ICMMA2020

The 14th International Conference on Multi-functional Materials and Applications

November 26~27th, 2020
KOREA

Sun Moon University

Organized by
Center for Next-Generation Semiconductor Technology
Sun Moon University, Asan, Korea
Anhui International Joint Research Center for Nano Carbo Based Materials and Environmental Health
Anhui University of Science and Technology, Anhui, China

Supported by
Department of Display and Semiconductor Engineering
Center for Next-Generation Display Evaluation
College of Engineering, Sun Moon University

Co-organizers

Hanseo Univ.
Bengbu Univ.
Anhui Univ. Sci. Technol.
Journal of Multifunctional Materials & Photoscience
Anhui Univ.
Yancheng Institute. Technol.
Anhui Jianzhu Univ.
Suzhou Univ. Sci. Technol.
Anhui Univ. Technol.
KhonKean Univ.
Nakhon Si Thammarat Rajabhat University
Hefei Univ.

The 14th International Conference on Multi-Functional Materials and Applications (ICMMA 2020)

Conference Chairman:

Prof. Ho-Seob Kim (Professor, Sunmoon University, Korea)

Conference Vice Chairman:

Prof. Jin Liu (Anhui Jianzhu University, China)
Prof. Won-Chun Oh (Hanseo University, Korea)

Advisory Chairman:

Prof. Mingxu Zhang (Anhui University of Science & Technology, China)
Prof. Zhigang Chen (Suzhou University of Science and Technology, China)
Prof. Saksit Chanthai (Khon Kaen University, Thailand)
Prof. Won-Chun Oh (Hanseo University, Korea)
Prof. Jin Liu (Anhui Jianzhu University, China)
Prof. Ding Ming (Bengbu University, China)
Prof. Chuyang Xu (Anhui University of Science & Technology, China)
Prof. Shin Mukai (Hokkaido University, Japan)
Dr. Chong-Hun Jung (Korea Atomic Energy Research Institute, Korea)
Prof. Cheol Gyu Kim (Hanbat National University, Korea)
Prof. Heon-Chang Kim (Hoseo University, Korea)
Prof. Masahiro Toyoda (Oita University, Japan)
Prof. Chan-Kyung Kim, (Inha University, Korea)
Prof. Daosung Sun (Hefei Normal University, China)
Dr. Kwang Yeon Cho, (Korea institute of Ceramic Eng. and Tech., Korea)
Prof. Zhaoqi Sun (Anhui University, China)
Prof. Chen-Hao Wang (National Taiwan University of Science and Technology, Taiwan)

Conference Local Chairman:

Prof. Ram Agarwal (AJC Editor Chief, India)
Prof. Shao-Jie Feng (Anhui Jianzhu University, China)
Dr. Hui-Jun Won (Korea Atomic Energy Research Institute, Korea)
Prof. Won-Kweon Jang (Hanseo University, Korea)
Prof. Chang-Sung Lim (Hanseo University, Korea)

Prof. Qinfang Zhang (Yancheng Institute of Technology, China)
Prof. Seung-Kyu Park (Hoseo University, Korea)
Prof. Dongtian Wang (Suzhou University of Science and Technology, China)
Prof. Yanmao Dong (Suzhou University of Science and Technology, China)
Dr. Hangkyo Jin (Korea Research Institute of Chemical Technology, Korea)
Prof. Benhong Yang (Hefei University, China)
Prof. Feng-Jun Zhang (Anhui Jianzhu University, China)
Prof. Young Chul Kim (Eulji University, Korea)
Prof. Prawit Nuengmatcha (Nakhon Si Thammarat Rajabhat University, Thailand)
Prof. Chew Tin Lee (Universiti Teknologi Malaysia, Malaysia)
Prof. Yin Liu, (Anhui University of Science and Technology, China)
Prof. Cheol-Kyu Jun, (Hoseo University, Korea)
Prof. Chunhu Wang (Bengbu University, China)
Dr. Suresh Sagadervan (Malaya University, Malaysia)
Prof. Minh-Vien Le (Ho Chi Minh City University of Technology , Vietnam)
Prof. Rachadaporn Benchawattananon (Khon Kaen University, Thailand)

Committee Board Members:

Prof. Bao-Lin Wang (Nanjing Normal University, China)
Prof. Ke Wu, (Hefei University, China)
Prof. Jong-Sung Yu, (Daegu Gyeungbuk Institute of Science & Technology, Korea)
Prof. Qingzeng Zhu (Shandong University, China)
Prof. Chengbao Liu (Suzhou University of Science and Technology, China)
Prof. Ze-Da Meng, (Suzhou University of Science and Technology, China)
Dr. Lei Zhu (Yancheng Institute of Technology, China)
Prof. Soon-Jik Hong (Kongju National University, Korea)
Prof. Jae-Won Lee (Dankook University, Korea)
Prof. Goutam Mukhopadhyay (B.C.D.A College of Pharmacy &Technology, India)
Prof. Zainal Arifin Ahmad (University Sains, Malaysia)
Prof. WeiChang Hao (BeiHang University, China)
Dr. Jyothi Rajesh Kumar (Korea Institute of Geoscience and Mineral Resources, Korea)
Dr. Yu-Jin Han (Korea Institute of Energy Research, Korea)
Prof. Sirinuch Loita (Khon Kaen University, Thailand)
Prof. Gaofeng Wang (Inner Mongolia University of Science and Technology, China)
Prof. Feng Liu (Nanchang University, China)

Prof. Hak-Soo Kim (Sun Moon University, Korea)

Prof. Jiahong Fan (Beijing Huabei Dianli University, China)

Prof. Yong Wook Park (Sun Moon University, Korea)

Prof. Seo hyung Cho (Sun Moon University, Korea)

Prof. Youn Soo Shim (Sun Moon University, Korea)

Prof. Jin Woo Kim (Sun Moon University, Korea)

Conference Academic Chairman:

Prof. Ho-Seob Kim (Professor, Sunmoon University, Korea)

Prof. Won-Chun Oh (Hanseo University, Korea)

Prof. Jin Liu (Anhui Jianzhu University, China)

Conference Registration

Deadline	**October 31 (Thursday), 2020**
All of presenters (Speakers) should be paid Registration fee.	

Registration fee

Regular : 50,000KWN, 50USD, 300RMB

Student : 30,000KWN, 30USD, 200RMB

Venue: Sun Moon University, Korea

Meeting Name	Meeting ID	PW
ICMMA2020_Room1_Zoom1	782 272 9549	icmma2020
ICMMA2020_Room2_Zoom2	366 357 0584	icmma2020
ICMMA2020_Room3_Zoom3	858 283 9675	icmma2020

Pesentation Guide

Plenary Lecture : 20 minutes speech, 5 minutes Q&A

Invited and Oral Lecture : 15 minutes speech, 5 minutes Q&A

Poster presentation : 2 minutes speech, 2 minutes Q&A (Only 1)

Full Paper Submission

1. **Molecules** (SCIE) , ISSN: 1420-3049

   Article processing charge (APC) : 1,600 CHF.

   Submission : https://www.mdpi.com/journal/molecules/special_issues/multi-func_material_ICMMA2020

   Guest Editor: Prof. Chan Kyung Kim (kckyung@inha.ac.kr)

molecules

an Open Access Journal by MDPI

IMPACT FACTOR
3.267

Multi - functional Materials and
Applications - - - Special Issue for
ICMMA2020

Guest Editor
Prof. Dr. Chan Kyung Kim

Deadline
28 February 2021

Special Issue

mdpi.com/si/62951

Invitation to submit

2. **Asian Journal of Chemistry** (SCOPUS), ISSN: 0975-427X (Online), ISSN: 0970-7077 (Print)

   APC : 450USD

   Guest Editor (Submission) : Prof. Won-Chun Oh (wc_oh@hanseo.ac.kr)

3. **Journal Multifunctional Materials and Photoscience**, ISSN: 2229-743x

   APC : Free Registration fee for submitter

   Editor-in-Chief (Submission) : Prof. Won-Chun Oh (wc_oh@hanseo.ac.kr)

4. **Korean Journal of Materials Research** (SCOPUS), ISSN : 1225-0562

   APC : 250USD

   Guest Editor (Submission) : Prof. Won-Chun Oh (wc_oh@hanseo.ac.kr)

Agenda of ICMMA2020-Opening Ceremony

(Host by Prof. Dr. **Ho-Seob Kim**)

09:00~09:10		Opening address by Prof. **Ho-Seob Kim** (Professor, Sun Moon University, Korea) –Conference Chairman -
09:10~09:20		Congratulation address by President Prof. **Sun Jo Hwang** (Prsident Professor, Sun Moon University, Korea) –President in Sun Moon University-
09:20~09:40	09:20~09:30	ICMMA News by Prof. Dr. **Won-Chun Oh** (Hanseo University, Korea) – Conference Vice Chairman -
	09:30~09:40	Address by Prof. Dr. **Prawit Nuengmatcha** (Nakhon Si Thammarat Rajabhat University, Thailand) **Introduction of ICMMA2021**
09:40~09:50		**"Award of Appreciation Plaque"** Plaque to Prof. Dr. **Ming Ding** (Bebgbu University, China) **“Award of Appreciation Plaque to Retired Scientists”** Prof. **Chuyang Xu** (Anhui University of Science and Technology, China) **“Best Paper Award – (Supported by Journal “Nanomaterials” : MDPI)”** Dr. **Chong-Hun Jung** (Korea Atomic Energy Research Institute, Kora) nanomaterials
09:50		The conference chairman announces **ICMMA 2020** begins
09:55		Group Photo
09:55~10:00		Break

Conference Program

November 26 (Thursday), 2020

Session I (Zoom A: No 782 272 9549, PW icmma2020) (10:00-10:50) (Session Chairman : Prof. Dr. Won-Chun Oh (Hanseo University), Feng-Jun Zhang (Anhui Jianzhu University))	
10:00-10:25	**Plenary Lecture 1** Prof. **Xiangke Wang** (College of Environmental Science and Engineering, North China Electric Power University, Beijing 102206 China) **Synthesis of C_3N_4-based photocatalysts for organic pollutants degradation and U(VI)/Cr(VI) sorption-reduction**
10:25-10:50	**Plenary Lecture 2** Dr. **Rajesh Kumar Jyothi** (Korea Institute of Geoscience and Mineral Resources KIGAM), Daejeon 34132, Korea) **Secondary recourse to clean energy materials via environmental management**
Session II-1(Zoom A: No 782 272 9549, PW icmma2020) (10:50-12:10) (Session Chairman : Prof. Dr. Chan-Kyung Kim (Inha University), Prof. Chin-Yang Yu (National Taiwan University of Science and Technology))	
10:50-11:10	**Invited Lecture 1** Prof. **Jia Hong Pan** (Colleague of Environmental Science and Engineering, North China Electronic Power University, Beijing 102206, China) **Self-Assembly of Hydrous TiO_2 Colloidal Spheres for Photo/electrochemical Applications**
11:10-11:30	**Invited Lecture 2** Prof. **Molang Cai** (State Key Laboratory of Alternate Electrical Power System with Renewable Energy Sources, Beijing Key Laboratory of Novel Thin-Film Solar Cells, North China Electric Power University, Beijing 102206, P. R. China) **Interfacial engineering of perovskite solar cell with efficient electron transport layers**
11:30-11:50	**Oral Lecture 1** **Kamrun Nahar Fatema** (Department of Advanced Materials Science & Engineering, Hanseo University, Seosan-si, Chungnam, Korea, 356-706) **A Comparative Study of Electrochemical Biosensors Based on Highly Efficient Mesoporous ZrO_2-Ag-G-SiO_2 and In_2O_3- G-SiO_2 for Rapid Recognition of E. coli O157: H7**
11:50-12:10	**Oral Lecture 2** **Zambaga Otgonbayar** (Department of Advanced Materials Science & Engineering, Hanseo University, Seosan-si, Chungnam, Korea, 356-706)

<table>
<tr><td></td><td>New modeling of Graphene-based Ternary nanocomposite and its photocatalytic reduction of CO$_2$ into Methanol</td></tr>
<tr><td colspan="2">Session II-2 (Zoom B: No 366 357 0584, PW icmma2020) (10:50-12:10) (Session Chairman : Jin Liu (Anhui Jianzhu University), Prof. Saksit Chanthai (Faculty of Science, Khon Kaen University))</td></tr>
<tr><td>10:50-11:10</td><td>Invited Lecture 3
Prof. K.L. Ameta (Department of Chemistry, School of Liberal Arts and Sciences, Mody University of Science and Technology, Lakshmangarh-332311, Rajasthan, India)
Synthesis of Bioactive Heterocycles Using Nanocatalytic Framework</td></tr>
<tr><td>11:10-11:30</td><td>Invited Lecture 4
Prof. Xianbiao Wang* ([a]Anhui Province International Research Center on Advanced Building Materials, School of Materials Science and Chemical Engineering, Anhui Jianzhu University, Hefei 230601, P. R. China)
Electrospinning Preparation of PAN/TiO$_2$/PANI hybrid Fiber membrane with Highly selective adsorption and photocatalytic regeneration properties</td></tr>
<tr><td>11:30-11:50</td><td>Oral Lecture 3
Prof. Kefayat Ullah (Department of Applied Physical & Material Sciences, University of Swat)
Graphene Based Nanomaterials, Towards Energy Storage and Production</td></tr>
<tr><td>11:50-12:10</td><td>Oral Lecture 4
Prof. Rambabu Kuchi (a. Powder & Ceramics Division, Korea Institute of Materials Science, Changwon, Gyeongnam 51508, South Korea, (b) Convergence research center for development of mineral resources, Korea Institute of Geoscience and Mineral Resources, Daejeon 34132, South Korea)
Advanced electromagnetic (EM) shielding materials for remediation of environmental pollution</td></tr>
<tr><td colspan="2">Session II-3 (Zoom C: No 858 283 9675, PW icmma2020) (10:50-12:10) (Session Chairman : Chuyang Xu (Anhui University of Sci. Tech.), Jing Wang (Anhui University of Sci. Tech.))</td></tr>
<tr><td>10:50-11:10</td><td>Invited Lecture 5
Prof. Shinichiroh Iwamura (Faculty of Engineering. Hokkaido University, Sapporo, Japan)
Improvement of Supercapacitor Performance of MnO$_2$/porous-carbon Nanocomposites by Tuning Pore Size of Porous Carbon Substrates</td></tr>
<tr><td>11:10-11:30</td><td>Invited Lecture 6
Prof. Hongzhi Liu (School of Chemistry and Chemical Engineering, Shandong University, Jinan, China)
Silsesquioxanes-Based Functional Porous Polymers</td></tr>
</table>

11:30-11:50	**Oral Lecture 5** Prof. **Yuhong Jiao** (Anhui Provincial Engineering Laboratory of Silicon-based Materials, School of Material and Chemical Engineering, Bengbu University, Bengbu, 233030, PR China) **In-situ synthesis SiC/MgO/$MgAl_2O_4$ in molten Al-30Si alloy：Flash pyrolysis phenolic resin**
11:50-12:10	**Oral Lecture 6** **Yonrapach Areerob** (Department of Industrial Engineering, Faculty of Engineering, King Mongkut's Institute of Technology Ladkrabang, Bangkok, 10520, Thailand) **Hybrid of Graphene based on quaternary $Cu_2ZnNiSe_4$ –WO_3 nanorods for counter electrode in Dye-sensitized Solar cell Application**
12:10-13:10 Lunch Time	
Session III (Zoom A : No 782 272 9549, PW icmma2020) (13:10-14:30) (Session Chairman : Prof. Shin Mukai (Hotkaido Uinversity), Prof. Masahiro Toyoda (Oita University))	
13:10-13:35	**Plenary Lecture 3** Prof. **Estelle Leonard (**T.I.M.R. EA 4297 ESCOM/UTC, 1 allée du réseau Jean-Marie Buckmaster, F-60200 COMPIEGNE) **Azo dyes – from biomass to sustainable development**
13:35-14:00	**Plenary Lecture 4** Prof. **Jiří Jaromír Klemeš** (Sustainable Process Integration Laboratory – SPIL, NETME Centre, Faculty of Mechanical Engineering, Brno, University of Technology - VUT Brno, Technická 2896/2, 616 00 Brno, Czech Republic) **Plastics: Material for the future?**
Break (14:00-14:10) : Refresh	
Session IV-1 (Zoom A : No 782 272 9549, PW icmma2020) (14:10-16:30) (Session Chairman : Prof. Ming Ding (Bengbu University), Dr. Yonrapach Areerob (King Mongkut's Institute of Technology))	
14:10-14:30	**Invited Lecture 7** Prof. **Minh-Vien Le*** (Faculty of Engineering, Ho Chi Minh city University of Technology, Ho Chi Minh City, 700000, Vietnam Chemical) **Synthesis N-doped TiO_2-SiO_2 coated honeycomb ceramic monolith to enhance photocatalytic degradation of phenol under UV-LED irradiation**
14:30-14:50	**Inivited Lecture 8** Prof. **Lin Shi** (School of Materials Science and Engineering, Yancheng Institute of Technology, Yancheng 224001, People’s Republic of China) **Ab initio Calculations of Light-Emitting Quantum Efficiency for Point Defects in Semiconductors**

14:50-15:10	**Oral Lecture 7** Prof. **Di Wang** (School of Materials and Chemical Engineering, Anhui Jianzhu University, 230601 Hefei, China) **Study of Stimuli-Responsive Organic Magneton Based on Nitroxide Radicals and Carbon Cation Radicals**
15:10-15:30	**Oral Lecture 8** Prof. **Xiaolong Fang** (College of Materials and Chemical Engineering, Anhui Jianzhu University, Hefei, 230601, China) **Ruthenium Catalysts with Metal-ligand Cooperation for Hydrogenation of Esters into Alcohols**
15:30-15:50	**Oral Lecture 9** Prof. **Janardhan Reddy Koduru** (Department of Environmental Engineering, Kwangwoon University, Seoul, 01897, South Korea) **Strategies and Opportunities of Magnetic Graphene-based Composites for Water Remediation**
15:50-16:10	**Oral Lecture 10** Prof. **Nichapha Senamart** (Materials Chemistry Research Center, Department of Chemistry, Faculty of Science, Khon Kaen University, Khon Kaen 40002, Thailand) **Influences of metal dispersion and H_2-spillover of Pt to lower reduction temperature of Ni/HZSM-5 catalyst investigated by TRXAS**
16:10-16:30	**Oral Lecture 11** Prof. **Rachadaporn Benchawattananon** (Integrated Science Faculty of Science Khon Kaen University Khon Kaen Thailand 40000) **Identity of rose wood (Dalbergia cochinchinensis) by FTIR SEM-EDX and SEM-EDS Utilization in Forensic Science**
16:30-16:50	**Oral Lecture 12** Prof. **Nur Indah Fajar Mukti** (Department of Chemical Engineering, Universitas Gadjah Mada, Indonesia) **Preparation of Carbon Supported Cobalt Oxide as Ethylene Scavenger for Fruit Preservation**
Session IV-2 (Zoom B: No 366 357 0584, PW icmma2020) (14:10-16:30) (Session Chairman : Dr. Rajesh Kumar Jyothi (KIGAM), Yu-Lin Kuo (National Taiwan University of Science and Technology))	
14:10-14:30	**Invited Lecture 9**

	Prof. **Teguh Ariyanto** (Carbon Material Research Group, Department of Chemical Engineering, Universitas Gadjah Mada, Indonesia) **Reusable Adsorbent of Fe/C for Metronidazole Removal**
14:30-14:50	**Invited Lecture 10** Prof. **Nunticha Limchoowong** (Materials Chemistry Research Center, Department of Chemistry and Center of Excellence for Innovation in Chemistry, Faculty of Science, Khon Kaen University, Khon Kaen 40002, Thailand) **A novel bead synthesis of the Chiron-SDS hydrogel and its kinetics-thermodynamics study of superb adsorption of alizarin red S from aqueous solution**
14:50-15:10	**Oral Lecture 13** Prof. **Yanmao Dong** (School of Chemistry and Life Sciences, Suzhou University of Science and Technology, Xuefu Road 99, Suzhou, China, 215009) **A novel Si-based Caged-structural Intumescent Additive for Improving Flame Retardance of Unsaturated Polyester Resin**
15:10-15:30	**Oral Lecture 14** Prof. **Jing Wang (**College of Materials Science and Engineering, Anhui University of Science And Technology, Huainan, Anhui 232001**)** **Fabrication and properties of transparen Eu:Lu_2O_3 scintillation ceramics**
15:30-15:50	**Oral Lecture 15** Prof. **Yanfen Wang** (School of Materials Science and Engineering, Anhui University of Science and Technology, Huainan 232001, PR China) **Facile preparation of ternary Ag@AgBr/TiO_2 nanorod arrays for enhanced photoelectrochemical and photocatalytical activity**
15:50-16:10	**Oral Lecture 16** Prof. **Chao Zhang** (School of Materials Science and Engineering, Anhui University of Science and Technology, Huainan 232001, China) **A new carbon allotrope: T_5-carbon**
16:10-16:30	**Oral Lecture 17** Prof. **Linfeng Xu** (Anhui University of Science & Technology, China) **Study on Titanium Dioxide Nanomaterials with Specific Crystal Facet for Enhanced Photocatalytic and Dye-Sensitized Solar Cells Performances**
16:30-16:50	**Oral Lecture 18** Prof. **Biao Hu** (School of Materials Science and Engineering, Anhui University of Science and Technology, Huainan, Anhui 232001, PR China)

	Thermodynamic modeling of the Ti–V system for the third generation CALPHAD database including metastable ω phase
Session IV-3 (Zoom C: No 858 283 9675, PW icmma2020) (14:10-16:30) (Session Chairman : Prof. Chew Tin Lee (Universiti Teknologi Malaysia), Dr. Suresh Sagadevan (University of Malaya))	
14:10-14:30	**Invited Lecture 11** Prof. **Feng Liu** (College of Chemistry, Nanchang University, Xuefu Avenue 999, Honggutan New District, Nanchang 330031, PR China) **Development of Low-Dielectric Polyimide Films: Effects of Alicyclic Functionality and Siloxane Segments**
14:30-14:50	**Invited Lecture 12** Prof. **Is Fatimah** (Department of Chemistry, Faculty of Mathematics and Natural Sciences, Universitas Islam Indonesia, Kampus Terpadu UII, Jl. Kaliurang Km 14, Sleman, Yogyakarta, Indonesia) **Porous Clay Heterostructure/Metal Oxide Nanocomposite as Photocatalyst Materials**
14:50-15:10	**Oral Lecture 19** Prof. **Jing-Tai Zhao** (School of Materials Science and Engineering, Guilin University of Electronic Technology, Guangxi, China) **Tuning of the thermoelectric properties of quaternary compounds, ABZnSb (A = Sr, Ba and rare earth elements; B = F and O) with the ZrCuSiAs structure type**
15:10-15:30	**Oral Lecture 20** Prof. **Annisa** (Department of Chemical Engineering, Universitas Gadjah Mada, Indonesia) **Influence of Gamma Irradiation to Modifying Nanoporous Carbon as Supercapacitor Material**
15:30-15:50	**Oral Lecture 21** Prof. **Paweena Porrawatkul** (Creative Innovation in Science and Technology, Nakhon Si Thammarat Rajabhat University, 80280, Thailand) **Green route for synthesis and characterization of Ag/zinc oxide nanoparticles for antibacterial activity application onto cotton fabrics**
15:50-16:10	**Oral Lecture 22** Prof. **Rungnapa Pimsen** (Nanomaterials Chemistry Research Unit, Department of Chemistry, Faculty of Science and Technology, Nakhon Si Thammarat Rajabhat University, 80280, Thailand) **Synthesis of nanozeolite-chitosan/sago starch for slow release fertilizer**
16:10-16:30	**Oral Lecture 23** Prof. **Ying-Wei Lu** (School of Materials Science and Engineering, Hefei University of

	Technology, Hefei, Anhui 230009, P. R. China) **Exploration of Improved Processes for Large-Scale Production of ZrO_2 Spheres**
16:30-16:50	**Oral Lecture 24** Prof. **P. Vajeeston (**Center for Materials Science and Nanotechnology, Department of Chemistry, University of Oslo,Box 1033 Blindern N-0315, Oslo, Norway**)** **Computational materials design and characterisation for functional inorganic materials**
16:50-17:00	**Zoom A : No 782 272 9549, PW icmma2020 Closing Remark (Prof. K. L. Ameta (Mody University of Science and Technology))**
17:00-18:00	**Zoom B : No 366 357 0584, PW icmma2020 : ICMMA2020 Committee Board Member Meeting (Prof. Won-Chun Oh)**

November 27 (Friday), 2020

Session VI (Zoom A: No 782 272 9549, PW icmma2020) (09:00-09:50) (Session Chairman : Prof. Chen-Hao Wang (National Taiwan University of Science and Technology), Prof. Molang Cai (North China Electric Power University))	
09:00-09:25	**Plenary Lecture 5** Prof. **Kyo-Seon Kim** (Department of Chemical Engineering, Kangwon National University, Chuncheon, Kangwon-Do, South Korea) **Application of Functionalized 1-D WO_3 prepared by Flame Vapor Deposition on Photoelectrochemical Oxygen Evolution**
09:25-09:50	**Plenary Lecture 6** Prof. **Saksit Chanthai** (Materials Chemistry Research Center, Department of Chemistry and Center of Excellence for Innovation in Chemistry, Faculty of Science, Khon Kaen University, Khon Kaen 40002, Thailand) **Recent chemical functions and applications of using carbon‒based nanomaterials to countermeasure for COVID‒19 outbreak: A Review**
Session VII-1 (Zoom A: No 782 272 9549, PW icmma2020) (09:50-11:50) (Session Chairman : Jia Hong Pan (North China Ele. Pow. University), Prof. Shinichiroh Iwamura (Hokkaido University)	
09:50-10:10	**Invited Lecture 13** Dr. **Suresh Sagadevan** (Nanotechnology & Catalysis Research Centre, University of Malaya, Kuala Lumpur 50603, Malaysia) **Synthesis, Physicochemical characterization, dielectric and electrical properties of ZnO/MgO Nanocomposite**

10:10-10:30	**Invited Lecture 14** Prof. **S Paiman** (Department of Physics, Faculty of Science, Universiti Putra Malaysia, 43400 UPM Serdang, Selangor, Malaysia) **Structural, Optical and Electrical Properties of Controlled Growth Zinc Oxide Nanowires**
10:30-10:50	**Oral lecture 25** Prof. **M. A. Motalib Hossain** (Nanotechnology and Catalysis Research Centre (NANOCAT), University of Malaya, 50603 Kuala Lumpur, Malaysia) **Recent advancement of molecular based techniques in the authentication of food products**
10:50-11:10	**Oral Lecture 26** Prof. **Kunhong Hu** (School of Energy Materials and Chemical Engineering，Hefei University，Hefei，230601, China) **The study on preparation and application of formed granular bentonite**
11:10-11:30	**Oral Lecture 27** Prof. **Asghar Ali** (Department of Advanced Materials Science & Engineering, Hanseo University, Seosan-si, Chungnam, Korea, 356-706.) **Novel and simple process for the photocatalytic reduction of CO2 with TMDSc-Graphene nanocomposite**
11:30-11:50	**Oral Lecture 28** Prof. **Wei Lian** (School of Materials Science and Engineering, Anhui University of Science and Technology, Huainan 232001, Anhui, China) **Effect of Flake-Shape and Content of Nano Mullite on Mechanical Properties and Fracture Process of Corundum Composite Ceramics**
Session VII-2 (Zoom B: No 366 357 0584, PW icmma2020) (09:50-11:50) (Session Chairman : Prof. Hongzhi Liu (Shandong University), Prof. Feng Liu (College of Chemistry, Nanchang University))	
09:50-10:10	**Invited Lecture 15** Prof. **Solhe F. Alshahateet (**Department of Chemistry, Mutah University, Jordan) **Design, Synthesis, and Applications of Novel V-shape Heterocyclic Derivatives**
10:10-10:30	**Invited Lecture 16** Prof. **Chen-Hao Wang** (Department of Materials Science and Engineering, National Taiwan University of Science and Technology, 10607, Taipei, Taiwan) **Development of Electrode Materials for Vanadium Redox Flow Batteries**
10:30-10:50	**Oral Lecture 29** Prof. **Yin Liu** (School of Materials Science and Engineering, Anhui University of Science and Technology, Huainan 232001, Anhui, China)

	Hydrothermal synthesis of organic perovskite and organic-inorganic hybrid three-dimensional perovskite ferroelectrics with H_2Dabco cation
10:50-11:10	**Oral Lecture 30** Prof. **Phacharaphon Tunthawiroon** (Department of Industrial Engineering, Faculty of Engineering, King Mongkut's Institute of Technology Ladkrabang, Bangkok 10520, Thailand) **Development of Co-based alloys for high temperature applications**
11:10-11:30	**Oral Lecture 31** Prof. **Hong Chen** (Department of Chemical Engineering, School of Energy Materials and Chemical Engineering, Hefei University, Hefei 230601, Anhui, China) **Solvating modulation effect of ionic liquids toward Fe_3O_4 nanomaterials**
11:30-11:50	**Oral Lecture 32** Prof. **Wu Ying** (School of Energy Materials and Chemical Engineering, Hefei University, Hefei, 230601, China) **Research on adsorption properties of rape straw biochar to dye wastewater**
Session VII-3 (Zoom C: No 858 283 9675, PW icmma2020) (09:50-11:50) (Session Chairman : Prof. Xianbiao Wang (Anhui Jianzhu University), Prof. Lin Shi (Yancheng Institute of Technology)	
09:50-10:10	**Invited Lecture 17** Prof. **Prawit Nuengmatcha** (Nanomaterials Chemistry Research Unit, Faculty of Science and Technology, Nakhon Si Thammarat Rajabhat University, Nakhon Si Thammarat, 80280, Thailand) **Enhanced sonocatalytic degradation of methylene blue using Fe_2O_3-graphene-Ag nanocomposite as catalyst**
10:10-10:30	**Invited Lecture 18** Prof. **Jing Wang (**College of Materials Science and Engineering, Anhui University of Science And Technology, Huainan, Anhui 232001**)** **Structures and Properties of Carbon-based Nanocomposites**
10:30-10:50	**Oral Lecture 34** Prof. **Jing Wang (**College of Materials Science and Engineering, Anhui University of Science And Technology, Huainan, Anhui 232001**)** **Preparation and Properties of Nitrogen-doped Carbon-based Electrode Material**
10:50-11:10	**Oral Lecture 35** Prof. **Jing Wang (**College of Materials Science and Engineering, Anhui University of Science And Technology, Huainan, Anhui 232001**)** **Preparation and Properties of Carbon-based Metal Oxide Composite Electrode Materials**

11:10-11:30	**Oral Lecture 36** Prof. **Guojun Cheng** (School of Materials Science and Engineering, Anhui University of Science and Technology, Huainan 232001, China) **The Functionalization of Two-Dimensional $Ti_3C_2T_x$ MXenes with TPME to Enhance Hydrophobicity and Stability**
11:30-11:50	**Oral Lecture 37** Prof. **Gao Meiling** (Anhui University of Science and Technology, School of Materials Science and Engineering, Huainan, 232001, Anhui) **Study on Preparation and properties of Permeable Composite Membrane based on PVA/PU and its Application**
11:50-12:50 Lunch Time	
Poster Session (12:50-17:00) (Session Chairman: Prof. Prawit Nuengmatcha (Nakhon Si Thammarat Rajabhat University), Prof. Minh-Vien Le (Ho Chi Minh city University of Technology)) (ZoomA: No 782 272 9549, PW icmma2020)	
Session VIII-1 (ZoomA: No 782 272 9549, PW icmma2020) (17:00-18:40) (Session Chairman : Prof. Prof. Estelle Leonard (ESCOM/UTC), Prof. Teguh Ariyanto (Universitas Gadjah Mada))	
17:00-17:20	**Invited Lecture 19** Prof. **Daming Gao** (Department of Chemical Engineering, School of Energy, Materials and Chemical Engineering, Hefei University, Hefei 230601, Anhui, China) **Constructed CdTe QDs Surface Fluorescence Probe to Detection of Ultratrace Herbicide Paraquat Free Radical Based on FRET Mechanism**
17:20-17:40	**Invited Lecture 20** Prof. **Chew Tin Lee** (School of Chemical and Energy Engineering, Faculty of Engineering. Universiti Teknologi Malaysia 81300 Johor Bahru. Malaysia) **Multi-functional Biochar for Sustainable Soil Management**
17:40-18:00	**Oral Lecture 38** **Prof. Lai Shengfa (**Anhui University of Science and Technology， Material Science and Engineering School， 232001**)** **Study on Preparation and Electrical Properties of Polyanline/Waterborne Polyurethane Composite**
18:00-18:20	**Oral Lecture 39** Prof. **Shen Tian** ([a]School of Materials Science and Engineering, Anhui University of Science and Technology, Huainan 232001, China)

	Fabrication of two-dimensional $Ti_3C_2T_x$ MXenes by ball milling pretreatment and mild etchant and their microstructure
18:20-18:40	**Oral Lecture 40** Prof. **Ziyue Xuan** ([a]School of Materials Science and Engineering, Anhui University of Science and Technology, Huainan 232001, China) **Flame-retardant behavior and Mechanism of SBR/MMT Composites Modified by Melamine Matrix Modifier**
Session VIII-2 (Zoom B : No 366 357 0584 , PW icmma2020) (17:00-18:40) (Session Chairman : Prof. Is Fatimah (Universitas Islam Indonesia), Prof. Kunhong Hu (Hefei University))	
17:00-17:20	**Invited Lecture 21** Prof. **Yu-Lin Kuo** (Department of Mechanical Engineering, National Taiwan University of Science and Technology, Taipei 10607, Taiwan.) **Enhanced Electrical Performance of the Graphene Felt for Energy Storage Devices by Atmospheric Pressure Plasma Jet**
17:20-17:40	**Invited Lecture 22** Prof. **Chin-Yang Yu** (Department of Materials Science and Engineering, National Taiwan University of Science and Technology, 43, Section 4, Keelung Road, Taipei 10607, Taiwan) **Preparation, Aggregation-Induced Emission and Nanoaggregates of the Copolymers Containing Different Ratios of Carbazoles and Tetraphenylethenes**
17:40-18:00	**Oral Lecture 41** Prof. **Chang-Peng Lv** (Anhui Provincial Engineering Laboratory of Silicon-based Materials, Engineering Technology Research Center of Silicon-based Materials Anhui, School of Material and Chemical Engineering, Bengbu University, Bengbu 233030, PR China) **$K_xSi_yNb_zO_w$ as a Low-Potential Anode Material for Lithium-Ion Battery**
18:00-18:20	**Oral Lecture 42** Prof. **Xiaochen Huang** (Anhui Provincial Engineering Laboratory of Silicon-based Materials, School of Material and Chemical Engineering, Bengbu University, Bengbu, 233030, PR China) **Research on irradiation properties of Max (Ti_3SiC_2, Ti_3AlC_2) materials**
18:20-18:40	**Oral Lecture 43** Prof. **Yang Benhong** (Department of Chemistry and Materials Engineering, Hefei University, Hefei, 230601, China) **Preparation and photocatalytic application of g-C_3N_4/WO_3 composites**
Session VIII-3 (Zoom C : No 858 283 9675, PW icmma2020) (17:00-18:40) (Session Chairman :	

Prof. Ben Hong Yang (Hefei University), Prof. Hak-Soo Kim (Sun Moon University)	
17:00-17:20	**Invited Lecture 23** Prof. **Yuwaraj K. Kshetri** ([1]Research Center for Eco-Multifunctional Nano Materials, Sun Moon University, Chungnam 31460, Republic of Korea) **Electronic structure, thermodynamic stability and high-temperature sensing properties of Er-α-SiAlON ceramics**
17:20-17:40	**Invited Lecture 24** Prof. **Na Yin** (Anhui Provincial Engineering Laboratory of Silicon-based Materials, School of Material and Chemical Engineering, Bengbu University, Bengbu, 233030, PR China) **Novel modifiedChitosan for remarkably high removal of heavy metal Cu (II)**
17:40-18:00	**Oral Lecture 44** Prof. **Chao Feng** (Anhui Provincial Engineering Laboratory of Silicon-based Materials, School of Material and Chemical Engineering, Bengbu University, Bengbu, 233030, PR China) **Highly supercapacitive performance on a Mn(II)-based MOF**
18:00-18:20	**Oral Lecture 45** Prof. **Jinlong Ge (**Department of Materials Science and Chemical Engineering, Anhui province Engineering Laboratory of Silicon-based Materials Bengbu University, Bengbu 233000, P.R. China **)** **Preparation of the mesoporous silica composite nanoparticles coated with biodegradable temperature/pH sensitive copolymer and their application in drug release**
18:40-18:50	**Closing Remark & Ceremony – Zoom A :** No 782 272 9549, PW icmma2020 **(Prof. Saksit Chantai (KhonKean University), Prof. Prawit Nuengmatcha (Nakhon Si Thammarat Rajabhat University))**

Timetable

09:00-10:00	**Zoom A** : Opening ceremony (**November 26 (Thursday), 2020**)			
	Zoom A : No 782 272 9549, PW icmma2020			
10:00-10:25	Plenary Lecture	Prof. Xiangke Wang., College of Environmental Science and Engineering, North China Electric Power University, Beijing 102206 China		
10:25-10:50	Plenary Lecture	Prof. Rajesh Kumar Jyothi., Korea Institute of Geoscience and Mineral Resources KIGAM), Daejeon 34132, Korea		
13:10-13:35	Plenary Lecture	Prof. Estelle Leonard., T.I.M.R. EA 4297 ESCOM/UTC, 1 allée du réseau Jean-Marie Buckmaster, F-60200 COMPIEGNE		
13:35-14:00	Plenary Lecture	Prof. Jiří Jaromír Klemeš., Sustainable Process Integration Laboratory – SPIL, NETME Centre, Faculty of Mechanical Engineering, Brno, University of Technology - VUT Brno, Technická 2896/2, 616 00 Brno, Czech Republic		
Second day				
09:00-09:25	Plenary Lecture	Prof. Kyo-Seon Kim., Department of Chemical Engineering, Kangwon National University, Chuncheon, Kangwon-Do, South Korea		
09:25-09:50	Plenary Lecture	Prof. Saksit Chanthai., Materials Chemistry Research Center, Department of Chemistry and Center of Excellence for Innovation in Chemistry, Faculty of Science, Khon Kaen University, Khon Kaen 40002, Thailand		
The information of Invited and Oral lectures				
		Zoom A **No 782 272 9549, PW icmma2020**	**Zoom B** **No 366 357 0584 , PW icmma2020**	**Zoom C** **No 858 283 9675, PW icmma2020**
10:50-11:10	Invited Lecture	Prof. Jia Hong Pan., Colleague of Environmental Science and Engineering, North China Electronic Power University, Beijing 102206, China	Prof. K. L. Ameta., Department of Chemistry, School of Liberal Arts and Sciences, Mody University of Science and Technology, Lakshmangarh - 332311, Rajasthan, India	Prof. Shinichiroh Iwamura., Faculty of Engineering. Hokkaido University, Sapporo, Japan
11:10-11:30	Invited Lecture	Prof. Molang Cai (State Key Laboratory of Alternate Electrical Power System with Renewable Energy Sources, Beijing Key Laboratory of Novel Thin-Film Solar Cells, North China Electric Power University, Beijing 102206, P. R. China	Prof. Xianbiao Wang*., [a]Anhui Province International Research Center on Advanced Building, Materials , School of Materials Science and Chemical Engineering, Anhui Jianzhu University, Hefei 230601, P. R. China	Prof. Hongzhi Liu., School of Chemistry and Chemical Engineering, Shandong University, Jinan, China
11:30-11:50	Oral Lecture	Kamrun Nahar Fatema., Department of Advanced Materials Science & Engineering, Hanseo University, Seosan-si, Chungnam, Korea, 356-706	Prof. Kefayat Ullah., Department of Applied Physical & Material Sciences, University of Swat	Prof. Yuhong Jiao, Anhui Provincial Engineering Laboratory of Silicon-based Materials, School of Material and Chemical Engineering, Bengbu University, Bengbu, 233030, PR China
11:50-12:10	Oral Lecture	Zambaga Otgonbayar., Department of Advanced Materials Science & Engineering, Hanseo University, Seosan-si, Chungnam, Korea, 356-706	Prof. Rambabu Kuchi., a. Powder & Ceramics Division, Korea Institute of Materials Science, Changwon, Gyeongnam 51508, South Korea	Yonrapach Areerob., Department of Industrial Engineering, Faculty of Engineering, King Mongkut's Institute of Technology Ladkrabang, Bangkok, 10520, Thailand
12:10-13:10	Lunch Time			
13:10-14:00	**Zoom A : No 782 272 9549, PW icmma2020** Plenary Lecture session			
14:00-14:10	Break time			
		Zoom A **No 782 272 9549, PW**	**Zoom B** **No 366 357 0584 , PW**	**Zoom C** **No 858 283 9675, PW**

		icmma2020	icmma2020	icmma2020
14:10-14:30	Invited Lecture	Prof. Minh-Vien Le*., Faculty of Engineering, Ho Chi Minh city University of Technology, Ho Chi Minh City, 700000, Vietnam	Prof. Teguh Ariyanto., Carbon Material Research Group, Department of Chemical Engineering, Universitas Gadjah Mada, Indonesia	Prof. Feng Liu., College of Chemistry, Nanchang University, Xuefu Avenue 999, Honggutan New District, Nanchang 330031, PR China
14:30-14:50	Invited Lecture	Prof. Lin Shi., School of Materials Science and Engineering, Yancheng Institute of Technology, Yancheng 224001, People's Republic of China	Prof. Nunticha Limchoowong., Materials Chemistry Research Center, Department of Chemistry and Center of Excellence for Innovation in Chemistry, Faculty of Science, Khon Kaen University, Khon Kaen 40002, Thailand	Prof. Is Fatimah., Department of Chemistry, Faculty of Mathematics and Natural Sciences, Universitas Islam Indonesia, Kampus Terpadu UII, Jl. Kaliurang Km 14, Sleman, Yogyakarta, Indonesia
14:50-15:10	Oral Lecture	Prof. Di Wang., School of Materials and Chemical Engineering, Anhui Jianzhu University, 230601 Hefei, China	Prof. Yanmao Dong., School of Chemistry and Life Sciences, Suzhou University of Science and Technology, Xuefu Road 99, Suzhou, China, 215009	Prof. Jing-Tai Zhao., School of Materials Science and Engineering, Guilin University of Electronic Technology, Guangxi, China
15:10-15:30	Oral Lecture	Prof. Xiaolong Fang., College of Materials and Chemical Engineering, Anhui Jianzhu University, Hefei, 230601, China	Prof. Jing Wang., College of Materials Science and Engineering, Anhui University of Science And Technology, Huainan, Anhui 232001	Prof. Annisa., Department of Chemical Engineering, Universitas Gadjah Mada, Indonesia
15:30-15:50	Oral Lecture	Prof. Janardhan Reddy Koduru., Department of Environmental Engineering, Kwangwoon University, Seoul, 01897, South Korea	Prof. Yanfen Wang., School of Materials Science and Engineering, Anhui University of Science and Technology, Huainan 232001, PR China	Prof. Paweena Porrawatkul (Creative Innovation in Science and Technology, Nakhon Si Thammarat Rajabhat University, 80280, Thailand
15:50-16:10	Oral Lecture	Prof. Nichapha Senamart., Materials Chemistry Research Center, Department of Chemistry, Faculty of Science, Khon Kaen University, Khon Kaen 40002, Thailand	Prof. Chao Zhang., School of Materials Science and Engineering, Anhui University of Science and Technology, Huainan 232001, China	Prof. Rungnapa Pimsen., Nanomaterials Chemistry Research Unit, Department of Chemistry, Faculty of Science and Technology, Nakhon Si Thammarat Rajabhat University, 80280, Thailand
16:10-16:30	Oral Lecture	Prof. Rachadaporn Benchawattananon., Integrated Science Faculty of Science Khon Kaen University Khon Kaen Thailand 40000	Prof. Linfeng Xu., Anhui University of Science & Technology, China	Prof. Ying-Wei Lu., School of Materials Science and Engineering, Hefei University of Technology, Hefei, Anhui 230009, P. R. China
16:30-16:50	Oral Lecture	Prof. Nur Indah Fajar Mukti, Department of Chemical Engineering, Universitas Gadjah Mada, Indonesia)	Prof. Biao Hu., School of Materials Science and Engineering,Anhui University of Science and Technology, Huainan, Anhui 232001, PR China	Prof. P. Vajeeston., Center for Materials Science and Nanotechnology, Department of Chemistry, University of Oslo,Box 1033 Blindern N-0315, Oslo, Norway
16:50-17:00	**Zoom A : No 782 272 9549, PW icmma2020 Closing Remark (Prof. K. L. Ameta (Mody University of Science and Technology)))**			
17:00-18:00	**Zoom B : No 366 357 0584 , PW icmma2020: ICMMA2020 Committee Board Member Meeting (Prof. Won-Chun Oh)**			
Second day (November 27 (Friday), 2020)				
09:00-09:50	**Zoom A** : **No 782 272 9549, PW icmma2020**: Plenary Lecture session			
		Zoom A **No 782 272 9549, PW icmma2020**	**Zoom B** **No 366 357 0584 , PW icmma2020**	**Zoom C** **No 858 283 9675, PW icmma2020**
09:50-10:10	Invited Lecture	Prof. Suresh Sagadevan., Nanotechnology & Catalysis Research Centre, University	Prof. Solhe F. Alshahatee., Department of Chemistry, Mutah University, Jordan	Prof. Prawit Nuengmatcha., Nanomaterials Chemistry Research Unit, Faculty of Science

		of Malaya, Kuala Lumpur 50603, Malaysia		and Technology, Nakhon Si Thammarat Rajabhat University, Nakhon Si Thammarat, 80280, Thailand
10:10-10:30	Invited Lecture	Prof. S Paiman., Department of Physics, Faculty of Science, Universiti Putra Malaysia, 43400 UPM Serdang, Selangor, Malaysia	Prof. Chen-Hao Wang., Department of Materials Science and Engineering, National Taiwan University of Science and Technology, 10607, Taipei, Taiwan	Prof. Jing Wang (College of Materials Science and Engineering, Anhui University of Science And Technology, Huainan, Anhui 232001)
10:30-10:50	Oral Lecture	Prof. M. A. Motalib Hossain (Nanotechnology and Catalysis Research Centre (NANOCAT), University of Malaya, 50603 Kuala Lumpur, Malaysia	Prof. Yin Liu., School of Materials Science and Engineering, Anhui University of Science and Technology, Huainan 232001, Anhui, China	Prof. Jing Wang., College of Materials Science and Engineering, Anhui University of Science And Technology, Huainan, Anhui 232001
10:50-11:10	Oral Lecture	Prof. Kunhong Hu., School of Energy Materials and Chemical Engineering, Hefei University, Hefei, 230601, China	Prof. Phacharaphon Tunthawiroon., Department of Industrial Engineering, Faculty of Engineering, King Mongkut's Institute of Technology Ladkrabang, Bangkok 10520, Thailand	Prof. Jing Wang., College of Materials Science and Engineering, Anhui University of Science And Technology, Huainan, Anhui 232001
11:10-11:30	Oral Lecture	Prof. Asghar Ali., Department of Advanced Materials Science & Engineering, Hanseo University, Seosan-si, Chungnam, Korea, 356-706	Prof. Hong Chen., Department of Chemical Engineering, School of Energy Materials and Chemical Engineering, Hefei University, Hefei 230601, Anhui, China	Prof. Guojun Cheng., School of Materials Science and Engineering, Anhui University of Science and Technology, Huainan 232001, China
11:30-11:50	Oral Lecture	Prof. Wei Lian., School of Materials Science and Engineering, Anhui University of Science and Technology, Huainan 232001, Anhui, China	Prof. Wu Ying., School of Energy Materials and Chemical Engineering, Hefei University, Hefei, 230601, China	Prof. Gao Meiling., Anhui University of Science and Technology, School of Materials Science and Engineering, Huainan, 232001, Anhui
11:50-12:50	Lunch Time			
12:50-17:00	Poster session (Zoom A) No 782 272 9549, PW icmma2020			
		Zoom A No 782 272 9549, PW icmma2020	Zoom B No 366 357 0584 , PW icmma2020	Zoom C No 858 283 9675, PW icmma2020
17:00-17:20	Invited Lecture	Prof. Daming Gao., Department of Chemical Engineering, School of Energy, Materials and Chemical Engineering, Hefei University, Hefei 230601, Anhui, China	Prof. Yu-Lin Kuo., Department of Mechanical Engineering, National Taiwan University of Science and Technology, Taipei 10607, Taiwan	Prof. Yuwaraj K. Kshetri, [1]Research Center for Eco-Multifunctional Nano Materials, Sun Moon University, Chungnam 31460, Republic of Korea, Electronic structure, thermodynamic stability and high-temperature sensing properties of Er-α-SiAlON ceramics
17:20-17:40	Invited Lecture	Prof. Chew Tin Lee., School of Chemical and Energy Engineering, Faculty of Engineering. Universiti Teknologi Malaysia 81300 Johor Bahru. Malaysia	Prof. Chin-Yang Yu., Department of Materials Science and Engineering, National Taiwan University of Science and Technology, 43, Section 4, Keelung Road, Taipei 10607, Taiwan	Prof. Na Yin, Anhui Provincial Engineering Laboratory of Silicon-based Materials, School of Material and Chemical Engineering, Bengbu University, Bengbu, 233030, PR China, Novel modifiedChitosan for remarkably high removal of heavy metal Cu (II)
17:40-18:00	Oral Lecture	Prof. Lai Shengfa., Anhui University of Science and Technology , Material Science and Engineering School, 232001	Prof. Chang-Peng Lv, Anhui Provincial Engineering Laboratory of Silicon-based Materials, Engineering Technology Research Center of Silicon-based Materials Anhui,	Prof. Chao Feng (Anhui Provincial Engineering Laboratory of Silicon-based Materials, School of Material and Chemical Engineering, Bengbu University, Bengbu, 233030, PR

			School of Material and Chemical Engineering, Bengbu University	**China)**
18:00-18:20	**Oral Lecture**	**Prof. Shen Tian., [a]School of Materials Science and Engineering, Anhui University of Science and Technology, Huainan 232001, China**	**Prof. Xiaochen Huang (Anhui Provincial Engineering Laboratory of Silicon-based Materials, School of Material and Chemical Engineering, Bengbu University, Bengbu, 233030, PR China)**	**Prof. Jinlong Ge (Department of Materials Science and Chemical Engineering, Anhui province Engineering Laboratory of Silicon-based Materials Bengbu University, Bengbu 233000, P.R. China)**
18:20-18:40	**Oral Lecture**	**Prof. Ziyue Xuan., [a]School of Materials Science and Engineering, Anhui University of Science and Technology, Huainan 232001, China**	**Prof. Yang Benhong., Department of Chemistry and Materials Engineering, Hefei University, Hefei, 230601, China**	
18:40-18:50	**Zoom A : No 782 272 9549, PW icmma2020 Closing Remark (Prof. Saksit Chantai, Prof. Prawit Nuengmatcha)**			

Presentation Guide

Plenary Lectures

Invited Lectures

Oral Lectures

Posters


New

신소재

- ✓ 유해가스제거용 다공성 무기 성형체 제조기술 (Co2제거기술)
- ✓ 미세먼지 및 중금속 제거 알코올 연료 변화기술
- ✓ 복합흡착제 제조기술
- ✓ 방사성 요오드 폐수정화 기술

환경사업

- ✓ 다중시설용 노필터실외공기청정기 (미세먼지, 오존)
- ✓ 대기오염물질 저감 제조시설
- ✓ 실내 필터형 대형 공기청정기
- ✓ 복합흡착제 제조기술 폐수정화 기술

연료사업

- ✓ 활성탄 생산
- ✓ 친환경 고체연료생산
- ✓ 체온상승 건강힐링 제품 생산

카본텍 다중용 공기청정기

- ✓ 직경 100m 미세먼지 85% 저감
- ✓ 오존(O_3) 저감
- ✓ VOC 저감
- ✓ 백연 제거 기술
- ✓ 염(질산염, 황산염) 제거 기술
- ✓ 유체역학에 기초한 '웨이브(wave)형 충돌판'(엘리미네이터) 설계 기술

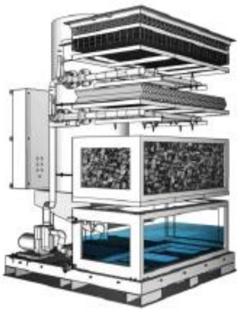

보유기술
산업용 미세먼지 저감시스템

비교우위 및 적용사례

적용사례

(주)카본텍 | 대표자 : 차제우

주소 : 충청북도 음성군 대소면 삼양로 838-11 | Tel : 043-881-2146 | Fax : 043-881-2148

사업자 번호 : 303-81-23842 | E-mail : carbon@carbontec.kr

Plenary Lecture

Synthesis of C_3N_4-based photocatalysts for organic pollutants degradation and U(VI)/Cr(VI) sorption-reduction

Xiangke Wang*

College of Environmental Science and Engineering, North China Electric Power University, Beijing 102206 China

Abstract

The degradation of organic pollutants by C_3N_4-based photocatalysts under visible light irradiation and sorption-reduction of U(VI)/Cr(VI) to U(IV)/Cr(III) by C_3N_4-based photocatalysts under different experimental conditions were studied from batch experiments, XPS and XAFS techniques and DFT calculations. The results showed that C_3N_4 could reduce U(VI) to U(IV) and reduce Cr(VI) to Cr(III), which is easy for the solidification of metal ions on solid particles. The organic pollutants were photocatalytic degraded effectively into water, CO_2 and other smaller molecules. This work is important for the elimination and solidification of pollutants in environmental pollution management

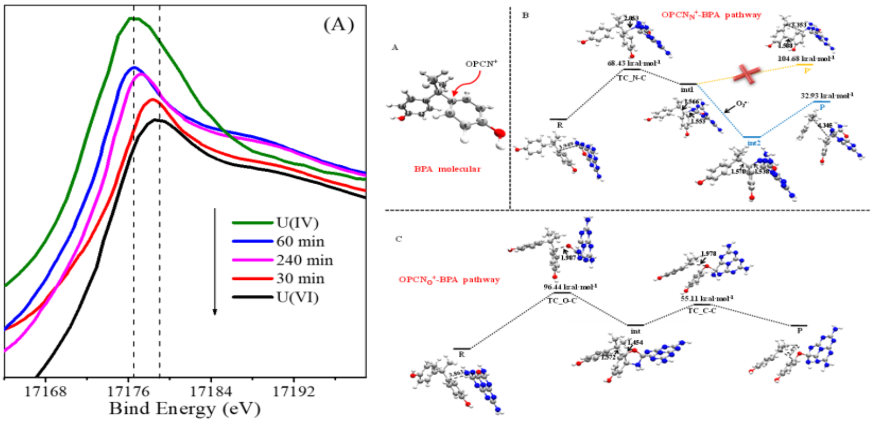

Fig. 1 XANES of U(VI) by C_3N_4 and DFT calculated structures of reactants, intermediates and transition state for the degradation of BPA attacked by OPCN catalysts with (B) N atoms or (C) doped O atoms as reactive sites

Keywords: C_3N_4; organic pollutants; reduction; DFT calculation; XAFS characterization

Secondary recourse to clean energy materials via environmental management

Rajesh Kumar Jyothi*

Korea Institute of Geoscience and Mineral Resources (KIGAM), Daejeon 34132, Korea

E-mail: *rkumarphd@kigam.re.kr*

Abstract

Rare earths (REs) playing key role in new modern lives; REs was having various uses in the areas of electrical, electronic fields as well as clean energy applications. Hydrometallurgy, the aqueous processing of metal ions tool is the cheapest and convenient for REs recovery from primary resources (ores and minerals) and secondary resources (industrial wastes and scraps). Countries like South Korea having many high-tech industries in the fields of electrical and electronic items manufacturing; as well as supply to global needs. At the same time this country has two major problems one is the landfilling problem (generated manufacturing waste and after usage scraps) and lack of natural resources. And the another major concern is the population densities, as per the world bank of economic co-operation and development (OECD) countries as on year 2018 top ten nations are as follows: South Korea-529, The Netherlands-511, Israel-410, Belgium-377, Japan-347, United Kingdom-275, Luxemburg-250, Germany-237, Italy-205 and Switzerland-215. REs having wide range applications in various fields. And REs demand worldwide in various fields are estimated magnets 26%, metal alloys 19%, polishing 16.5%, catalysts 15%, glass/phosphors 6% and ceramics/others 5.5%. REs reserves and production global wide China occupies the major role the other nations such as India, Australia, Malaysia, Brazil, USA, and Russia. Four REs recognized by the DoE, USA as critical rare earth elements such as neodymium, praseodymium, dysprosium, and terbium based on their reserves, supply and demand. Du and Graedel estimated the REs global in-use stocks for the Nd-Fe-B permanent magnets. Out of these four REs neodymium estimated high amount of global in-use stocks followed by Pr/Dy and Tb.

In recycling topic, is the most favorable option always is prevention of as much as waste followed by minimization. In second option reuse the minimized materials then go for recycling and energy recovery processing's. The least favored option is disposal in a proper place. Once generated the waste it will gives another challenge is landfilling problem. To face these two major issues, one is less natural resources another one is landfilling problem the resources recycling tool can reach national demand of REs by using environmentally friendly routes (Fig. 1). Various stages involved in REs products life cycles from primary/secondary

resources to manufacturing the REs products. The recycling tendency showed the effect on coast of the particular metal.

Fig. 1 Stages of rare earths product life cycles from primary and secondary resources

PL-3

Azo dyes – from biomass to sustainable development

Estelle Leonard*

T.I.M.R. EA 4297 ESCOM/UTC, 1 allée du réseau Jean-Marie Buckmaster, F-60200 COMPIEGNE

E-mail: e.leonard@escom.fr

Abstract

Photochromic molecules such as azobenzenes can involve a huge amount of applications, such as forensics, food coloring or textile dyes. But chemists are really encouraged to use one or more of the twelve principles in green chemistry for their syntheses or their processes. Here we will see how they can integrate a sustainable concept, especially for photochromic micellar catalysis.[1] Indeed, their capability of isomerization can lead to a better on-off catalysis, with a better products recovery and thus a better recyclability of the media.[2,3] We will see also how these photochromes can have a biocide activity,[4] and how to make their synthesis greener.

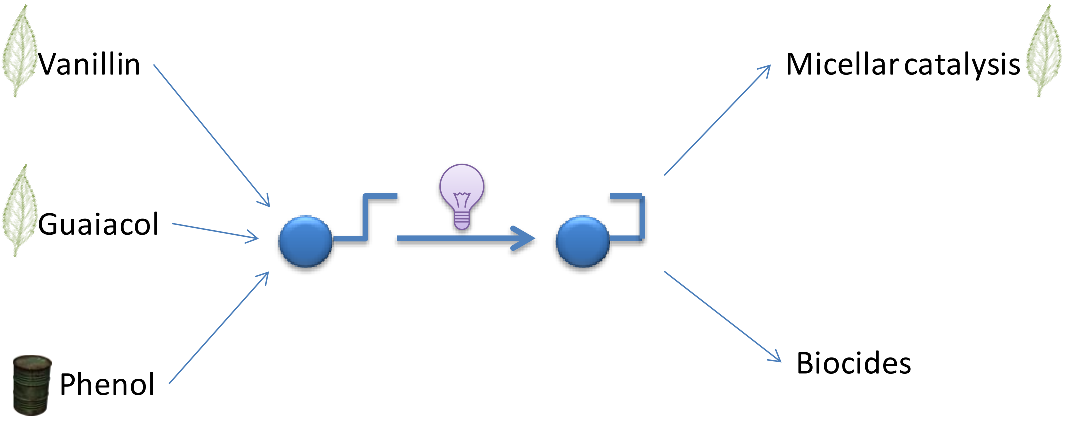

Keywords: Azobenzenes, biomass, micellar catalysis, biocides

References

(1) Léonard, E.; Mangin, F.; Villette, C.; Billamboz, M.; Len, C. Azobenzenes and Catalysis. *Catal. Sci. Technol.* **2016**, *6* (2), 379–398. https://doi.org/10.1039/C4CY01597E.

(2) Billamboz, M.; Mangin, F.; Drillaud, N.; Chevrin-Villette, C.; Banaszak-Léonard, E.; Len, C. Micellar Catalysis Using a Photochromic Surfactant: Application to the Pd-Catalyzed Tsuji–Trost Reaction in Water. *J. Org. Chem.* **2014**, *79*, 493–500. https://doi.org/10.1021/jo401737t.

(3) Drillaud, N.; Banaszak-Léonard, E.; Pezron, I.; Len, C. Synthesis and Evaluation of a Photochromic Surfactant for Organic Reactions in Aqueous Media. *J. Org. Chem.* **2012**, *77* (21), 9553–9561. https://doi.org/10.1021/jo301466w.

PL-4

Plastics: Material for the future?

Jiří Jaromír Klemeš, Yee Van Fan

Sustainable Process Integration Laboratory – SPIL, NETME Centre, Faculty of Mechanical
Engineering, Brno, University of Technology - VUT Brno, Technická 2896/2, 616 00 Brno, Czech
Republic.
E-mail jiri.klemes@vutbr.cz

Abstract:

The plastic, more correctly to be addressed as polymers, are one of the most important materials of the present time and obviously of the future. The plastics have been branded as an evil, which must be replaced, in some cases at any cost. However, a coldblooded analysis and assessment are needed comparing all pros and cost based on environmental footprints quantification with full life cycle assessment. This should include assessment of possible health risks, consumed energy, released emissions and effluents, as well as consumption of raw materials, water and dealing with the wastewater. The assessment of recyclability, reprocessing and environmental burden is needed.

The presentation tends to contribute to the discussion of what recommendations should be developed to the industry and business to minimise the environmental impacts. A Plastic Footprint has been assessed, and a novel Plastic Waste Footprint introduced.

Acknowledgements

The authors gratefully acknowledge financial support from the EU project Sustainable Process Integration Laboratory – SPIL, funded as project No. CZ.02.1.01/0.0/0.0/15_ 003/0000456, by Czech Republic Operational Programme Research and Development, Education, Priority 1: Strengthening capacity for quality research.

Keywords: Plastic, assessment of management, waste treatment, pollution, emissions and plastic footprints

References:

Klemeš, J.J., Fan, Y.V., Jiang, P., 2020. Plastics: friends or foes? The circularity and plastic waste footprint. Energy Sources, Part A: Recovery, Utilisation, and Environmental Effects, 1-17. doi: 10.1080/15567036.2020.1801906.

Klemeš, J.J., Fan, X.Y., Tan R.R., Jiang P., 2020, Minimising the present and future plastic waste, energy and environmental footprints related to COVID-19, Renewable and Sustainable Energy Reviews, 127 109883.

PL-5

Application of Functionalized 1-D WO_3 prepared by Flame Vapor Deposition on Photoelectrochemical Oxygen Evolution

Kyo-Seon Kim*

Department of Chemical Engineering, Kangwon National University, Chuncheon, Kangwon-Do, South Korea

E-mail: kkyoseon@kangwon.ac.kr

Abstract

In this study, we could prepare 1-D WO_3 nanowires (NW) on fluorine-doped tin oxide (FTO) glass as photoanode framework by a rapid, facile and low-cost flame vapor deposition method. The vertically aligned NW-structured WOx was fabricated in a combustion system incorporated with wire feeders. By adding the wire feeder and by applying 2 flame burners, we could prepare the hetero NW-structures of multicomponent on FTO by the combustion system, which showed a higher photoelectrochemical (PEC) efficiency. $BiVO_4$ layer was spin coated on the WO_3 nanowires to prepare 1-D WO_3/ $BiVO_4$ heterojunction photoanodes, which also showed the higher efficiency to harvest solar energy. Co-Pi was also deposited on the prepared 1-D WO_3/$BiVO_4$ photoanodes by photo-assisted electrodeposition process. Detailed PEC study has revealed that applying Co-Pi to the 1-D WO_3/$BiVO_4$ for photoelectrochemical oxygen evolution is a vital strategy to improve the overall water oxidation efficiency of composite photoanode. The hetero NW-structures of multicomponent on FTO was fabricated by combustion process incorporated with double burners and extra horizontal wire feeder and was modified to prepare the high functional photocatalyst system, which was applied to enhance the water splitting reaction efficiency.

PL-6

Recent chemical functions and applications of using carbon-based

nanomaterials to countermeasure for COVID-19 outbreak: A Review

Won-Chun Oh[1] and Saksit Chanthai[2]*

[1]Department of Advanced Materials Science & Engineering, Hanseo University, 46, Hanseo1ro,
Haemi-myun, Seosan, Chungnam, Korea

[2]Materials Chemistry Research Center, Department of Chemistry and Center of Excellence for
Innovation in Chemistry, Faculty of Science, Khon Kaen University, Khon Kaen 40002, Thailand
**e-mail: sakcha2@kku.ac.th*

Abstract

Carbon-based nanomaterials have much emerging roles for many industrial applications and can be used with potential biocompatibility and antiviral properties. In this review, such graphene quantum dots, carbon dots or other carbon-based matters have been subject to be antiviral ones. Different carbon-based materials allow several strategies to be applied in peculiar antiviral properties. Some nanomaterials have been used as a platform for functional molecules attributing for their inhibitory viral activity. Possibility of using the nanomaterials is now on-going done. At present, human beings often find themselves helpless arising from the emergence of the COVID-19 outbreak. Lack of tools to fight virulent infections and/or a slow down the outbreak of the world pandemic can have bad economic impacts and social implications. Face masks against COVID-19 have been numerous applied with various potential utilities in association with instant hand hygiene. Besides, physical distancing, face masks, and eye protection are the main systematic prevention policies throughout every community.

Keywords: Carbon based nanomaterials, Graphene, Face mask, COVID-19, Virus,

Selected References:

1) Derek K Chu, Elie A Akl, Stephanie Duda, Karla Solo, Sally Yaacoub, Holger J Schunemann, www.thalancet.com Vol 395 June 27, 2020, 1973-1987.
2) Jeramy Howard, Austin Huang, Zhiyuan Li, Zeynep Tufekci, Zdimal Vladimir, Helene-Mari van der Westhuizen et al., www.pnas.org/cgi/doi/10.1073/pnas. PNAS, April 10, 2020, 1-8.

Invited Lectures

Self-Assembly of Hydrous TiO_2 Colloidal Spheres for Photo/electrochemical Applications

Jia Hong Pan

Colleague of Environmental Science and Engineering, North China Electronic Power University, Beijing 102206, China

E-mail: pan@ncepu.edu.cn

Abstract

Owning to their monodisperse nature, structural diversity at nano- and microscale, excellent structural stability, large surface area, and close-packing capability, mesoporous anatase TiO_2 spheres (MAS) have attracted increasing interest for photoelectrochemical applications. Traditional template and template-free (e.g. hydro/solvothermal) methods have been developed for the preparation of MAS with solid or hollow inner structure; however, mass production and textural property control have not well realized. Thanks to the colloidal science, monodisperse, amorphous hydrous TiO_2 spheres (HTS) derived from the forced hydrolysis of titanium alkoxides has been recently employed as a versatile self-template for the controllable synthesis of mesoporous TiO_2 spheres consisting of well-organized anatase nanocrystallites and possessing hierarchical structures and large surface area.

In this talk, synthetic technique, and the underlying formation mechanism of HTS will be first introduced. The key parameters, such as water dosage and the type of the structure-directing agents, are discussed to achieve size-controllable synthesis. Phase and structural transformation from HTS to solid/hollow MTS and perovskite titanates by posttreatments such as hydro/solvothermal process or UV irradiation are then addressed. Photoelectrochemical applications of these elaborated mesoporous TiO_2-based spheres in the fields of environmental photocatalysis, mesoscopic solar cells will be discussed.

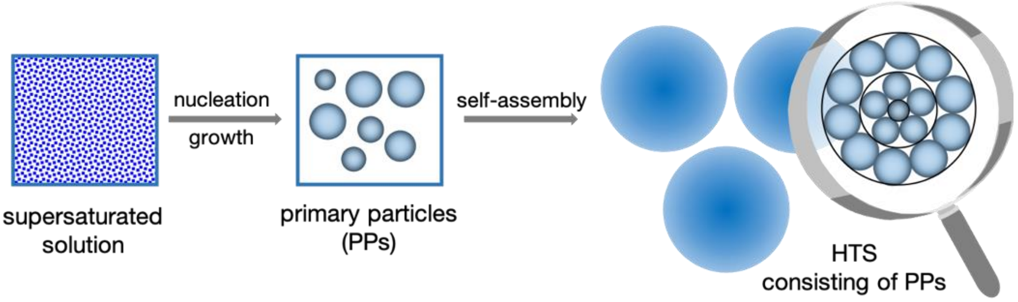

Figure 1. Self-assembly formation and structural properties of HTS derived from sol-gel process.

References

[1] *Prog. Mater. Sci.*, 2020, 109, 100620.
[2] *ACS Appl. Energy Mater.*, 2020, 3, 4186–4192.
[3] *Langmuir*, 2020, 36 (26), 7447–745; 2015, *31*, 4566−4572.
[4] *Catal. Today* **2014**. *230*, 197-204.

Interfacial engineering of perovskite solar cell with efficient electron transport layers

Molang Cai

State Key Laboratory of Alternate Electrical Power System with Renewable Energy Sources, Beijing Key Laboratory of Novel Thin-Film Solar Cells, North China Electric Power University, Beijing 102206, P. R. China
E-mail: molangcai@ncepu.edu.cn

Abstract

Perovskite solar cell (PSC) has attracted much attention due to the fast development of device performance. The dynamic processes such as electron transfer and collection at interfaces, energy alignment and electric potential distribution are critical to efficiency and long-term stability of perovskite solar cell. The control of film growth kinetics as well as interfacial engineering for active layers were considered as effective methods to further promote the efficiency and stability of device.

We have investigated the heterojunction properties of the mesoporous and planar TiO_2 solar devices based on different self-doping perovskite film to elaborate the interfacial transfer mechanism. It is found that the interface is critical for the compact TiO_2 based device performances while mesoporous TiO_2 based device depends on the perovskite film properties [1]. Then the C60/*u*-TiO_2 bilayer is prepared to improve the stability and electron transfer at interfaces. Both the open-circuit voltage and fill factor were largely improved to obtain a PCE of 19.38% with a rigid device. The C60/*u*-TiO_x bilayer-based PSC shows outstanding stability, retaining 83% and 90% of its initial performance after 312 h UV irradiation and 1000 h exposure to ambient air, respectively [2-3]. The trap-assisted carrier recombination of SnO_2 based PSC is suppressed by using passivator via the formation of coordination with under-coordinated Sn and Pb^{2+} ions. The champion device demonstrated a promising efficiency of 21.28% with negligible hysteresis and much improved environmental stability, i.e. retaining 98% of the initial efficiency under ambient atmosphere over 1000 h[4]. we introduce a non-ionic additive of polyethyleneimine (PEI) with multiple amino-groups to form hydrogen bond with I^-/Br^- ions and coordinate with Pb^{2+}/Cs^+ ions simultaneously. The strong interplay between PEI and $CsPbI_2Br$ achieves a well-controlled grain size, reduced defects, and reinforced phase structure of $CsPbI_2Br$ film, which boosts the efficiency of perovskite solar cells to 15.48%. An impressed PCE of 13.37% is achieved by the device based on $CsPbI_2Br$-PEI film processed under ambient condition [5].

Reference

[4] Molang Cai, ‡ Nobuyuki Ishida, ‡ Xing Li, Xudong Yang,* Takeshi Noda, Yongzhen Wu, Fengxian Xie, Hiroyoshi Naito, Daisuke Fujita, Liyuan Han,* Joule, 2018,2, 21,296–306

[2] Pengju Shi, Yong Ding,* Yingke Ren, Xiaoqiang Shi, Zulqarnain Arain, Cheng Liu, Xuepeng Liu, Molang Cai*, Guozhong Cao, Mohammad Khaja Nazeeruddin,* and Songyuan Dai*, Adv. Sci. 2019, 6, 1901591

[3] Xiaoqiang Shi, Yahan Wu, Jieqiong Chen, Molang Cai*, Yi Yang, Xuepeng Liu, Ye Tao, Mina Guli, Yong Ding, Songyuan Dai*, J. Mater. Chem. A, 2020, 8, 7205-7213

[4] Cheng Liu,‡ Molang Cai,‡ Yi Yang, Zulqarnain Arain, Yong Ding,* Songyuan Dai*, Guozhong Cao, J. Mater. Chem. A, 2019, 7, 11086–11094

[5] Huirong Peng, Molang Cai*, Jiyu Zhou, Yi Yang, Xihong Ding, Ye Tao, Gao Wu, Xuepeng Liu, Jia Hong Pan, Songyuan Dai*, Sol. RRL. doi:10.1002/solr.202000216

Synthesis of Bioactive Heterocycles Using Nanocatalytic Framework

K. L. Ameta

Department of Chemistry, School of Liberal Arts and Sciences,

Mody University of Science and Technology, Lakshmangarh-332311, Rajasthan, India

E-mail: klameta77@hotmail.com

Abstract

Over the past few decades, heterocyclic compounds have been considered as a significant synthetic target compounds due to their intense applications as therapeutic agents. Heterocyclic compounds containing nitrogen, sulphur and oxygen with five or six-membered rings have occupied diverse pharmacological activities.

Now a day's the heterogeneous catalysis, especially nanocatalysis is widely used by organic chemists in research to give excellent activity, selectivity, consumption of low energy, and longer lifetime. This is achieved by controlling the size, shape, electronic structure, and spatial distribution, and surface composition, thermal and chemical stability of the individual nanocomponents. Nanocatalysis also opens a new corridor to synthesize value added heterocycles not only in low cost but also increases high product selectivity that directly influence in industrial research.

Electrospinning Preparation of PAN/TiO$_2$/PANI Hybrid Fiber Membrane with Highly Selective Adsorption and Photocatalytic Regeneration Properties

Bao Xu[a], Xianbiao Wang[a]*, Yuanyuan Huang[a], Jin Liu[a], Di Wang[a], Shaojie Feng[a], Xianhuai Huang[b], Huanting Wang[c]
[a]*Anhui Province International Research Center on Advanced Building Materials, School of Materials Science and Chemical Engineering, Anhui Jianzhu University, Hefei 230601, P. R. China*
[b]*Key Laboratory of Water Pollution Control and Wastewater Reuse of Anhui Province, Anhui Jianzhu University, Hefei 230601, P. R. China*
[c]*Department of Chemical Engineering, Monash University, VIC 3800, Australia*
Corresponding author, E-mail: xbwang@ahjzu.edu.cn (X. Wang)

Abstract

Fiber membranes for pollutants removal have attracted more and more attentions owing to their high adsorption performance and easy recovery properties. However, some adsorption membranes are short of reusability performance due to lack of environment-friendly regeneration approach and low regeneration efficiency especially in terms of chemical adsorption. Herein a polyacrylonitrile/ titanium dioxide/ polyaniline (PAN/TiO$_2$/PANI) hybrid fiber membrane was successfully prepared by electrospinning of PAN solution with TiO$_2$ particles and subsequent in-situ oxidative polymerization of aniline (ANI) on PAN/TiO$_2$ fiber membranes. The obtained fibers have ~200 nm in width with PANI and TiO$_2$ particles dispersed uniformly. Importantly, such hybrid membrane could remove Congo red effectively and completely in water. Detailed investigation reveals that the adsorption behavior fits Langmuir model well which indicates chemical related adsorption. In addition, the membranes could be recycled by photocatalytic degradation under visible light irradiation. After 4 times photocatalytic regenerations, the regeneration efficiency and removal rate could still remain ~ 60% and upon 50%, respectively, higher than that of water-wash regeneration (only 2%). Such extraordinary performance could also extend to heavy metals [such as Cr (VI)]. After equilibrium adsorption, the adsorbed Cr(VI) on membrane could be reduced and desorbed through visible light photocatalytic procedure, leading to an effective regeneration. This work not only demonstrates the possibility and validity of the PAN/TiO$_2$/PANI hybrid fiber membrane as promising environment-friendly adsorbent for pollutants removal, but also gives insight into understanding the adsorptive behavior of the hybrid membrane.

Key words: Electrospinning; Membrane; PANI; Adsorption; Regeneration

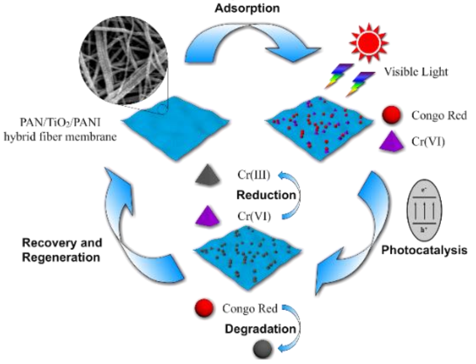

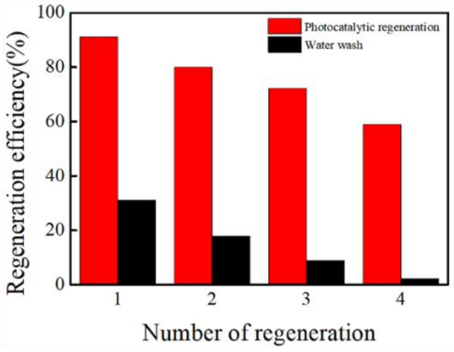

Improvement of Supercapacitor Performance of MnO_2/porous-carbon Nanocomposites by Tuning Pore Size of Porous Carbon Substrates

Shinichiroh Iwamura1*, Ryotaro Umedu2, Shin R. Mukai1
1 Faculty of Engineering. Hokkaido University, Sapporo, Japan
2 Graduate School of Chemical Sciences and Engineering, Sapporo, Japan
*e-mail: iwamura@eng.hokudai.ac.jp

Introduction

MnO_2 can be potentially utilized as an electrode material for redox capacitors. The deposition of MnO_2 particles with poor electrical conductivity onto porous carbons supplies them with additional conductive paths; as a result, the capacitance of the electrical double layer formed on the porous carbon surface can be utilized together with the redox capacitance of MnO_2. However, the obtained composites are not generally suitable for industrial production because they require the use of expensive porous carbons and/or inefficient fabrication methods. Thus, to develop an effective preparation procedure of the composite, a suitable structure of porous carbons must be determined. In this study, MnO_2/C composites have been prepared from activated carbon gels (CGs) with various pore sizes, and their electrical properties were investigated via cyclic voltammetry.

Experimental

Resorcinol (R)-formaldehyde (F) gels were synthesized and carbonized. To control their pore size, the R/C (C = sodium carbonate as a polymerization catalyst) ratio in the solution used to synthesize them was adjusted in the range between 200 and 1000. The carbonized samples were activated at 1000°C under a CO_2 flow. Hereafter, the resulting samples will be referred to by the R/C ratio, such as “CG1000”. CG samples and activated carbon (AC) were stirred in 1 M $KMnO_4$ solution to introduce Mn species and deposit MnO_2 into their pores, and finally, MnO_2/C nanocomposites were obtained.

Results and discussion

The porous structure of the samples prior to and after MnO_2 deposition was analyzed by N_2 adsorption experiments. The N_2 adsorption isotherms revealed that MnO_2 were mainly deposited in mesopores and macropores of mesoporous CG200 and macroporous CG1000, respectively (Fig. 1). In contrast, MnO_2 was deposited on the outer surface of the microporous AC.

Fig. 2 shows capacitances of the MnO_2/porous-carbon nanocomposites measured at various scan rates. CG200 and AC formed a composite with relatively low capacitance (~100 F/g-composite) and poor rate performance despite the moderate redox capacitance obtained for MnO_2 (200-300 F/g-MnO_2). On the other hand, CG1000 increased the MnO_2 redox capacitance (399 F/g-MnO_2) as well as the capacitance and rate performance of the entire material (203 F/g-composite). Both capacitance and rate performance can be improved by increasing the pore size of the carbon substrate, suggesting that the existence of macropores increases the diffusibility of the electrolyte. The obtained results can be used in the industrial manufacturing of MnO_2/C composites for supercapacitor electrodes from the commercially available porous carbons.

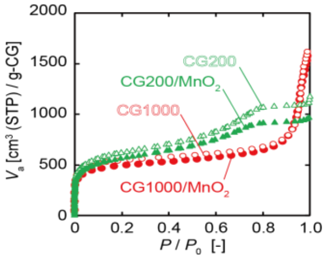

Fig. 1 N_2 adsorption isotherms of porous carbons prior to and after MnO_2 deposition.

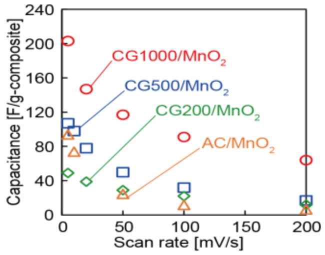

Fig. 2 Capacitances of MnO_2/porous-carbon nanocomposites measured at various scan rates.

IL-6

Silsesquioxanes-Based Functional Porous Polymers

Hongzhi Liu
School of Chemistry and Chemical Engineering, Shandong University, Jinan, China
Email:*liuhongzhi@sdu.edu.cn*

Abstract

Recently, more attention has been devoted to hybrid porous polymers considering their exhibiting some unique properties by combination with the advantages of inorganic and organic components. Cage silsesquioxane has proven to be an ideal building block to prepare hybrid nanoporous polymers with enhanced thermal and mechanical properties in view of their rigidity and multifunctionality. [1] Very recently, octavinylsilsesquioxane (OVS) has been successfully used to prepare silsesquioxanes-based porous materials *via* Friedel-crafts reaction and Heck reaction, cationic polymerization by us.[2-5] Moreover, the bulky cage could prevent the aggregation of chromophores and enhance luminescence in silsesquioxanes-based porous materials.[6] These hybrid porous polymers exhibited high surface areas, thermal stabilities and excellent luminescence, which make them to be multifunctional and potentially apply in gas storage, water treatment, energy storage and sensors *etc.*

References:

1. Watcharop, C.; Masaru, K.; Takahiko, M.; Ayae, S. N.; Atsushi, S.; Tatsuya, O. Porous Siloxane-Organic Hybrid with Ultrahigh Surface Area Through Simultaneous Polymerization-Destruction of Functionalized Cubic Siloxane Cages. *J. Am. Chem. Soc.* **2011,** *133*, 13832-13835.
2. Yang, X.; Liu, H. Ferrocene-Functionalized Silsesquioxane-Based Porous Polymer for Efficient Removal of Dyes and Heavy Metal Ions. *Chem. Eur. J.* **2018,** *24*, 13504-13511.
3. Ge, M.; Liu, H. A Silsesquioxane-Based Thiophene-Bridged Hybrid Nanoporous Network as A Highly Efficient Adsorbent for Wastewater Treatment. *J. Mater. Chem. A.* **2016,** *4*, 16714-16722.
4. Yang X.; Liu H. Diphenylphosphine-Substituted Ferrocene/Silsesquioxane-Based Hybrid Porous Polymers as Highly Efficient Adsorbents for Water Treatment. *ACS Appl. Mater. Interfaces* **2019**, 11, 26474−26482.
5. Du Y.; Ge M.; Liu H.; Porous Polymers Derived from Octavinylsilsesquioxane by Cationic Polymerization. *Macromol. Chem. Phys.* **2019**, *220*, 1800536-1800543.
6. Yan Y.; Laine M.; Liu H. In Situ Methylation Transforms Aggregation-Caused Quenching into Aggregation-Induced Emission: Functional Porous Silsesquioxane-Based Composites with En Near-Infrared Emission. *ChemPlusChem* **2019**, *84*, 1630–1637.

IL-7

Synthesis N-doped TiO_2-SiO_2 coated honeycomb ceramic monolith to

enhance photocatalytic degradation of phenol under UV-LED irradiation

Huynh Huu Tai[1,2], Ngoc-Quoc-Duy Vo[1,2], Ngo Manh Thang[1,2], Ho Thi Ngoc Suong[1,2] and Minh-Vien Le[1,2]

[1]Faculty of Chemical Engineering, Ho Chi Minh city University of Technology, Ho Chi Minh City, 700000, Vietnam

[2]Vietnam National University Ho Chi Minh City, Ho Chi Minh City,700000, Vietnam

** E-mail: lmvien@hcmut.edu.vn*

Abstract

In the recent years, TiO_2-based photocatalysts was developed to reduce a high band gap energy (3.2 eV) to increase absorption in visible region to achive degradation efficiency of organic substances from water. Nitrogen doping has been investigated to reduce band gap energy and prevent electron recombination expand adsorption in visible region. Despite the high photocatalytic activity and proven ability of suspended N-doped TiO_2 photocatalysts in degrading organic compounds, the challenge of their application is the need to separate and recover the nanoparticles for reuse after treatment. Immobilization of the N-doped TiO_2 photocatalyst on a substrate is a possible remedy. The cordierite honeycomb monoliths (CHMs) have advantages that include efficient mass transport, low pressure drops, high thermal stability, good chemical durability, highly refractory properties, good mechanical strength, and ease of scaling. Accordingly, a CHM become an ideal substrate for surface-coating by a catalyst. The coating photocatalyst on a carrier has also shown improvement in stability and reusability. This study has focused on the synthesis and evaluation the photocatalytic properties of nitrogen modification of TiO_2-SiO_2 coated on CHM through the degradation of phenol in aqueous solution with initial concentration to be 10 ppm under 100W 395 nm UV-LED irradiation. Different N-doped TiO_2-SiO_2 composite samples was investigated, in which molar ratio of N to TiO_2 was 3%, 5% and 7% and molar ratio of TiO_2:SiO_2 to be 95:5 (TS5). The 3N-TS5 photocatalyst suspension, which was prepared from 3 mol % N-doped TiO_2 show the highest phenol efficiency degradation 95% in 4h, high reaction rate constant of 0.0102 min^{-1} due to the narrow band gap energy of 3.05 eV. The 3NTS5/CHM monolithic photocatalyst which was synthesized from the dipcoating of 750 °C calcined SiO_2 coated CHM into the 3N-TS5 precursor solution and then calcined at 500 °C for 2h, shown the achievement with 82.2% degradation of phenol for 4h irradiation and rate constant to be 0.0061 min^{-1}. The photocatalytic degradation reactions of all photocatalysts followed a pseudo first-order kinetics and obey Langmuir – Hinshelwood model. Moreover, the 3NTS5/CHM photocatalyst show outstanding stability and reusability, namely that after six cycles reuse, the monolithic photocatalyst still achieved 80.4% degradation efficiency, the reaction rate constant of 0.0056 min^{-1}. The N-doped TiO_2/SiO_2 coated cordierite honeycomb monoliths photocatalyst could be a promising photocatalyst for removal and degradation of organic pollutants.

Keyword: N doped – TiO_2-SiO_2, photocatalytic degradation phenol, cordierite honeycomb monolith substrate, dip-coating.

IL-8

Ab initio Calculations of Light-Emitting Quantum Efficiency for Point

Defects in Semiconductors

Lin Shi [1,2*]

[1]*School of Materials Science and Engineering, Yancheng Institute of Technology, Yancheng 224001, People's Republic of China*

[2]*Suzhou Institute of Nano-Tech and Nano-Bionics, Chinese Academy of Sciences, Suzhou 215123, People's Republic of China*

*Email: linshi.ycit@foxmail.com

Abstract

Point defects play an important role in the photoelectrical properties of semiconductor materials, and they can be luminescence centers. However, the relationships among the observed luminescence wavelengths, intensities, and the microscopic processes are in most cases unknown, or depend heavily on parameter fitting. In order to apply different multiphonon assisted electron transition formalisms, we have calculated the electron-phonon coupling constants by *ab initio* density functional theory for all phonon modes. Compared with different methods, the capture coefficients calculated by the static coupling theory are in good agreement with the experiment results.[1] In this work, the light-emitting quantum efficiencies for point defects using *ab initio* density functional theory are calculated. The study of radiation recombination for electrons and nonradiation recombination for holes is reported here. The results show that the defect C_N transition between "–" and "0" charged levels and the defect C_N+O_N transition between "0" and "+" charged levels both may be responsible for the yellow luminescence (YL) which is observed in experiment. This work shows that it is possible to use *ab initio* calculations to understand the microscopic mechanisms and the competitions among different channels for the light emissions caused by defects.[2]

Keywords: quantum efficiencies, DFT calculations, point defects, radiation recombination, non-radiation recombination

References

[1] Lin Shi, Ke Xu, and Lin-Wang Wang, ***Phys. Rev. B*** **97**, 077302 (2018).

[2] Hai-Shan Zhang, Lin Shi*, Xiao-Bao Yang, Yu-Jun Zhao, Ke Xu, and Lin-Wang Wang*, ***Adv. Optical Mater.*** **5**, 1700404 (2017).

Reusable Adsorbent of Fe/C for Metronidazole Removal

Teguh Ariyanto[1,2 a)], Farhah Ayu Fajrin[1,2 b)], Imam Prasetyo[1, 2, c)]

[1]Department of Chemical Engineering, Universitas Gadjah Mada, Indonesia

[2]Carbon Material Research Group, Department of Chemical Engineering, Universitas Gadjah Mada, Indonesia

Email: a) teguh.ariyanto@ugm.ac.id, b) farhah.ayu.f@mail.ugm.ac.id, c) imampras@ugm.ac.id

Abstract:

The presence of antibiotics in wastewater discharged to waterbody has negative effects to environment such as antibiotic-resistant microbes, the change of fish reproduction, and inhibition of photosynthesis in aquatic organisms. Hence, efforts to control the concentration of antibiotics in wastewater are required. In this work, removal of antibiotics of metronidazole was performed by adsorption using nanoporous carbon in the form of monolith. The porous carbon was prepared by pyrolysis of templated resorcinol formaldehyde polymer at different temperature. The material was characterized systematically by XRD, SEM-EDX and N_2-sorption analyzer. As comparison, commercial carbon of coconut shell-derived carbon was also employed in the study. The characterization showed that porous carbon monolith has high specific surface area up to 600 m^2/g. In the adsorption test, the results indicated that porous carbon monolith were better at adsorbing antibiotics compared to the commercial one. Furthermore, the study showed that with simple oxidation process using peroxide the adsorbent can be regenerated and reused with only small decrease in the adsorption performance.

Keywords: adsorption; metronidazole; porous carbon; wastewater

IL-10

A novel bead synthesis of the Chiron-SDS hydrogel and its kinetics-thermodynamics study of superb adsorption of alizarin red S from aqueous solution

Nunticha Limchoowong[1,2]*, Phitchan Sricharoen[1], Saksit Chanthai[1]**

[1]Materials Chemistry Research Center, Department of Chemistry and Center of Excellence for Innovation in Chemistry, Faculty of Science, Khon Kaen University, Khon Kaen 40002, Thailand

[2]Department of Chemistry, Faculty of Science, Srinakharinwirot University, Sukhumvit 23, Wattana, Bangkok 10110, Thailand

Abstract

In this study, we present the first time a novel strategy for one step synthesis of iron)III(hydroxide doped chitosan)“Chiron”(without using acidic solvent via sodium dodecyl sulfate)SDS(as surfactant gelation, namely, Chiron-SDS hydrogel bead. The Chiron-SDS bead is developed as a potentially attractive adsorbent for an investigation of the noxious anionic dye from aqueous solution. Various experimental parameters were optimized including chitosan and surfactant concentrations in the modification process of the beads, pH, adsorbent dose, contact time, ionic strength, and temperature. Under optimum conditions, the amount of iron)III(in chitosan solution was achieved with a mass ratio of 1:1. The hydrogel bead formation was obtained from 20 µL of the Chiron solution, and their uniform bead diameter was observed about 179 ± 0.13 µm in average, of which containing 86.7% moisture or $6x10^{-5}$ g DW per bead. Alizarin red S)AR(, anionic dye was chosen as pollutant model and was monitored spectrophotometrically at 425 nm.

The bead size after AR adsorption was slightly larger)185 ± 0.10 µm(than that of its original one. Fourier transform infrared)FTIR(analysis indicated that the Fe)OH($_3$ were chelated with chitosan structure in the Chiron-SDS beads. The equilibrium data fit to Langmuir as the best representative model)R^2 0.99(, and their kinetics data are well fitted with the pseudo-second order. It was found that the maximum adsorption capacity)q_m(from Langmuir model for AR by Chiron-SDS bead is 294 mg g^{-1}, which was much higher than those previously reported data. The calculated thermodynamic parameters show that the dye adsorption is spontaneous and endothermic process. The advantage characteristics of ease, low cost, eco-friendly, and superb high adsorption efficiency demonstrate that this output gives a great deal to step forward for a huge scale elimination of toxic dye contaminants from aqueous solution, leading usefulness further for an environmental remediation.

Keywords: Chitosan, Ferric)III(oxide, Sodium dodecyl sulfate, Hydrogel bead, Alizarin red S

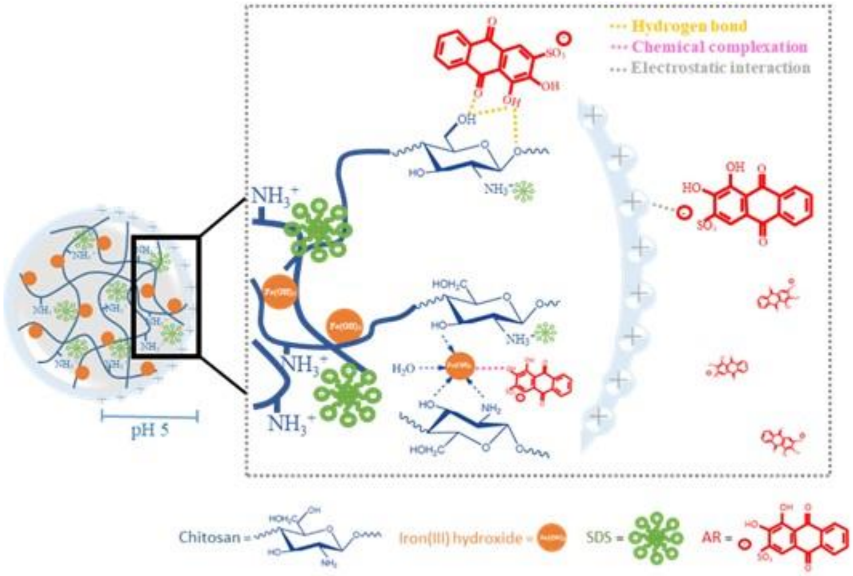

Development of Low-Dielectric Polyimide Films: Effects of Alicyclic Functionality and Siloxane Segments

Haixia Qi, Xiulong Wang, Juan Li, Shuaike Zhu, Feng Liu*
College of Chemistry, Nanchang University
Xuefu Avenue 999, Honggutan New District, Nanchang 330031, PR China
Correspondence to Feng Liu, email: liuf@ncu.edu.cn , Tel: 086-791 83969984

Abstract

To date, the development of transparent and low dielectric constant (low-k) PIs is highly required and has been intensively studied from the viewpoint of their potential application to optoelectronics and high-frequency microelectronics fields. Dielectric properties of the PIs are important when considering their microelectronic applications as insulating materials, as the signal propagation and fidelity and device heating are highly dependent on the dielectric constant and dielectric loss of the insulating material.

A new series of alicyclic-functionalized polyimide monomers have been prepared by structurally transforming natural-(D)-camphor, a renewable forestry compound extracted from cinnamomum camphora, as shown in Figure 1.

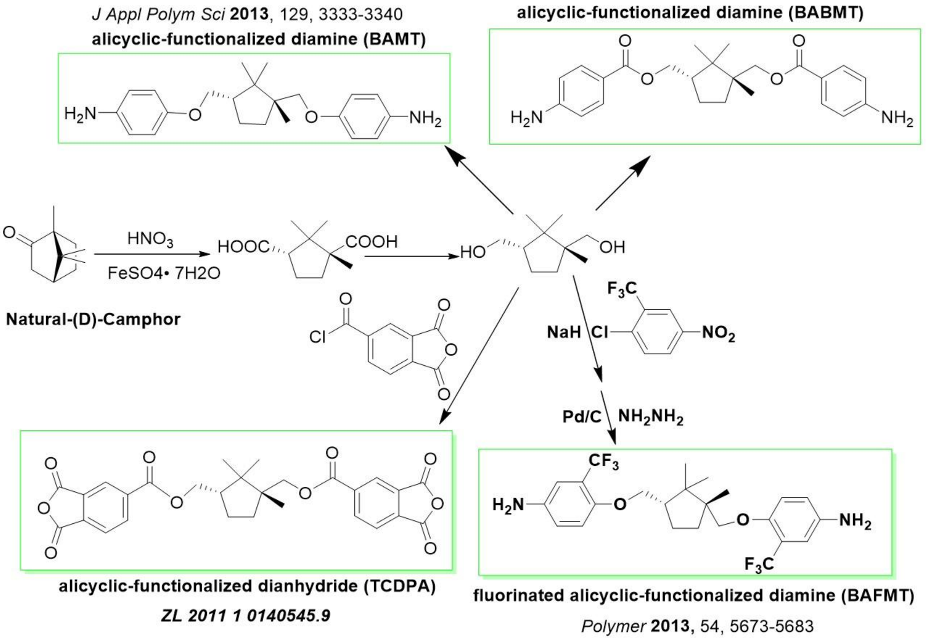
J Appl Polym Sci **2013**, 129, 3333-3340

alicyclic-functionalized diamine (BAMT)

alicyclic-functionalized diamine (BABMT)

Natural-(D)-Camphor

alicyclic-functionalized dianhydride (TCDPA)

ZL 2011 1 0140545.9

fluorinated alicyclic-functionalized diamine (BAFMT)

Polymer **2013**, 54, 5673-5683

Figure 1.

It is revealed that the presence of fluorinated alicyclic-functionalized group endows FAl-PI the with lower dielectric constant and dielectric loss than commercial Kapton HN, as shown in Table 1.

Table 1

Polymer	Dielectric constants (ε')				Dielectric loss (ε")	
	1Hz	100Hz	1KHz	1MHz	1Hz	1KHz
FAl-PI	3.01	2.92	2.88	2.79	0.0058	0.0041
Ref	3.24	3.22	3.19	3.13	0.006	0.0044

Novel soluble PI films containing adjustable siloxane segments content have been developed and exhibit high optical transparence and peculiar low dielectric constant characteristics, as shown in Figure 2. These materials present competitiveness for practical application in microelectronics and optoelectronics.

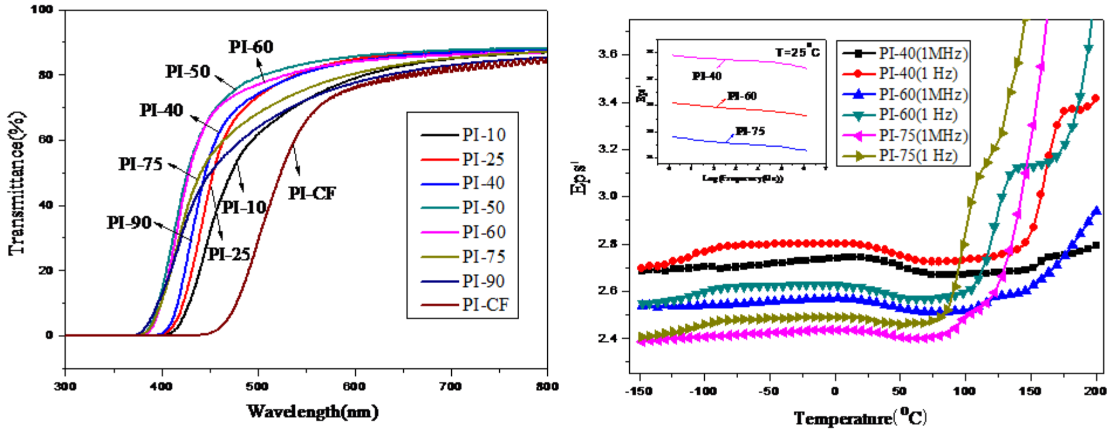

Figure 2

Key words: alicyclic-functionalized polyimide; natural-(D)-camphor; siloxane segments; microelectronics; optoelectronics.

Porous Clay Heterostructure/Metal Oxide Nanocomposite as Photocatalyst Materials

Is Fatimah[a], Ganjar Fadillah[a], Amri Yahya[a], Putwi Widya Citradewi[a], Ruey-an Doong[b]

[a]Department of Chemistry, Faculty of Mathematics and Natural Sciences, Universitas Islam Indonesia, Kampus Terpadu UII, Jl. Kaliurang Km 14, Sleman, Yogyakarta, Indonesia
[b]Institute of Analytical and Environmental Sciences, National Tsing Hua University, 101, Sec 2, Kuang Fu Road, Hsinchu 30013, Taiwan

Abstract

Metal oxide nanocomposites are the class of nanocomposite giving elaborated properties among the metal nanoparticles related with the applications of environmental remediation, energy and medical. Within the scheme, combination of semiconductor metal oxide and porous materials for photocatalytic purposes is an interested functional material. In many aspects, photocatalysis delivered some advantageous compared to other method such as adsorption and chemical treatment for water and wastewater treatment. The reusability of the process and its economical efficient procedure due to no further treatment are better alternative compared to other technique such as adsorption, chemical coagulation, etc. Among the various photocatalysts studied recently, the design of TiO_2 and ZnO with clay-based porous material was studied. The porous clay heterostructure was prepared by templated sol-gel pillarization with focus study in effect of synthesis method to the physicochemical characterization. Such intensification methods consist of microwave assisted method and hydrothermal method were applied, and correlation between physicochemical character of materials to the kinetics of photocatalysis along with optimization were discussed.

Synthesis, Physicochemical characterization, dielectric and electrical properties of ZnO/MgO Nanocomposite

Suresh Sagadevan*

Nanotechnology & Catalysis Research Centre, University of Malaya, Kuala Lumpur 50603, Malaysia

*Corresponding author email Id: drsureshnano@gmail.com

Abstract

The present work deals with the feasibility of incorporating the oxides of Zn and Mg for the high-frequency electronic devices and for that the ZnO/MgO nanocomposites with different Mg ratios formed by the sol-gel method were analyzed thoroughly for the physical characteristics. The XRD study confirms the presence of wurtzite ZnO and the cubic MgO phase, while the FESEM micrograph of the synthesized ZnO/MgO nanocomposites showed mixed morphologies of nanoflakes and spherical shaped particles. The values of dielectric constant, dielectric loss factor, and tangent loss were found to be increasing with increasing temperature and decreasing with increasing frequency of the applied field. The AC conductivity of ZnO/MgO nanocomposites is found to be frequency independent at low frequency, but weakly temperature dependent. The temperature dependence of conductivity (σ_{AC}) shows that it is a thermally activated process and hence the synthesized ZnO/MgO nanocomposite exhibits the semiconductor behavior. The activation energy of the synthesized nanocomposite calculated using the Arrhenius plot indicated that the values are getting decreased with that of increased frequency. Based on the overall analysis, the observation of excellent dielectric and magnetic properties of the synthesized ZnO/MgO nanocomposite makes it a potential candidate for high-frequency electronic devices.

Keywords: ZnO/MgO nanocomposite; Dielectric properties; AC conductivity; Impedance analysis; Semiconductivity; High-frequency electronic devices.

Structural, Optical and Electrical Properties of Controlled Growth Zinc Oxide Nanowires

S Paiman[1,2*], T Hui Ling[1], M. Husham[3] and Suresh Sagadevan[4]
[1]Department of Physics, Faculty of Science, Universiti Putra Malaysia, 43400 UPM Serdang, Selangor, Malaysia
[2]Functional Device Laboratory, Institute of Advanced Technology, Universiti Putra Malaysia, 43400 UPM Serdang, Selangor, Malaysia
[3]Department of Physics, Faculty of Education, Tishk International University, Erbil, KRG, Iraq.
[4]Nanotechnology & Catalysis Research Centre, University of Malaya, Kuala Lumpur 50603, Malaysia
Corresponding author Email: suriati@upm.edu.my

Abstract

We report the effect of various growth parameters on the morphology, optical and electrical properties of ZnO nanowires grown on indium tin oxide-coated-coated glass substrates. FESEM and PL studies have revealed that the morphological and optical properties of ZnO NWs can be controlled by controlling the annealing of the substrates. It has been found that ZnO NWs grown onto unannealed ITO-coated glass substrates have larger diameter with a high tapering morphology compared to those grown onto annealed ITO-coated glass substrates. The resistivity of ZnO NWs was found to be decreased by annealing, thus the conductivity of the NWs was improved. This study revealed that controlling the annealing process of ITO-coated glass substrates would significantly improve the properties of ZnO.

IL-15

Design, Synthesis, and Applications of Novel V-shape Heterocyclic Derivatives

Solhe F. Alshahateet

Department of Chemistry, Mutah University, Jordan

Email: s_alshahateet@mutah.edu.jo

IL_15_Solhe
Alshahateet.pdf

Abstract

We are currently developing series of new V-shape heterocyclic lattice inclusion compounds using our general crystal engineering design illustrated in Figure 1. The target heterocyclic molecules are constructed from three distinct structural components: two planar aromatic wings, a flexible central linker group able to provide molecular *C*2 symmetry, and two exo-oriented sensor groups. A series of new molecules was synthesized, and their various applications were studied. Our studies attempted to use these V-shape compounds as host molecules for compounds with different functional groups and properties in a host-guest inclusion process.

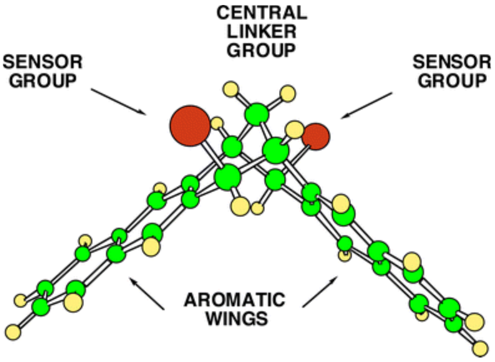

Figure 1

[1] Alshahateet, S.F., Bishop, R., Craig, D.C., Kooli, F., Scudder, M.L. *CrystEngComm*, **2008**, *10*, 297-305.

[2] Alshahateet, S.F., Bishop, R., Craig, D.C., Scudder, M.L. *Cryst. Growth Des.*, **2011**, *11*, 4474-4483.

[3] Alshahateet, S.F., Bhadbhade, M.M., Bishop, R., Scudder, M.L. *CrystEngComm*, **2015**, 17(4), 877-888.

[4] Alshahateet, S.F., Bhadbhade, M.M., Bishop, R., Craig, D.C., Scudder, M.L. *CrystEngComm*, **2015**, 17, 9111-9122

[5] Alshahateet, S.F. *Molecular Crystals & Liquid Crystals,* **2016,** 625(1), 186-194.

Development of Electrode Materials for Vanadium Redox Flow Batteries

Chen-Hao Wang*

Department of Materials Science and Engineering, National Taiwan University of Science and Technology, 10607, Taipei, Taiwan.

**Corresponding author (Prof. C. H. Wang): chwang@mail.ntust.edu.tw*

Abstract

In the recent years, sustainable energy has become the major tendency around the world. To stabilize power grids, energy storage system plays an indispensible role and vanadium redox flow battery (VRFB) is one of the most promising one. It can store and release energy by converting the oxidation state of vanadium ions such as the redox couples of V^{2+}/V^{3+} and VO^{2+}/VO_2^{+}. Moreover, it possesses the advantages of high design flexibility, long service life, low cross-contamination, without explosion risk, etc. About electrode materials, due to the usage of acidic electrolyte, carbon-based materials with the features of anti-corrosion and high conductivity are always the priority. However, it has the nature of low catalytic activity toward vanadium ions and hydrophobicity and need to be improved by the modification which our research team always focuses on. Electrode modification can be divided into surface modification and catalyst attachment. Taking water activation for the example of the former, graphite felt (GF) can have higher porosity, higher hydrophilicity, and more active sites when it was annealed at 700℃ with water vapor. At the current density of 50 mA cm^{-2}, the energy efficiency was raised from 78.63% and 81.93% which were provided by pristine GF and heat-treated GF respectively to 83.10%, and it also can perform outstanding stability after water activation. On the other hand, in the case of catalyst, $W_{18}O_{49}$ will become a powerful catalyst after sintering at 450℃ in 5%H_2/95%Ar. The reasons are the increase of surface hydrophilicity and the creation of active sites such as oxygen vacancies which was confirmed by Raman spectra and XPS. In the single cell test with 80 mA cm^{-2}, H_2-treated $W_{18}O_{49}$ GF can raise the energy efficiency about 12.5% than that of heat-treated GF and didn't decline after 100 cycles. From the above, we can know that the electrode modification is apparently focused on the increase of active sites and hydrophilicity. For enhancing the industrial competitiveness of VRFB, the development of superior electrode materials will play an essential role.

Keywords: Energy storage system, vanadium redox flow battery (VRFB), electrode modification, energy efficiency

Enhanced sonocatalytic degradation of methylene blue using Fe_2O_3-graphene-Ag nanocomposite as catalyst

Prawit Nuengmatcha[1,2†] **Amnuay Noypha**[1], **Yonrapach Areerob**[3], **and Saksit Chanthai**[4]

[1]Creative Innovation in Science and Technology, [2]Nanomaterials Chemistry Research Unit, Faculty of Science and Technology, Nakhon Si Thammarat Rajabhat University, Nakhon Si Thammarat, 80280, Thailand.

[3]Department of Industrial Engineering, Faculty of Engineering, King Mongkut's Institute of Technology Ladkrabang, Bangkok, 10520, Thailand

[4]Materials Chemistry Research Center, Department of Chemistry and Center of Excellence for Innovation in Chemistry, Faculty of Science, Khon Kaen University, Khon Kaen 40002, Thailand

Abstract

In the present research work, Fe_2O_3-graphene-Ag (FGA) was synthesized by a simple hydrothermal method. The sonocatalytic activity of the FGA particles was evaluated by the degradation of methylene blue (MB) under ultrasonic irradiation, revealing their good sonocatalytic activity. The effects of various experimental factors, such as dosage, time, and ultrasonic frequencies on the sonocatalytic efficiency were investigated; a significant influence of different factors on the sonocatalytic degradation of MB was observed, whereas the best degradation conditions were obtained when ultrasonic irradiation was performed for 90 min at room temperature considering MB concentration = 0.5 g/L, $C_{catalyts}$ = 1g/L, and pH 6.5. Moreover, the sonocatalytic activity of the FGA was compared to that of Fe_2O_3 (F), graphene (G), and Fe_2O_3-graphene (FG). As a result, the FGA was found to exhibit higher sonocatalytic activity than other catalysts (FGA > FG > G > F), which evidenced the practical utility of the synthesized FGA as a highly effective catalyst for the removal of dye pollutants. Finally, the plausible sonocatalytic mechanism of FGA is also discussed in this work

Keywords: Sonocatalytic degradation, Graphene, Catalyst, Fe_2O_3

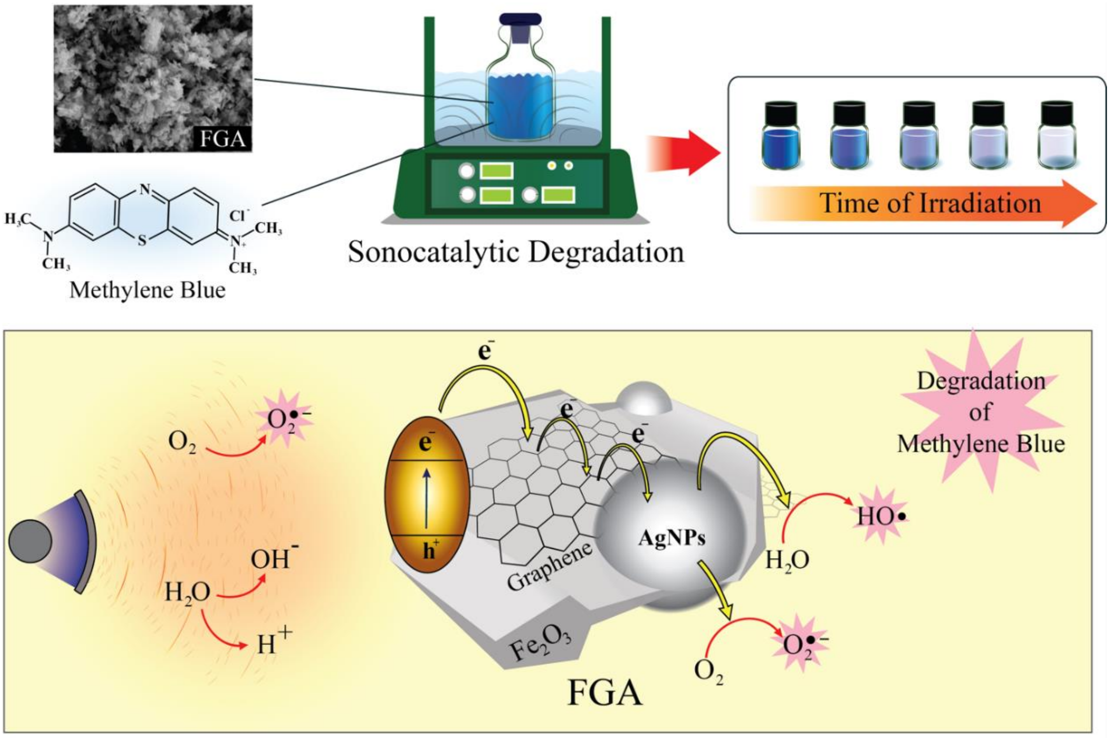
FGA
H3C
CH3
N
S
Cl-
CH3
CH3
Methylene Blue
Sonocatalytic Degradation
Time of Irradiation
O2
O2•-
H2O
OH-
H+
e-
h+
Graphene
AgNPs
Fe2O3
FGA
H2O
HO•
O2
O2•-
Degradation of Methylene Blue

IL-18

Structures and Properties of Carbon-based Nanocomposites

Jing Wang *, Ye Ge, Guotao Dong, Tianhao Hu, Youyang Chen
College of Materials Science and Engineering, Anhui University of Science And Technology,
Huainan, Anhui 232001
*Corresponding author (Phone and WeChat: + 0086 (13855418833); jingwang@aust.edu.cn)

Abstract： Based on various carbon nano materials, the ternary composite functionalized carbon nanotubes (FMWCNTs) @ carbon quantum dots (CQDs) @ polyaniline (PANI) was prepared by in-situ polymerization and hydrothermal method. The carbon-based material was made into an electrode sheet. The morphology and microscopic nanostructures were characterized by FTIR, field emission scanning electron microscopy and field emission transmission electron microscopy. Cyclic voltammetry and galvanostatic charge discharge method was adapted to study the electrochemical properties of these active materials. Our results showed that the specific capacitance of FMWCNTs @ CQDs @ PANI was as high as 534 F/g, while it was 362 F/g, 319 F/g and 279 F/g for PANI @ FMWCNTs, PANI @ CQDs and polyaniline. It means that the specific capacitance of FMWCNTs @ CQDs @ PANI is increased by 47.5%, 67.4% and 91.4% comparing with the capacitance of PANI @ FMWCNTs, PANI @ CQDs and polyaniline, respectively. Moreover, the specific capacitance retention rate of the ternary active electrode after 1000 times of constant current charge and discharge cycle reached 86%, while it was 60% for PANI @ FMWCNTs, 72% for PANI @ CQDs and 65%

for polyaniline.

Key words: Carbon Quantum Dots; Functionalized Multi-Walled Carbon Nanotubes; Polyaniline; Composite Electrode Material; Specific Capacitance

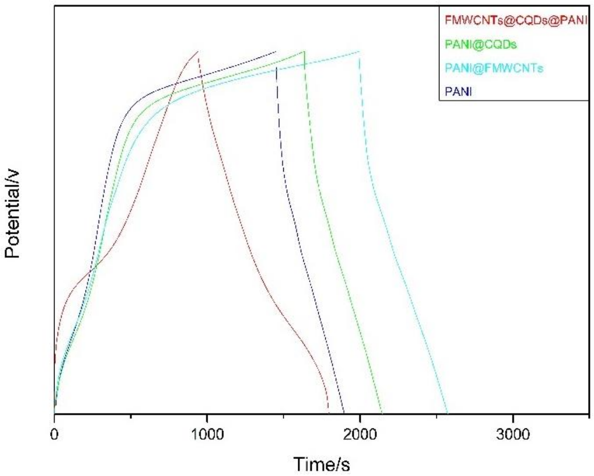

Figure 1. Constant current charge and discharge curves of PANI, PANI @ CQDs, PANI @ FMWCNTs and FMWCNTs @ CQDs @ PANI in 1 M H_2SO_4 electrolyte

Reference

1. XU F, JAMAL R, UBUL A, et al. Characterization and electrochemical properties of poly(aniline-co-o-methoxyaniline)/multi-walled carbon nanotubes composites synthesized by solid-state method [J]. Fibers and Polymers, 2013, 14(1): 8-15.
2. DYACHKOVA T P, ANOSOVA I V, TKACHEV A G, et al. Synthesis of Composites from Functionalized Carbon Nanotubes and Polyaniline [J]. Inorganic Materials: Applied Research, 2018, 9(2): 305-310.
3. ZHOU Y, QIAN W, HUANG W, et al. Carbon Nanotube-Graphene Hybrid Electrodes with Enhanced Thermo-Electrochemical Cell Properties [J]. Nanomaterials (Basel), 2019, 9(10): 1450.
4. Kurra, N.; Jiang, Q.; Alshareefn, H.N. A general strategy for the fabrication of high performance microsupercapacitors. Nano Energy 2015, 16, 1–9.
5. Chen H S, Drag Y. Progress in electrical energy storage system: A critical review[J]. Progress in Natural Science, 2009, 19(3): 291-312.
6. Li Y L, Zheng Y Y. Preparation and electrochemical properties of polyaniline/reduced graphene oxide composites [J]. Journal of Applied Polymer Science, 2018, 135(16): 235-262.
7. LIU L, NIU Z, CHEN J. Flexible supercapacitors based on carbon nanotubes [J]. Chinese Chemical Letters, 2018, 29(4): 571-581.
8. PEI X Y, MO D C, LYU S S, et al. Synthesis of MnCO(3)/Multiwalled Carbon Nanotube Composite as Anode Material for Lithium-Ion Batteries [J]. J Nanosci Nanotechnol, 2019, 19(9): 5743-5749.

9. WULANDARI S A, ARIFIN, WIDIYANDARI H, et al. Synthesis and characterization carboxyl functionalized Multi-Walled Carbon Nanotubes (MWCNT-COOH) and NH_2 functionalized Multi-Walled Carbon Nanotubes ($MWCNTNH_2$) [J]. Journal of Physics: Conference Series, 2018, 1025(1): 12005.
10. AZIZ S A A, UBAIDILLAH, MAZLAN S A, et al. Implementation of functionalized multiwall carbon nanotubes on magnetorheological elastomer [J]. Journal of Materials Science, 2018, 53(14): 10122-10134.

IL-19

Constructed CdTe QDs Surface Fluorescence Probe to Detection of Ultratrace Herbicide Paraquat Free Radical Based on FRET Mechanism

Yuan Cheng, Jing Wang, Jiadong Zhao, Zhihui Wang, Caiyu Ni, Xiaoxiao Xia, Hui Zhang, Daming Gao*, [1], and Chan Kyung Kim*, [2]
1. Department of Chemical Engineering, School of Energy, Materials and Chemical Engineering, Hefei University, Hefei 230601, Anhui, China.
2. Department of Chemistry, Inha University, 100 Inharo, Michuholgu, Incheon 22212, Korea

Abstract

The recognition and detection of trace amounts of pesticide residues is a considerable challenge for a strategy of efforts made to construct the sensors between the sensible material and target analyte. The real dilemma is how to build the output of sensitive signal response between sensing material and target analyte based on the fundamental principles, in essence, which embody the innate laws of things in physics and chemistry fields. This paper reports a strategy for a resonance energy transfer fluorescence quenching at the surface of CdTe quantum dots (QDs) for the detection of ultratrace herbicide paraquat free radical existed by quantum chemical (QC) simulation in solution environments. Thioglycolic acid (TGA) was tightly attached onto the surface of CdTe QDs to form a functional monolayer of carboxylic group by a number of coordination bonds. The fluorescent CdTe QDs can specifically bind paraquat free radical by the cation-anion pair’s complexing interaction between negative

carboxylic group of TGA and positive bipyridinium ion of paraquat free radical. The resultant paraquat free radical-carboxyl complexes bound at the CdTe QDs surface can strongly suppress the fluorescence emission of the chosen CdTe QDs by the fluorescence resonance energy transfer (FRET) from CdTe QDs donor to the irradiative acceptor of paraquat free radical-carboxyl complexes through intermolecular polar-polar interactions at spatial proximity.

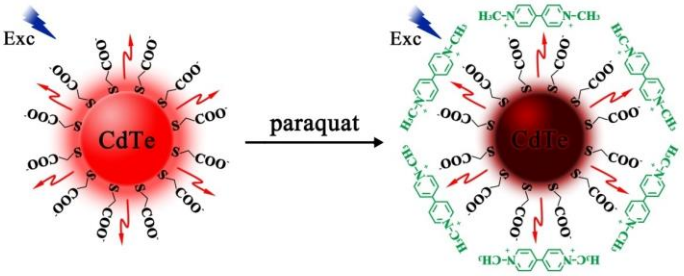

Figure 1. Schematic illustration for the quenching mechanism of the CdTe quantum dots fluorescence probe towards the trace detection of paraquat free radical based on fluorescence resonance energy transfer

References

1. Dey N, Bhagat D, Cherukaraveedu D, Bhattacharya S (2017) Utilization of red-light-emitting CdTe nanoparticles for the trace-level detection of harmful herbicides in adulterated food and agricultural crops. Chem-Asian J 12:76-85.
2. Kishikawa N, Higuchi S, Ohyama K, Nakashima K, Kuroda N (2013) A simple and rapid chemiluminescence assay for on-site analysis of paraquat using a portable luminometer. Forensic Toxicol 31:301-306.
3. Su YC, Ma SH, Jiang KP, Han XJ (2015) CdTe-paper-based visual sensor for detecting methyl viologen. Chinese J Chem 33:446-450

Acknowledgements

This work was supported by Natural Science Foundation of China (Nos. 21075026)

IL-20

Multi-functional Biochar for Sustainable Soil Management

Chew Tin Lee*, Cassendra Phun Chien Bong

School of Chemical and Energy Engineering, Faculty of Engineering. Universiti Teknologi Malaysia

81300 Johor Bahru. Malaysia.

E-mail: ctlee@utm.my

Abstract:

Biochar is widely reported to enhance the physical, chemical and biological properties of soil by improving the sorption of nutrients and reducing nutrient leaching from the soil. It is also reported to remediate soil polluted by heavy metals and salts. Recent studies aim to enhance the multi-functionality of biochar by integrating other materials such as polymer and ions. Such modifications have shown both positive and negative effects on the properties of the biochar composites towards specific applications. This paper reviews the various role of multi-functional biochars, derived through the pyrolysis of biomass and other materials to form composites to improve the properties of soil. The properties include soil porosity, soil aggregation, water holding capacity, hydraulic conductivity, organic carbon content, pH, electrical conductivity, exchangeable sodium percentage and sodium adsorption ratio to fulfil the various need of soil management. The efficiency of the biochar composites on their designated applications brought by the changes in the properties and the respective mechanisms are classified to serve a different application for soil management.

Acknowledgements

The authors gratefully acknowledge financial support from the Malaysian Ministry of Higher Education under the Fundamental Research Grant Schemes (FRGS) with grant no.

R.J130000.7809.5F147.

Keywords: Biochar, surface functionality, electrostatic, composites, soil management

References:

1. Bong C.P., Lim L.Y., Lee C.T., Ong P.Y., Klemeš J.J., Li C., Gao Y., 2020, Lignocellulosic Biomass and Food Waste for Biochar Production and Application: A Review, Chemical Engineering Transactions, 81, 427-432 DOI:10.3303/CET2081072
2. Dahlawi S., Naeem A., Rengel Z., Naidu R., 2018, Biochar application for the remediation of salt-affected soils: Challenges and opportunities, Science of The Total Environment, 625, 320-335

IL-21

Enhanced Electrical Performance of the Graphene Felt for Energy Storage Devices by Atmospheric Pressure Plasma Jet

Yu-Lin Kuo*1, Chen-Hao Wang2, Chiu-Feng Lin3,4, Song-Yu Chen1, Jhao-Yu Guo1, Yao-Ming Wang3, Wei-Mau Hsu3

1Department of Mechanical Engineering, National Taiwan University of Science and Technology, Taipei 10607, Taiwan.

2Department of Materials Science and Engineering, National Taiwan University of Science and Technology, Taipei 10607, Taiwan.

3Metal Industries Research & Development Centre, Kaohsiung 81160, Taiwan

4Department of Vehicle Engineering, National Pingtung University of Science and Technology, Neipu, Pingtung 91207, Taiwan.

**Corresponding author (Prof. Y. L. Kuo): ylkuo@mail.ntust.edu.tw*

With the exhaustion of energy, the development of energy storage technology is the popular research topic in the world. Vanadium redox flow battery is an environment friendly energy storage technology that has many advantages, such as high safety, flexible adjustment of capacitance, high stability and so on. In order to improve the electrochemical activity of graphite felt (GF) electrodes, we employed atmospheric pressure plasma technology to modify the surface of the GF. The optical emission spectroscopy (OES) is used to analyze the plasma species generated by atmospheric pressure plasma jet. The characteristic peak of functional OH group to give a surface hydrophilicity is located at 306 nm. The pristine GF represented a water contact angle of 133°, while plasma treatment process definitely reduced to reach the value under 10°which means apparently increased the wettability of GF. The plasma temperature analyzed with the working distance between plasma

jet and substrate of 15 mm around 200℃ detected by thermal couple. According to Raman spectrum, the ratio variation is the defect generation under with high plasma energy to bombard the GF to increase the reactive area. The electrical properties of GF are tested by cyclic voltammetry (CV). The ration of $I_{Anode}/I_{Cathode}$ becomes larger and potential change becomes smaller, which means that the surface is grafted the functional groups to be more hydrophilic and created more active sites for further electrochemical reaction. We believed that plasma treatment using air APPJ system is an efficient and costly process on GF for Vanadium redox flow battery.

Keywords：Energy storage technology, Atmospheric pressure plasma, Electrochemical activity, Graphite felt

IL-22

Preparation, Aggregation-Induced Emission and Nanoaggregates of the Copolymers Containing Different Ratios of Carbazoles and Tetraphenylethenes

Yu-Wei Tu, Chao-Chi Wang, Alis Shano Godana, Chin-Yang Yu*

Department of Materials Science and Engineering, National Taiwan University of Science and Technology, 43, Section 4, Keelung Road, Taipei 10607, Taiwan

**Corresponding author (Prof. C. -Y. Yu): cyyu@mail.ntust.edu.tw*

Abstract

Copolymers comprising of the different ratios of decyl or triethylene glycol substituted 2,7-carbazoles and tetraphenylethenes were synthesized by palladium-catalyzed Suzuki Miyaura cross coupling reaction of their corresponding comonomers. The copolymers containing carbazoles and tetraphenylethenes showed aggregation induced emission characteristics in both solid state and aggregate state when the composition of the tetraphenylethenes reached to 50%. N-triethylene glycol substituted carbazole based polymers revealed lower bandgap and higher HOMO level compared to that of the N-decyl substituted ones. When the composition of the tetraphenylethenes is higher, the HOMO level and the bandgap of the polymers is deeper and larger, respectively. Copolymers with 1:1 molar ratio of the carbazoles and the tetraphenylethenes exhibited sphere-like nanoparticles with an average diameter of around 30 nm. In addition, the copolymers containing carbazole and tetraphenylethene units with 3:1 or 1:3 molar ratio self-assembled to form nanoaggregates with a size of around 100 nm.

Keywords: copolymers, carbazoles, tetraphenylethenes, aggregation induced emission, nanoaggregates

IL-23

Electronic structure, thermodynamic stability and high-temperature sensing properties of Er-α-SiAlON ceramics

Yuwaraj K. Kshetri[1,*], Bina Chaudhary[2], Jin Hyuk Choi[3], Tae-Ho Kim[4], Soo Woo Lee[3]

[1]Research Center for Eco-Multifunctional Nano Materials, Sun Moon University, Chungnam 31460, Republic of Korea
[2]Department of Fusion Science and Technology, Sun Moon University, Chungnam 31460, Republic of Korea
[3]Department of Environment and Bio-Chemical Engineering, Sun Moon University, Chungnam 31460, Republic of Korea
[4]Division of Mechanics and ICT Convergence Engineering, Sun Moon University, Chungnam 31460, Republic of Korea

[*]Corresponding author: *yuwarajkhatri@gmail.com*

α-SiAlON ceramics have been in use as engineering ceramics in the most arduous industrial environments such as molten metal handling, cutting tools, gas turbine engines, extrusion molds, thermocouple sheaths, protective cover for high-temperature sensors, etc., owing to their outstanding mechanical, thermal and chemical stability. Taking advantage of the intrinsic properties of α-SiAlONs, we investigate, in this paper, the possibility of using the Er-doped α-SiAlON (Er-α-SiAlON) ceramic as a high-temperature sensing material via its unique near-infrared to visible upconversion property. We first use neutron diffraction and density functional theory calculations to study the electronic structure and thermodynamic stability of Er-α-SiAlON. It is found that the interstitial doping of Er stabilizes the α-SiAlON structure via chemical bonds with O-atoms with N:O ratio of 5:2 in the seven-fold coordination sites of the

Er^{3+} ion. Temperature-dependent upconversion emissions are then studied under 980 and 793 nm excitations over a temperature range of 298-1373 K and the fluorescence intensity ratio (FIR) technique has been employed to investigate the temperature sensing behavior. Temperature-dependent Raman behavior is also investigated. We demonstrate that using Er-α-SiAlON as a sensing material, the limit of temperature measurement via the FIR technique can be pushed well beyond 1273 K.

Keywords: Er-doped α-SiAlON, DFT calculations, upconversion, temperature se
temperature-dependent Raman

IL-24

Novel modifiedChitosan for remarkably high removal of heavy metal Cu (II)

Ke Wang, QingxiangShu, Zongqun Li, Na Yin*

Anhui Provincial Engineering Laboratory of Silicon-based Materials, School of Material and Chemical Engineering, Bengbu University, Bengbu, 233030, PR China

* To whom all correspondence should be addressed.

Tel.: +86-552-317-9528; +86-371-8660-9672;Fax: +86-552-317-9368;
E-mail:yn@bbc.edu.cn.

Abstract:

Heavy metal wastewater poses a great threat to human health. In this paper, high temperature modified chitosan was used to adsorptive removal of heavy metal ions. The obtain chitosan was investigated by infrared spectroscopy (FT-IR) and X-ray diffraction analysis (XRD). A crystalline structure was newly confirmed. Thermogravimetric analysis (TG) showed that the chitosanrevealed high temperature resistance. Effects of adsorption time, pH value, adsorption temperature and the concentration of Cu(II) on the adsorption were then studied. The suitable operating conditions were at adsorption time of 120 min, pH was 4, adsorption temperature was 35 °C, and the concentration of Cu(II) was as high as 180 mg/L. The adsorption kinetics of modified chitosan on heavy metal ions was calculated, and the data fit the quasi-secondary kinetic model.The adsorption mechanisms were also confirmed by X-ray photoelectron spectrum (XPS), which was absolutely not the coordination interaction between the –$NH_2$from Chitosan and Cu (II). The modified chitosan has shown great potential in heavy metal wastewater treatment.

Key words: Chitosan; High temperature modification; Heavy metal ions;Adsorption

Oral Lectures

A Comparative Study of Electrochemical Biosensors Based on Highly Efficient Mesoporous ZrO_2-Ag-G-SiO_2 and In_2O_3- G-SiO_2 for Rapid Recognition of *E*. coli O157: H7

Kamrun Nahar Fatema[1], Yin Liu[2], Kwang Youn Cho[3], & Won-Chun Oh[1,3]

[1]*Department of Advanced Materials Science & Engineering, Hanseo University, Seosan-si, Chungnam, Korea, 356-706*

[2] *College of Materials Science and Engineering, Anhui University of Science & Technology, Huainan 232001, PR China*

[3] *Korea Institute of Ceramic Engineering and Technology, Soho-ro, Jinju-Si, Gyeongsangnam-do, South Korea*

Abstract

Here, we reported an innovative and electrochemical biosensor for the rapid detection of *E. coli O157: H7.* We fabricated the mesoporous ZrO_2-Ag-G-SiO_2 (ZAGS) and In_2O_3-G-SiO_2 (IGS) sensors and cyclic voltammetry (CV) was employed to detect the bacteria. The development of these portable sensors that address the challenges of conventional time consuming and more expensive laboratory-based analyses. Hence, the biosensors were highly selective to detect *E. coli.* The sensor could recognize an individual *E. coli* cell in a 1 μL sample volume within 30 s. *E. coli* live cells tied down on sample nanoparticles worked as the definite acquirement of *E. coli*. The high thickness of negative charge on the surface of *E. coli* cells effectively regulates the concentration of dominant part charge carriers in the mesoporous channel, allowing a continuous check of *E. coli* concentration in a known sample. The signals current was decreasing linearly while the *E. coli* concentration increasing from 1.0×10^1 to 1.0×10^{10} CFU/mL. The ZAGS and IGS biosensor detect the *E. coli* from 10^1 CFU/mL to 10^{10} CFU/mL. The ZAGS and IGS biosensor in this investigation showed great specificity, reproducibility, stability, and selectivity is expected to have a great impact on applications in the detection of foodborne pathogens.

New modeling of Graphene-based Ternary nanocomposite and its photocatalytic reduction of CO_2 into Methanol

Zambaga Otgonbayar [1], Chong-Hun Jung [3], *Won-Chun Oh* [1, 2]

[1] *Department of Advanced Materials Science & Engineering, Hanseo University, Seosan-si, Chungnam, Korea, 356-706*

[2] *College of Materials Science and Engineering, Anhui University of Science & Technology, Huainan 232001, PR China*

[3] *Decommissioning Technology Research Division, Korea Atomic Energy Research Institute, Daedeok-daero, Daejeon, Republic of Korea*

E-mail: wc_oh@hanseo.ac.kr

Abstract

Effective separation of photogenerated charge is the key factor and can define the catalytic activity of the photocatalyst material. The recombination of electron and holes on the photocatalyst surface can block the effect of hydrogen in the holes for the CO_2 reduction, causing the eventual of inhibition of the catalytic activity. A new challenge that scientists need to overcome is the unification of a well-structured photocatalyst material for transforming CO_2 into a product, and the graphene-based chalcogenide photocatalyst has shown a great-deal of promising attributers in this area due to variable bandgap energy. The role of graphene is an electron acceptor/transporter, whereby this presents the most important part of the partition of electron-hole transport in coupling of graphene with metal semiconductor. The ternary and quaternary chalcognide nanocomposite has semi-insolating feature was observed with band-gaps from small (< 1 eV) to large (> 3 eV) and noted a suppleness large amount of electron hole pairs. The ternary nanocomposite is a stable, environmentally friendly, and efficient visible-light photocatalyst, which advanced the research field of photocatalytic carbon dioxide reduction under sunlight irradiation. The morphology structure, charge-carrier separation properties are main understanding points of graphene-based metal semiconductor which can offers a promising route for the rational design of a new class of graphene-based ternary photocatalyst for various applications in environmental protection and solar energy conversion.

Keywords : Graphene, Chalcogenide quaternary nanocomposite, ternary, CO_2 reduction, methanol.

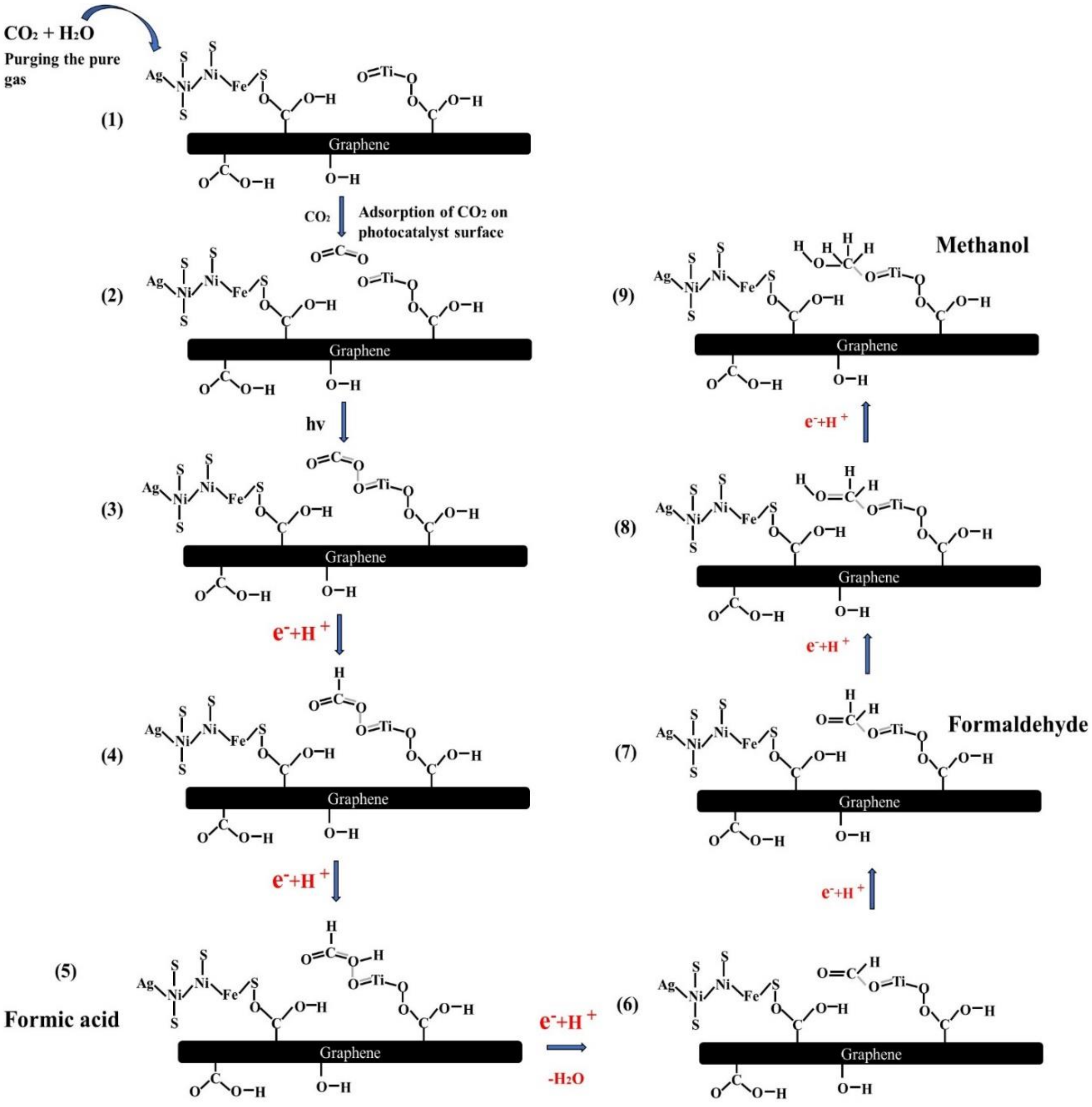

Schematic illustration of photocatalytic CO_2 reduction on Graphene-based ternary nanocomposite.

References

1. Zambaga Otgonbayar, Kwang Youn Cho and Won-Chun Oh. Enhanced photocatalytic activity of CO_2 reduction to methanol through the use of a novel-structured $CuCaAg_2Se$–graphene–TiO_2 ternary nanocomposite, *New J. Chem.***,** 2020, 44**,** 16795-16809.

OL-3

Graphene Based Nanomaterials, Towards Energy Storage and Production

Kefayat Ullah

Department of Applied Physical & Material Sciences, University of Swat.

Abstract

Graphene, a 2D material with unexpected mechanical, optical, and electrical properties has recently attracted enormous interest in photocatalysis and nano science. Graphene stands out among many promising candidate materials because of its low cost and favorable band gap.

However, its properties are hindered by issues like, photo generated charge carriers, short hole diffusion length and mobility of charge carriers. To address these limitations nanostructure composites with a solid-state electron mediator graphene act as an ideal material. The enormous charge transport properties of graphene have been widely discussed and proved by the scientist globally. Graphene has been considered as support material to work as a mediator between two semiconductor materials to boost their optical and electrical properties. It has been experimentally observed as the most useful unit for the construction of numerous nanocomposite materials in environmental and energy applications.

Key words: Microwave; Raman; Graphene; DRS, Solar cell, Supercapacitors.

OL-4

Advanced electromagnetic (EM) shielding materials for remediation of

environmental pollution

Rambabu Kuchi[a,b,*]

[a] *Powder & Ceramics Division, Korea Institute of Materials Science, Changwon, Gyeongnam 51508, South Korea*

[b] *Convergence research center for development of mineral resources, Korea Institute of Geoscience and Mineral Resources, Daejeon 34132, South Korea*

E-mail: rambabu.kuchi@kigam.re.kr

Abstract

Nowadays, the electromagnetic (EM) wave radiation in the gigahertz (GHz) range has been subjected as a serious problem for advanced electronic technologies: biological systems, industrial and military safety equipment's, etc. Since the EM wave interference from the interaction of EM waves with the device signal and thereby EMI pollution generated. It has been treated as a serious issue since it could become harmful to the human health deteriorate the performance of advanced electronic systems (biological systems, industrial and military safety equipment etc.). Therefore, the demand for the advanced EMI shielding material is increasing continuously. For this purpose, magnetic nanoparticles (MNP) and its composites have been drawn the huge attention of research in recent years due to their effective utilization to remediate the EMI pollution. EMI shielding performance was evaluate by the reflection and absorption processes, which can affect by the electromagnetic parameters of materials. It is important that proper combination of MNP with another material for the preparation of MNC to obtain the excellent EMI properties. Thus, focused on the different approaches of synthesis of MNP and its composites consisting with dielectric carbon materials and other dielectric material and discussed the EMI properties of MNP and its composites through adequate analysis of electromagnetic parameters.

Keywords: Magnetic nanoparticles (MNP), composites, electromagnetic interference shielding, electromagnetic parameters.

In-situ synthesis SiC/MgO/$MgAl_2O_4$ in molten Al-30Si alloy：Flash pyrolysis phenolic resin

Yuhong Jiao[1,2], Jianfeng Zhu[2], Chunjie Shi[1]

1 Anhui Provincial Engineering Laboratory of Silicon-based Materials, School of Material and Chemical Engineering, Bengbu University, Bengbu, 233030, PR China

2 Shaanxi Key Laboratory of Green Preparation and Functionalization for Inorganic Materials, School of Materials Science and Engineering, Shaanxi University of Science & Technology, Xi' an, 710021, PR China

* Corresponding author: E-mail: j7963936@126.com, Tel: +86-552-317-9368

Abstract

SiC/$MgAl_2O_4$/MgO enhanced Al matrix composite was obtained by in-situ synthesis process in rapid pyrolysis model of phenolic resin. XRD, SEM and EDS were used to analyze phase contents, microstructure and fractures microstructures, which reveal the enhancement or reaction mechanism. Including Al matrix, Si, $MgAl_2O_4$ and a small amount of SiC consist the samples, as showed in the XRD results, which were obtained from in-situ synthesis. It was observed that in-situ synthesis process uniformly scattered nano-ceramic particles (SiC/$MgAl_2O_4$/MgO) in Al matrix composite, which was confirmed that the pyrolysis gas as carbon and oxygen source has been joined the reactions of forming MgO, SiC and Spinel. An obvious change was showed in SEM graphs of phenolic resin addition that a dramatic decrease of inclusion in the matrix was found, and the pore in the matrix were increased. Nevertheless, a hypothesis which nano-ceramic powders are beneficial to the mechanical properties of composites was denied. Strain-stress curves are showed decreased trend due to the enhancement was concealed by the primary fracture factor which huge size particles of Si in matrix snicked the matrix, and then destroyed the continuity of matrix.

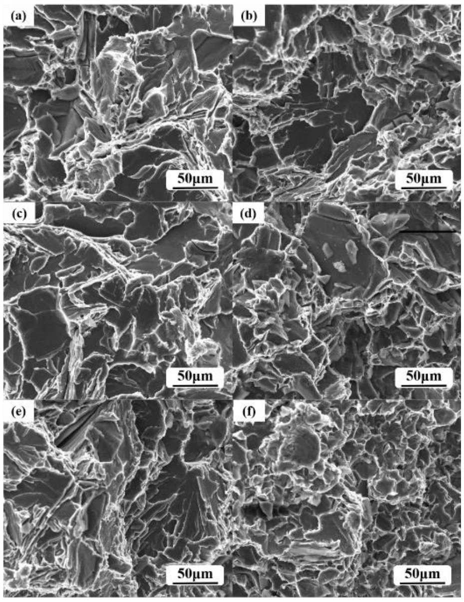

Fig.1 SEM graphs of fracture

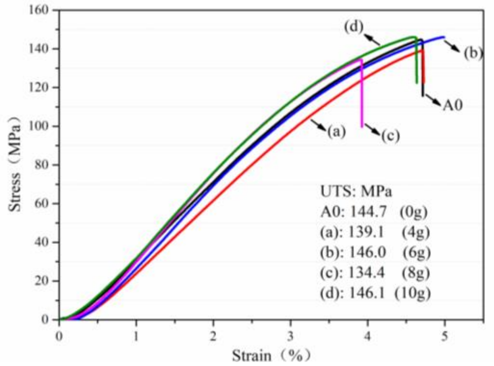

Fig.2 Strain-stress curves of the composites.

References

1 Dong, C. Cui, R.; Wang, R.; et al. *Transactions of Nonferrous Metals Society of China* 2020, 30 (4), 863-871.

2 Ghanaraja S ; Rajashekar H ; Ravikumar K S. *Materials Today Proceedings* 2018, 5 (1), 2765-2772.

Acknowledgments

The work was supported by the National Natural Science Foundation of China (No. 51472153, 51572158).

OL-6

Hybrid of Graphene based on quaternary $Cu_2ZnNiSe_4$ –WO_3 nanorods for counter electrode in Dye-sensitized Solar cell Application

Won-Chun Oh[a]*, Yonrapach Areerob[b],

[a] Department of Advanced Materials Science & Engineering, Hanseo University, Chungnam 356-706, South Korea

[b] Department of Industrial Engineering, Faculty of Engineering, King Mongkut's Institute of Technology Ladkrabang, Bangkok, 10520, Thailand

Corresponding E-mail: wc_oh@hanseo.ac.kr

Abstract

A novel nanohybrid of graphene-based $Cu_2ZnNiSe_4$ with WO_3 nanorods (G-CZNS@W) was successfully synthesized via a simple hydrothermal method to use as a counter electrode (CE) for dye-sensitized solar cells (DSSCs). The characterization technique confirmed the structural and morphologies of the G-CZNS@W nanohybrid, which could show rapid electrons transfer pathway through the WO_3 nanorods. Moreover, the as-fabricated G-CZNS@W nanohybrid exhibited synergetic effect between G-CZNS and a WO_3 nanorod, which could affect the electrocatalytic activity towards triiodide reaction. The nanohybrid exhibits an excellent photovoltaic performance of 12.16%, which is higher than that of the standard Pt electrode under the same conditions. the G-CZNS@W nanohybrid material as CE thus offers a promising low-cost Pt-free counter electrode for DSSC.

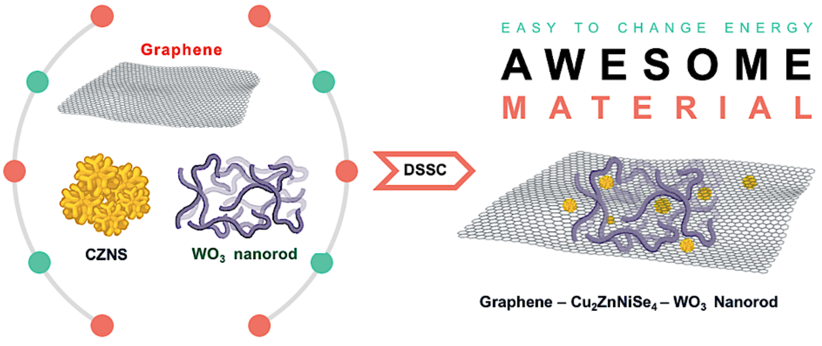

Keywords: Dye-sensitized solar cells, Nanorod, Graphene and Counter Electrode

References

1. W.C. Oh, K.Y. Cho, C.-H. Jung, and Y. Areerob, *Sci. Rep.*, **10**, 4738 (2020).

Study of Stimuli-Responsive Organic Magneton Based on Nitroxide Radicals and Carbon Cation Radicals

Di Wang[1], Jin Liu[1], Martin Baumgarten[2]*

[1] School of Materials and Chemical Engineering, Anhui Jianzhu University, 230601 Hefei, China）

[2] Max Planck Institute for Polymer Research, Ackermannweg 10, 55128 Mainz, Germany）

Abstract

Organic spin-magnetic molecules, especially stimuli responsive magneton with magnetic controllable properties have received wide attentions and possessed huge potential applications. Nowadays, these research concerned are limited mainly in some certain organic molecules or metal-organic compositions. Due to the low chemical stability of spin centers upon light, thermo and redox stimuli factors, the control of spin-magnetic transition decreased. In this study, nitroxide radicals or aromatic carbon cation radicals and temperature or redox sensitive units will be used as precursors to synthesize the stimuli responsive magneton in a proper way. During spin magnetic transitions, the aromatic carbon skeleton could convert to stable cation radicals under mild redox situations. By regulating the type, length or positons between conjugated bridges with spin centers and the configuration change upon external stimuli, the transitions of spin multiplicity and magnetic interaction (high / low spin state or ferro / antiferro-magnetic coupling) will be achieved among the multi-spin centers. The inner relationships or mechanisms between the multi-dimensional structure change and the transitions of spin magnetism would be discovered. In addition, our research would further provide structures and theoretical support for the acquirements of entire organic ferro / antiferro-magnetic materials with high value of saturation susceptibility.

Key words: Stimuli Response、Nitroxide Radicals、Spin-Magnetic Controllable、Carbon Cation、High/Low Spin State

Acknowledgments: This work was supported by the SFB/TR 49 and the Max Planck Society. D.W. is grateful for a scholarship from the China Scholarship Council No. 201306340011.

Ruthenium Catalysts with Metal-ligand Cooperation for Hydrogenation of Esters into Alcohols

Xiaolong Fang[1]

[1] College of Materials and Chemical Engineering, Anhui Jianzhu University, Hefei, 230601, Chin）

Abstract

The *Noyori-type* Ru-NH catalyst has been successfully applied in homogeneous hydrogenation of esters into alcohols, in which the Ru-*H* and N-*H* intramolecular cooperation determines the catalytic process. To modulate the effect of this type cooperation, we have developed a variety of bis(aminophosphine)ruthenium catalysts, which exhibit excellent catalytic activity in aliphatic and cyclic esters hydrogenation.

However, the typical catalyst (o-$Ph_2PC_6H_4NH_2)_2RuCl_2$ (**1a**) has limit to catalyze the hydrogenation of sterically hindered esters (eg. methyl benzoate, etc.), and requires a large amount of base. Thus, two novel catalysts (o-$PPh_2C_6H_4CH_2NH_2$)(o-$PPh_2C_6H_4NH_2$)$RuCl_2$ (**2a**) and (o-$PPh_2C_6H_4NH_2$)($EtNH(CH_2)_2NHEt$)$RuCl_2$ (**3a**) containing two or more NH functional groups in different chemical environments were synthesized. Interestingly, the coexistence of rigid and flexible aminophosphine ligands in the structure of **2a** shows good performance in hydrogenation of sterically hindered substrates.

Moreover, compound **3a** performs well under mild conditions, and the TOF value was raised up to 3920 h^{-1} under optimized reaction conditions. This is due to the presence of $(CH_2NHEt)_2$ ligand, which significantly increases the electron density of ruthenium center, therefore enhances the nucleophilicity of the ruthenium hydride as the catalyst intermediate.

Keywords: ester; alcohol; catalytic hydrogenation; Ru-NH catalyst

Acknowledgments: This research was financially supported by Natural Science Foundation of China (No. 21802010).

Strategies and Opportunities of Magnetic Graphene-based Composites for Water Remediation

Dr. Janardhan Reddy Koduru

Department of Environmental Engineering, Kwangwoon University, Seoul, 01897, South Korea

Abstract

Technological advances are need of this society and growing at a rapid pace to cater the requirements of human beings in various sectors. Nevertheless, this industrial growth leads to the release of toxic chemicals into the air, water, and land, thus contaminated them. Water pollution is a global environmental concern and concentration of toxic pollutants in the water bodies are well above the designated limits established by world health organization (WHO) and environmental protection agency (EPA). Heavy metals are one of the primary contaminants in the aqueous environment, and continuous exposure leads to high-risk health problems for humans. In pursuit of removal of toxic pollutants from the aqueous environment, researchers have been developed many techniques. Among these techniques, magnetic separation has caught research attention, as this approach has shown excellent performance in the removal of toxic pollutants from aqueous solutions. However, magnetic graphene oxide-based nanocomposites (MGO) possess unique physicochemical properties including excellent magnetic characteristics, high specific surface area, surface active sites, high chemical stability, tunable shape and size, and the ease with which they can be modified or functionalized. As results of their multi-functional properties, affordability, and magnetic separation capability, MGO's have been widely used in the removal of heavy metals, radionuclides, and organic dyes from the aqueous environment, and are currently attracting much attention. This provides insights into preparation strategies and approaches of MGO's utilization for the removal of pollutants for sustainable water purification. It also reviews the preparation of magnetic graphene oxide nanocomposites and primary characterization instruments required for the evaluation of structural, chemical and physical functionalities of synthesized magnetic graphene oxide nanocomposites. Finally, we summarized some research challenges to accelerate the synthesized MGO's as adsorbents for the treatment of water pollutants such as toxic and radioactive metal ions and organic and agricultural pollutants.

Influences of metal dispersion and H_2-spillover of Pt to lower reduction temperature of Ni/HZSM-5 catalyst investigated by TRXAS

Nichapha Senamart[1], Yingyot Poo-arporn[2], Pimrapas Tawachkultanadilok[3], Sirinuch Loiha[1]

[1] Materials Chemistry Research Center, Department of Chemistry, Faculty of Science, Khon Kaen University, Khon Kaen 40002, Thailand
[2] Synchrotron Light Research Institute, Nakhon Ratchasima 30000, Thailand
[3] School of Chemistry, Institute of Science, Suranaree University of Technology, Nakhon Ratchasima 30000, Thailand

Abstract

Nickel-supported HZSM-5 zeolite is widely used as a catalyst for hydrogenation process due to its high activity and stability. The reducibility of nickel plays important role in the catalytic activity. This work aims to improve the reducibility of the Ni/HZSM-5 catalysts at low reduction temperature for mild condition approach of the levulinic acid (LA) hydrogenation. The reducibility of nickel is investigated by temperature evolution of time-resolve X-ray absorption spectroscopy (TRXAS) technique under H_2/N_2 flow. Effects of Ni loading (3 and 5wt%) and Pt-addition (30Pt:70Ni mole ratio) on the Ni reduction are determined. In addition, the structural stability to LA-adsorption at 250-450ºC of the Ni catalysts is deduced. Ni^{2+} on the as-synthesized Ni/HZSM-5 catalysts could be partially reduced to Ni^0 during calcination step at about 300 ºC due to dehydration of the oxide structure. A 3Ni/HZSM-5 clearly exhibits a higher reducibility than 5Ni/HZSM-5 at 420ºC. XANES profiles of 5Ni/HZSM-5 are relevant to large particle size of Ni. The catalysts are completely reduced at 500ºC with holding time of 1.5h. The complete reduction temperature is reduced to 300ºC on a bimetallic 30Pt70Ni/HZSM-5 catalyst indicating a strong influence of H_2-spillover on Pt. The metallic nickel on all catalysts is stable through LA-adsorption step. Therefore, the catalysts are enabling to use for hydrogenation of LA at mild condition.

Identity of rose wood (*Dalbergia cochinchinensis*) by FTIR SEM-EDX and SEM-EDS Utilization in Forensic Science

Rachadaporn Benchawattananon

Integrated Science Faculty of Science Khon Kaen University Khon Kaen Thailand 40000

Email: rachadaporn@kku.ac.th

Abstract

In response to its higher value and demand, international trade is great and lead to dramatically increase to illegal logging. Lost of rosewood is about 20% in the past 6 years. *Dalbergia cochinchinensis* or rosewood is an important plant listed in the Appendix II of CITES. There are smuggling rosewood criminal acts cross over Thailand, Laos and Cambodia. This research aims to identified rosewood from various sources, including Thailand, Laos, Cambodia to determine specific characteristic for identification of endemic species. The elemental compositions of the soil and wood sample were analyzed using FTIR, SEM-EDX and SEM-EDS. The relationship between the elemental components of rosewood trees and soil properties was established using PCA. The result found the different pattern of graph of FTIR. Cambodia has unique than Laos and Thailand. The soil from the result by SEM-EDX, and SEM-EDS have different pattern which each country. The results of the study can be used as a basis planning for surveillance or prevent illegally logging of rosewood or used as a basis for investigation in the case of illegally logging of rosewood.

Keywords: *Dalbergia cochinchinensis*, FTIR SEM-EDX and SEM-EDS
illegal logging, Cambodia, Laos, Thailand

Preparation of Carbon Supported Cobalt Oxide as Ethylene Scavenger for Fruit Preservation

Nur Indah Fajar Mukti[1,2,3 a)], Imam Prasetyo[1, 2, b)], Teguh Ariyanto[1,2c)]

[1]Department of Chemical Engineering, Universitas Gadjah Mada, Indonesia

[2]Carbon Material Research Group, Department of Chemical Engineering, Universitas Gadjah Mada, Indonesia

[3]Department of Chemical Engineering, Islamic University of Indonesia, 55584 Yogyakarta, Indonesia

Email: a)165210101@uii.ac.id, b)imampras@ugm.ac.id, c)teguh.ariyanto@ugm.ac.id

Abstract.

Ethylene is a compound produced naturally by fruit that can accelerate the maturity of the fruit. Controlling ethylene gas as a product of metabolism of fruit during storage will prolong the shelf life of the fruit. Controlling ethylene gas is carried out by adsorption process using carbon-impregnated cobalt oxide. In this study, carbon as a support made by pyrolysis of biomass at a temperature of 850°C for 15 minutes. Furthermore, the process of impregnating of cobalt oxide into the carbon pore network was carried out by using the incipient wetness impregnation method by adding a cobalt salt solution into the carbon pore network, followed by calcination at a temperature of 200oC for 6 hours. Ethylene adsorption test performed at 30°C using a static volumetric test. While Cavendish banana fruit preservation process was carried out at ambient temperature (20-32oC) by observing the changing of skin color from day to day. Adsorption test results showed that the ethylene uptake increased with the increasing of the composition of cobalt oxide on the carbon surface. The highest ethylene uptake of 6.094 mmol/(gram of adsorbent) was obtained from adsorption of ethylene using carbon-impregnated 30% cobalt oxide. Fruit preservation process indicated that the increasing of amount of adsorbent can improve the shelf life of bananas Cavendish. The highest result was obtained from the addition of 15 grams of carbon-impregnated cobalt oxide and silica gel that can extend the shelf life of bananas Cavendish for 15 days.

Keywords: adsorption; metal oxide; ethylene scavenger; porous carbon

OL-13

A novel Si-based Caged-structural Intumescent Additive for Improving Flame Retardance of Unsaturated Polyester Resin

Gang Zhang, Yanlin Wang, Yanmao Dong*
School of Chemistry and Life Sciences, Suzhou University of Science and Technology
Xuefu Road 99, Suzhou, China,215009
*E-mail: dongyanmao@163.com

Abstract

Abstract: To improve the flame-retardant performance of unsaturated polyester resin (UPR), a novel mono-component intumescent flame retardant (IFR) containing caged structure named phosphonyltris (N, N, N-trimethylol clathrate methylamine) amine (PTSA) was synthesized. The PTSA as prepared was characterized by nuclear magnetic resonance (NMR), fourier transform infrared (FTIR), elemental analysis (EA) and Thermogravimetric analysis (TGA). The efficiency of flame retardant UPR/PTSA composites was investigated by using the limiting oxygen index (LOI), vertical burning (UL-94) tests and cone calorimeter tests. As the loading of PTSA is as low as 18 wt%, the composites reached UL-94 V-0 rate without dripping and the LOI value was 29.1%. Cone calorimeter tests revealed the peak of heat release and CO production of UPR/PTSA-18 were obviously declined with the reduction of 57.2 and 39.9% compared with that of neat UPR. The addition of PTSA greatly increased the stability of UPR composites. The structural analysis of UPR/PTSA materials after the cone calorimeter tests was characterized by scattering electron microscopy (SEM). It was founded that the incorporation of PTSA stimulated the UPR matrix to generate char layer in advance and the char layer inhibited the decomposition process and limited the smoke emission. This presented research provided a new way to obtain flame retardant UPR composites with high performance.

Key words: unsaturated polyester resin, intumescent flame retardant, synergistic charing agents, caged structure

---

OL-14

Fabrication and properties of transparent

Eu:Lu_2O_3 scintillation ceramics

Ye Ge, **Guotao Dong, Tianhao Hu, Youyang Chen**, **Zhihao Hu**, **Jing Wang ***
College of Materials Science and Engineering, Anhui University of Science And Technology,
Huainan, Anhui 232001
*Corresponding author (Phone and WeChat: + 0086 (13855418833); jingwang@aust.edu.cn)

Abstract: Lu_2O_3 is a kind of semi oxide which is widely concerned, which is beneficial to the preparation of Lu_2O_3 transparent material[1-2]. Lu_2O_3 can be used as a matrix material for high performance scintillation detectors, laser media and other functional materials. It has excellent X-ray and other high energy particle blocking ability. Eu-doped Lu_2O_3 material has potential application value in X-ray imaging field[3-5]. The Eu:Lu_2O_3 ceramic precursor was synthesized by wet chemical method, and the morphologies, microstructures and phases of both Eu:Lu_2O_3 ceramic precursor and the calcined Eu:Lu_2O_3 ceramic powders were studied by SEM and XRD. The results showed that the powders are spherical, well-dispersed and good crystalline. The particle size is calculated to be about 68.5nm. Using the powders calcined at 1100°C for 4h as raw material, the highly transparent Eu:Lu_2O_3 ceramics were successfully fabricated by vacuum sintering at 1650°C for 30h. The grain size is calculated to be about 46 μm, and in-line transmittance of the Eu:Lu_2O_3 ceramics reaches 66.7% at 611nm. What's more, the absorption curve, the excitation spectrum, the emission spectrum and the X-ray excited emission spectrum of the Eu:Lu_2O_3 ceramics were studied. It can be observed that the absorption curve of Eu:Lu_2O_3 ceramics is consisted of the matrical absorption and active ion absorption. It can be seen from the photo-luminescence emission spectrum and X-ray excited emission spectrum of the Eu:Lu_2O_3 ceramics that an extremely strong peak is located at 611 nm, corresponding to the $^5D_0\rightarrow{}^7F_2$ transition of Eu^{3+} ions. By comparison with the BGO crystal, the light output of the Eu:Lu_2O_3 ceramics is estimated to be about ~85000 ph/MeV. Eu:Lu_2O_3 ceramics have an excellent X-ray stopping power due to its high density and effective atomic number. It is indicated that Eu:Lu_2O_3 ceramics are a potential ceramic scintillator for the application of X-ray detection imaging.

Key words: Transparent Eu:Lu_2O_3 scintillation ceramics, vacuum sintering, photo-luminescence, X-ray excited emission spectrum；light output

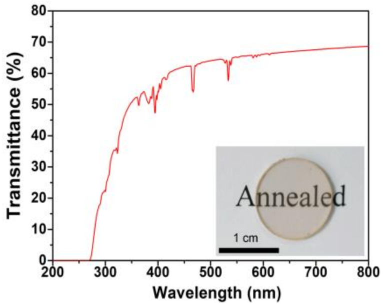

Fig.1 5at%Eu：Lu_2O_3 straight line transmittance curve of ceramics, illustrated as physical picture of sample (1 mm thickness)

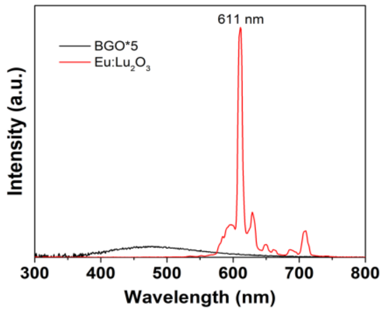

Fig.2 5at%Eu：Lu_2O_3 X ray excitation emission spectra of ceramics and commercial BGO single crystals

References

[1] Lvchao Zhuang,Zhijun Zhang,Yong Wang, et al.Afterglow Behavior, Energy Transfer and Trap States in Lu_2O_3:Eu Single Crystal Scintillator[J]. ECS Journal of Solid State Science and Technology, 2018, R17-R20.

[2] T. Zorenko, V. Gorbenko, N. Safronova, et al. Comparative study of the luminescent properties of oxide compounds under synchrotron radiation excitation: Lu_2O_3 :Eu nanopowders, ceramics and films[J]. Journal of Luminescence, 2018:461-464.

[3] Seferis I E , Michail C , Zeler J , et al. Detective quantum efficiency (DQE) of high X-ray absorption Lu 2 O 3 :Eu thin screens: the role of shape and size of nano- and micro-grains[J]. Applied Physics A, 2018, 124(9):1-7.

[4] Hu Y , Gu M , Li Q , et al. Influence of Annealing Temperature on the Performance of LuO:Eu Nanowire Arrays Synthesized by Sol–Gel Method Using AAO Template[J]. IEEE Transactions on Nuclear ence, 2020, 67(8):1899-1903.

[5] N.A. Safronova, R.P. Yavetskiy, O.S. Kryzhanovska, et al. Fabrication and VUV luminescence of Lu_2O_3 :Eu^{3+} (5 at.%) nanopowders and transparent ceramics[J]. Optical Materials,2020, 101(Mar.):109730.1-109730.7.

Facile preparation of ternary Ag@AgBr/TiO_2 nanorod arrays for enhanced photoelectrochemical and photocatalytical activity

Yanfen Wang[a,b], Yin Liu[a], Haocheng Yang[b], Hai Yu[b], Miao Zhang[b], Gang He[b], Zhaoqi Sun[b]

[a] *School of Materials Science and Engineering, Anhui University of Science and Technology, Huainan 232001, PR China*

[b] *School of Physics & Materials Science, Anhui University, Hefei 230601, PR China*

*Corresponding author (zhongbo@hit.edu.cn).

E-mail address: szq@ahu.edu.cn (Z.Sun)

Abstract:

A new and fast-electron-transfer heterostructure was successfully constructed by the deposition of Ag@AgBr nanoparticles on well-ordered TiO_2 nanorod array (TNR) via a facile solvothermal process. The microstructure, composition, morphology, optical property, photoelectrochemical and photocatalytic properties of the as-synthesized Ag@AgBr/TNR (ABT) were studied. The results showed that varying reaction time yielded Ag@AgBr nanoparticles with diameters ranging from 10-200 nm, which was closely attached to top and side of TiO_2 nanorods. The sensitization of Ag@AgBr nanoparticles on TNR significantly extended photoresponse region, promoted charge transfer, and suppressed their recombination. 12ABT photoelectrode with 12 h reaction time had the lowest transfer resistance for interfacial charges and highest transient photocurrent intensity of 130 $\mu A/cm^2$, which was about 13 times as that of bare TNR. In the degrading of methyl orange, 12ABT showed the optimal photocatalycal efficiency of 95.6 % and rate constant of 0.0167 min^{-1} under full spectral irradiation, which was 18.6 times of TNR (14.5 %). The favorable sunlight-driven photocatalytic activity originated from synergistic effect of three components in Ag@AgBr/TNR sample, such as the improved solar light response through surface plasmon resonance (SPR) and photosensitive effect of Ag@AgBr co-sensitizers, as well as the high-efficiency carrier transfer in the ternary heterojunction.

A new carbon allotrope: T_5-carbon

Xian-Yong Ding[1], Chao Zhang[1,4,5,*], Dong-Qi Wang[2], Bing-Sheng Li[3], Qingping Wang[1], Zhi Gen Yu[4], Kah-Wee Ang[5] and Yong-Wei Zhang[4]

[1]School of Materials Science and Engineering, Anhui University of Science and Technology, Huainan 232001, China

[2]Multidisciplinary Initiative Center, Institute of High Energy Physics, Chinese Academy of Sciences, Beijing 100049, China

[3]State Key Laboratory for Environment-friendly Energy Materials, Southwest University of Science and Technology, Mianyang, Sichuan 621010, China

[4]Institute of High-Performance Computing, A*STAT, Singapore, 138632

[5]Department of Electrical and Computer Engineering, National University of Singapore, Singapore, 117583

Abstract

A novel carbon allotrope is predicted by first-principles calculations. This allotrope is obtained by replacing one of the two atoms in the primitive cell of diamond with a carbon tetrahedron, thus it contains five atoms in one primitive cell, termed T_5-carbon. The stabilities of T_5-carbon are checked in structural, thermal, and vibrational calculations. T_5-carbon is a wide band gap semiconductor with an indirect band gap of 4.30 eV and has a lattice thermal conductivity of 409 W/mK. Mechanical analyses reveal that T_5-carbon shows good mechanical performances. Furthermore, by modifying T_5-carbon with replacing some carbon atoms with Si or Ti atoms, we can obtain SiC_4 or TiC_4 structures. Importantly, the TiC_4 system has a moderate conduction and valance band edges, comparable larger absorption capacity of visible light and smaller effective masses of electron and hole carriers than TiO_2, confirming its photocatalysis applications.

Study on Titanium Dioxide Nanomaterials with Specific Crystal Facet for Enhanced Photocatalytic and Dye-Sensitized Solar Cells Performances

Linfeng Xu

Anhui University of Science & Technology, China

Abstract

TiO_2, as one of the most promising semiconductor materials, has become a topic of intense research. It has been reported that the main influencing factors on the photocatalytic activity are surface area, crystallinity, and crystal-facet on the surface. Most recently, intense attention has been paid to well-exposed high-surface-energy facets, such as {010}-, {001}- and [111]-facets. Up to now, [111]-faceted TiO_2 nanocrystals were synthesized and showed excellent photocatalytic and DSSC performance. However, these TiO_2 nanocrystals were synthesized using hydrofluoric acid solution. In the present study, we report an environment-friendly and facile one-pot process for [111]-faceted anatase TiO_2 nanocrystals and research their photocatalytic and DSSC performance and the influence of crystal-facet on the blue shift of bandgap.

To synthesize anatase nanocrystals, TTIP was mixed with TMAOH aqueous solution (TMAOH/TTIP mole ratio=0.3) at room temperature to obtain a suspension solution. And then the suspension solution was hydrothermally treated at 200 ^{o}C for 24h after adjusting to a desired pH value. The product is named 0.3-200-X (X: pH value of solution). Fig 1 shows TEM images of anatase TiO_2 nanocrystals synthesized at different pH conditions. The crystal size is strongly dependent on the pH value of reaction solution which increases with the increasing of pH value. The cuboidal anatase nanocrystals with uniform crystal size and [111]-facet on the surface can be synthesized easily by the hydrothermal treatment of the TMA-TTIP suspension solution in the pH range of 9-12 and their crystallinity increases with increasing pH value.

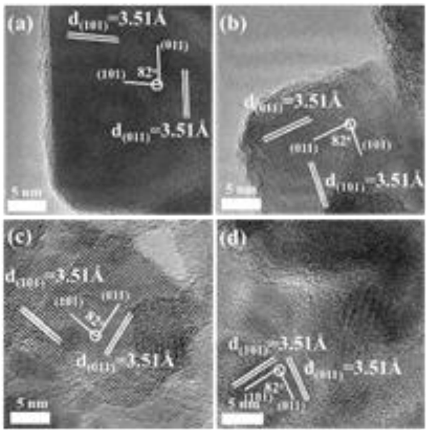

Fig. 1. TEM images of (a) 0.3-200-11; (b) 0.3-200-9; (c) 0.3-200-5; (d) 0.3-200-3.

In the formation process of the [111]-faceted TiO_2 anatase nanocrystals, firstly an intermediate of layered titanate is formed by the hydrolysis reaction of TTIP in TMAOH solution. The layered titanate is exfoliated to the titanate nanosheets, and then stacking of

titanate nanosheets, structural transformation to anatase, and dissolution-deposition reaction of anatase polycrystalline particles occur gradually.

Table I shows the characteristics of synthesized [111]-faceted anatase nanocrystals, P25 (40% [111]-faceted nanocrystals), and ST-20 (non-facet) nanoparticles. Fig.2 exhibits bandgap dependence on the crystal size of anatase with different facets on the surface. The bandgap blue shift increases in an order of: non-face < [111]-facet < {010}-facet, revealing the surface energy affects the blue shift behavior. The photocatalytic activity of MB degradation increases in an order of ST-20 < 0.3-200-11 < P25 < 0.3-200-9 < 0.3-200-5, which matches with the bandgap energy increasing order. The higher bandgap energy of the [111]-faceted nanocrystals is a reason why it shows higher surface photocatalytic activity than that of non-faceted nanocrystals (ST-20). The higher bandgap energy causes higher potential reductive electrons for the photocatalytic reduction reaction. The DSSCs results also reveal that the [111]-faceted anatase nanocrystals present a higher DSSCs performance than that of the non-faceted nanocrystals due to the strong binding of dye molecule on TiO_2 [111]-faceted surface.

Sample	Exposed facet	Crystal phase	Eg (eV)	Crystal size(nm)	S_{BET} (m^2/g)
0.3-200-5	[111]	Anatase	3.08	10	112.3
0.3-200-9	[111]	Anatase	3.06	20	56.3
P25	40% [111]	Anatase/ rutile	3.04	20	54.6
0.3-200-11	[111]	Anatase	3.02	50	37.9
ST-20	Non-facet	Anatase	3.01	20	62.6

Table I. Exposed facet, crystal phase, bandgap, crystal size and surface area of TiO_2 nanocrystals

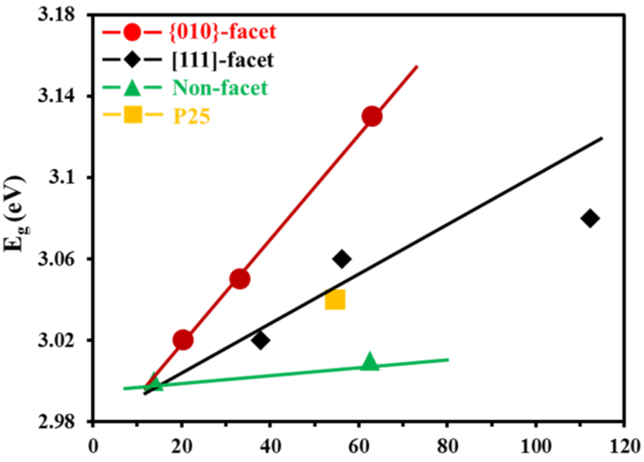

Fig. 2. Dependences of bandgap energy on crystal size for anatase with different facets

Thermodynamic modeling of the Ti–V system for the third generation CALPHAD database including metastable ω phase

Biao Hu*, Jin Zhang, Yu Zhang

School of Materials Science and Engineering, Anhui University of Science and Technology, Huainan, Anhui 232001, PR China

*E-mail address: hubiao05047071@163.com, bhu@aust.edu.cn

Abstract

Thermodynamic model based on the Einstein function with more physical significance has been used to describe the hcp, bcc, fcc, ω, liquid and amorphous phases for titanium and vanadium from high temperature down to 0 K by the CALPHAD (Calculation of Phase Diagrams) approach for the third generation of thermodynamic databases. The liquid and amorphous phases have been treated as one phase by the generalized two-state model. The Debye temperatures and the ground state energy differences at 0 K for different allotropes of titanium and vanadium have been computed by *ab initio* calculations based on the density functional theory (DFT). The Ti–V system has been reassessed based on the new Gibbs energy functions of titanium and vanadium obtained in the present work and experimental data available in the literature. The metastable phase diagram of the Ti–V system with $T_0(\beta/\alpha)$ and $T_0(\beta/\omega)$ curves has been calculated using the obtained thermodynamic parameters. The calculated results indicate that almost all of the reliable experimental data are satisfactorily reproduced by the present modelling.

Keywords: Ti–V; ω phase; Lattice stability; CALPHAD; T_0 curve; Martensitic transformation

The financial support from the National Natural Science Foundation of Anhui Province (No. 2008085QE200) and Anhui Province University Natural Science Research Projects of China (No. KJ2019A0113) are greatly acknowledged.

Reference:

1. [1] Q. Chen, B. Sundman, *J. Phase Equilib*. 22 (2001) 631-644.
2. [2] B. Hu et al., *Intermetallics*, 122 (2020) 106791.

OL-19

Tuning of the thermoelectric properties of quaternary compounds, ABZnSb (A = Sr, Ba and rare earth elements; B = F and O) with the ZrCuSiAs structure type

Jing-Tai Zhao
School of Materials Science and Engineering, Guilin University of Electronic Technology, Guangxi, China
Email：jtzhao@guet.edu.cn

Abstract

Quaternary layered compounds ABZnSb (A = Sr, Ba, and rare earth elements; B = F and O) adopt the tetragonal ZrCuSiAs structure ($P4/nmm$), consisting of [AB] layer and [ZnSb] layer alternately stacking along the c axis. In the [ZnSb] layer, Zn is tetrahedrally coordinated with four Sb atoms, forming edge-sharing tetrahedrons [$ZnSb_{4/4}$]. [ZnSb] layer has been viewed as a promising carrier tunnel due to the weak scattering and high carrier mobility, can be tuned by substitution of both Zn and Sb sites by other elements which can modify the carrier concentration and mobility. The similar effects have been studied in the Zintl systems of AZn_2Sb_2 and related systems. The [AB] layers matched with the ZnSb layer will play an important role in lowering thermal conductivity acting as some sort of thermal barrier, resulting to an overall potential optimization of the thermal property. The flexible chemical adjustments in these layered compounds provide great potential for the tuning of the electronic conductivity, thermal conductivity, carrier concentration and mobility, structural anisotropy. The phase stabilities of a series of rare earth compounds have been predicted and approved experimentally. The samples of some compounds and their substitutional variants in this system have been prepared and their thermoelectric parameters characterized. The so far maximal thermoelectric figure of merit ZT for $NdOZn_{0.96}Ag_{0.04}Sb$ reaches 0.44 at 725 K. Further optimizations of the electrical and thermal transport properties for other compounds are undergoing.

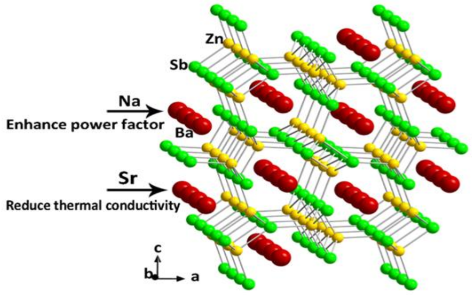

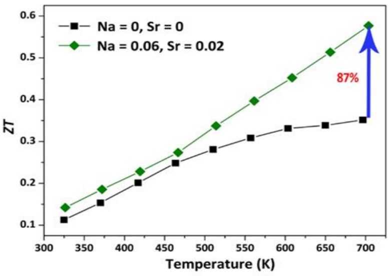

OL-20

Influence of Gamma Irradiation to Modifying Nanoporous Carbon as

Supercapacitor Material

Annisa[1,2 a)], Imam Prasetyo[1, 2, b)], Deni Swantomo[3, c)], Teguh Ariyanto[1,2d)]

[1]Department of Chemical Engineering, Universitas Gadjah Mada, Indonesia

[2]Carbon Material Research Group, Department of Chemical Engineering, Universitas Gadjah Mada, Indonesia

[3]Polytechnic Institute of Nuclear Technology, Indonesia

Email : a)annisa96@mail.ugm.ac.id, b)imampras@ugm.ac.id, c)deni_sttn@yahoo.co.id

d)teguh.ariyanto@ugm.ac.id

Abstract

The effect of gamma irradiation to modify surface chemistry of nanoporous carbon synthesized from coconut shell was examined. Nanoporous carbons, due to high specific surface area, high pore accessibility, and controlled pore structure, have been utilized as material electrode supercapacitors. To obtain high power and energy densities, it is necessary to introduce functional groups in the carbon surface. Alterations of surface chemistry were studied by using Fourier Transform Infrared Spectroscopy (FTIR), surface morphology by scanning electron microscopy and textural pore changes were determined by nitrogen sorption analysis. Irradiated sample in the absence of water showed oxygen functional groups increased and reached optimum point at radiation dose 25 kGy. After gamma irradiation exposed, there were the cavities on the surface of material and the size of cavities got bigger as irradiation dosage increased. While the specific surface area of nanoporous carbon decreased insignificantly after subjected to irradiation. Cyclic Voltammetry (CV) was employed to analyze the capacitive behavior of nanoporous carbon. CV measurements showed an improvement of specific capacitance for the irradiated nanoporous carbon. The highest specific capacitance of 64 F/g was achieved at radiation dose 25 kGy.

Keywords: Gamma irradiation; porous carbon; supercapacitors

OL-21

Green route for synthesis and characterization of Ag/zinc oxide

nanoparticles for antibacterial activity application onto cotton fabrics

Paweena Porrawatkul[1] and Prawit Nuengmatcha[*2]

[1]Creative Innovation in Science and Technology, [2]Nanomaterials Chemistry Research Unit,
Department of Chemistry, Faculty of Science and Technology, Nakhon Si Thammarat Rajabhat
University, 80280, Thailand

Email: prawit_nue@nstru.ac.th

Abstract

The present study reported a green route for synthesis of silver/zinc oxide (Ag/ZnO) nanocomparticles using *Averrhoa carambola* fruit extract by microwave assisted method. The synthesized Ag/ZnO nanocomposite was characterized by using UV–visible spectroscopy, X-ray diffraction (XRD), scanning electron microscopy (SEM), transmission electron microscopy (TEM), energy dispersive X-ray spectroscopy (EDS) techniques. The XRD analysis revealed wurtzite crystalline structure of Ag/ZnO nanocomposite. Electron microscopy images showed agglomeration of Ag/ZnO nanocomposite having spherical shaped structure with size in the range of 30–50 nm. The antibacterial activity of uncoated cotton, *Averrhoa carambola* fruit extract and Ag/ZnO NPs coated cotton fabrics were investigated against Gram positive (*S. aureus*) and Gram negative (*E. coli*) via using agar well diffusion method. It showed that Ag/ZnO NPs coated cotton fabric has higher antibacterial activity than other test samples against both bacteria's. Finally, the modified cotton fabrics were washed through a certain number of laundering cycles and their surfaces and antibacterial performances were investigated. It was found that the modified cotton fabrics remains has antibacterial activity for *E. coli* and *S. aureus* even after 20 washing cycles.

Keywords: *Averrhoa carambola*, cotton fabric, silver/zinc oxide (Ag/ZnO) nanocomparticles

OL-22

Synthesis of nanozeolite-chitosan/sago starch for slow release fertilizer

Rungnapa Pimsen

[1]Nanomaterials Chemistry Research Unit, Department of Chemistry, Faculty of Science and Technology, Nakhon Si Thammarat Rajabhat University, 80280, Thailand.

[*]Corresponding author. Email: rungnapa_pim@nstru.ac.th

Abstract

This study developed the slow-release fertilizers using nanozeolite (NZ) composite chitosan (CS)/sago starch (ST)-based biopolymer. The biopolymer nanocomposite was prepared by ionotropic gelation process using sodium tripolyphosphate as a cross-linking agent. The NZ was synthesized by the co-precipitation method and annealing at 650°C and characterized by scanning electron microscope and energy dispersive X-ray spectrometry, X-ray diffractometry, and transmission electron microscope. The average particle size of NZ is 12.80 nm. The biopolymer nanocomposite was a considerable rise in the swelling ratio when molecular weight of CS and crosslinking times increased. The NZ-CS/ST nanocomposite showed the percentage amount release of phosphorus and urea at the 14th day to be 64.00 and 41.93%, respectively. The obtained fertilizer was applied to grow *Philodendron sp.*, resulting in better growth indicators than the control and urea. Consequently, the prepared nanocomposite maintains the water level and can further be used as slow-release fertilizers in agriculture.

Keywords: Chitosan, Starch, Nanozeolite, Biopolymer, Slow release fertilizer

References

1. Giroto AS, Guimarães GGF, Foschini M, Ribeiro C. Role of Slow-Release Nanocomposite Fertilizers on Nitrogen and Phosphate Availability in Soil. Vol. 7, Scientific Reports. 2017.
2. Riza F, Ftikos C, Tietz F, Fischer W. Preparation and characterization of slow-release and water-retention fertilizer based on starch and halloysite. J Eur Ceram Soc. 2001;21(10–11):1769–73.
3. Lateef A, Nazir R, Jamil N, Alam S, Shah R, Khan MN, et al. Synthesis and characterization of environmental friendly corncob biochar based nano-composite – A potential slow release nano-fertilizer for sustainable agriculture. I Nanotechnology, Monit Manag. 2019;11.

OL-23

Exploration of Improved Processes for Large-Scale Production of ZrO_2 Spheres

Ying-Wei Lu [1]*, Jun Chen [1], Chang-Ming Xu [2,3]*

[1] School of Materials Science and Engineering, Hefei University of Technology, Hefei, Anhui 230009, P. R. China

[2] Suzhou Nutpool Materials Technology Co., Ltd, Suzhou, 215513, P. R. China

[3] Jiangxi Nutpool Industrial Co., Ltd, Yongfeng, 331500, P. R. China

*Corresponding author (Ying-Wei Lu: luyw@hfut.edu.cn, Chang-Ming Xu: nanopure@qq.com)

Abstract

It is well known that ZrO_2 is one of the most important ceramic materials, which has been widely employed in various application fields due to its unique physical and chemical properties, among which, the monodispersity and high sphericity of ZrO_2 spheres are two key factors to achieve ZrO_2 products with better performance. Many fabrication methods, for instance microemulsion method **오류! 참조 원본을 찾을 수 없습니다.**, colloid-aggregation process, sol-gel process and so on, have been reported to fabricate ZrO_2 spheres with monodispersity and high sphericity. However, there are some disadvantages in these techniques, such as high cost, low product yield and complicated procedures. We hereby respectively carried out an improved traditional process (Spray Granulation) and an advanced technique (Micro-Droplet Spray Forming) to fabricate monodispersed ZrO_2 ceramic spheres with high sphericity and promising mechanical performance. Based on the demonstration of the parameter effects on the morphology and mechanical properties of ZrO_2 spheres, we believe both of our two preparation methods could serve for the industrial production of zirconia and other ceramic materials since they are stable process with high yield and excellent quality.

Key words: ZrO_2 spheres, Spray Granulation, Micro-Droplet Spray Forming, Optimization, Forming mechanism, Mechanical performance

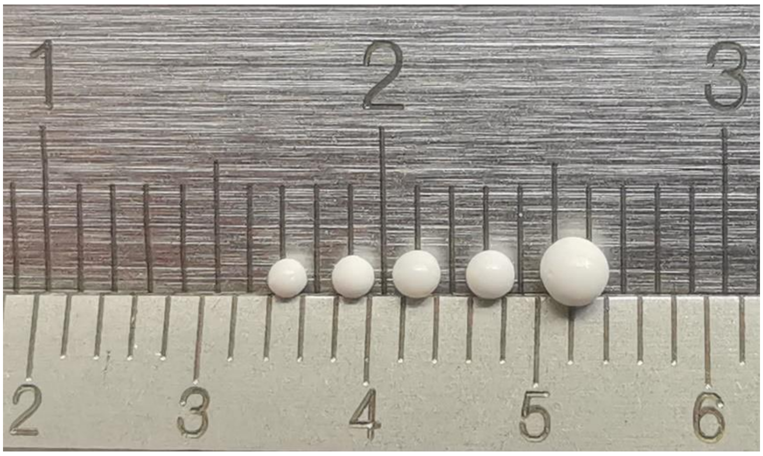

Fig.1 Sintered ZrO_2 spheres with different sizes

References

1. Yao HB, Jia DM, Zhang HM. A new approach of fabricating monodisperses micrometer hollow zirconia spheres. Ceram Int. 2015, 41(1):1531-1534.

2. Park KY, Jung YG, Kim IS, Yang BI. Effects of purity and phase content of feedstock powder on thermal durability of zirconia-based thermal barrier coatings. J Therm Spray Tech. 2017, 26(6):1161-1167.

3. Bergamaschi VS, Carvalho FMS, Rodrigues C, Fernandes DB. Preparation and evaluation of zirconia microspheres as inorganic exchanger in adsorption of copper and nickel ions and as catalyst in hydrogen production from bioethanol. Chem Eng J. 2005, 112(1-3):153-158.

4. Silva ADR, Rigoli WR, Osiro D, Mello DCR, Vasconcellos LMR, Lobo AO, et al. Surface modification using the biomimetic method in alumina-zirconia porous ceramics obtained by the replica method. J Biomed Mater Res B. 2018, 106(7):2615-2624.

5. Couland M, Fourcaudot S, Abril RJ, Fernandez-Carretero A, Somers J. Novel production route of yttria-stabilized zirconia fuel kernels and pellets for nuclear fuel applications. J Am Ceram Soc. 2012, 95(1):133-137.

6. Yan BW, McNeff CV, Chen F, Carr PW, McCormick AV. Control of synthesis conditions to improve zirconia microspheres for ultrafast chromatography. J Am Ceram Soc. 2001, 84(8):1721-1727.

7. Kim JW, Bae K, Kim HJ, Son J, Kim N, Stenfelt S, et al. Three-dimensional thermal stress analysis of the re-oxidized Ni-YSZ anode functional layer in solid oxide fuel cells. J Alloy Compd. 2018, 752:148-154.

8. Liang SS, Li J, Li XM, Man J, Nunes JK, Chen HS. Microfluidic fabrication of ceramic microspheres with controlled morphologies. J Am Ceram Soc. 2018, 101(8):3787-3796.

9. Walter M, Somers J, Fernandez A, Specht ED, Hunn JD, Boulet P, et al. Structure of yttria stabilized zirconia beads produced by gel supported precipitation. J Mater Sci. 2007, 42(12):4650-1658.

10. Wang GG, Ma JT, Gao Y. A comparative study of small-size ceria–zirconia microspheres fabricated by external and internal gelation. J Sol-Gel Sci Techn. 2016, 78(3):673-681.

11. Xu R, Chen JS, Zhao SJ, Hao SC, Zhao XY, Li JJ, et al. Preparation of monodisperse ZrO_2 ceramic microspheres (>200μm) by co-axial capillary microfluidic device assisted internal gelation process. Ceram Int. 2019, 45(16):19627-19634.

OL-24

Computational materials design and characterisation for functional inorganic materials

P. Vajeeston

Center for Materials Science and Nanotechnology, Department of Chemistry, University of Oslo, Box 1033 Blindern N-0315, Oslo, Norway, e-mail: ponniahv@kjemi.uio.no

O23_Vajeeston.pdf

Abstract

High-throughput computational materials design is an emerging area of materials science and technology. By combining advanced computational methods with intelligent database construction and exploiting the power of current supercomputer architectures one can generate, manage and analyse enormous data repositories for the discovery of novel materials for energyrelated technologies. Although the demand for materials is endlessly growing, experimental discovery is bound by high costs and time-consuming procedures of synthesis. Computational materials science is an alternative burgeoning area for computational materials design. It is based on the bridge between computational quantum-mechanical, thermodynamic and spectroscopic approaches. In this presentation, I am going to present our recent activities on battery materials and light-absorbing materials for photovoltaic applications. Although a commercial success, lithium ion batteries are still the object of intense research mainly aimed to the characterization of improved electrode and electrolyte materials. We have modelled relative stability, electronic structure, thermodynamical, electrochemical and mechanical properties of several potential cathode and electrolyte materials for Li/Na ion batteries. This study presents a short review of our recent progress dedicated to the electrode and electrolyte materials that have the potential to fulfil the crucial factors of cost, safety, lifetime, durability, power density, and energy density.

Recent advancement of molecular based techniques in the authentication of food products

M. A. Motalib Hossain

Nanotechnology and Catalysis Research Centre (NANOCAT), University of Malaya, 50603 Kuala Lumpur, Malaysia

Abstract

Authentication of food products has become an important and routine work under the supervision framework of most countries to prevent diseases transmitted by meat and bone meal as well as meat adulteration by mixing materials of different animal origins. Specifically, adulteration of animal materials is of serious religious, health and economic concerns. protein-based methods are less effective since the target biomarkers could be modified throughout the processing treatments. On the other hand, molecular based techniques have gained wider acceptance and reliability because of the superior stability and universality of DNA in all tissues and cells. Among the molecular based techniques, multiplex polymerase chain reaction (PCR) assays are greatly promising for the screening of multiple species targets in a single assay platform, saving analytical cost and time. Recently, nanotechnology-based biosensor approaches for DNA detection have attracted the attention of scientists as well as end-users due to its rapidness, stability, low cost and in-field application. The biosensor is an analytical device which integrates a biologically active component like DNA, antibodies, aptamers etc. with a suitable physical transducer to generate a quantifiable signal proportional to the amount of analyte exist in the sample.

The study on preparation and application of formed granular bentonite

Kunhong Hu*, Nana Zhou, Guangchao Qin

(School of Energy Materials and Chemical Engineering, Hefei University, Hefei, 230601, China)

**Corresponding author, Email: hukunhong@163.com*

Abstract

Ammonia nitrogen is one of the most common water pollutants with a wide range of sources. It can lead to eutrophication and the deterioration of water environments and has serious impact on the ecological environment and human health. Therefore, the pollution control of ammonia nitrogen wastewater is crucial. Bentonite, a nonmetallic mineral material, is a rich resource with a low cost. It is commonly used as an environment-friendly adsorbent due to its good water absorption, expansibility, and adsorbability. In this study, sodium bentonite and porous agent $NaHCO_3$ were used as the primary raw materials to prepare granular bentonite via extrusion granulation. The structure, composition, and morphology of sodium bentonite powder and the formed granular bentonite were tested and analyzed. Sodium bentonite exhibits good adsorption property, and bentonite powder is formed into particles via extrusion and granulation, avoiding the disadvantage of powder of being easy to bond and separate while being used. The operation method is simple, and the formation of granules is easy to control.

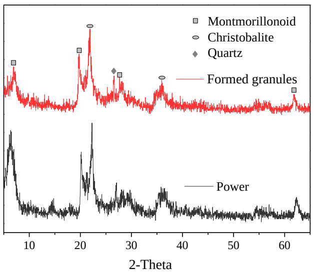

Granular bentonite exhibits good water absorption, rapid agglomeration, and high strength. It can wrap and absorb pet waste and odor. Bentonite raw materials are nontoxic, tasteless, and noncorrosive. The formed particles are dust-free. Cat litter can solve the problem of fecal and urine contamination caused by household pets; thus, it is good for indoor cleaning and the healthy growth of pets. This study provides a theoretical basis for the preparation of granular bentonite and the treatment of ammonia nitrogen wastewater. Moreover, results have a certain reference value for the application research of granular bentonite as cat litter.

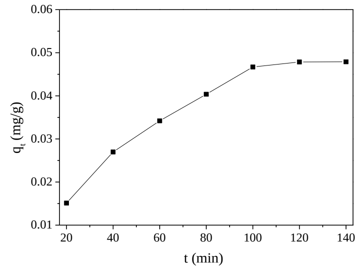

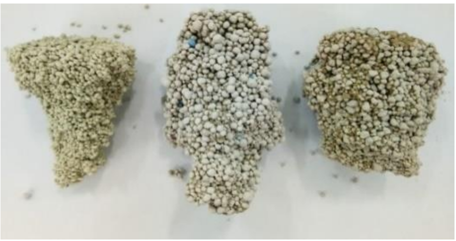

References

[1] Mazloomi F , Jalali M . Environmental Monitoring and Assessment, 2017, 189(8):415.

[2] Yin Q , Zhang B , Wang R , et al. Environmental Science and Pollution Research, 2017, 24:26297-26309.

Novel and simple process for the photocatalytic reduction of CO_2 with TMDSc-Graphene nanocomposite

Asghar Ali[1], and Won-Chun Oh[1] *

1.Department of Advanced Materials Science & Engineering, Hanseo University, Seosan-si, Chungnam, Korea, 356-706.

Abstract

In present work, the new binary composite WSe_2-Graphene are synthesized using hydrothermal as well as X-ray diffraction (XRD), scanning electron microscopy (SEM), transmission electron microscopy (TEM), X-ray photoelectron spectroscopy (XPS), Raman spectroscopy, and UV–Visible diffuse-reflectance spectra (DRS) analyses. The prepared photocatalysts were tested for the CO_2 photocatalytic reduction in a reactor, and the main detected reaction product is CH_3OH. The optimum loading graphene of 12% exhibits maximum photoactivity, achieving a total CH_3OH yield of 9.240 μmol g−1 h−1after 4days. This outstanding photoreduction activity is due to the positive synergistic relation between the WSe_2 and the graphene components in our heterogeneous system. The present work provides a novel application regarding the improvement of nanoscale WSe2-Graphene materials for photocatalytic applications.

References

1. Yuan, L. & Xu, Y.-J. Photocatalytic conversion of CO_2 into value-added and renewable fuels. Applied Surface Science 342, 154–167, (2015).
2. Voiry, D. et al. Enhanced catalytic activity in strained chemically exfoliated WS_2 nanosheets for hydrogen evolution. Nature materials (2013).
3. H. Kyung, J. Lee, and W. Choi, Environmental science & technology 39 (7), 2376-2382 (2005).
4. R. Vinu and G. Madras, Applied Catalysis A: General 366 (1), 130-140 (2009).

Corresponding author
E-mail: wc_oh@hanseo.ac.kr
Tel: +82-41-660-1337, Fax:+82-41-688-3352

Effect of Flake-Shape and Content of Nano Mullite on Mechanical Properties and Fracture Process of Corundum Composite Ceramics

Wei Lian[1], **Yan Liu**[1], **Wenjie Wang**[1], **Yangtao Dong**[1], **Sheng Wang**[1], **Rui Zhu**[1], **Nan Xie**[1], **Yueqin Wang**[2], **Zhenying Liu**[1], **Yin Liu**[1,3], **Lingbing Kong**[4]

1. *School of Materials Science and Engineering, Anhui University of Science and Technology, Huainan 232001, Anhui, China*
2. *School of Mechanics and Optoelectronic Physics, Anhui University of Science and Technology, Huainan 232001, Anhui, China*
3. *State Key Laboratory of Mining Response and Disaster Prevention and Control in Deep Coal Mines, Anhui University of Science and Technology, Huainan 232001, Anhui, China*
4. *College of New Materials and New Energies, Shenzhen Technology University, Shenzhen 518118, Guangdong, China*

Corresponding author: Tel:86-554-6668643; E-mail: yinliu@aust.edu.cn (Liu Yin)

Abstract: Coal gangue is used to prepare flake nano mullite with a molten salt method. In order to increase the utilization value, corundum composite ceramics were prepared from the nano-mullite and alumina. The effect of particle size of the raw material size and the content of mullite on mechanical properties of the corundum composite ceramics was studied. It is found that the mullite with appropriate sizes can be filled in between the corundum grains, thus increasing the density of the samples. The mechanical properties were enhanced due to the variation in the crack propagation mode. The optimized sample exhibited flexural strength and fracture toughness of 263.73 MPa and 5.01 MPa·$m^{1/2}$, respectively. Griffith fracture theory analysis results indicated that the critical crack size reached173.86 μm and the fracture energy was 127.55 J/m^2. Coal gangue has realized deep resource utilization, and the mechanical properties of composite ceramics are higher than alumina ceramics prepared under the same conditions. Flake nano-mullite contributes to mechanical properties.

Keywords: Corundum composite ceramics; Mechanical properties; Gangue

Hydrothermal synthesis of organic perovskite and organic-inorganic hybrid three-dimensional perovskite ferroelectrics with H_2Dabco cation

Yang Fan[a], Yin Liu[a, b,*]

a. School of Materials Science and Engineering, Anhui University of Science and Technology, Huainan 232001, Anhui, China

b. State Key Laboratory of Mining Response and Disaster Prevention and Control in Deep Coal Mines, Anhui University of Science and Technology, Huainan 232001, Anhui, China

Abstract: Perovskite piezoelectric ferroelectric materials are widely used in aerospace, national defense and military industry, mobile phones and submarine sonar. Compared with inorganic perovskites, organic perovskites are more flexible, light, environmentally friendly and biocompatible. In this paper, we designed a kind of organic perovskite ferroelectric materials, in which NH_4X was dissolved in water, then phosphoric acid and 1,4-diazabicyclo [2.2.2] octane ($C_6H_{12}N_2$) was added and stirred continuously. A temperature dielectric responsive organic perovskite (H_2Dabco)NH_4X_3 was prepared by heating the final mixture in a Teflon lined steel autoclave at 160 ℃ for about 3 days, and then cooling to room temperature. The principle of this method is to replace the B site in the general formula ABX_3 (doubly protonated 1,4-diazabicyclo [2.2.2] octane = H_2Dabco). At the same time, a similar structure hybrid perovskite (H_2Dabco)KX_3 was designed as a control. The piezoelectric and ferroelectric properties of pure organic perovskite and organic-inorganic hybrid perovskite with H_2Dabco cation were compared. On the other hand, the order disorder transition of their organic "spherical" cation (H_2Dabco) is believed to result in their phase transition and dielectric response switching. In view of its excellent ferroelectric and piezoelectric properties, (H_2Dabco)NH4X_3 organic perovskite will gradually replace inorganic perovskite in the potential application of piezoelectric and ferroelectric devices in the future.

Key words: ferroelectric, piezoelectric, organic cation, perovskite

Development of Co-based alloys for high temperature applications

Phacharaphon Tunthawiroon

Department of Industrial Engineering, Faculty of Engineering, King Mongkut's Institute of Technology Ladkrabang, Bangkok 10520, Thailand

Abstract

Recently, Co-based alloys have been widely used for the replacement of current hot-working tool steels and heat-resistance components because they exhibit high degree of corrosion resistance. Nevertheless, direct exposure to high temperature during the service life always leads to the oxidation process that continuously attacks the surface of alloys, resulting in metal surface deterioration. Therefore, it is practically essential to characterize and control the oxide films formed on the surface of alloys. In this work, the high temperature oxidation behavior of the Si-doped Co–Cr–Mo alloy was investigated. The isothermal oxidation heat treatment at 700 ºC was conducted in air. The Si concentration (x) was varied between 0.1, 0.5, 1.0, 3.0, and 5.0 wt.%. The morphologies of oxide film formed on the oxidized surface of Co–Cr–Mo alloys were characterized using a scanning electron microscope (SEM). Meanwhile, the chemical compositions of the oxide were analyzed using the SEM equipped with an energy-dispersive spectroscope (EDS). The X-ray photoelectron spectroscopy (XPS) was conducted to identify the compositions, oxidation states, and thickness of the oxide film formed on the surface of the oxidation-treated alloys. The chemical compositions of the surface analysis revealed that Si concentrations played a role in the stabilization of Cr oxides on the surface of Co–Cr–Mo–xSi alloys. With the increasing Si concentration in the Co–Cr–Mo–xSi alloy, the Co-oxide was suppressed by Cr-oxide owing to the selective oxidation of Cr atoms. The SiO_2 was both found along the grain boundaries and interface between the outmost oxide and matrix. In addition, the existence of a considerably stable Cr-oxide and sub-layered SiO_2 when compared with the Co-oxide became a barrier in inhibiting the inward and outward diffusion of O and Cr. Thus, the oxide thickness was reduced with the increase in Si concentration. This investigation might help in manufacturing and design engineering for the optimization of other alloyed element conditions.

Solvating modulation effect of ionic liquids toward Fe_3O_4 nanomaterials

Hong Chen*, Qin Zhan, and Caiyu Ni

Department of Chemical Engineering, School of Energy Materials and Chemical Engineering, Hefei University, Hefei 230601, Anhui, China

Abstract

Herein, ionic liquids were selected as the medium to design, synthesize and magnetic functionalize imidazole ionic liquids. The solvation effect of two ionic liquids in the preparation of Fe_3O_4 nanomaterials was investigated. The main work is one-step synthesis of imidazole ionic liquid [C4mim]Br by ultrasonic-assisted method and magnetic functionalization to [C4mim]$FeBrCl_3$. Fe_3O_4 nanomaterials were prepared by coprecipitation method using [C4mim]Br and [C4mim]$FeBrCl_3$ as media respectively. The characteristics of Fe_3O_4 nanomaterials in different media were analyzed by SEM, XRD, IR and TG, including particle size, saturation magnetic field strength, morphology and other parameters. The solvation control effect of ionic liquid on metal oxide nano-materials was investigated, and its application in photocatalytic degradation of wastewater was compared. The degradation of malachite green wastewater was used as a probe reaction to investigate the catalytic activity of Fe_3O_4 nanomaterials. The results showed that the catalytic decolorization rates of Fe_3O_4 (medium 1) and Fe_3O_4 (medium 2) were 95.37% and 94.94% respectively. Compared with 86.81% in aqueous medium, the catalytic performance of Fe_3O_4 prepared in ionic liquid medium was improved more.

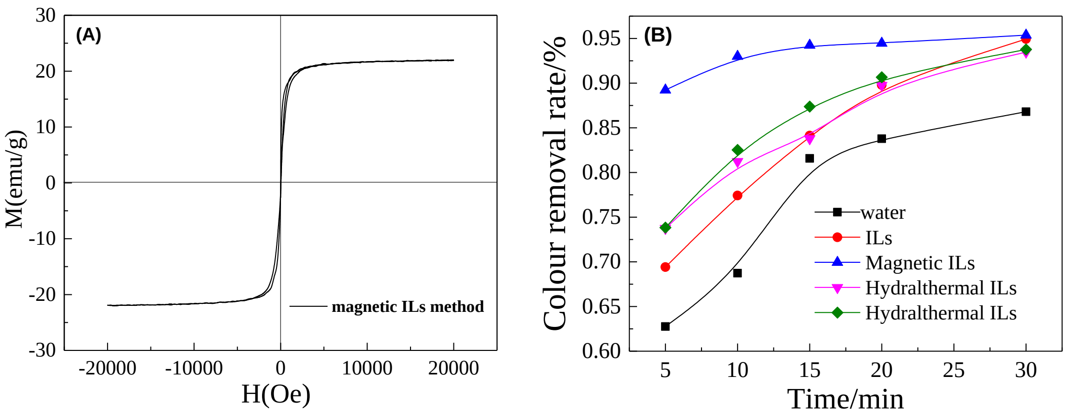

Figure 1 Fe_3O_4 Hysteresis loop (A) and effect of Fe_3O_4 on decolorization rate of malachite green (B)

Key words: Ionic liquids； Magnetic ionic liquid, Ferroferric oxide, Acknowledgements: This work was supported by Natural Science Foundation of China

OL-32

Research on adsorption properties of rape straw biochar to dye wastewater

WU YING[1]*，LIU Yunfeng[1,2]

(1.School of Energy Materials and Chemical Engineering, Hefei University, Hefei, 230601, China

3. Shanghai Tofflon Science&Technology Co.,Ltd. Shanghai, Shanghai, China)

**Corresponding author, Email: wuying@hfuu.edu.cn*

Abstract

To rape straw as raw material, using zinc chloride modified prepared modified rapeseed straw biochar. The study of modified biochar to printing and dyeing wastewater of reactive brilliant red X-3B adsorption performance, pH, temperature, reactive brilliant red X-3B, initial concentration and adsorbent additive quantity's influence on the removal rate.

The optimum temperature, pH, dosage of adsorbent and initial concentration of active brilliant red X-3B were determined by static adsorption experiment. Selected pH, reactive brilliant red X-3B initial concentration and adsorbent additive amount of three variables to orthogonal experiment, get the optimal experimental conditions of adsorption pH6.55, reactive brilliant red solution of the initial mass concentration of 75 mg/L, dosing quantity is 0.6 g/L, under the condition of the equilibrium adsorption capacity of 76.19 mg/g. To explore the sequence of factors influencing the removal rate, including the initial mass concentration, adsorbent dosage and pH of active brilliant red X-3B. By some kinds of characterization, suggests $ZnCl_2$ modification has brought obvious changes in the microstructure of biochar, very beneficial to straw biomass charcoal adsorption active brilliant red X-3B, for electrostatic adsorption effect, and is accompanied by chemical adsorption.

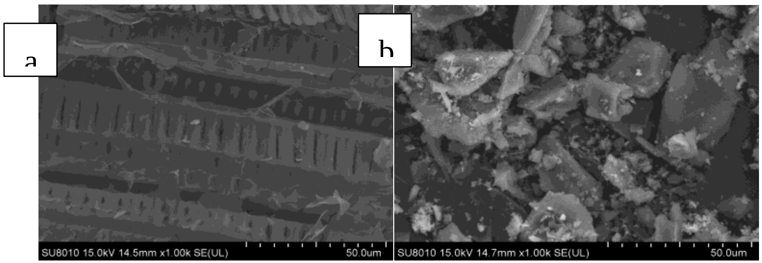

Fig.1 SEM photos of the samples（a:Raw rape straw; b: modified straw biochar）

Keywords: Biochar; Reactive brilliant red X-3B; Adsorption

Acknowledgments: This project was supported by Anhui province natural science research fund follow-up project. (No.1800031822)

References

1. Surchi K M S. Agriculture wastes as low-cost adsorbents for Pb removal: Kinetics, equilibrium and thermodynamics[J]. International Journal of Chemistry, 2011, 3(3): 102-113.
2. Zhu Z Q. Research on printing and Dyeing Wastewater Treatment Technology[J].Jiangxi Chemical Industry,2017,(6):55-57
3. Wang Y, Wu Y. Adsorptive removal of Co(Ⅱ) from aqueous solution by using modified cole straw[J].Chinese Journal of Environment Engineering, 2016,10(1):379-384.
4. Huang X Q, Li T Y. Competitive effects and mechanisms of the biosorption for removal Pb(Ⅱ) by rape straw powders from multi-ion aqueous solutions[J].Environmental Science of China,2017,37(9):3363-3370.
5. Zhang J Y, Li G. Preparation of biochar adsorbent from straw and its adsorption capability [J]. Transactions of the Chinese Society of Agricultural Engineering, 2011,27 (2): 104-109
6. Ji X Q, Lu L. Sorption properties and mechanisms of organic dyes by straw biochar[J].Chinese journal of environment science,2016,36(5):1648-1654.

Preparation and Properties of Nitrogen-doped Carbon-based Electrode Materials

Tianhao Hu ,Guotao Dong, Ye Ge，Zhihao Hu，Youyang Chen，Jing Wang *

College of Materials Science and Engineering, Anhui University of Science And Technology, Huainan, Anhui 232001

Corresponding author (Phone and WeChat: + 0086 (13855418833); jingwang@aust.edu.cn)

Abstract: With the development of new energy sources, such as supercapacitors and battery storage devices have attracted attention. Therefore, in order to improve the energy density of supercapacitors, we can increase the specific capacitance of the electrode. The specific capacitance of the electrode is related to the electrode materials, among which porous carbon materials have wide sources, stable structure, large specific surface area and adjustable aperture, and are widely used in the field of energy storage.

It is of great significance to select suitable preparation methods and carbon sources for controlling the size of carbon materials and reducing the cost. Nitrogen-doped porous carbon materials for high performance supercapacitors were synthesized by one-step activation with the introduction of nitrogen source and activation reagent. Specific steps are as follows: first, the peanut shells, biomass of longan shell shattered, then mixed with activated reagent, and nitrogen source in a certain proportion, the mixture of distilled water was added into the impregnation after a period of time, the drying time, finally the mixture in the tube furnace high temperature activation for a period of time, filtration, washing and drying the solid super capacitor with high-performance nitrogen doping multistage aperture carbon materials. In addition, the combustion reaction can also be used to synthesize nitrogen-doped porous carbon materials.

Nitrogen-doped porous carbon materials have become one of the research hotspots in the field of carbon materials. The product has obvious porous structure, large specific surface area and nitrogen doping, so it has a broad application prospect.

Keywords: Supercapacitor；Nitrogen-doped porous carbon material；One-step activation method；Combustion method；Electrochemical performance

References:

[1] Samahe Sadjadi, Masoumeh Malmir, Bastien Léger, et al. Palladium nanoparticles supported on nitrogen doped porous carbon material derived from cyclodextrin, glucose and melamine based polymer: promising catalysts for hydrogenation reactions. 2020, 92(6):827-

837.

[2] Zhao X , Li A , Quan X , et al. Efficient electrochemical reduction of nitrobenzene by nitrogen doped porous carbon[J]. Chemosphere, 2020, 238(Jan.):124636.1-124636.8.

[3] He G , Yan G , Song Y , et al. Biomass Juncus Derived Nitrogen-Doped Porous Carbon Materials for Supercapacitor and Oxygen Reduction Reaction[J]. Frontiers in Chemistry, 2020, 8:226.

[4] Hoque M K , Behan J A , Stamatin S N , et al. Capacitive storage at nitrogen doped amorphous carbon electrodes: structural and chemical effects of nitrogen incorporation[J]. Rsc Adv, 2019, 9(7):4063-4071.

[5] Jinxing Z , Chang L , Kun X , et al. In-Situ Template Formation Strategy for the Preparation of Nitrogen Doped Carbon Nanocage with Graphitic Shell as Electrode Material for Supercapacitor[J]. Journal of Nanoscience and Nanotechnology, 2018, 18(10):6949-6956.

[6] Mao Z , Zhao S , Wang J , et al. Facile synthesis of nitrogen-doped porous carbon as robust electrode for supercapacitors[J]. Materials Research Bulletin, 2018, 101(MAY):140-145.

[7] Zhang H , Mo Z , Guo R , et al. Facile preparation of three-dimensional honeycomb nitrogen-doped carbon materials for supercapacitor applications[J]. Journal of Materials Research, 2019, 34(7):1200-1209.

[8] Wang P , Tao L , Luo H , et al. Organosilica-based ionogel derived nitrogen-doped microporous carbons for high performance supercapacitor electrodes[J]. Inorganic Chemistry Frontiers, 2018, 5(12):3091-3098.

OL-35

Preparation and Properties of Carbon-based Metal Oxide Composite

Electrode Materials

Guotao Dong, Tianhao Hu, Ye Ge, Zhihao Hu, Youyang Chen, Jing Wang *

College of Materials Science and Engineering, Anhui University of Science And Technology, Huainan, Anhui 232001

**Corresponding author (Phone and WeChat: + 0086 (13855418833); jingwang@aust.edu.cn)*

Abstract: The development of new energy technology has become an important means to solve the traditional energy crisis and protect the environment[1,2]. Compared with traditional energy storage devices,supercapacitors have the advantages of high specific capacitance, fast charge and discharge, green environmental protection and excellent cycle stability[3-5]. Therefore, supercapacitors have a broad space for development in the fields of industry, equipment and transportation[6]. Transition metal oxides have typical pseudo-capacitance behavior, which depends on reversible redox reaction and chemical adsorption/desorption process to store charge[7]. However, transition metal oxides have some disadvantages such as poor conductivity and poor cycle stability. A large number of studies have shown that the composite of transition metal oxides and carbon materials is an effective way to solve the above problems[8].

This paper focuses on the application of carbon-based metal oxide electrode materials in supercapacitors. Carbon-based metal oxide electrodes were prepared by microwave hydrothermal method and their pseudo-capacitance properties were studied.$NiCo_2O_4$ crystal was synthesized by microwave-assisted hydrothermal method and subsequent calcination process. The effect of microwave reaction time on the crystal structure and morphology of $NiCo_2O_4$ was investigated. Carbon nanotubes were compounded with $NiCo_2O_4$ by hydrothermal method, and their electrochemical properties were tested. The results show that the electrode has excellent pseudo-capacitance properties and good cycle stability.

Keywords: Metallic Oxide；$NiCo_2O_4$；Carbon Nanotubes；Hydrothermal Method, Electrochemical Performance

References:

[1] Dajun Wu, Haochi Han, Xuekun Hong, et al. A novel self-branching $MnCo_2O_4$/nanographene hybrid composites on macroporous electrically conductive network as bifunctional electrodes for boosting miniature supercapacitors and sodium ion batteries. 2020, 846:155720-155732.

[2]Ipsita P. Swain, Shantanu K. Behera. Nanoporous carbon hybrids derived from polymethylsilsequioxane for ultracapacitor electrodes. 2020, 303:110290-110295.

[3]BoopathiRaja, M. Parthibavarman. Desert rose like heterostructure of $NiCo_2O_4$ /NF@PPy composite has high stability and excellent electrochemical performance for asymmetric super capacitor application. 2020,

346:136270-136279.

[4]Liang Shao, Juanjuan Xu, Jianzhong Ma, et al. MXene/RGO composite aerogels with light and high-strength for supercapacitor electrode materials. 2020, 19:108-113.

[5]ZHANG S, ZHU J, QING Y, et al. Ultramicroporous carbons puzzled by graphene quantum dots: Integrated high gravimetric, volumetric, and areal capacitances for supercapacitors [J]. Advanced Functional Materials, 2018, 28(52):223-230.

[6]Chaoxian Chen, Chenyang Zhao, Cuihua Li, et al. Porous NiCo2O4 Nanowire Arrays as Supercapacitor Electrode Materials with Extremely High Cycling Stability. 2020, 36(4):715-720.

[7]Mingming Liu,Chao Cai,Zhijie Zhang,Rui Liu.Transition metal oxides loaded with nano-carbon materials as electrode materials for supercapacitors[J].Materials Reports, 2019, 33(01): 103-109.

[8]Qiaoqin Li, Xiaoqin Wang, Nana Yang, et al. Hydrangea- like NiCo- based Bimetal- organic Frameworks, and their Pros and Cons as Supercapacitor Electrode Materials in Aqueous Electrolytes. 2019, 645(16): 1022-1030.

The Functionalization of Two-Dimensional $Ti_3C_2T_x$ MXenes with TPME to Enhance Hydrophobicity and Stability

Guojun Cheng[a,b,*], Shen Tian[a], Ziyue Xuan[a], Feixiang Sha[a], Guoxin Ding[a],

Zhoufeng Wang[a], Xianglong Wan[a,b,], Konghu Tian[a], Junshan Gao[a]

[a]*School of Materials Science and Engineering, Anhui University of Science and Technology, Huainan 232001, China*

[b] Institute of Environment-friendly Materials and Occupational Health of Anhui University of Science and Technology (Wuhu), Wuhu 241003, China

**Corresponding authors E-mail:* chengguojun0436@126.com (G. Cheng)*

Abstract: The $Ti_3C_2T_x$ MXenes have excellent electrical, magnetic and mechanical properties. However, the strong hydrophilic properties limit its compatibility with polymer. The functional $Ti_3C_2T_x$-TPME was prepared by wet method process using 3-(trimethoxysilyl) propyl 2-methylprop-2-enoate (TPME). The results showed that the $Ti_3C_2T_x$-TPME had smaller particle sizes and distinct lamellar microstructure in organic solvent. The grafting rate of the TPME on the surface of $Ti_3C_2T_x$ reached 62.5 %. Its thermal stability was further improved and the contact angle of $Ti_3C_2T_x$-TPME have increased to 119 °. The hydrophilicity of $Ti_3C_2T_x$ was reduced owing to a large amount of -OH groups consumed through the hydrolysis and condensation of TPME. The covalent bonds (Ti-O-Si) of $Ti_3C_2T_x$-TPME due to the introduction of TPME into the interlamination was confirmed by Fourier transform infrared spectroscopy and X-ray photoelectron spectroscopy. The 2θ of the $Ti_3C_2T_x$-TPME moved to a smaller angle and the layer spacing was further increased via X-ray diffraction analysis. The TPME's layer acts as a physical barrier to increase the steric hindrance between $Ti_3C_2T_x$ particles and improve the dispersion and stability. A kind of 2D layered structural $Ti_3C_2T_x$-TPME with high hydrophobicity and stability was successfully prepared by the introduction of TPME.

Keywords: MXenes; Ti_3AlC_2; Modification; Hydrophobicity; Stability; Functionalization.

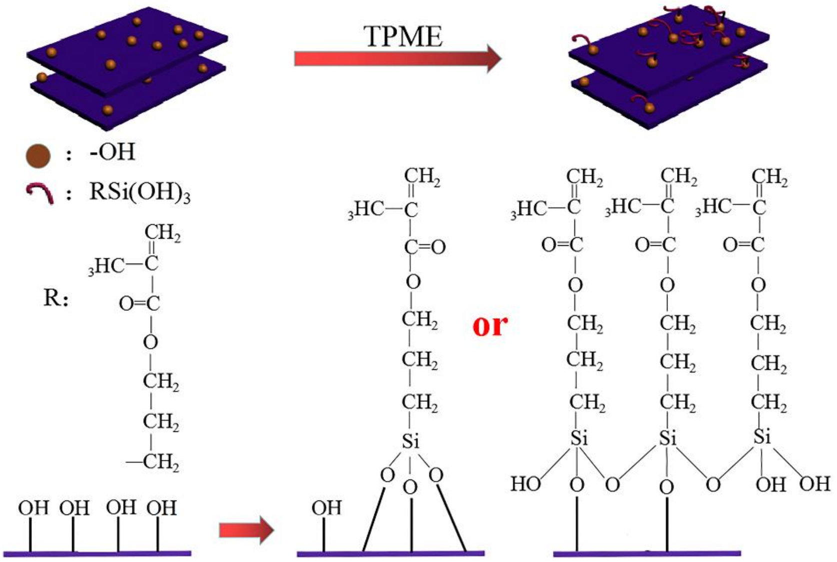

Fig.1. Schematic diagram of sample modification mechanism.

Acknowledgments

The financially support of works was provided to the Foundation of Provincial Natural Science Research Project of Anhui Colleges (KJ2019A0118), Research Foundation of the Institute of Environment-friendly Materials and Occupational Health of Anhui University of Science and Technology (Wuhu) (ALW2020YF15 and ALW2020YF12), University outstanding young talents support program (gxyq2017006 and gxyq2018015), Doctor’s Start-up Research Foundation of Anhui University of Science and Technology (ZY017), Key Laboratory of Photovoltaic and Energy Conservation Materials, Chinese Academy of Sciences (PECL2018KF010), Anhui Provincial Natural Science Foundation (1908085QE244) and the Guidance Science and Technology Plan Project of Huainan City（2020B150).

OL-37

Study on Preparation and properties of Permeable Composite Membrane based on PVA/PU and its Application

Gao Meiling Lai Shengfa Hu Kaiqiang Chen Zhibo Yuan Panpan Wan Xianglong*

(Anhui University of Science and Technology, School of Materials Science and Engineering, Huainan, 232001, Anhui)

Abstract： Permeable composite membranes have become a research hotspot due to their broad application prospects in the fields of seawater desalination, green energy, sewage reuse, aerospace, and energy collection. In this paper, the swellability of polyvinyl alcohol (PVA) and the high strength of polyurethane (PU) were used to prepare permeable composite membranes. The permeability and discharge performance of permeable composite membranes with different mass fractions of PVA in PU were studied. The results show that the hydrophilicity of the permeable composite membrane increases with PVA content and its thickness. The swelling degree of the permeable composite membrane varies with The PVA in the permeable composite membrane. Observed on composite membrane by scanning electron microscope, the phase separation degree of the surface layer of the permeable composite membrane and the internal pores were increased with the mass fraction of PVA. A permeable composite membrane with a wet film thickness of 300 μm, 7% PVA and controllable pore size was prepared by controlling the mass fraction of PVA in PU for a battery. The discharge voltage of the battery can reach 90.6mV, which provides potential application of composite membranes in batteries.

Keywords: permeable composite membrane; PVA; thickness; swelling; discharge voltage

OL-38

Study on Preparation and Electrical Properties of Polyanline/Waterborne

Polyurethane Composite

Lai Shengfa, **Hu Kaiqiang**, **Gao Meiling**, **Chen Zhibo**, **Cui Hao**, **Qian Yanfeng, Wan Xianglong***

(Anhui University of Science and Technology, Material Science and Engineering School, 232001)

Abstract: When polyaniline acted as an electrode material, its stability and processability are more prominent issues. The compatibility of waterborne polyurethane (WPU) and polyaniline (PANI) was improved by adding polyvinylpyrrolidone, and the PANI/WPU composite was synthesized by in-situ polymerization. Fourier infrared spectrometer, scanning electron microscope, X-ray diffractometer, ultraviolet-visible spectrophotometer, electrochemical workstation was used to study the influence of different amounts of WPU on the electrochemical performance of PANI/WPU composites. The results show that hydrogen bonds are formed between the NH- groups of PANI and the NHCOO- groups of PU, and the PANI/WPU composites are successfully prepared. When the ratio of WPU to aniline is 1:0.5, the cyclic voltammetry curve can be seen that the polyaniline composite material presents a good rectangular shape, indicating the ideal electric double layer performance. From the AC impedance curve, it shows the highest conductivity compared to other ratio composite materials, when the current density is 1A /g, the specific capacitance reached 439.1F/g, indicating that the addition of WPU significantly improved the specific capacitance performance of polyaniline. This can solve the processability and stability problems of polyaniline, making polyaniline more widely used in flexible electrode materials.

Keywords: polyaniline; waterborne polyurethane; composite materials; electrochemical performance

OL-39

Fabrication of two-dimensional $Ti_3C_2T_x$ MXenes by ball milling

pretreatment and mild etchant and their microstructure

Shen Tian[a], Guojun Cheng[a,b,*], Feixiang Sha[a], Ziyue Xuan[a], Guoxin Ding[a],

Zhoufeng Wang[a], Xianglong Wan[a,b,], Konghu Tian[a], Junshan Gao[a]

[a]*School of Materials Science and Engineering, Anhui University of Science and Technology, Huainan 232001, China*

[b] *Institute of Environment-friendly Materials and Occupational Health of Anhui University of Science and Technology (Wuhu), Wuhu 241003, China*

**Corresponding authors E-mail: chengguojun0436@126.com (G. Cheng)*

Abstract: 2D transition metal carbide/nitride (MXenes) have demonstrated wide application potential in energy storage and composite materials. In this article, a kind of 2D sheet structure and thermally stable $Ti_3C_2T_x$ MXenes was prepared through ball milling pretreatment, followed by mild etching with HCl and LiF. After ball grinding, the size of Ti_3AlC_2 was uniform and D_{50} decreases from 4.488 μm to 1.454 μm, which is conducive to the preparation of MXenes $Ti_3C_2T_x$ with a well-defined 2D sheet structure. The microstructure of the $Ti_3C_2T_x$ was analyzed by X-ray diffraction (XRD) and scanning electron microscopy (SEM). Results of XRD showed that the (002) peak of Ti_3AlC_2 broadened and shifted from $2\theta=9.82°$ to $2\theta=6.63°$. The corresponding interlayer distance was increased from 8.99 Å to 13.32 Å. The $Ti_3C_2T_x$ MXenes phase were uniform and showed a “Tyndall effect”. Obvious “accordion-like” structures were formed in $Ti_3C_2T_x$ MXenes, which could achieve the etching effect of the hydrofluoric acid method. The thermogravimetric results showed that $Ti_3C_2T_x$ MXenes phase prepared by this method absorbed many functional groups on the surface and had a high weight loss rate of 38.2%. All results demonstrated that the obtained $Ti_3C_2T_x$ MXenes by HCl and LiF etchant via ball milling pretreatment has not only a well-defined 2D sheet structure, but also dispersion stability and thermal stability. This article provides a new idea for the preparation of $Ti_3C_2T_x$ MXenes phase.

Keywords:MXenes; Two dimensional $Ti_3C_2T_x$; Ball milling; Etching; Microstructure

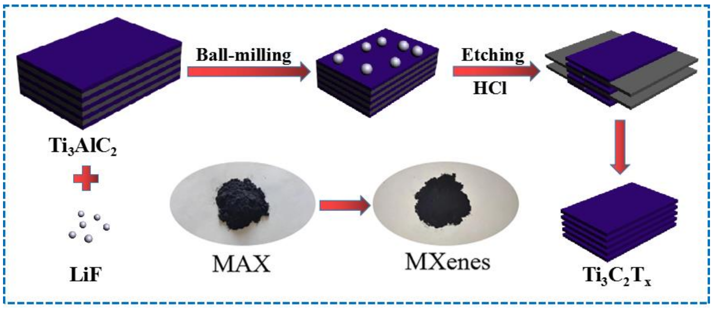

Fig. 1. The schematic of the process of $Ti_3C_2T_x$ MXenes.

Acknowledgments

The financially support of works was provided to the Foundation of Provincial Natural Science Research Project of Anhui Colleges (KJ2019A0118), Research Foundation of the Institute of Environment-friendly Materials and Occupational Health of Anhui University of Science and Technology (Wuhu) (ALW2020YF15 and ALW2020YF12), University outstanding young talents support program (gxyq2017006 and gxyq2018015), Doctor’s Start-up Research Foundation of Anhui University of Science and Technology (ZY017), Key Laboratory of Photovoltaic and Energy Conservation Materials, Chinese Academy of Sciences (PECL2018KF010), Anhui Provincial Natural Science Foundation (1908085QE244) and the Guidance Science and Technology Plan Project of Huainan City（2020B150).

OL-40

Flame-retardant behavior and Mechanism of SBR/MMT Composites Modified by Melamine Matrix Modifier

Ziyue Xuan,Guojun Cheng[a,b,*], Feixiang Sha[a], Shen Tian[a], Guoxin Ding[a],

Zhoufeng Wang[a], Xianglong Wan[a,b,], Konghu Tian[a], Junshan Gao[a]

[a]*School of Materials Science and Engineering, Anhui University of Science and Technology, Huainan*

232001, China
[b] *Institute of Environment-friendly Materials and Occupational Health of Anhui University of Science and Technology (Wuhu), Wuhu 241003, China;*
**Corresponding authors E-mail: chengguojun0436@126.com (G. Cheng)*

Abstract: Melamine quaternary ammonium salt (MQAS), a novel flame-retardant intercalation modifier, was used to prepare the flame-retardant organic sodium-based montmorillonite (FOSM), and which was added to SBR by a two-roll mixing and molding process to prepared the SBR/FOSM composites. The synergistic flame-retardant effects of sodium-based montmorillonite (MMT) and MQAS were investigated by the various methods. The results showed that the combustion residues of the SBR/FOSM samples are dense and continuous, and its total heat release rate and peak of heat release rate were reduced by 81.39% and 86.08%, respectively. Its fracture surface was smooth without pores due to the dispersion stability of the MMT MQAS modifier. Meanwhile, the FOSM can significantly reduce the loss factor of SBR composites. The XRD results showed that the introduction of MQAS further expands the interlayer spacing of MMT about 20%. Furthermore, it can improve effectively the flame-retardant properties of SBR/MMT composites.

Keyword: montmorillonite, SBR, modifier, flame-retardant, melamine, mechanism

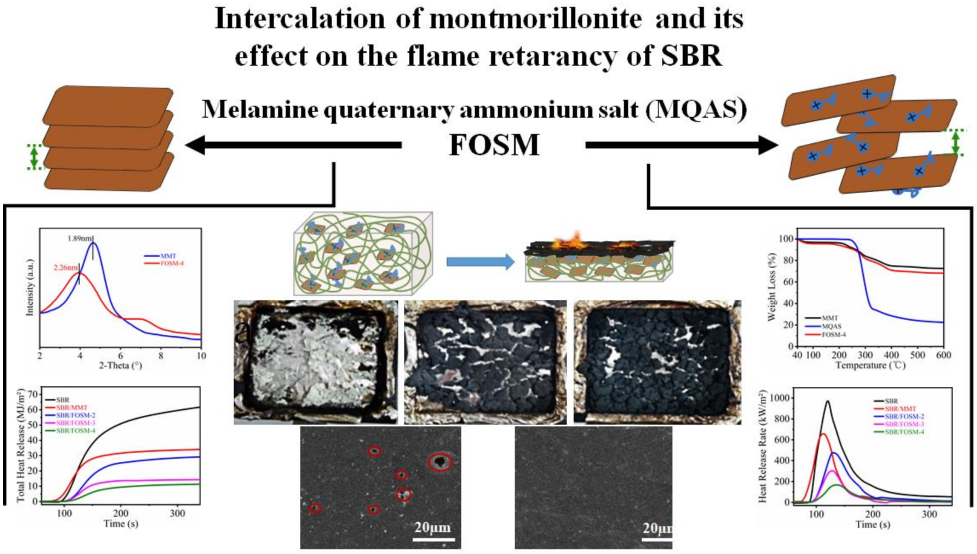

Acknowledgments

The financially support of works was provided to the Foundation of Provincial Natural Science Research Project of Anhui Colleges (KJ2019A0118), Research Foundation of the Institute of Environment-friendly Materials and Occupational Health of Anhui University of Science and Technology (Wuhu) (ALW2020YF15 and ALW2020YF12), University outstanding young talents support program (gxyq2017006 and gxyq2018015), Doctor's Start-up Research Foundation of Anhui University of Science and Technology (ZY017), Key Laboratory of Photovoltaic and Energy Conservation Materials, Chinese Academy of Sciences (PECL2018KF010), Anhui Provincial Natural Science Foundation (1908085QE244) and the Guidance Science and Technology Plan Project of Huainan City（2020B150).

OL-41

$K_xSi_yNb_zO_w$ as a Low-Potential Anode Material for Lithium-Ion Battery

Chang-Peng Lv*, Wen-Jie Du, Chao Feng, Zong-Qun Li

Anhui Provincial Engineering Laboratory of Silicon-based Materials, Engineering Technology

Research Center of Silicon-based Materials Anhui, School of Material and Chemical Engineering,

Bengbu University, Bengbu 233030, PR China

*Corresponding author, E-mail: lvcp1213@gmail.com , Tel.:+8615155257976

Abstract

A new oxide $K_xSi_yNb_zO_w$ have been synthesized by solid-state reaction, was found to reversibly (de)intercalate lithium by utilizing the Nb(V)/Nb(III) redox couple. Registering a low operational voltage at 0.65 V vs. Li^+/Li, it delivered a reversible capacity of 280 $mAh{\cdot}g^{-1}$ at a rate of C/2. Excellent rate performance was observed retaining 122 $mAh{\cdot}g^{-1}$ even at a fast rate of 10C. Without electrode optimization, it delivered robust cycling stability by maintaining 85% capacity retention at a high rate of 10C after 200 cycles. The structure changes of this material during discharge/charge processes were investigated by using in situ X-ray diffraction. The results indicated that Fast lithium (de)insertion without any significant capacity loss can be linked to the rigid endless distorted pentagonal channels built from Si_2O_7 groups linked with NbO_6 octahedra.

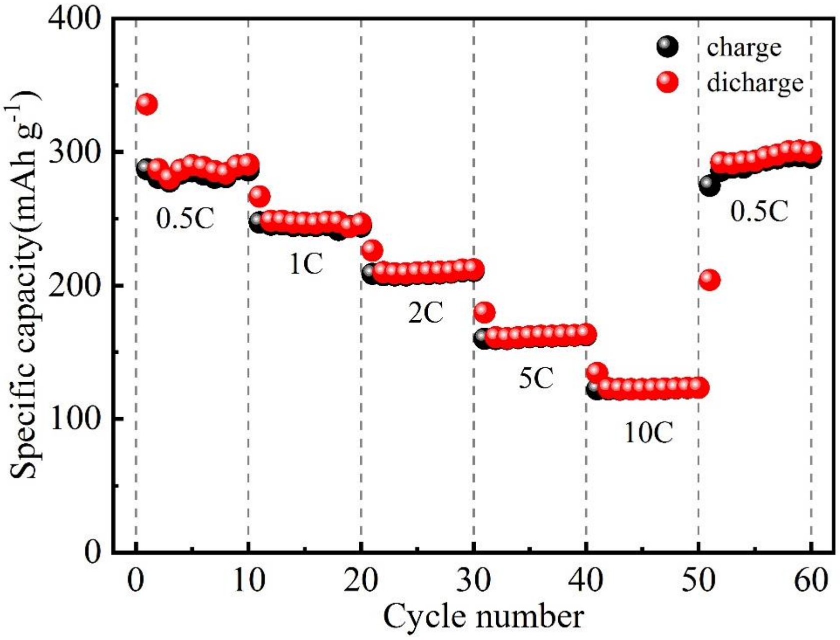

OL-42

Research on irradiation properties of Max (Ti_3SiC_2, Ti_3AlC_2) materials

Xiaochen Huang*

Anhui Provincial Engineering Laboratory of Silicon-based Materials, School of Material and

Chemical Engineering, Bengbu University, Bengbu, 233030, PR China

Abstract

Effect of irradiation on MAXmaterials (Ti_3AlC_2 and Ti_3SiC_2) by using electron-beams are discussed here. After irradiated with different electrical voltages, the changes of selected area electron diffraction (SAED) patterns are different. After 200 keV electron irradiation, the high-resolution transmission electron microscopy (HRTEM) shows that sputtering of atoms occurs. While the SAED patterns demonstrate that there's no amorphization occurred, but interplanar spacings decrease. The results obtained here indicate that MAXmaterials (Ti_3AlC_2 and Ti_3SiC_2) have high radiation tolerance with the energy below 200 keV.

Keywords：MAXmaterial;electron irradiation; SAED; HRTEM

References

[1] B. Han, H. Wang, Y. Kong, J. Wang. Mater. Lett. , **100**,159(2013)

[2]P. A. Robles-Dutenhefner, K.A.D.S. Rocha, E.M.B. Sousa, E.V. Gusevskaya. J. Catal. , **265**,72(2009)

[3] Feng, C.; Lv. C. P.; Zhao, H.; Li, Z. Q.; Xie, W. N.; Sun, L. N.; Wang, Y. Structural elucidation and supercapacitive performance on a Mn(II)-based MOF. *Cryst. Growth Des.* 2020, 20, 5682−5687.

OL-43

Preparation and photocatalytic application of g-C_3N_4/WO_3 composites

Huang Youpeng[1]，Wu Fuli[1]，LI Bing[2]，Yang Benhong[2*]

1. Deparyment of Biological and Environmental Engineering, Hefei University, Hefei, 230601.

2. Deparyment of Chemistry and Materials Engineering, Hefei University, Hefei, 230601, China.

Introduction

P-type and n-type semiconductors are easy to form heterojunction due to the matching of energy band structures, which can expand the visible light response and improve the efficiency of electron-hole separation, thus greatly improving the photocatalytic activity. Mahdi [1] studied the effect of g-C_3N_4/WO_3 on the degradation process of azo dyes and found that the excellent photocatalytic performance was caused by the enhanced light absorption. g-C_3N_4 has a relatively negative conduction band (CB) potential, WO_3 has a positive conduction band (VB) potential light response, which can be well matched in theory to form p-n heterostructure complex and improve the electron hole separation efficiency and photocatalytic activity. Related reports on the complex also confirmed this[2].

Experimental procedure

In this paper, melamine and thiourea were used as raw materials and NH_4Cl as porogen template to prepare flake like g-C_3N_4. Sodium tungstate and hydrochloric acid were used as raw materials, and sodium chloridewas used as ion buffer The efficient and stable catalyst g-C_3N_4/WO_3 was used to investigate the degradation of RhB.With $C_3H_6N_6$ and CH_4N_2S as precursors and NH_4Cl as template agent, thin-flake g-C_3N_4 was prepared by thermal polymerization.$Na_2WO_4 \cdot 2H_2O$ was used as precursor, NaCl was used as acid buffer, and WO_3 was prepared by hydrothermal method. The composite semiconductor g-C_3N_4/WO_3 was successfully prepared by low temperature thermal polymerization.The photocatalytic performance of different mass ratio g-C_3N_4/WO_3 composite semiconductor on RhB was investigated.

Result and discussion

It can be seen from Fig. 1(a) that g-C_3N_4 presents graphene-like lamellar structures and stacked on each other, and the slice is thin and micro coiled with a large number of voids. This is due to the large amount of NH_3 produced by the template in high temperature atmosphere. It can be seen from Fig. 1 (b) that WO_3 presents blocks with a side length of 200nm. It can be seen from Fig. 1 (c) and 1(d), It can be seen that WO_3 blocks are uniformly attached to the g-C_3N_4, and part of WO_3 is wrapped by the g-C_3N_4. This structure is conducive to increasing the specific surface area by uniform dispersion and uniform morphology. increasing the reaction sites and improving the photocatalytic activity. The results showed that g-C_3N_4/WO_3 had a certain ability to degrade the five dyes. The degradation rates of MO, BG, AF, MB and RhB were 3.6%, 45.6%, 64.2%, 66.4% and 94.3% respectively.

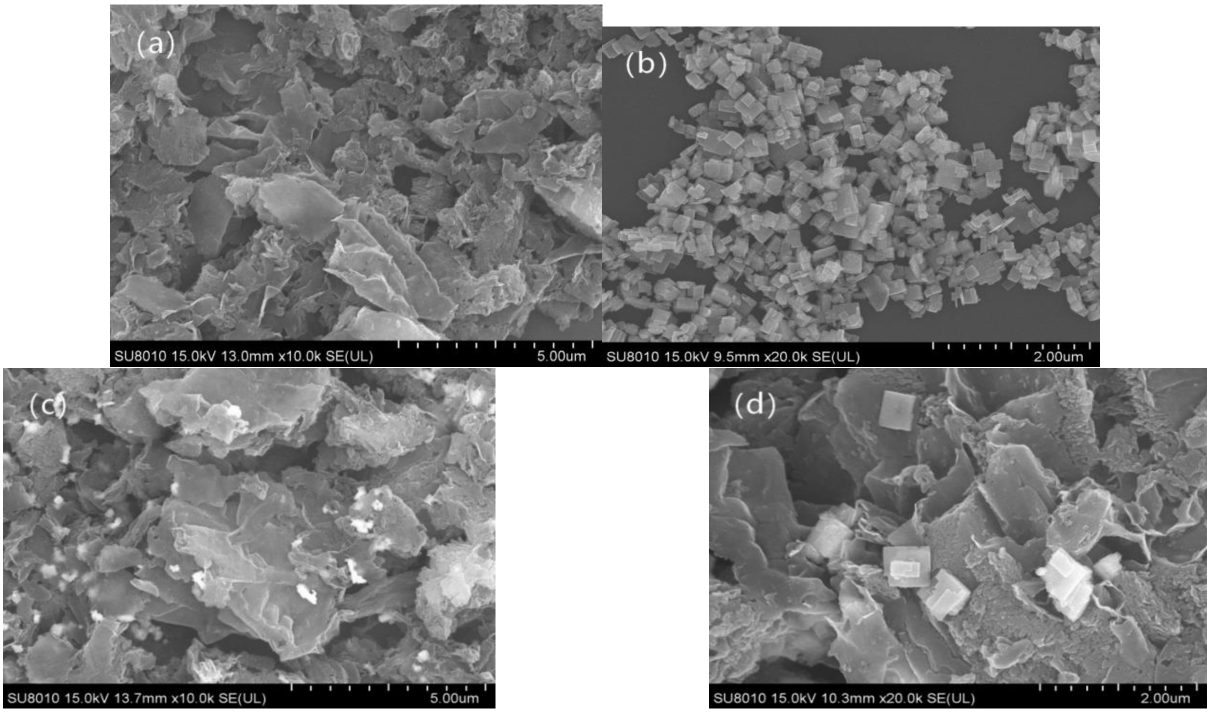

Fig.1 SEM images of g-C_3N_4、WO_3 and g-C_3N_4/WO_3-20

(a)g-C_3N_4; (b)WO_3; (c)g-C_3N_4/WO_3-20(×10k); (d)g-C_3N_4/WO_3-20(×20k)

The degradation rate can reach 95% under the visible light irradiation for 60min with certain stability, and the degradation rate can still reach 90% after four cycles of use. It has certain degradation ability for different dyes, especially for positively charged dyes with good photodegradation performance. The mechanism experiments found $\cdot O_2^-$ is the main active specie which degraded RhB, and $\cdot OH$ and h^+ played some roles, accounting for a double charge transfer mechanism in the photocatalytic activity.

References

[22]Mahdi Karimi-Nazarabada, Elaheh K. Goharshadi. Highly effiffifficient photocatalytic and photoelectrocatalytic activity of solar light driven WO_3/g-C_3N_4 nanocomposite[J]. Solar Energy Materials and Solar Cells, 2017, 160: 484–493.

[23]Liu Xin. Synergy of adsorption and visible-light photocatalytic degradation of methylene blue by a bifunctional Z-scheme heterojunction of WO_3/g-C_3N_4 [J]. 2017, 405: 359-371.

OL-44

Highly supercapacitive performance on a Mn(II)-based MOF

Chao Feng*, Jing-Jing Guo, Zong-Qun Li, Chang-Peng Lv, Shu Ye

Anhui Provincial Engineering Laboratory of Silicon-based Materials, School of Material and Chemical Engineering, Bengbu University, Bengbu, 233030, PR China

* Corresponding author: E-mail: fchg042@163.com, Tel: +86-552-317-9368

Abstract

Metal–organic frameworks (MOFs) used directly in supercapacitors have attracted much attention for their potential high performance. Herein, one new Mn-based MOF, [Mn(Hpzca)$_2$]$_n$ (**1**) has been obtained *via* one-step hydrothermal method with the ligand (H$_2$pzca = 1*H*-pyrazole-4-carboxylic acid). After characterization, the Mn-MOF exhibits a 3D structure bridged through the carboxylic group, which is beneficial for the charge transfer and ion transport for supercapacitors. In the three-electrode system, this Mn-MOF electrode showed a high specific capacitance and a good cycling stability. Its maximum specific capacitance was 443 F g^{-1} at 1 Ag^{-1}, along with a high capacitance of 86 % retained after 1000 cycles at a current density of 5 A g^{-1} in the 6 M KOH solution. All these results demonstrate that the title Mn-MOF is a kind of promising electrode material for high-performance supercapacitors.

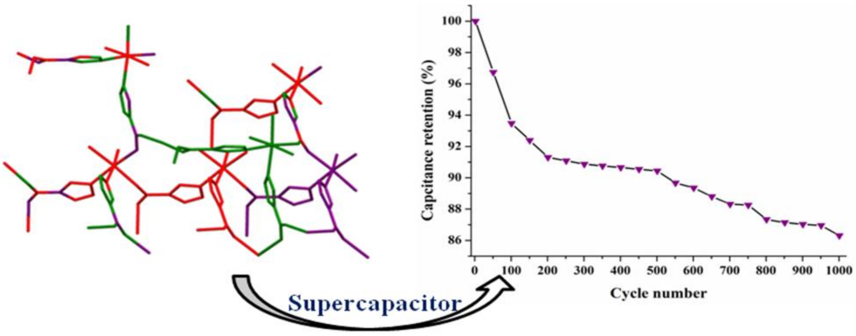

Fig.1 3D Mn-based MOF with high supercapacitive performance

References

[1] Feng, C.; Lv, C. P.; Li, Z. Q.; Zhao, H.; Huang, H. H. A porous 2D Ni-MOF material with a high supercapacitive performance. *J. Solid State Chem.* **2018**, *265*, 244-247..

[2] Feng, C.; Lv. C. P.; Zhao, H.; Li, Z. Q.; Xie, W. N.; Sun, L. N.; Wang, Y. Structural elucidation and supercapacitive performance on a Mn(II)-based MOF. *Cryst. Growth Des.* 2020, 20, 5682−5687.

Acknowledgments

The work was supported by National Science Foundation for Cultivation of Bengbu University (2018GJPY03), Starting Research Fund of Bengbu University (BBXY2018KYQD15) and the P of College Students Innovation of Laboratory Construction (2016ckjh116).

OL-45

Preparation of the mesoporous silica composite nanoparticles coated with

biodegradable temperature/pH sensitive copolymer and their application in drug release

Xiaoqi Jin, Jinlong Ge, Qiuqin Wang, Yan Gao

Department of Materials Science and Chemical Engineering, Anhui province Engineering Laboratory of Silicon-based Materials Bengbu University, Bengbu 233000, P.R. China

Abstract

In this work, we have synthesized the biodegradable and temperature/pH- sensitive copolymer PEG-PLA-P(NIPAM-co-AA) by emulsion copolymerization method with the modified of Poly(ethylene glycol)-co-(L-lactic acid) as crosslinker[1]. Then the structural composition and temperature/pH-sensitive properties were characterized by using ^{1}HNMR, FT-IR and Dynamic light scattering (DLS) techniques. Furthermore, the Ibuprofen as the model drug , the copolymer was encapsulated on the surface of modified mesoporous silica nanoparticles MSNs-NH$_2$ using "grafted to" method. We preliminary investigated the performance of drug release in the difference release conditions. The results showed that the copolymer had rapidly temperature/pH dual stimuli responsive. Moreover, the resultant composite nanoparticles PEG-PLA-P(NIPAM-co-AA)@ MSNs exhibited excellent property of drug-controlled release, as shown in Fig.1. Therefore, the copolymer is expected to apply in the field of controlled drug release as intelligent drug carried.

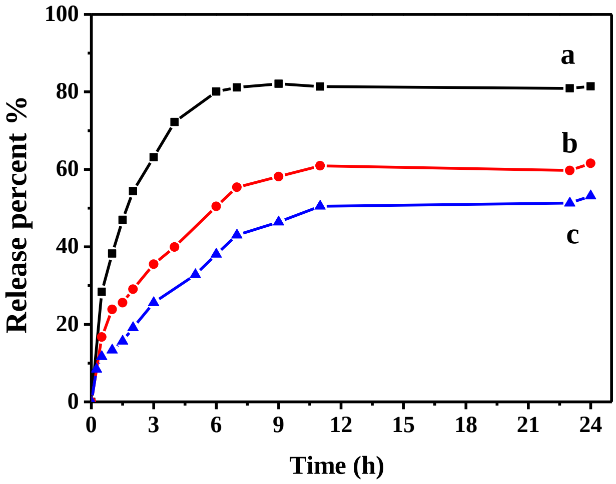

Fig.1 Release profiles of ibuprofen from composite nanoparticles (a) pH=7.4 PBS 40℃(b) pH=2.0 PBS 40℃ (c) pH=7.4 PBS 25℃

Keywords: mesoporous silica nanoparticles, biodegradable; pH/temperature sensitivity; controlled drug release

Acknowledgments: This project was supported by the Key Research Project of Natural Science

from Provincial Bureau of Education, Anhui, China (KJ2018A0567)

References:

[1] Dong W. L., Tae G. P. Stereocomplex formation between enantionmeric PLA-PEG-PLA triblock copolymers; Characterization and use as protein-delivery microparticulate carriers [J]. J Appl Polym Sci, 2000, 75(13):1615-1623.

Posters

Recent studies on semiconducting material for sonophotocatalytic hydrogen evolution under visible light irradiation with scavenger effect.

Md Nazmodduha Rafat, Chang Sung Lim and Won-Chun Oh *

Department of Advanced Materials Science & Engineering, Hanseo University, Seosan-si,

Chungnam, Korea, 356-706

E-mail: wc_oh@hanseo.ac.kr

Abstract

To solve the global energy problem, hydrogen has been getting enormous attention because of its zero-carbon content. A promising strategy for producing clean and carbon-neutral hydrogen fuel is photocatalytic water splitting. Although different kinds of semi-conductive materials have been invented, modification of a solar-light-driven impressive material with low cost is the main goal in this decade. The goal of our research is to make a novel material with low band-gap energy. In this regard we used sonication for preparing quaternary material. The homogeneous structure is the main advantage of using ultrasonic a method, which causes it to have nanoparticles with high reactivity. In our lab, we are trying to design combined semiconducting material to get efficient photocatalysts. In our work, we find out that as a photocatalyst LaCdSe-GO-TiO2 (LCS) has shown a good potential in photoelectrochemical water splitting for hydrogen evolution. In this work, LCS nanoparticles were synthesized by ultrasonic process under ambient pressure. The small particle size plays a key role in suppressing the recombination of photo-induced carriers, and thus promoting the photocatalytic activity. In the presence and absence of 20% methanol as a sacrificial agent, its show good photocatalytic activity. This work provides a good example on size control, low-cost synthesis and photocatalysts' design. Small size particles or low-dimension materials enable shorter diffusion distance of electrons and holes which could facilitate the surface redox reaction as compared to their bulk counterparts. Various synthetic techniques have been applied in controlling particle size, including solvothermal, sonochemical and wave-assisted hydrothermal methods in recent years. It is well-known that most of these methods demand harsh reaction conditions such as good quality equipment, high temperature or high pressure. Therefore, for the purpose of meeting the requirements of industrial application, it is highly competitive to make use of ultrasonic process under ambient pressure conditions. Our group has demonstrated that LaCdSe-GO-TiO2 (LCS) can be prepared by ultrasonic method. We reckon, in the future it will be applicable for synthesizing novel materials.

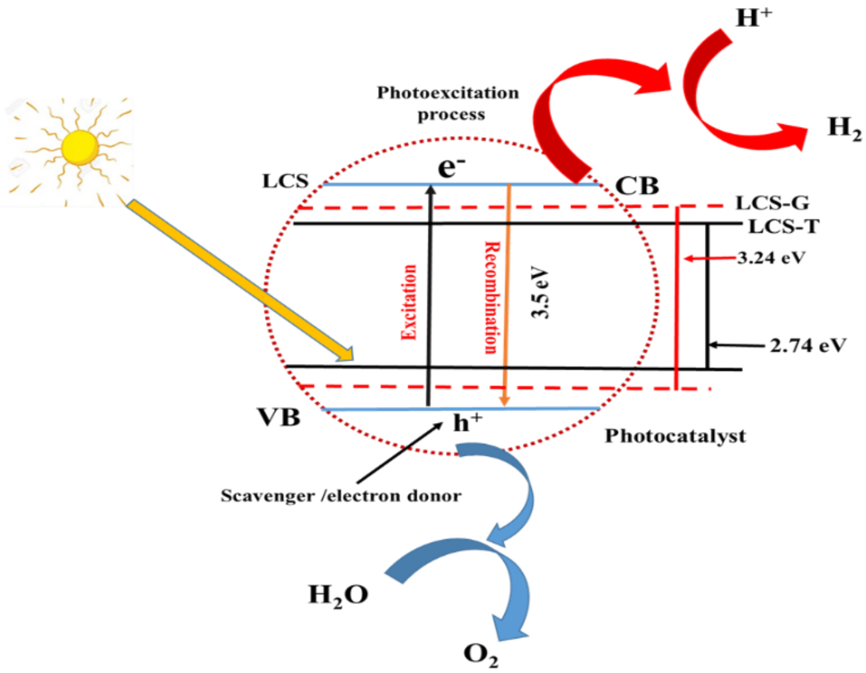
H^+
H_2
Photoexcitation process
LCS
e^-
CB
LCS-G
LCS-T
3.24 eV
Excitation
Recombination
3.5 eV
2.74 eV
VB
h^+
Photocatalyst
Scavenger /electron donor
H_2O
O_2

Removal of organic dye from wastewater by using zinc oxide nanoparticle cooperated with graphene and iron oxide as catalyst by photocatalysis process

Prawit Nuengmatcha[1*], Rungnapa Pimsen[1], Arnannit Kuyyogsuy[1], Paweena Porawatkul[1], and Piyawan Nuengmatcha[1,2]

*[*1]Nanomaterials Chemistry Research Unit, Department of Chemistry, [2]Department of Environmental Science, Faculty of Science and Technology, Nakhon Si Thammarat Rajabhat University, Nakhon Si Thammarat 80280, Thailand.*

*Corresponding author: E-mail:*pnuengmatcha@gmail.com,

Abstract

Zinc oxide-graphene-iron oxide (ZGF) nanocomposite was synthesized by solvothermal method. The obtained sample was characterized by XRD, SEM, EDX, TEM and HR-TEM techniques. The data from all techniques confirmed the formation of ZGF catalyst. Photocatalytic activities of the as-prepared ZGF nanocomposite were investigated through photodegradation of methylene blue (MB) under visible light irradiation. The suitable conditions for MB degradation were 10 mg/L, 90 min, 0.03 g, and 100 watt for initial concentration of MB, irradiation time, catalyst dosage, and irradiation intensity, respectively. The as synthesized photocatalysts exhibited excellent stability and reusability for five successive operating cycles.

Keywords: Zinc oxide nanoparticle; Graphene; Iron oxide; Photocatalysis

Introduction

Currently, several techniques have been established in many research fields claiming successful organic dyes removal from wastewater such as adsorption, membrane, precipitation, coagulation, electrochemical oxidation, sonocatalysis, and photocatalysis [1-3]. Among these mentioned techniques, photocatalysis has much contribution as a promising one to solve the pollution problem. Using photocatalysis technique to degrade dyes from wastewater it might results in not only decolorization, but also use of complete degradation. Of various heterogeneous photocatalysts, zinc oxide (ZnO), graphene, and iron oxide (Fe_2O_3) have been widely used because of its both photoconductive and photochemical properties, since it exhibits various advantage properties [4]. However, the synthesis and application of ternary ZnO-graphene-Fe_2O_3 nanocomposite in visible light driven photocatalysts system has not yet been reported. Therefore, in this study, the magnetic materials such as Fe_2O_3, graphene and ZnO was synthesized as a co-operated ternary ZnO-graphene-Fe_2O_3 composite would lead to improved photocatalytic activity and excellent magnetic separation ability.

Experimental

Synthesis of ZGF catalyst

ZGF catalyst was prepared via four steps. Firstly, 2.0 g of citric acid was heated to 260 °C for 10 min. And then the obtained solution was mixed with 100 mL of 0.25 mol/L NaOH and stirred for 30 min. The obtained product is graphene quantum dots stock solution. Secondly, 5 g of $FeCl_3{\cdot}6H_2O$, 2.5 g of $FeSO_4{\cdot}7H_2O$ and DI water were mixed into a 500 mL three-necked flask. Then, 20 mL of 28% NH_4OH was slowly dropped into the solution. To obtain the colloidal solution, the solution was heated at 80·C for 30 min under N_2 atmosphere. The obtained solid is Fe_2O_3. Thirdly, the GQDs solution and Fe_2O_3 were mixed in round bottom. Then, the suspension was stirred and heated at 80 °C for 30 min. The obtained sample is Fe_2O_3-graphene (FG). Finally, 0.5 g of FG and 250 mL of 0.1 mol/L $Zn(NO_3)_2$ were mixed and stirred for 5 h while heating at 90 °C. After that, the solid sample was heat at 600 °C for 1 h to obtain ZnO-graphene-Fe_2O_3 (ZGF). All samples were charaterized using XRD, SEM, EDX, TEM and HR-TEM techniques.

Photocatalytic degradation of MB

Photocatalytic performances of all catalysts were performed in a closed chamber with various conditions including initial concentration of MB (5-40 mg/L), irradiation time (0-180 min), catalyst dosage (0-0.12 g), and irradiation intensity (25-130 watt). The obtained supernatant was analyzed by using a UV-Visible spectrophotometer at λ_{max} 665 nm for the maximum absorption of MB.

Results and Discussion

Characterization of ZGF catalyst

The XRD results of ZGF catalyst showed the refection peaks of the hexagonal phase of hematite (α-Fe_2O_3) (JCPDS card No. 33-0664) [5]. at $2\theta = 24.1°$, 33.2°, 35.6°, 40.9°, 49.5°, 54.1°, 62.4° and 64.1°. And the XRD pattern of ZnO appears at $2\theta = 31.86°$, 34.52°, 36.36°, 47.66°, 56.72°, 62.98°, 66.50°, 68.08° and 69.24° (JCPDS No. 36-1451) [6]. From the XRD patterns of ZGF, it is evident that the prepared sample shows the major phase of both α-Fe_2O_3 and ZnO. In addition, it was found that the prepared sample gave the characteristic diffraction peak $2\theta = 25.1°$ which corresponded to the plane of graphene [7], indicating that the presence of graphene, α-Fe_2O_3 and ZnO on the ZGF nanocomposite.

Optimum conditions for photocatalytic degradation of MB

The optimum conditions for photocatalytic degradation of MB by using ZGF as catalyst are summarized in Table 1. The suitable conditions for MB degradation were 10 mg/L, 90 min, 0.03 g, and 100 watt for initial concentration of MB, irradiation time, catalyst dosage, and irradiation intensity, respectively.

Table 1. The optimum conditions for photocatalytic degradation of MB

Parameter	Suitable condition
initial concentration of MB (mg/L)	10
irradiation time (min)	90
catalyst dosage (g)	0.03
irradiation intensity (watt)	100

Conclusion

ZGF nanocomposite was synthesized by simple solvothermal method. The XRD, SEM, EDX, TEM and HR-TEM confirmed its formation. The suitable conditions for MB degradation were 10 mg/L, 90 min, 0.03 g, and 100 watt for initial concentration of MB, irradiation time, catalyst dosage, and irradiation intensity, respectively. The as synthesized photocatalysts exhibited excellent stability and reusability for five successive operating cycles. Therefore, the ZGF composites are exceptional material for applications in a number of environmental issues.

Acknowledgements

This research was financially supported by Nakhon Si Thammarat Rajabhat University Research Fund (NSTRU 004/25613 and Nanomaterials Chemistry Research Unit, Department of Chemistry, Faculty of Science and Technology, Nakhon Si Thammarat Rajabhat University, Thailand.

References

1. N. Boudechiche, M. Fares, S. Ouyahia, H. Yazid, M. Trari, Z. Sadaoui. Comparative study on removal of two basic dyes in aqueous medium by adsorption using activated carbon from Ziziphus lotus stones. *Microchem. J.* 146 (2019) 1010-1018.
2. S. Zereshki, P. Daraei, A. Shokri, Application of edible paraffin oil for cationic dye removal from water using emulsion liquid membrane. *J. Hazard. Mater.* 356 (2018) 1-8.
3. C.H. Nguyen, C.C. Fu, R.S. Juang, Degradation of methylene blue and methyl orange by palladiumdoped TiO_2 photocatalysis for water reuse: Efficiency and degradation pathways. *J. Cleaner Prod.* 202 (2018) 413-427.
4. P. Nuengmatcha, P. Porrawatkul, S. Chanthai, P. Sricharoen, N. Limchoowong. Enhanced photocatalytic degradation of methylene blue using Fe_2O_3/graphene/CuO nanocomposites under visible light. *J. Environ. Chem. Eng.* 7 (2019) 103438.
5. S. Zhang, F. Ren, W. Wu, J. Zhou, L. Sun, X. Xiao, C. Jiang, Size effects of Ag nanoparticles on plasmon-induced enhancement of photocatalysis of Ag-α-Fe_2O_3

nanocomposites. *J. Colloid Interface Sci.* 427 (2014) 29-34.

6. F.T. Johra, W.G. Jung. RGO–TiO_2–ZnO composites: synthesis, characterization, and application to photocatalysis. *Appl. Catal.,* A. 491 (2015) 52-57.

7. L. Zhu, S.B. Jo, S. Ye, K. Ullah, W.C. Oh, Rhodamine B degradation and reactive oxygen species generation by a ZnSe- graphene/TiO_2 sonocatalyst, *Chin. J. Catal.* 5 (2014) 1825-1832.

Synthesis, Characterization, and Properties of ZnO Nanoparticles for Antifungal Activity in Durian

Arnannit Kuyyogsuy[*1], **Prawit Nuengmatcha**[1] **and Wilaiwan Chaisorn**[2]

[1]*Nanomaterials Chemistry Research Unit, Department of Chemistry,* [2] *Department of Biology*

Faculty of Science and Technology, Nakhon Si Thammarat Rajabhat University, 80280, Thailand.

[*]*Corresponding author. e-mail: arnannit.k@gmail.com; Fax +66-7537-7443*

Abstract

ZnO nanoparticles have been synthesized by precipitation method from Zinc acetate dihydrate. The powder was characterized by X-ray diffraction, scanning electron microscopy, transmission electron microscopy, and laser particle size analysis. XRD patterns showed that ZnO nanoparticles have hexagonal unit cell structure. SEM and TEM pictures reveal the rod morphology and LPSA analysis exhibited the particle size of prepared ZnO nanoparticles as 88 nm. The UV-vis absorption spectrum shows an absorption band at 380 nm due to ZnO nanoparticles. The synthesis method has potential for application in agriculture due to inhibit the growth of fungi. The antifungal action of the ZnO nanoparticles on *Phytophthora palmivora* fungal strains, causing fruit rot disease in durian was then determined. Those with rod morphology showed a more efficient antifungal activity for the concentrations considered, showing the percentage of inhibition as 70±0.08%.

Keywords: synthesis, characterization, ZnO nanoparticles, morphology and antifungal activity

Introduction

Durian (*Durio zibethinus* Murray) is the most popular fruit in Southeast Asia, particularly in Thailand [1]. It is well known as the “king of fruit”. The main cause of symptom disease in durian is fungal which lead to economic lost. The genus *Phytophthora* is one of the most important plant pathogens worldwide, and many economically important crop species in Southeast Asia, such as durian, rubber, cocoa, jackfruit, papaya, coconut, pepper, potato, plantation forestry, and citrus are susceptible. Fruit rot of durian caused by *Phytophthora palmivora* that it appears as watersoaked lesions with light brown centres 3–5 days after infection, depending on the host. The lesions expand rapidly and can completely rot an entire fruit. Nanotechnology is a research which interested in modern materials science. This technology can be able to apply in a wide range of innovative textile compounds, food processing, and agricultural production to complex medicinal techniques [2]. It is considered as the synthesis, characterization, and exploration of materials in the nanometer region (1–100 nm) which at this scale, the properties and functions of living systems are defined [3]. In this technology, the materials are those whose structures reveal new and considerably increased and physicochemical as well as obvious phenomena and functionalities as biological properties a result of the nanoscale size [4]. Nano-sized ZnO reveals varying morphologies and presents significant antimicrobial activity over a wide spectrum of microbial species explored by a large body of researchers [5]. ZnO is currently being investigated as an antimicrobial agent in both microscale and nanoscale formulations. ZnO shows significant antimicrobial activities when particle size is reduced to the nanometer range, then nano-sized ZnO can interact with microbial surface and/or with the microbial core where it enters inside the cell, and subsequently exhibits distinct bactericidal mechanisms [6]. The interactions between these unique materials and bacteria are mostly toxic, which have been exploited for antimicrobial applications such as in food industry. Interestingly, ZnO-NPs are reported by several studies as non-toxic to human cells [7], this aspect necessitated their usage as antibacterial agents, noxious to microorganisms, and hold good biocompatibility to human cells [8]. The various antifungal mechanisms of nanomaterials are mostly attributed to their high specific surface area-to-volume ratios [9], and their distinctive physicochemical properties. The aim of this work was to synthesize the optimum of ZnO nanoparticle and the characterization of ZnO nanoparticles using X-ray diffraction, scanning electron microscopy (SEM), transmission electron microscopy (TEM) and Laser particle size analysis (LPSA) including antifungal activity *P. palmivora*, causing fruit rot disease in durian.

Materials and Methods

Synthesize of ZnO nanoparticles (ZnO-NPs)

Synthesis of the ZnO-NPs was carried out using modification of the method of Li and coworker [10]. Briefly, 1.5 g of Zinc acetate dihydrate [$Zn(CH_3COO)_2.2H_2O$] was dissolved in 40 ml of distilled water, then the mixture was sonicated for 10 min until the solution was clear. After that the solution was adjusted with 1 M NaOH until the solution was pH10, at this stage, the resulting solution was a milky white viscous gel, and then stirred for 30 min. The solution was heated in an oil bath at 50 °C for 3 h until the solution was a white precipitate. The sediment was then filtered and rinsed with distilled water several times to neutral pH. Once the sediment was obtained, it was dried at 80 °C for 8 h until dry and ground for further study use. In the synthesis of ZnO-NPs, the optimal conditions for the synthesis of nanoparticles were studied such as substantial weight (1.5, 2, 2.5 and 3 g), pH (pH6, 8.5, 10 and 12), time (1, 2, 3 and 5 h) and temperature. (50, 60 and 90 °C).

Characterization of the nanosized ZnO colloids synthesized

The prepared ZnO-NPs were characterized for their optical and nanostructural properties. The morphology, size, crystallinity of ZnO-NPs were determined through a number of helpful techniques, such as scanning electron microscope (SEM), transmission electron microscopy (TEM), energy dispersive X-ray (EDS), laser particle size analysis (LPSA) and powder X-ray diffraction (XRD). The UV-VIS spectroscopy technique was used to support the ZnO-NPs.

Phytophthora palmivora and the synthesized ZnO-NPs preparation

P. palmivora was isolated from durian fruit rot, kindly provided by the Prince of Songkhla University, Thailand, and grown in potato dextrose agar (PDA) plate at room temperature for 7 days. After that, the synthesized ZnO-NPs solution was mixed with the PDA medium until the final concentration at 1% (w/v). Sterile distilled water was used as a control.

Evaluation of Antifungal activity of the synthesized ZnO-NPs

To carry out the evaluation of antifungal activity of the synthesized ZnO-NPs, the *in vitro* methodology was performed by the mycelial disc of *P. palmivora* was put on the center PDA medium amended with the synthesized ZnO-NPs (final concentration 1% (w/v)). Plates were incubated at room temperature for 7 days. After that, the diameters of the fungal colonies were assayed by an equation of Gamliel and coworker [11], which presented as %inhibition. Each treatment was replicated using three plates, and experiment was performed three times.

$$\%\text{inhibition} = 100-[(R^2/r^2)100])$$

(when R is radial of the fungal colonies for control, r is radial of the fungal colonies for treatment)

Results and Discussion

Synthesis of ZnO-NPs: Process optimization and UV characterization

The nanoparticles size plays an important role in changing the entire properties of materials. Thus, the nanoparticle size becomes very essential to identify the properties of the materials. UV-visible absorption spectroscopy is widely being used technique to determine the optical properties of nanoparticles. In the present study, the optimized condition for the synthesis of ZnO-NPs were 1.5 g of Zinc acetate dihydrate (Figure 1A), pH10 (Figure 1B), temperature 50 °C (Figure 1C) and 3 h reaction time (Figure 1D). Good stability of the synthesized ZnO-NPs was observed at room temperature up to 100 days with no aggregation. The absorption spectrum of the synthesized ZnO nanopowder was shown in Figure 1E. It was exhibited a strong absorption band at about 380 nm.

Characterization of ZnO-NPs

The SEM and TEM image of ZnO-NPs showed that the particles were rod in shape with a hexagonal base (Figure 2A and 2B) while, LPSA analysis was presented the size of ZnO-NPs as 88 nm (Figure 2C).

EDS spectra of the samples indicated the presence of the elements zinc, oxygen and carbon in the powders of ZnO-NPs analyzed, where the percentages of these indicated that the highest of Zinc while a lower presence of oxygen and carbon (Figure 2D), evidencing the nonstoichiometric character of the synthesized ZnO and a high concentration of oxygen vacancies in the obtained ZnO-NPs.

The X-ray diffraction pattern of ZnO nanopowder (Figure 2E), a definite line broadening of the XRD peaks indicated that the prepared material consists of particles in nanoscale range. From this XRD patterns analysis, the diffraction peaks located at 31.84°, 34.52°, 36.33°, 47.63°, 56.71°, 62.96°, 68.13°, and 69.18° have been keenly indexed as hexagonal wurtzite phase of ZnO [12, 13] with lattice constants $a = b = 0.324$ nm and $c = 0.521$ nm (JPCDS card number: 36-1451) [14].

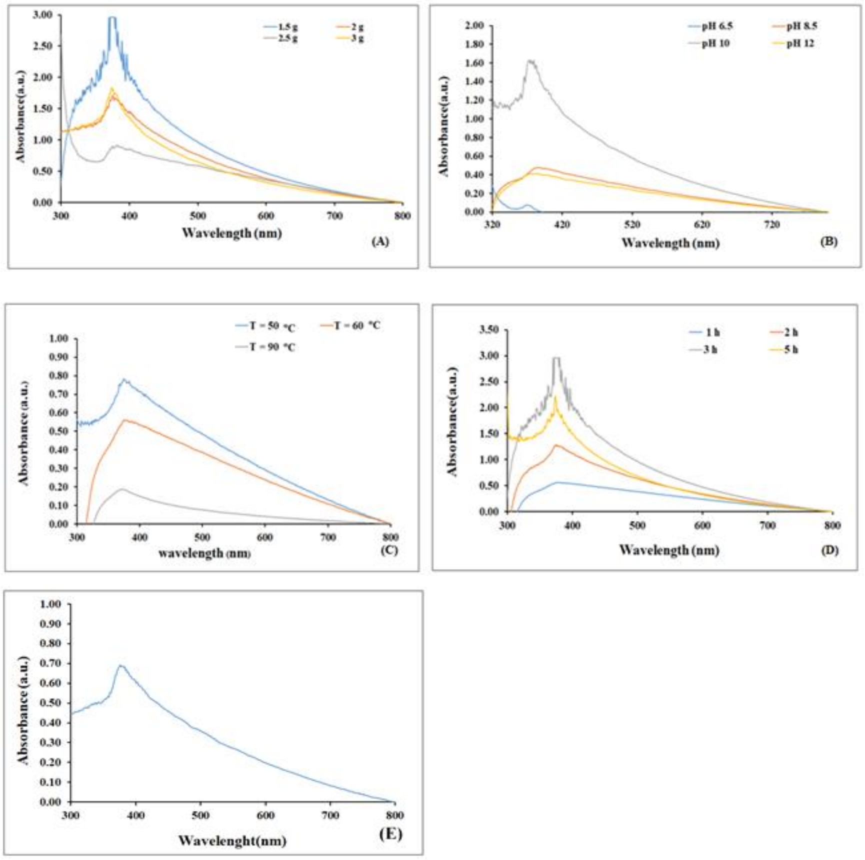

Figure 1. The optimum of the synthesized Zn-NPs at different parameters: (A) concentration, (B) pH, (C) temperature, (D) time and (E) the optimized for the synthesized Zn-NPs

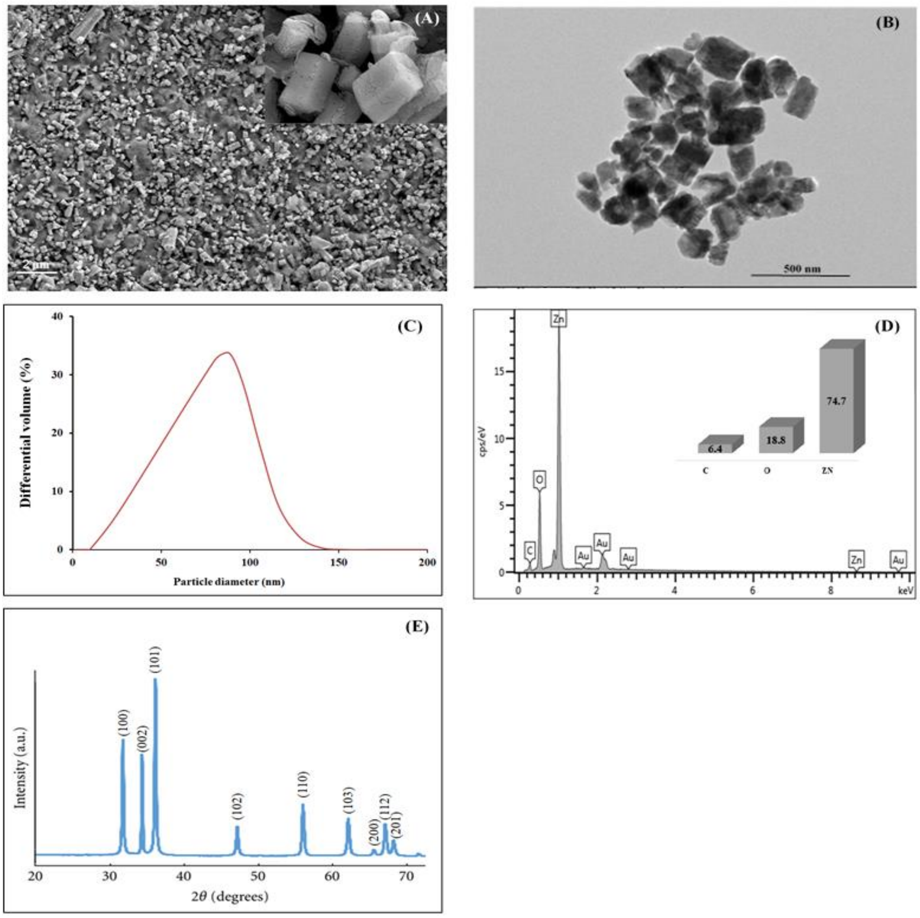

Figure 2. Characterization of ZnO-NPs: (A) SEM image; (B) TEM image; (C) LPSA analysis; (D) EDS and (E) XRD

Evaluation of antifungal capacity of the synthesized ZnO-NPs

In Figure 3 we can see the growth of *P. palmivora*, *in vitro*, without treatment as a control (Figure 3A) and treated with the synthesized ZnO-NPs (Figure 3B). The results showed that the synthesized ZnO-NPs can be able to inhibit the growth of fungi *P. palmivora* when compared to the control set for 7 days after the start of the trial, showing a percentage of inhibition as 70±0.08%.

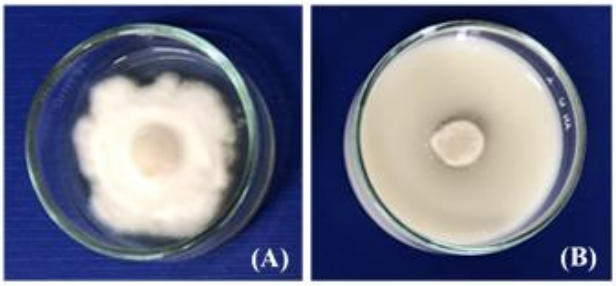

Figure 3. Antifungal activity of the synthesized Zn-NPs: (A) control and (B) 1%(w/v) Zn-NPs

Conclusions

In this work a methodology was structured that made it possible to obtain zinc oxide nanoparticles (ZnO-NPs) in a controlled and reproducible way, with predetermined characteristics and sizes. It was seen during the course of the study that the nature of the solvent used in the synthesis process of ZnO, the pH of the system and the temperature of heat treatment appreciably affected the characteristics of the final product. ZnO-NPs with rod morphology (with a size of 88 nm) were obtained. In addition, the antifungal action of the synthesized ZnO-NPs on strains of *P. palmivora* was evidenced, being more efficient in inactivating *P. palmivora*. The results obtained reiterate the importance of the synthesis methods used to obtain the ZnO-NPs and the effect these methods have on the final physicochemical characteristics.

Acknowledgements

This work was financially supported by Nanomaterials Chemistry Research Unit, Department of Chemistry, Faculty of Science and Technology, Nakhon Si Thammarat Rajabhat University.

References

[1] P. Booncherm, J. Siriphanich, *Kasetsart Journal*, **25**, 119–125 (1991).

[2] B. Xing, C. Vecitis, N. Senesi, *John Wiley & Sons, Inc., Hoboken, New Jersey,* (2016).

[3] V. Yadav, *a review; AEEE,* **3**, 771–778 (2013).

[4] S. Pal, Y.K. Tak, J.M. Song, *Appl.Environ. Microbiol*, **73**, 1712–1720 (2007).

[5] K.R. Raghupathi, R.T. Koodali, A.C. Manna, *Langmuir*, **27**, 4020–4028 (2011).

[6] J.T. Seil, T.J. Webster, *Int. J. Nanomed*, **7**, 2767–2781 (2012).

[7] G. Colon, B.C. Ward, T.J. Webster, *J. Biomed. Mater. Res*, **78**, 595–604 (2006).

[8] N. Padmavathy, R. Vijayaraghavan, *Sci. Technol. Adv. Mater*, **9**, 035004 (2008).

[9] J. Pasquet, Y. Chevalier, E. Couval, D. Bouvier, G. Noizet, C. Morliere, M.A. Bolzinger, *Int. J. Pharm,* **460**, 92–100 (2014).

[10] G.R. Li, T. Hu, G.L. Pan, T.Y. Yan, X.P. Gao, H.Y. Zhu, *J. Phys. Chem. C,* **112**, 11859-11864 (2008).

[11] A. Gamliel, J. Kantan, and E. Cohon, *Phytoparasitica*., **17**, 101–106 (1989).

[12] L.R. Khot, S. Sankaran, J.M. Maja, R. Ehsanie, E.W. Schuster, *Crop Prot.,***35**, 64–70 (2012).

[13] R. Raliya, J.C. Tarafdar, *Agric. Res.*, **2**, 48–57 (2013).

[14] J. Wojnarowicz, T. Chudoba, W. Lojkowski, *Nanomaterials,* **10**, 1086 (2020).

P-4

Influence of Edge Sites of Carbon Gels on their Performance as

Li-Air Battery Cathodes

Shintaroh Nagaishi[1], Shinichiroh Iwamura[2], Shin R. Mukai[2]

1Graduate School of Chemical Science and Engineering, Hokkaido University, N13W8, Kita-ku, Sapporo 060-6828, Japan.

2Faculty of Engineering, Hokkaido University, N13W8, Kita-ku, Sapporo 060-6828, Japan. Email: smukai@eng.hokuai.ac.jp

PO_4__nagaishi.pdf

Introduction

Lithium air batteries (LABs) have a high theoretical energy density. However, their poor cyclability inhibits their practical application. Surface properties of carbon materials used for the cathode significantly influences cell performance. This is because the surfaces of carbon materials show catalytic activities towards oxygen reduction reactions, which affects the state of Li_2O_2 deposition during discharging, and the rates of side reactions involving the decomposition of the electrolyte [1]. In this study, we quantitatively investigated how oxygen-containing functional groups (OCFGs) and edge-hydrogen (H) of porous carbons influence the cathode performance of the carbon by using a temperature programmed desorption (TPD) technique, which is conducted under high vacuum and up to a high maximum temperature of 1500 to 1800°C [2]. Carbon gels were selected as a model material for cathodes, because they have a large volume of mesopores, which are effective for rapid O_2 diffusion and Li_2O_2 storage.

A series of carbon gels which have almost the same pore structure, but different surface properties was prepared, and the influence of surface properties on cathode performance was investigated. In addition to as-prepared carbon gels (CG), 2 types of surface modified carbon gels were prepared by HNO_3 treatment at room temperature (Ox-CG) and an additional heat-treatment to Ox-CG at 300°C for 3 h under a N_2 flow (Ox- 300°C-CG). The edge sites of resulting materials were quantitatively analyzed by the TPD technique. The cathodes were prepared by coating the sample on a carbon paper using a PVDF binder. 2032-type coin cells having small holes on the cathode side were assembled using the obtained electrode and a Li foil as working and counter electrode, respectively. Tetraethylene glycol dimethyl ether (TEGDME) mixed with CF_3SO_3Li at a molar ratio of 4 : 1 was used as the electrolyte. The cells were discharged and charged in the range of 2.0-4.4 V at a current density of 50 mA (g-sample)-1 after a 10-hour rest in an oxygen atmosphere. During cycling, charge and discharge capacities were limited to 500 mAh (g-sample)-^{1}. The desorption curves of CO, CO_2 and H_2 obtained by TPD measurement were analyzed and the amount of each type of OFCG in each sample was quantified. By acid treatment, the total amount of OCFGs increased from 0.37 mmol g-1 to 2.1 mmol g-1, and the COOH content increased from 0.038 mmol g-1 to 0.22 mmol g-1. The amount of H decreased from 2.8 mmol g-1 to 2.3 mmol g-1 by acid treatmentsuggesting that H atoms bonded to the edge sites were substituted with OCFGs by acid treatment. In Ox-300°C-CG, the total amount of OCFGs was 2.0 mmol g-1 and the amount of COOH was 0.005 mmol g-1, indicating that COOH was selectively removed by heat treatment.

Fig. 1 shows the results of the discharge-charge cycle tests of the samples. The discharge capacity of CG was maintained at 500 mAh g-1 for 20 cycles, while that of Ox-CG was maintained only for 4 cycles. This is probably because the OCFGs increased by acid treatment promoted side reactions during discharge and charge cycles. On the other hand, the discharge capacity of Ox-300°C-CG was maintained at 500 mAh g-1 for 26 cycles. As mentioned above, there were almost no differences between the total amounts of OCFGs existing in Ox-CG and Ox-300°C-CG, while the amount of COOH existing in them was quite different. From these results, it was concluded that the important factor governing cycle performance is the type of OCFGs rather than the total amount of OCFGs. In particular, COOH groups probably promote side reactions which lead to a significant degradation in cycle performance.

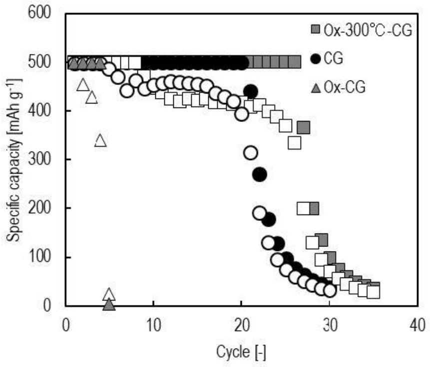

Reference

[1] Daniil M. Itkis, Dmitry A. Semenenko, et al., Nano Letters, 13, 10, (2013), 4697-4701.

[2] Takahumi Ishii, Susumu Kashihara, et al, Carbon, 80, (2014) 135-145.

Acknowledgement

This work was partly supported by the ALCA-SPRING project of JST.

P-5

Effect of nano TiO_2 on the properties of white UPHC

Rui Ma[1, 2], Wei Zhang[1, 2], Aiguo Wang[1, 2], Daosheng Sun[1, 2]*

[1] Anhui Province Engineering Laboratory of Advanced Building Materials, Anhui Jianzhu University, Hefei, 230601, China）

[2] Anhui Province Key Laboratory of Advanced Building Materials, Anhui Jianzhu University, Hefei, 230601, China）

Abstract

With the rapid development of urbanization, the demand of concrete construction is keep increasing and the aesthetical properties becomes more and more important. White cementitious materials exhibited good appearance for constructions and was popularly researched in recent years. However, as a decoration material, the structure properties of white concrete is not pay enough attention, the maintenance and the service life of normal white concrete building is still a big problem. Ultra-high-performance concrete (UHPC) has good mechanical properties and corrosion resistance. Preparation white UHPC (WUHPC) and used as a protect shield for normal concrete, will both improve the out looking performance and strength, and prolong the durability by prevent the environment corrosion. In this work, ecological WUHPC was prepared with quaternary binders, and the improvement of mechanical properties was studied. High volume of limestone and white silica was used to partly substitute white Portland cement to decline the environment impact and materials costs. Since the hydration reactivity of mineral admixtures was lower than cement, nano TiO2 was added to offset the strength decline and improve the matrix properties. The workability, whiteness, and strength development of WUHPC with various mix proportion was studied. The isothermal conduction calorimetry, XRD, SEM-EDS and TG-DSC methods was used to investigate the hydration rate, the component, morphology, and the formation process of hydration products to reveal the synergistic reaction mechanism of multiple binders system. Further, the micro-mechanical properties of hydration products, pore structure and the interfacial transition zone were studied, to demonstrate the micro mechanism of strength development, and the enhancement mechanism of nano materials on WUHPC.

Key words: white ultra-high-performance concrete; mineral admixtures; nano TiO_2, strength development; micro-structure

Acknowledgments: This research was financially supported by Ph.D initial funding of Anhui Jianzhu University (Grant. 2019QDZ15) Natural Science Found Foundation of Anhui

Provance. (Grant. 2008085QE246)

Synthesis and Characterization of MoS_2/Graphene-TiO_2 Ternary Photocatalysts for High-Efficiency Hydrogen Production under Visible Light

Cui Kong[1], Feng-Jun Zhang[1, 2*], Yi Ding[2], Jin Liu[2], Wen- Jie Xie[2]

（1 Key Laboratory of Functional Molecule Design and Interface Process, Anhui Jianzhu University, Hefei Anhui, P. R. China, 230601）

（2 Anhui Key Laboratory of Advanced Building Materials, Anhui Jianzhu University, Hefei Anhui, P. R. China, 230022）

[*]Corresponding author: Zhang Feng-Jun, E-mail: fjzhang@ahjzu.edu.cn

Abstract

Ternary MoS_2/graphene (G)-TiO_2 photocatalysts were prepared by a simple hydrothermal method. The morphology, phase structure, band gap, and catalytic properties of the prepared samples were investigated by X-ray diffraction, Raman spectroscopy, scanning electron microscopy, UV-vis spectrophotometry, and Brunauer-Emmett-Teller surface area measurement. The H_2 production efficiency of the prepared catalysts was tested in methanol-water mixture under visible light. MoS_2/G-TiO_2 exhibited the highest activity for photocatalytic H_2 production. For 5 wt% and 1 wt% MoS_2 and graphene (5MT-1G), the production rate of H_2 was as high as 1989 $\mu mol^{-1}h^{-1}$. The catalyst 5MT-1G showed H_2 production activity that was ~11.3, 5.6, and 4.1 times higher than those of pure TiO_2, 1GT, and 5MT, respectively. The unique structure and morphology of the MoS_2/G-TiO_2 photocatalyst contributed to its improved hydrogen production efficiency under visible light.

Key words: Heterojunction; Hydrogen production; Visible light

Acknowledgments:

This work was financially supported by the Major Projects of Natural Science Research in Anhui Colleges and Universities (KJ2018ZD050, GXXT-2019-017), Natural Science Foundation of Anhui province (1808085ME129), Key research and development plan of Anhui Province (202004a05020060), Outstanding Young Talents Support Program in Colleges and Universities (gxyqZD2018056).

Deterioration of Mortars Immersed in Sodium- and Ammonium-Sulfate Solutions

Kaiwei Liu, Zeying Li, Daosheng Sun, Xingxing Chen, Wanyu Xu
（Anhui Province Engineering Laboratory of Advanced Building Materials, Anhui Jianzhu University, Hefei, 230022, China）

Abstract

Sulfate ions from natural soil and groundwater will react with cement hydration products that limit the lifetime of concrete constructions. An aggressive type of acid–sulfate damage, ammonium sulfate attack, has drawn great attention from scientists as ammonium-based salts are often left in soil after industrial and agricultural applications. The appearance, mass change and expansion were studied to investigate the damage process of the mortars exposed in sodium- and ammonium-sulfate solutions with different concentrations. pH value, X-ray diffraction (XRD) and scanning electron microscopy (SEM) were further studied to analyze the deterioration mechanism. As the concentration increases from 0.1mol/L to 0.6mol/L, the damage of the mortar becomes more serious in sodium- and ammonium-sulfate solutions, especially in ammonium sulfate solution. Mortars immersed in $(NH_4)_2SO_4$ solution show rapid expansions and all samples collapse after 25 weeks of immersion, while samples immersed in Na_2SO_4 solution still maintain a complete appearance. Ammonium sulfate attack provides a potentially acid environment for cement mortars as the pH of solution is maintained at 9-10, which causes the decomposition of calcium hydroxide. The decomposed calcium ions are beneficial to the formation of large amounts of gypsum at a lower pH environment and it is the main reason for accelerated damage of mortars in ammonium sulfate solution.

Key words: sulfate attack; ammonium sulfate; deterioration mechanism; Portland cement

Caulerpa racemosa extract mediated synthesis of ZnO nanoparticles is for antibacterial finishing over cotton fabrics

Paweena Porrawatkul*[1], Rungnapa Pimsen[1], Prawit Nuengmatcha[1], Naengnoi Saengsane[1]
Montakarn Thongsom[2], Sunanta Khongsai[3] and Luksamee Vittaya[3]
[1]Nanomaterials Chemistry Research Unit, Department of Chemistry, [2]Department of Biology Science, Faculty of Science and Technology, Nakhon Si Thammarat Rajabhat University, 80280, Thailand.
[3]Faculty of Fisheries Science and Technology,Trang Campus,Rajamangala University of Technology Srivijaya, 92150, Thailand.
**Corresponding author. e-mail : paweena.n@gmail.com; Tel. +66-7537-7443, Fax +66-7537-7443*

Abstract

In recent times, treatment of natural fibers, like cotton, with antimicrobial finishing using material nanoparticles has become increasingly high due to their tunable nature. In this study, using the *Caulerpa racemosa* extract, zinc acetate was reduced to obtain ZnO nanoparticles using synthesis routes sonication methods. The effected of pH, time reaction and temperature of synthesized ZnO nanoparticles were studied. The ZnO nanoparticles were subjected to X-ray diffraction, scanning electron microscope and energy-dispersive X-ray spectroscopy to ascertain its structure/morphology. The modified cotton fabric possessed excellent inhibited Gram-negative bacterium and Gram-positive bacterium and also maintained the basic properties of cotton fabric. These results suggest that the modified cotton fabrics may find potential applications in a wide variety of areas such as sportswears, socks, and medical textiles.

Keywords: Antibacterial, *Caulerpa racemosa*, Cotton fabric

Introduction

Cotton fabrics are widely used due to their excellent properties such as flexibility, comfortability, water absorptivity, and air permeability. Nevertheless, its extremely easy to cause the growth of bacteria bringing about the degradation of wearability exerts adverse effect on human health [1,2]. Numerous techniques for the surface modification of cotton fabrics have been reported to create additional functionalities, including water repellence, antimicrobial effect, fire resistance, and UV protection. One method, the surface modification using zinc oxide nanoparticles (ZnO NPs) to prepare antimicrobial cotton textiles, has been widely studied due to their nontoxic nature and has diverse physical, chemical and biological properties together with high chemical balance, wide bandgap (3.37 ev), high binding energy (60 MeV) and impressive photo stability [3]. Moreover, the food and drug administration (FDA, USA) listed, ZnO is a safe material compared to other nanomaterials [4]. In recent times, ZnO NPs are also used as external antibacterial agents in textile fabrics, food packages, ointments, mouthwash and lotions to prevent microbial contamination [5–8]. Generally, synthesis of ZnO NPs can be achieved by various physical and chemical methods such as hydrothermal, microwave assisted, co-precipitation, ultrasonic synthesis, thermal decomposition, electrochemical and sol-gel methods [9–11]. All of these methods contain the use of toxic chemicals and solvents, which are harmful to human health and the environment. Recently, bio-inspired synthesis of ZnO NPs, particularly using plants has received much attention due to being eco-friendly, low cost, and facile synthesis process. Plants contain various phytocompounds such as alkaloids, flavonoids, terpenoids, carotenoids, tannins and chlorophylls. The presence of these phytocompounds in plants can be used as a reducing, and capping agents for the synthesis of ZnO NPs [12].

In this work, we are interested in bio-synthesis of ZnO NPs by using the *Caulerpa racemose* as reducing agent, because *Caulerpa racemosa* showed the potential antibacterial activity against pathogenic skin bacteria such as *Staphylococcus aureus*, *Staphylococcus epidermidis* and *Pseudomonas aeruginosa*. In the Southeast Asian, *Caulerpa racemosa* is a green seaweed that is spread widely throughout tropical regions along in the Andaman coastal area such as Trang, Satun, Krabi and Pang-nga province. Local people were usually used *Caulerpa racemosa* as food [13]. Herein, antibacterial cotton textile with a ZnO NPs coating is successively prepared by applying *Caulerpa racemosa* onto cotton fiber surface. The temperature, pH and incubation time were optimized during the process of biosynthesis of ZnO NPs under ultrasonic field. The antibacterial activity of ZnO nanofluids and modified cotton fabric were tested against *S. aureus* and *E. coli* via agar-well diffusion method.

Materials and methods

Caulerpa racemosa was collected from Had-Sam-Ran district, Trang province, Thailand. All analytical reagents used in the study were of analytical grade and were purchased from Merck. Nutrient agar for bacterial culture and Mueller–Hinton broth and agar for antimicrobial activity were purchased from Hi-Media, Mumbai, India.

Collection of seaweeds

Caulerpa racemosa was collected from Had-Sam-Ran district, Trang province, Thailand. This seaweed was cleaned well with seawater to remove all the extraneous matter such as epiphytes and other contaminated materials. Samples were then thoroughly washed with tap water followed by distilled water and kept under sunshade until nearly dry followed by oven drying at 50 °C for 24 hours and powdered using mixer grinder.

Synthesis of zinc oxide nanoparticles

10 g of dry *Caulerpa racemosa* was mixed with 100 mL of double ionized water. The solution was heated at 50 °C and then, doubles filtered using Whatman filter paper no.1. Freshly prepared *Caulerpa racemosa* extract was used for ZnO NPs synthesis. 0.01 M Zinc acetate dihydrate solution was kept on a magnetic hot plate at 80 °C for 20 min. 5 mL of freshly prepared extract was added to it and the solution was stirred for 10 min the pH of the reaction mixture was adjusted by dropwise addition of 1 M NaOH. The temperature, pH and incubation time were optimized during the synthesis process under ultrasonic field. The change of color from colorless to white solution after continuous stirring indicated the synthesis of ZnO NPs. Synthesized ZnO NPs were centrifuged at 10,000 rpm for 5 min and double washed using deionized water and 95% ethanol. ZnO NPs synthesis mechanism and reactions have been studied. Colloidal stability of nanoparticles was tested using UV–Visible spectrophotometer.

Characterization of biosynthesized zinc oxide nanoparticles

Visual observation was considered to comprehend the synthesis of ZnO NPs process. Double beam UV–Vis was used to monitor the absorption spectra of ZnO NPs. Surface plasmon resonance peak of ZnO NPs was measured for their maximum absorbance using UV–Visible Spectrophotometry in the range of 300–700 nm. Their structure and composition were studied by SEM (Scanning electron microscope), XRD (X-Ray Diffractometer) and EDX (Energy-dispersive X-ray spectroscopy).

Coating of ZnO NPs on cotton fabrics

About 0.5 g of ZnO NPs was dissolved in 20 mL chitosan solution (20 mg of chitosan in 20 mL of 1% acetic acid) and stirred for 1 h with magnetic stirrer at room temperature. The mixture was sonicated for 30 min improve the dispersion of ZnO NPs particles in the solution. About 4 g of bio scoured cotton fabric was immersed in the ZnO NPs into chitosan solution for 30 min and padded in the padding mangle, squeezed between two squeezing rollers for 80% wet pick-up. The padded fabric was dried in an oven at 70 ◦C for 10 min and cured in an oven at 150 ◦C for 5 min. The cured fabric was washed well with 1% sodium hydroxide solution, neutralised with 1% acetic acid, washed again and air-dried.

Antibacterial study

Caulerpa racemosa extract and modified cotton fabric were tested for their antibacterial activity against *S. aureus* and *E. coli* by using the agar-well diffusion method. The bacteria culture was spread evenly on the nutrient agar plate using sterile cotton swab. Wells were prepared on agar plates. To these wells standard antibiotic disc (chloramphenicol) were added. After incubation at 37 °C for 24 h, the diameter of inhibition zones around samples were measured and compared with that around the commercial standard antibiotic chloramphenicol and ethanoic extract.

Result and discussion

Synthesis of ZnO nanoparticles

In the present study, zinc oxide nanoparticles were synthesized from *Caulerpa racemosa* ethanolic extract, which were collected from healthy plants and it contains the phytochemical constituents such as alkaloids, tannins, saponins, phenols, glycosides, steroids, terpenoids and flavonoids as main constituents. After the addition of ethanolic *Caulerpa racemosa* extract into zinc nitrate solution under alkalinity condition, color of the reaction mixture was changed from light yellow-green to white color. The color change arises due to the excitation of surface plasmon resonance in the metal nanoparticles, indicating the formation of ZnO nanoparticles and it may be the electron rich functional groups of *Caulerpa racemosa* ethanolic extract were responsible for the conversion of ZnO NPs. Thus, it is concluded that the *Caulerpa racemosa* extract acts as capping and stabilizing agents for the formation of ZnO NPs.

Effect of pH for synthesis of ZnO nanoparticles

The effect of pH was studied at four different pH conditions. The UV–visible spectra of the ZnO NPs were measured at pH 9.0, 10.0, 11.0 and 12.0 of synthesis condition. The result showed that the synthesized ZnO NPs occurred at pH 9 condition and yielded of products increase when the pH value increase. Fig. 1(a) shows the effect of the pH on the synthesis of ZnO NPs. At the pH 12 showed highest absorbance meaning to highest concentration of product. This result due to zinc acetate dihydrate is a soluble metal salt and undergoes precipitation to form zinc hydroxide when dissolved in water or treated with a base. For effective growth and formation of ZnO NPs, enough OH^- concentration is needed in the solution.

Effect of for synthesis of ZnO nanoparticles

Fig. 1(b) shows the UV–vis spectra of the ZnO NPs at four different temperatures: at 50 °C, 60 °C, 70°C and 80 °C, respectively. We found that the rate of ZnO nanoparticle formation increased with increasing temperature from 50 °C to 60 °C, whereas the nearly concentration of product synthesis at 60 °C, 70°C and 80 °C. However, when the reaction was carried out at a temperature more than 60°C, the extract will be degraded. Therefore, the temperature of reaction at 60 °C is a best condition for synthesis of ZnO NPs.

Effect of time for synthesis of ZnO nanoparticles

The time is one of the most important factors in the realization of nanoparticles during the green synthesis. Fig. 1(c) showed an increase in the reaction time resulted in a gradual increase in the absorbance around 360 nm and it was found that the color intensity increased with the duration of the incubation with the maximum absorbance reached at 120 min of the reaction time.

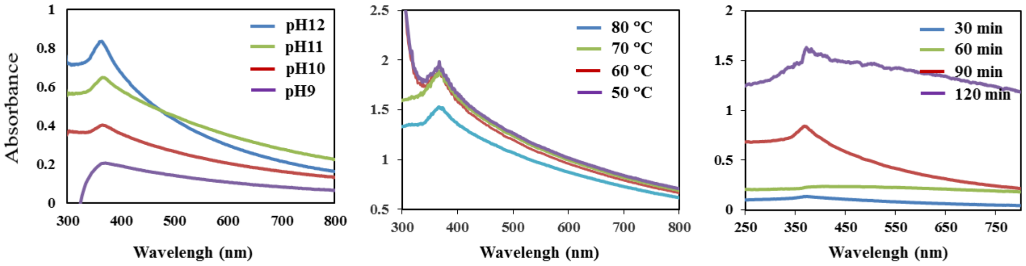

Fig. 1 UV spectra showing (a) the effect of pH (b) the effect of temperature and (c) the effect of time on the ZnO nanoparticles synthesis

X-ray diffraction analysis of ZnO nanoparticles

Fig. 2 shows the XRD pattern of ZnO NPs synthesized at pH 12. The XRD pattern displays the crystalline nature of ZnO NPs by formation of intense peaks at diffraction angles 31.69°, 34.35°, 36.18°, 47.56°, 56.54°, 63.00°, 68.05° and 77.04° corresponding to (100), (002), (101), (102), (110), (103), (200) and (202) plane respectively. The peak patterns could be attributed to the hexagonal phase of synthesized ZnO NPs. Similar lattice plane was observed by *Caulerpa racemosa* extract synthesized ZnO NPs [14]. Sharp diffraction peaks observed in the XRD pattern depicts a good degree of ZnO NPs crystallinity. The observed pattern agreed with JCPDS card no 36–1451 data. Absence of any random peak in XRD pattern established the pure nature of ZnO NPs [15].

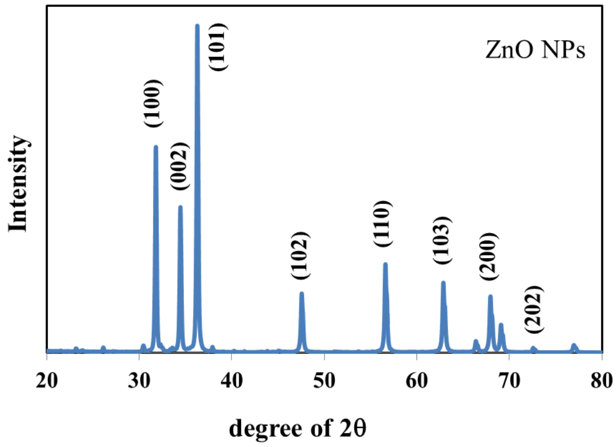

Fig. 2 XRD patterns of ZnO NPs synthesis by using *Caulerpa racemosa* extract.

SEM image and EDX analysis

The surface morphology of ZnO NPs was determined by scanning electron microscopy. The SEM images of synthesized ZnO NPs exhibits spherical morphology (Fig. 3). Energy dispersive x-ray spectrum of ZnO NPs showed the peaks of zinc, oxygen and carbon elements, which confirmed ZnO prepared was free from impurities. The absence of any extra peaks in the EDS spectrum shows the formation of pure zinc oxide nano particles. The EDX spectra of the ZnO samples reveal prominent EDX peaks at 0.3 keV, 0.5 keV and 1.0 keV were observed. These X-ray energies represent the emissions from the K-shell of carbon (54.0%), K-shell of oxygen (16.5%) and L-shell of zinc (78.1%) respectively. The EDX spectrum of ZnO NPs was showed in Fig. 3.

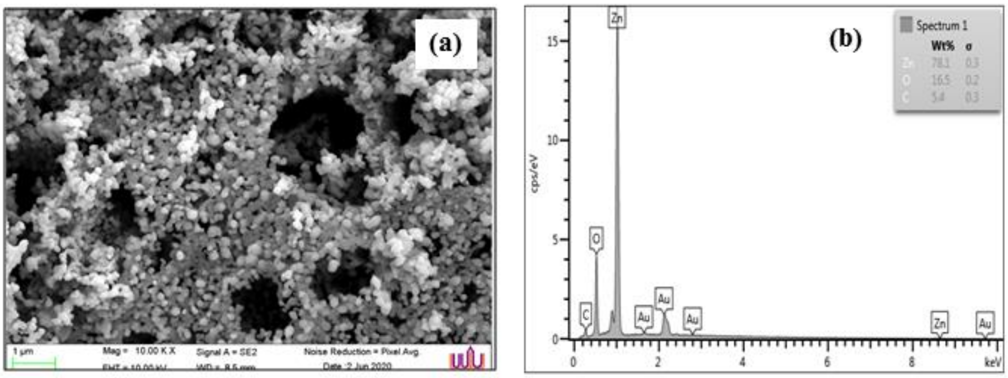

Fig. 3 SEM image and Energy dispersive x- ray spectroscopy of synthesized ZnO NPs.

Surface morphology of the unmodified and modified fabrics

The surface morphology of the untreated cotton fabric and cured cotton fabrics treated with *Caulerpa racemosa* extract capped ZnO-NPs was investigated by SEM and illustrated in Fig. 4. Obviously, the SEM image of the unmodified cotton fabrics (Fig. 4a) that the surface of cotton fiber appears relatively smooth at low magnification and display clear grooves at high magnification. While the cotton fabrics treated with ZnO NPs exhibits the surface morphology of cotton fabrics treated with ZnO NPs (Fig. 4b). The ZnO NPs that coated on fiber fabric effected to antibacterial property of cotton fabric.

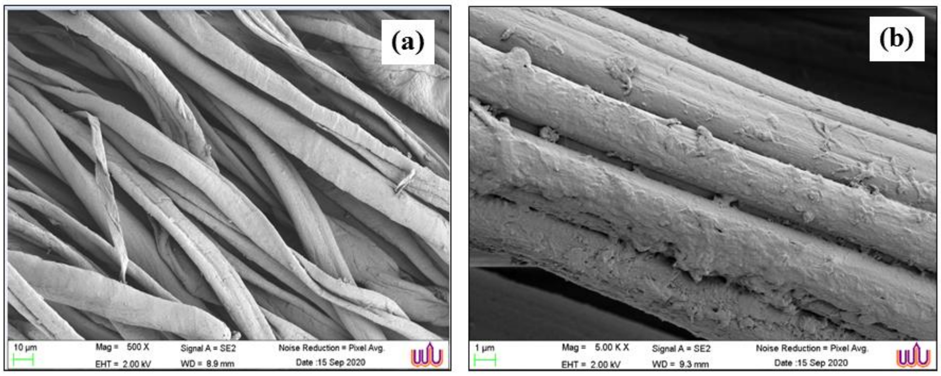

Fig. 4 SEM image of unmodified fabric and modified ZnO NPs on fabric.

Antibacterial activities test

Gram-negative bacterium (*E. coli*) and Gram-positive bacterium (*S. aureus*) were used as models for the investigation of the antibacterial activities of the cotton and modified fabrics. Samples of diameters of 1.5 cm were placed with a bacterial culture in a Mueller–Hinton agar medium following the Kirby–Bauer protocol for the zone of inhibition test. The results are shown in Fig. 5 no inhibition zones were detected in the unmodified cotton fabric (Fig. 5a4, b4).

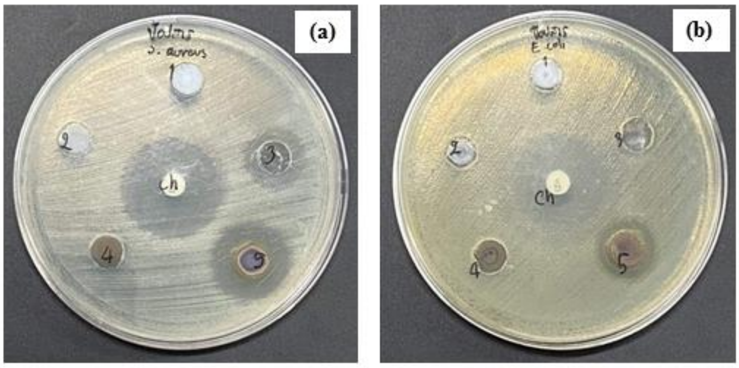

Fig. 5 Antibacterial of unmodified and modified fabric (a) *E. coli* (b) *S. aureus*

In contrast, after the in-situ formation of the ZnO (Fig. 5a5, b5) layer on the surface of cotton, the inhibition zones are obviously visible, indicating that the functional coating provided a significant growth inhibition for both bacteria. The antibacterial activity of zinc oxide is believed to be derived from the H_2O_2 generated from the surface of ZnO which damages the cell membrane of bacteria, leads to some type of injury, and suppresses the growth of the cells or even kills them [16].

Conclusion

In summary, ZnO NPs synthesized by using *Caulerpa racemose* extract was successfully coated on cotton fabric for inhibited bacterial. The modified cotton fabric possessed excellent inhibited Gram-negative (*E. coli*) bacterium and Gram-positive (*S. aureus*) bacterium and also maintained the basic properties of cotton fabric. Results from this study may be exploited for the preparation of cotton textile materials with strong antimicrobial and anti-mildew properties that can find use in practical applications, especially in biomedical textiles.

Acknowledgements

This work was supported by Research and Development Institute, Nakhon Si Thammarat Rajabhat University and Nanomaterials Chemistry Research Unit, Department of Chemistry, Faculty of Science and Technology, Nakhon Si Thammarat Rajabhat University.

References

[1] A. El-Shafei, M. ElShemy, and A. A. Okeil, Carbohydr. **(2015).** A novel chitosan 3 amino-1,2,4-triazole hybrid: Preparation and its effects on cotton fabric properties. *Journal of Taibah University*

for Science., 11(5), 768-774.

[2] Q. Yu, Z. Q. Wu, and H. Chen, Acta Biomater. (2015). Dual-function antibacterial surfaces for biomedical applications. Acta Biomaterialia., 16(1), 1-13.

[3] S. Preethi, K. Abarna, M. Nithyasri, P. Kishore, K. Deepika, R. Ranjithkumar, V. Bhuvaneshwari, D. Bharathi, **(2020).** Synthesis and characterization of chitosan/zinc oxide nanocomposite for antibacterial activity onto cotton fabrics and dye degradation applications. *Int. J. Biol. Macromol*., 164, 2779–2787

[4] T.G. Smijs, S. Pavel, **(2011).** Titanium dioxide and zinc oxide nanoparticles in sunscreens: focus on their safety and effectiveness. *Nanotechnol. Sci. Appl*. 4, 95–102.

[5] H. Moustafa, A.M. Youssef, N.A. Darwish, A.I. Abou-Kandil, (2019). Eco-friendly polymer composites for green packaging: future vision and challenges. *Compos. Part B Eng*. 172, 16–25.

[6] A.M. Youssef, S.M. El-Sayed, H.S. El-Sayed, H.H. Salama, F.M. Assem, M.H. El-Salam, **(2018).** Novel bionanocomposite materials used for packaging skimmed milk acid coagulated cheese (Karish), *Int. J. Biol. Macromol*., 115, 1002–1011.

[7] P.C. Nagajyothi, S.J. Cha, I.J. Yang, T.V.M. Sreekanth, K.J. Kim, H.M. Shin, **(2015).** Antioxidant and anti-inflammatory activities of zinc oxide nanoparticles synthesized using Polygala tenuifolia root extract. *J. Photochem. Photobiol. B*., 146, 10–17.

[8] L. Dobircau, P.A. Sreekumar, R. Saiah, N. Leblanc, C. Terri, R. Gattin, J.M. Saiter, **(2009).** Wheat flour thermoplastic matrix reinforced by waste cotton fibre:agrogreen- composites. *Compos. Part A Appl. Sci. Manuf*. 40, 329–334.

[9] L. Gan, S. Shang, C.W.M. Yuen, S.X. Jiang, **(2015).** Graphene nanoribbon coated flexibleand conductive cotton fabric. Compos. Sci. *Technol*. 117, 208–214.

[10] N.A. Samat, R.M. Nor, **(2013).** Sol–gel synthesis of zinc oxide nanoparticles using Citrus aurantifolia extracts. *Ceram. Int.*, 39, S545–S548.

[11] M. Hasanpoor, M. Aliofkhazraei, H. Delavari, **(2015).** Microwave-assisted synthesis of zinc oxide nanoparticles. *Procedia Mater. Sci*., 11, 320–325.

[12] R.K. Sharma, R. Ghose, **(2015).** Synthesis of zinc oxide nanoparticles by homogeneous precipitation method and its application in antifungal activity against Candida albicans,. *Ceram. Int*., 41, 967–975.

[13] Khongsai, S., Chareondat, U., Chalad, C. **(2017)**. The performance of *Caulerpa racemosa* extracts on inhibition of some pathogenic skin bacteria. *Rajamangala University of Technology Srivijaya Research Journal*. 9 (1), 68 – 75.

[14] A.Z. Noah,M.A. El Semary, A.M. Youssef,M.A. El-Safty, **(2017).** Enhancement of yield point at high pressure high temperature wells by using polymer nanocomposites based on ZnO and $CaCO_3$ nanoparticles. *Egypt. J. Pet*., 26, 33–40.

[15] L.H. Li, J.C. Deng, H.R. Deng, Z.L. Liu, L. Xin, **(2010).** Synthesis and characterization of chitosan/ZnO nanoparticle composite membranes. *Carbohydr. Res*. 345, 994–998.

[16] Zhang, S., Lu, M., Li, Y., Sun, F., Yang, J., Wang, S., **(2013).** Synthesis and electrochemical properties of Zn2SiO4 nano/mesorods. Mater. Lett. 100, 89–92.

P-9

Influence of aggregate characteristics on concrete volume stability and its control measures: A critical review

Aiguo Wang[1], Yingjie Chu[1], Kaiwei Liu[1], Haiyan Xu[1], Xiusheng Wu[1], Daosheng Sun[1*]

（1 Anhui key laboratory of advanced building materials, Anhui Jianzhu University, Hefei 230022, China）

Abstract

Improving the volume stability of concrete is an important research content and a key issue to be solved urgently for improving the durability of modern concrete and realizing high performance. Aggregate properties are one of the important factors affecting the volume stability of concrete. The shape and gradation, mineral compositions, pore and pore structure, elastic modulus and thermal properties of aggregate will all affect the volume stability of concrete. Most of the past research works focused on the influence of one or several characteristics of aggregate on the volume stability of concrete under single factors such as temperature or humidity, and failed to fully clarify the mapping relationship between aggregate characteristics and concrete volume stability. At the same time, the interaction of aggregate properties and the mechanism of their influence on the volume stability of modern concrete have not been studied in depth. Therefore, this article focuses on the different characteristics of aggregates, in terms of shape, pore and pore structure, elastic modulus and mineral composition of aggregate, summarizing its influence on the volume stability of concrete, revealing the mapping relationship between aggregate properties and concrete volume stability. It also clarifies the interaction mechanism of aggregate characteristics and the influence mechanism of the interaction on the volume stability of modern concrete. In view of concrete temperature deformation, drying shrinkage deformation and self-volume deformation, measures to control the volume stability of concrete are proposed from the perspective of aggregate characteristics.

Key words: aggregate characteristics; modern concrete; volume stability; lifting technology

Acknowledgments: The research was the financially supported by the Key Research and Development Projects of Anhui Province (202004b11020033).

P-10

Adsorption of Cr(VI) ions from aqueous solution by ZnO/cellulose

composites

Chinnawat Hoisang Supattra Tangtubtim and Kongsak Pattarith*

Department of Chemistry, Faculty of Science, Buriram Rajabhat University,

Buriram 31000, Thailand

Corresponding author: e-mail kongsak.pr@bru.ac.th; Fax :+66 44612858

Abstract

ZnO impregnated cellulose composites were successfully synthesized via ultrasonic process. The characterization of all materials is carried out through Fourier transform infrared spectroscopy (FTIR) and Scanning electron microscopy (SEM). The remove heavy metal activities were also evaluated for the adsorption of Cr(VI) ions on ZnO/cellulose composites from aqueous solutions. The effects of various parameters including pH of solution, contract time, and temperature were studied. The adsorption of Cr(VI) ions reached the optimum at pH 3 and adsorption equilibrium was reached within 180 min. The maximum adsorption capacity of ZnO/cellulose composites was 200.23 mg/g at 30 ^{o}C which was higher than that of cellulose at the same temperature. The purposed mechanism of Cr (VI) ions adsorption was discussed.

Keywords: Zinc oxide; impregnation; adsorption; cellulose composites; Cr(VI) removal

Introduction

Heavy metals are the most serious pollutants, becoming an extreme public health problem. Heavy metal contamination exists in aqueous waste streams of many industries, such as metal plating facilities, mining operations and tanneries. Cr(VI) ions is a well-known a hazardous waste and highly toxic to humans and environment, considered a priority pollutant[1-2]. Industrial sources of Cr(VI) ions include pesticide application, leather tanning, electroplating, textile manufacturing, dyeing industry etc. A long list of methods has been available for the removal of Cr(VI) ions from wastewater such as chemical precipitation, adsorption, reverse osmosis, ion exchange, electrocoagulation, and membrane separation etc.[3-4]. Among these processes, the adsorption process is easier to operate than other processes, and t low cost for the removal of Cr(VI) from wastewater[5]. For our work, we want to synthesize cellulose and zinc oxide impregnated cellulose composites from waste bamboo and apply as adsorbent for removal of Cr(VI) ions from aqueous solution.

Experimental

Synthesis and characterization of adsorbents

In first step, The waste Bamboo was dried under sunlight. Ten g of waste bamboo were placed in 250 ml of sodium hydroxide solution at 30% in a plastic beaker with agitation for one week at ambient temperature. Then they were filtered, washed with distilled water, and dried at a temperature of 60 ^{o}C. Next, bamboo cellulose fibers were immersed in 1 mM Zinc acetate and sonicated for 1 h. with ultrasonic horn homogenizer, followed by treating with 10 mM NaOH solution to reduce Zinc into nanoparticles. Finally, the cellulose was washed with ethanol and obtained residue was rinsed with deionized water. The synthesized composite was vacuum-dried over night at 30 ^{o}C. All samples were characterized using FTIR and SEM techniques.

Adsorption experiment

Batch experiments were conducted in 100 mL Erlenmeyer flasks, with 0.005 g of the cellulose and ZnO/cellulose being brought into contact with 50 mL Cr(VI) solutions of known concentrations at various pH values. The flasks were agitated using a thermostatic shaker at 150 rpm and kept at various temperatures. The concentrations of Cr(VI) ions in the aqueous samples were determined using a spectrophotometer at 540 nm using diphenyl carbazide as a complexing agent

Results and Discussion

Characterization of adsorbents

Characteristics peaks of cellulose and ZnO/cellulose composites, in case of FTIR analysis, appeared at 3400 cm^{-1} and 2926 cm^{-1} due to O-H stretching and C-H stretching, while 1749–1579 cm^{-1} are due to C-O stretching. While deposition of ZnO on cellulose do not show new peaks different from the cellulose, verifying that no chemical reactions occurred on cellulose revealing coating of ZnO on the cellulose surface only due to physical deposition. Comparison of the SEM images of cellulose and ZnO/cellulose showed that ZnO significantly changed the morphology of cellulose. The ZnO/Cellulose surface was rougher and denser than that of cellulose.

Adsorption study

Cr(VI) ions adsorption capacity of ZnO/cellulose composites was 200.23 mg/g at 30 ^{o}C. The adsorption capacity reached a maximum at pH 3 and adsorption equilibrium was reached after 180 min. The optimal experimental conditions shown in Table 1

Table 1. The optimum conditions for adsorption of Cr(VI) ions by ZnO/cellulose composites

Parameter	Optimum condition
Initial concentration of Cr(VI) (mg/L)	250
Contact time (min)	180
pH	3.0
Temperature (oC)	30

Conclusions

The adsorption of Cr (VI) by ZnO/cellulose composites reached the optimum at pH 3 and adsorption equilibrium was reached within 180 min. The maximum adsorption capacity of ZnO/cellulose composites was 200.23 mg/g at 30 ^{o}C which was higher than that of cellulose (95.62 mg/g) at the same temperature. The present work revealed that the waste Bamboo was the promising materials for the removal of Cr (VI) from aqueous solutions.

Acknowledgements

This research was financially supported by Nakhon Si Thammarat Rajabhat University Research Fund (NSTRU 004/25613 and Nanomaterials Chemistry Research Unit, Department of Chemistry, Faculty of Science and Technology, Nakhon Si Thammarat Rajabhat University, Thailand.

References

1. P. Jain, S. Varshney, S, Srivastava. Synthetically modified nano-cellulose for the removal of chromium: a green nanotech perspective. ET Nanobiotechnology 11 (2017) 45 – 51.

2. N. A. Awang, W. N. Wan Salleh, A. F. Ismail, N. Yusof, F. Aziz, J. Jaafar. Adsorption Behavior of Chromium(VI) onto Regenerated Cellulose Membrane. Ind. Eng. Chem. Res., 58 (2019) 720–728.

3. V. E. Pakade, N.T. Tavengwab and L. M. Madikizelac Recent advances in hexavalent chromium removal from aqueous solutions by adsorptive methods. RSC Adv., 9 (2019) 26142-26164.

4. A. Khan, M. Nazir, I. Ali, A. Kumar. Removal of Chromium(VI) from aqueous solution using guar gum–nano zinc oxide biocomposite adsorbent. Arabian J. Chem., 10 (2017) S2388-S2398.

5. A. Ali, S. Ambreen, Q. Maqbool, S. Naz, M. F. Shams, M. Ahmad, A. R. Phull, M.Zia. Zinc impregnated cellulose nanocomposites: Synthesis, characterization, and applications. J. Phys. Chem. Solids., 98 (2016) 174-182.

Antioxidant Capacity and Total Phenolic Content of Leaf Extracts from *Sonneratia caseolaris* (L.)

Naengnoi Sangsane[*1], **Rattana Wongchuphan**[2], **Paweena Porrawatkul**[1], **Yanisa Tepchuay**[1]

[1]*Nanomaterials Chemistry Research Unit, Department of Chemistry,*
Faculty of Science and Technology, Nakhon Si Thammarat Rajabhat University, 80280, Thailand.
[2]*Program of Chemistry, Faculty of Science and Technology, Suratthani Rajabhat University,84100, Thailand.*
[*]*Corresponding author. e-mail* : s.saengsane@gmail.com

Abstract

Sonneratia caseolaris (L.) *also called* Lam Phu in Thai, belongs to Lythraceae family and has been traditionally used in local cuisine and herbal medicines in Thailand. In this study, antioxidant capacity and total phenolic content of ethanolic leaf extracts were evaluated. The results were calculated as an inhibitory concentration at 50% (IC_{50}) using ascorbic acid as a reference compound (IC_{50} = 23.62±0.02 mg/L). As the result, in the leaflet exhibited the higher antioxidant activity with IC_{50} of 20.57±0.04 mg/L than leaf with IC_{50} = 21.42±0.05 mg/L. The ethanolic leaflet and leaf extracts showed their closely total phenolic contents (29.77±0.03 and 26.09±0.04 mg GAE/100 g of dry weight, respectively). The results suggest that *Sonneratia caseolaris* (L.) was an alternative source of good natural antioxidants.

Keywords: *Sonneratia caseolaris* (L.), Lam Phu, DPPH assay, Total phenolic content

Introduction

Lam Phu in Thai or Crabapple Mangrove, Mangrove Apple and Firefly Mangrove in English common name (*Sonneratia caseolaris* (L.)) from mangrove areas belongs to the genus Sonneratia and the family Lythraceae [1,2]. The plant distribution includes Cambodia, China, India, Indonesia, Malaysia, New Guinea, Sri Lanka, Thailand, Vietnam, Australia, and Pacific islands. Ahmad Fuad Morad has written up on this plant [3] as followed: small to medium-sized tree, up to 15 m, rarely up to 20 m tall, with many, often very strong, vertical pneumatophores and a rather lax crown, much like a (weeping) willow tree. Crown rounded, spreading, not dense. The ends of the branches droop and are quadrangular when young. Leaves are simple, opposite, variable in size, measuring 5-13 by 2-5 cm (Fig. 1). Tip of most leaves has a minute, recurved point. The leaf stalk is broad and very short. Flowers occur in groups of 1-3 together at the ends of stems. The flower buds are broadly oval, less than twice as long as broad. When in full flower, the calyx tube is shallowly cup-shaped and smooth, usually without ribs. The calyx lobes (6, rarely 7 or 8) are usually distinctly longer than the tube, green outside, greenish- or yellowish-white inside. The narrow petals measure about 17-35 mm by 1.5-3.5 mm and are dark red. The numerous stamens are 2.5-3.5 cm long and are soon shed: filaments carmine below, white above. They are red in their lower part, and white in their upper part. The green fleshy fruit occurs on the flattened calyx tube with its nearly horizontally-spreading lobes. It is flattened-round, measuring 3-4 by 5-7.5 cm. The sour young fleshy fruit is edible. Poor quality timber, but occasionally used to salt-water piling. After having been boiled in water, the pneumatophores are an inferior substitute for cork. Pneumatophores are also used for making wooden soles of shoes.

Figure 1. Appearence of *Sonneratia* leaves

Fruits, vegetables and herb extracts containing the phenolic compounds are benificial due to their potential antioxidative properties [4]. Thus, the aims of this study was to identify phytochemicals and to assess the antioxidant capacity of phenolic compounds of the ethanol extract derived from *Sonneratia* leaves by 2,2-diphenyl-1-picrylhydrazyl radical scavenging capacity (DPPH).

Materials and Methods

Chemicals

The organic solvents were used in the experiments for analytical grade and purchased from Merck, Thailand.

Ethanolic extraction of *Sonneratia* leaves

Sonneratia leaves were collected from Tha Sala district, Nakhon Si Thammarat province. Clean *Sonneratia* leaflets and leaves were used as plant samples for extraction.
The ethanolic extracts from both parts were used for analyses: phytochemical screening, DPPH assay and total phenolic content.

Phytochemical screening

Qualitative phytochemical tests for identifying anthraquinones, flavonoids, steroids, terpenoids, saponins, steroids and tannins in the extracts were carried out [3].

DPPH assay

The antioxidant activity was determined using DPPH radical scavenging model with a slight modification. Various concentrations of test compounds in methanol were mixed with the ethanolic solution having a final DPPH radical concentration of 0.1 mM. The mixture was shaken vigorously and kept in dark for 30 min. Reading at 515 nm [4] was obtained using UV-Vis spectrophotometer (Lambda12, Perkin Elmer). The percentage of DPPH inhibition was calculated from the following equation:

$$DPPH\ inhibition\ (\%) = \frac{Abs_{control} - Abs_{sample}}{Abs_{control}} \times 100$$

Determination of total phenolic content

Total phenolic content in the extracts was determined using Folin-Ciocalteu reagent according to the AOAC method. Gallic acid was used as a standard. Samples 0.1 mL were introduced to test tubes and followed by adding 0.3 mL of Folin-Ciocalteu reagent and 2 mL of Na_2CO_3 (15%). The absorbance of all samples was measured at 765 nm using UV–Vis spectrophotometer (Lambda12, Perkin Elmer). Results were expressed as milligrams of gallic acid equivalent (GAE) per 100 grams of dry weight (DW).

Results and discussion

In Table 1, phytochemical screening showed that *Sonneratia* leaves composed of saponins, tannins, terpenoids, steroids, flavonoids and alkaloids.

Table 1 Phytochemicals found in *Sonneratia* leaflet and leaf extracts

Phytochemicals	Leaflet extract	Leaf extract
Saponins	F	F
Tannins	F	F
Terpenoids	F	F
Steroids	F	F
Anthraquinones	ND	ND
Flavonoids	F	F
Alkaloids	F	F

F = Found; ND = Not Detectable

In Table 2, *Sonneratia* leaflet extract showed lower antioxidant activities (IC_{50} = 20.57±0.04 mg/L) and higher total phenolic content (29.77±0.03 mg GAE/100 g DW) than those of leaf extracts. Antioxidant capacity of *Sonneratia* leaves (20.57-21.42 mg/L) was comparable to ascorbic acid (23.62±1.10 mg/L) as their lower IC_{50}. Moreover, antioxidative property of *Sonneratia* leaves may occur because of their phenolic compounds and other active antioxidants.

Table 2 DPPH assay and total phenolic content of *Sonneratia* leaflet and leaf extracts.

Standard and samples	IC_{50})mg/L(	Total phenolic content (mg GAE/100 g DW)
Ascorbic acid	23.62±0.02	-
Leaflet extract	20.57±0.04	29.77±0.03
Leaf extract	21.42±0.05	26.09±0.04

Conclusions

Positive result of six phytochemicals in *Sonneratia* leaves was obtained except anthraquinones. Also, good antioxidant capacity of *Sonneratia* leaves was given as they contain phenolic compounds but not the main active antioxidant. The results suggest that *Sonneratia caseolaris* (L.). leaf was an alternative source of natural antioxidants provided. Further studies should be undertaken for their pharmacological properties.

Acknowledgement

This work was financially supported by Nanomaterials Chemistry Research Unit, Department of Chemistry, Faculty of Science and Technology, Nakhon Si Thammarat Rajabhat University

References

[1] Thailand Nature Project. (2020). *Sonneratia caseolaris* (L.) Engl. Accessed from https://www.thailandnatureproject.com/sonneratia-caseolaris.html.

[2] The Plant List. (2010). A working list of all plant species: *Sonneratia caseolaris* (L.) Engl. Accessed from http://www.theplantlist.org/tpl/record/tro-29700010.

[3] Morad, AF. (2014). Article about *Sonneratia caseolaris* (L.) Engl. Accessd from https://www.flickr.com/photos/adaduitokla/12137411665/.

[4] Wetwitayaklung, P., Limmatvapirat, C., & Phaechamud, T. (2013). Antioxidant and anti-cholinesterase activities in various parts of *Sonneratia caseolaris* (L.). Indian Journal of Pharmaceutical Sciences, **75**(6), 649–656.

Green synthesis of silver nanoparticle-graphene quantum dots against *V. parahaemolyticus* in pacific white shrimp (*Litopenaeus Vannamei*)

Rungnapa Pimsen[*], **Paweena Porrawatkul**[1], **Prawit Nuengmatcha**[1], **and Montakarn Thongsom**[2]

[1]*Nanomaterials Chemistry Research Unit, Department of Chemistry,*
Nakhon Si Thammarat Rajabhat University, 80280, Thailand.
[2] *Department of Biology Nakhon Si Thammarat Rajabhat University, 80280, Thailand.*
[*]*Corresponding author. e-mail : rpimsen@gmail.com*

Abstract

Early Mortality Syndrome (EMS) or Acute Hepatopancreatic Necrosis Syndrome (AHPNS) is a disease produced by gram-negative bacteria *Vibrio parahaemolyticus* (*V. parahaemolyticus*), which has caused declines in worldwide production of a white shrimp *Litopenaeus vannamei* (*L. vannamei*) In this work, we have synthesized a silver nanoparticle-graphene quantum dots (AgNPs/GQDs) using *Barringtonia acutangula* (L.) Gaertn leaf extract and graphene quantum dots as reducing agent and stabilizer. The synthesized GQDs and AgNPs/GQDs hybrid have been characterized by ultraviolet–visible spectroscopy (UV-Vis), X-ray diffraction (XRD) and transmission electron microscopy (TEM). Results indicated that mono-dispersed AgNPs were obtained with particles size around 20 nm, and the lattice spacing is 0.214 nm, which corresponds to the (1 0 0) lattice fringes of graphene. The antibacterial activity of Ag-GQDs was evaluated of bare GQDs and AgNPs/GQDs against *V. parahaemolyticus* in pacific white shrimp (*Litopenaeus Vannamei*).

Keywords: Green synthesis, silver nanoparticle-graphene quantum dots, *V. parahaemolyticus*, pacific white shrimp (*Litopenaeus Vannamei*)

Introduction

Vibrio is a bacterium belonging to the genus that is gram negative. Several species of this bacteria can cause foodborne infection, usually associated with seafood [1]. In 2013, a laboratory infection model found that a pathogenic strain of *V. parahaemolyticu*s provokes an AHPNS illness, disease that has affected severely shrimp industry. Because it can infect wild and cultivated shrimps [1]. Several strategies have been addressed to control diseases that affect a shrimp, such as tank water replacements, good personnel management practices On the one hand, given the inefficiency of conventional treatments, the development of new agents for pathogen treatment has been opted for, such as nanomaterial development and implementation, including antibiotic resistance [2]. On the other hand, green synthesis is a viable strategy for nanomaterial generation, since it is a process that uses plant extracts, algae, fungi, yeast, etc., as reducing agents, and is safe and an eco-friendly strategy [3]. Silver nanoparticles (AgNPs) are emerging as an antimicrobial candidate with particular promise because of their unprecedented function as a bactericide against a broad spectrum of microorganisms through the mechanism of releasing Ag^+ and generating reactive oxygen species (ROS). However, it is usually a challenge for nanostructured Ag substrates to achieve such effective capture because of the weak affinity of some target molecules toward the metal surface [18]. In particular, plant extracts have been utilized for AgNP synthesis, in nanotechnology field, highlighting how this has shown a very promising effect as a bactericide [4].

In this work, we propose the implementation of AgNPs/GQDs synthesized with *Barringtonia acutangula* (L.) Gaertn leaf extract and graphene quantum dots as reducing agent and stabilizer as an alternative on *V. parahaemolyticus* control in pacific white shrimp (*Litopenaeus Vannamei*)

Materials and methods

Analytical reagents used in the study were of analytical grade and were purchased from Merck. Nutrient agar for bacterial culture and Mueller–Hinton broth and agar for antimicrobial activity were purchased from Hi-Media, Mumbai, India.

Preparation of leaf extract

10 grams of *B. acutangula* (L.) Gaertn leaves was weighed, cut into fine pieces, crushed with 100 mL of distilled water for 1 h at 60 °C, and filtered through Whatman No.1 filter paper. The filtrate aqueous extract was used as a reducing agent.

Synthetic Graphene Quantum Dots (GQDs)

2 grams of citric acid was heated and melted at 170°C, which then converted into dark orange color within 15 min. 0.75 M solution of NaOH was added dropwise in the melted dense solution of citric acid at room temperature, adjust pH with 0.75M NaOH until pH 7 (neutral). The resulting solution was quantum graphene graphene and was identified with UV-Vis, SEM, EDX, XRD, and TEM techniques.

Optimization of AgNPs synthesis and characterization of AgNPs

The aqueous solution of silver nitrate ($AgNO_3$) was prepared in a flask. 2 mL of the leaf extract was mixed with $AgNO_3$ solution under magnetic stirring. Silver nanoparticle formation was visually observed by the gradual change in color of the mixture, which was incubated under different time and temperature. To achieve the maximum product yield, the optimization of these factors was analyzed by UV-visible absorption.

Optimization of AgNPs-GQDs synthesis and characterization of AgNPs-GQDs

AgNPs-GQDs solution using 0.1M AgNO3 2mL, the 2 mL dose of the extract with different volumes of GQDs was 1, 2, 3, and 4 mL. under sonication temperature 80 ° C for 1 h., which was incubated under different time and temperature. To achieve the maximum product yield, the optimization of these factors was analyzed by UV-visible absorption.

Antibacterial study

AgNPs-GQDs biosynthesized from *B. acutangula* (L.) Gaertn leaf extract and the aqueous leaf extract were tested for their antibacterial activity against *V. parahaemolyticus* using the Agar-well diffusion method. The bacteria culture was spread evenly on the nutrient agar plate using sterile cotton swab. Wells were prepared on agar plates. To these wells nanoparticles solution (30 mg/L) and standard antibiotic disc (chloramphenicol, 30 μg) were added. After incubation at 37 °C for 24 h, the diameter of inhibition zones around AgNPs-GQDs were measured.

Results and discussion

AgNPs-GQDs characterization

The UVevis absorbance spectroscopy first demonstrates the formation of Ag NPs in the aqueous solution of GQDs. In Fig. 1(a), a sharp characteristic peak at ca. 228 nm and several other broad absorption bands at ca. 270 nm, 305 nm and 370 nm can be observed for GQDs. The sharp one is corresponded to the π-π^*transition of carbon-carbon bonds, whereas the rest ones arise from the n-π^* transition of carbon-oxygen bonds. The appearance of those broad absorption bands well documents that the electrochemically prepared GQDs contain oxygen functional groups on either side of its basal plane and at the sheet edges [3][4]. After adding AgNO3 aqueous solutions with different volume ratios into the GQDs aqueous solution and subsequent continuous UV exposure of the mixture solutions, a strong absorption band centered at ca. 430 nm can be observed in Fig. 1.

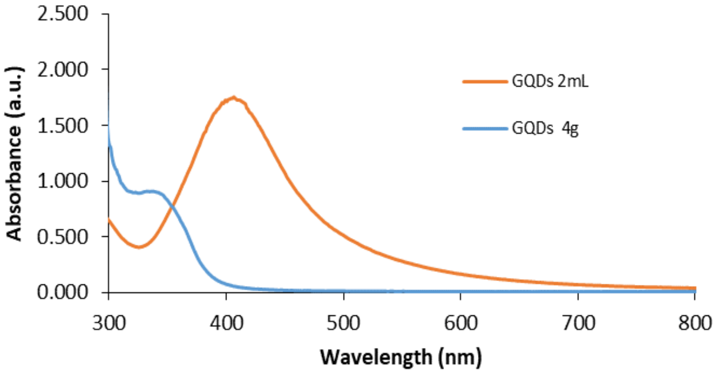

Fig. 1 UV–vis spectra of AgNPs-GQDs solution using 2 mL of 0.1M $AgNO_3$ with 2 mL of extract.

The FTIR spectroscopy of the leaf extract (Fig. 2) showed prominent peaks at 1042, 1350, 15617 and 3406 cm^{-1} attributed to C–N stretching (aliphatic amines), C-H group (aromatic) [5], C=O stretching [6] and O–H stretching [7], respectively. The majority of the IR bands are characteristic of phenolic compounds present in the leaf extract. The FTIR spectroscopy of AgNPs shows a broad peak that decreases in intensity at around 3211 cm^{-1} corresponding to the OH stretching vibrations of phenolic compounds. The shift from 3406 to 3211 cm^{-1} may indicate the involvement of OH functional group in the reduction of Ag^+ ions [8].

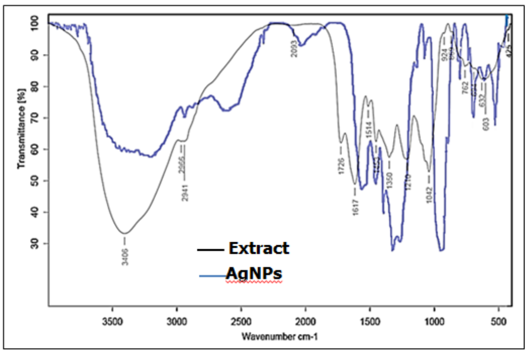

(a)

Fig. 2 AgNPs Characterization (a) FTIR spectra of AgNPs vs leaf extract

Effect of time

The time is one of the most important factors in the realization of nanoparticles during the green synthesis. Found that an increase in the reaction time resulted in a gradual increase in the absorbance at 420 nm and it was found that the color intensity decreased with the duration of the incubation with the maximum absorbance reached at 2 h of the reaction time. The optimum time was 0.5 h, that is unstable for the formation of AgNPs-GQDs [3].

Effect of temperature

The UV–vis spectra of the AgNPs-GQDs at three different temperatures; at 60, 70 °C and 80 °C, respectively. We found that the spectra intensity of AgNPs-GQDs decreased with increasing temperature. The maximum synthesis of silver nanoparticles occurred at 60 °C.

However, when the reaction was carried out at a temperature more than 60°C, the leaf extract will be degraded.

Antibacterial activity

The antibacterial activity of the AgNPs-GQDs was studied by the well diffusion method according to the protocol as described in the previous section. The zones of inhibition are shown in Fig. 3. the synthesized AgNPs displayed an efficient antibacterial activity against *V. parahaemolyticus*. The AgNPs showed the largest zone of inhibition, at around 26 mm.

Fig. 3 Zone of Inhibition Area (in mm) exhibited by the formed AgNPs-GQDs against *V. parahaemolyticus*.

Conclusion

We reported a simple and efficient green synthesis of AgNPs using the aqueous leaf extract of *B. acutangula*)L.) Gaertn. The synthesized AgNPs-GQDs were characterized by UV–Vis spectroscopy, FTIR, LPSA, SEM, and TEM analyses. The UV-vis spectra showed a maximum absorption peak at 430nm, which represents the characteristic surface plasmon resonance of nanosilver. FTIR analysis was carried out to probe the possible functional groups involved in the synthesis of AgNPs. In addition, the synthesized AgNPs-GQDs showed the good antibacterial for *V. parahaemolyticus.* inhibition.

References

[1] J. Cesar *et al.*, “Silver nanoparticles applications (AgNPS) in aquaculture,” vol. 6, no. 2, pp. 5–11, 2018.

[2] J. M. Lacave *et al.*, “Acute toxicity, bioaccumulation and effects of dietary transfer of silver from brine shrimp exposed to PVP/PEI-coated silver nanoparticles to zebrafish,” *Comp. Biochem. Physiol. Part - C Toxicol. Pharmacol.*, vol. 199, pp. 69–80, 2017, doi: 10.1016/j.cbpc.2017.03.008.

[3] J. Ge, Y. Li, J. Wang, Y. Pu, W. Xue, and X. Liu, “Green synthesis of graphene quantum dots and silver nanoparticles compounds with excellent surface enhanced Raman scattering performance,” *J. Alloys Compd.*, vol. 663, pp. 166–171, 2016, doi: 10.1016/j.jallcom.2015.12.055.

[4] H. V. Tran, A. D. Chu, T. Van Nguyen, N. D. Nguyen, T. D. Le, and C. D. Huynh, “An investigation of silver nanoparticles formation under presence of graphene quantum dots as reducing reagent and stabilizer,” *Mater. Trans.*, vol. 59, no. 7, pp. 1106–1111, 2018, doi:

10.2320/matertrans.MD201713.

[5] S. Das, J. Das, A. Samadder, S. S. Bhattacharyya, D. Das, and A. R. Khuda-bukhsh, “Colloids and Surfaces B : Biointerfaces Biosynthesized silver nanoparticles by ethanolic extracts of Phytolacca decandra , Gelsemium sempervirens , Hydrastis canadensis and Thuja occidentalis induce differential cytotoxicity through G2 / M arrest in A375 cells,” *Colloids Surfaces B Biointerfaces*, vol. 101, pp. 325–336, 2013, doi: 10.1016/j.colsurfb.2012.07.008.

[6] S. Dinesh, S. Karthikeyan, P. Arumugam, T. Nadu, T. Nadu, and T. Nadu, “Biosynthesis of silver nanoparticles from Glycyrrhiza glabra root extract,” vol. 4, no. 1, pp. 178–187, 2012.

[7] T. Y. Suman, S. R. R. Rajasree, A. Kanchana, and S. B. Elizabeth, “Colloids and Surfaces B : Biointerfaces Biosynthesis , characterization and cytotoxic effect of plant mediated silver nanoparticles using Morinda citrifolia root extract,” *Colloids Surfaces B Biointerfaces*, vol. 106, pp. 74–78, 2013, doi: 10.1016/j.colsurfb.2013.01.037.

[8] R. Vivek, R. Thangam, K. Muthuchelian, and P. Gunasekaran, “Green biosynthesis of silver nanoparticles from Annona squamosa leaf extract and its in vitro cytotoxic effect on MCF-7 cells,” *Process Biochem.*, vol. 47, no. 12, pp. 2405–2410, 2012, doi: 10.1016/j.procbio.2012.09.025.

A STUDY OF TEENAGER BEHAVIOR PROCEEDING TO COMMITTING CRIMINAL ACTS

Watcharaporn Khunthanee[1] and Rachadaporn Benchawattananon[2]*

[1]*Forensic Science Faculty of Science, Khon Kaen University, Khon Kaen 40002, Thailand.*

[2]** Integrated Science, Forensic Science, Faculty of Science, Khon Kaen University, Khon Kaen 40002, Thailand.*

** Corresponding Author: Benchawattananon, R.; Email: rachadaporn@kku.ac.th*

Abstract

Adolescents or youths in Thailand today find themselves in a crime problem and social violence tends to increase. The cause may be due to different behavioral conditions, different factors such as social conditions, family, friends, external environment may include the use of technology. Nowadays, physical development, such as hormones, may be a factor affecting behavior. In this research, the factors that contributed to the crime were selected and studying hormones, substances from the brain that may influence criminal behavior. Its objectives are to study the behavior of adolescents induced to commit crime and to study hormones that influence the behavior of crimes. The ethic of this research is HE632234 from the sample studied, 60 people aged 17-21 years the number of samples was divided into 2 groups, group 1 of 30 people to study crime-related factors using data of the criminal sample group collected by the back-base and police officer group 2. 30 people to study the hormone, the neurotransmitter that may have the effect of causing criminal behavior, is dopamine. The results of the study showed that the tendency of violent behaviors that resulted in crime was largely substance abuse and the neuronal hormone Dopamine has a slight effect on violent behavior.

Keyword: Adolescents, Crime, Dopamine, Risk behavior

Synthesis of Solid Dye Laser Materials

JU YONG CHO,[1] AND WON KWEON JANG[1,*]

[1]*Department of Aeronautic Electricity, University of Hanseo, Hanseo 1-ro 46, Seosan-si 31962, South Korea*

*Email: *jwk@hanseo.ac.kr*

Abstract

Dye lasers have been attractive sources for long years though its disadvantage of liquid flow system with handling inconvenience. It has been suffered from technical complexity of the flow system for constant turbulence and flow. Solid state dye has been developed with improving many defects because it has still a strong candidate in some wavelength range with wide tunability. In this paper, solid state dye is synthesized, in order to replace liquid solution in the dye lasers, and transmittance spectrum of the dye with different concentration is investigated. This solid-state dye can be used for tunable laser.

1. Introduction

Broad absorption and emission spectra are shown in dye molecules. Therefore, dye laser is very attractive source to implement tunable laser. Many dyes have been investigated to cover the spectral range from ultraviolet to the near infrared. This versatility gives many applications in spectroscopy, medicine, and industry. One of major drawbacks is photodegradation that results from thermal destruction[1]. This drawback can be solved by flow system of the dye solution, but the the size of flow system is huge[1]. Moreover, there is inconvenicence to hold constant flow rate[1]. In this paper, solid state dye is synthesized to overcome the major drawback that conventional dye system has. Transmittance spectrum of the dye solution with different concentration was investigated to examine the change of absorption peak. The solid-state dye laser system provides advantage such as compact system, easy operation, and avoidance from toxicity and flammability.

2. Synthesis of solid-state dye

In order to synthesize solid state dye, polymethymethacrylate(PMMA) and dye solution should be mixed, and initiator is mixed with the mixed solution. the prepared solution needs to be heat up to initiate polymerization. Rhodamine 590 was chosen for this synthesis. The dye was dissolved by ethanol before the dye and PMMA are mixed, because PMMA and the dye powder are not easily mixed. 0.5wt% initiator was used. The prepared solution was 10ml.

In order to hold the temperature of surface of cylinder that contains prepared solution during polymerization, water was filled in large size beaker and was bolied. Water was bolied at 90℃ by stirrer until the prepared solution is viscous, and temperature water was kept being 70℃ until the solution becomes solid state. Figure 1 shows polished solid-state dyes.

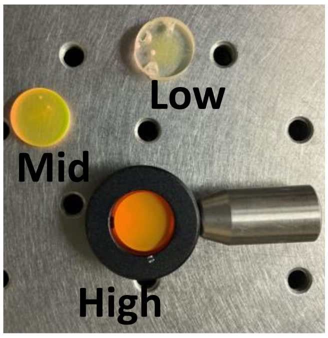

Figure 1. Synthesized solid state dye.

3. Transmittance spectrum of solid-state dye

Transmittance spectrum of solid-state dye is investigated for the choose of appropriate pump wavelength and is shown in figure 2. Transmittance quickly decay according to increase concentration of Rhodamine 590 in solid state dye. Lowest tranmittance of low concentrated solid-state dye is at 530nm.

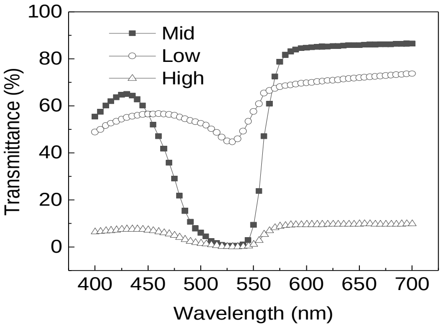

Figure 2. Transmittance spectrum of solid-state dye.

4. Conclusion

Procedure of synthesis of solid-state dye is briefly discussed and transmittance spectrum of solid-state dye are investigated in this paper. Change of absorption of solid-state dye with various concentration needs to be investigated. Laser cavity with synthesized dye will be built to investigate properties for the tunable laser.

References

A. Costela, L. Cerdán, and I. García-Moreno, “Solid state dye lasers with scattering feedback”, Progress in Quantum Electronics 37 (2013), Vol. 37, pp. 348-382(2013).

Extending maximum wavenumber in a spatially modulated Fourier transform spectrometer

JU YONG CHO,[1] AND WON KWEON JANG[1,*]

[1]*Department of Aeronautic Electricity, University of Hanseo, Hanseo 1-ro 46, Seosan-si 31962, South Korea*

*Email: *jwk@hanseo.ac.kr*

Abstract

Spatially modulated Fourier transform spectrometers are able to detect the chemical compounds in wide range of spectrum. One of major drawbacks of the spatially modulated Fourier transform spectrometers is the limited sampling points that have been treated importantly in extending the maximum wavenumber. The spectral distortion is commonly observed in the measurement of broadband wavelength range due to insufficient sampling points. In this paper, the interpolation method was tried to the spatially modulated interferogram to avoid aliasing. Maximum wavelength was increased by 7 times after interpolation in our experimental resuls.

1. Introduction

The spatially modulated Fourier transform spectrometers are a powerful tool to measure widely spread chemical compounds. The spectrometers produce spatially modulated interferogram that contains information of the light. Overlapped sector that spatially modulated interferogram is observed is so small that pixels to detect overlapped sector are insufficient. Therefore, one of major disadvantage of the spectrometers is aliasing.

Sampling points and maximum optical path difference are trade-off relationship. In the case of low optical path difference, many sampling points can be acquired, and aliasing is not easily appeared, but the spectral resolution is bad because resolution is inversely proportional to optical path difference.

In this paper, interpolation in order to increase maximum wavenumber is briefly introduced. Sampling points in the spectrometer is discussed to avoid spectral aliasing.

2. Required resolution

Spectral resolution δ_R in the spectrometer depends on spectral range and sampling points N_S, and the spectral resolution is given as follow:

$$\delta_R = \frac{\tilde{\nu}_{\max} - \tilde{\nu}_{\min}}{N_s} \tag{1}$$

Where $\tilde{\nu}_{\max}$ is maximum wavenumber and $\tilde{\nu}_{\min}$ is minimum wavenumber. Wavenumber $\tilde{\nu}$ is inversely proportional to wavelength. In the experiment, Sagnac interferometer is chosen because optical path difference is adjustable. Equivalent optical layout of the interferometer is equal to double slits. Therefore, eq. 1 can be written as below[1]:

$$\delta_R = \frac{f}{d \cdot l \cdot N_s} \tag{2}$$

Where f is focal length of the lens, d is pixel pitch of detector, and l is distance between two separated beams.

3. Results and discussions

LED that has 90nm spectral width at 1550nm central wavelength is used. its spectral range in wavenumber is from 6269.6cm^{-1} to 6644.8cm^{-1}. For this experiment, lens of 400mm focal length and detector that has 25 μm pixel pitch and 512 total pixels is used. In this case, calculated maximum distance between two separated beams and overlapped sector are 11.3mm and 1.2mm, respectively. Maximum resolution that can avoid spectral aliasing is 27.6cm^{-1}[1]. In order to increase maximum wavenumber by interpolation, the interferogram acquired at 1.41mm distance is used. Calculated resolution was 266.5cm^{-1}. Data points in overlapped sector is 443. In order to be 27.6cm^{-1}, 4096 data points are needed. Original interferogram and interferogram after interpolation are shown in figure 1.

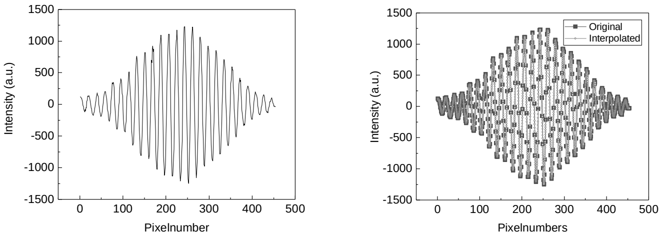

(a) (b)

Figure 1. Interferogram acquired at 1mm distance between two separated beams. (a) is original interferogram, and (b) is interferogram after interpolation.

Interferograms in figure 1 are Fourier transformed and are shown in figure 2. Compared to the acquired spectrum from monochromator, spectral width is wide because of resolution. The spectral line, that interferogram after interpolation is Fourier transformed, has same spectral line of original interferogram. Maximum wavenumber for original interferogram is 69189cm^{-1} and maximum wavenumber for interpolated interferogram is 511550cm^{-1}. Maximum wavenumber after interpolation is incrased approximately by 7 times, which is shown in figure 2.

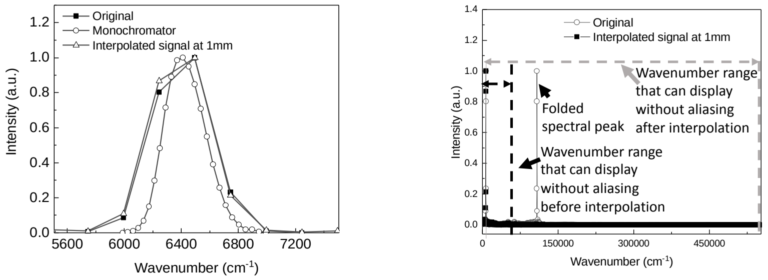

(a) (b)

Figure 2. (a) Spectral line of interferograms in figure 1. Spectrum measured by monochromator is used as reference. (b) entire spectra of interferogram in figure 1.

4. Conclusion

Spatially modulated Fourier transform spectrometer is built with Sagnac interferometer. Required sampling points are briefly discussed in order to increase maximum wavenumber. In this paper, any spectral information change is not observed after interpolation and maximum wavenumber can be increased by interpolation. This interpolation technique for spatially modulated Fourier transform spectrometer can be used to avoid aliasing when broad wavenumber range needs to be measured.

References

1. Ju Yong Cho, Seung Hoon Lee, and Won Kweon Jang, “Improvement of spectral resolution by signal padding method in the Spatially modulated Fourier transform spectrometer based on a Sagnac interferomter”, *Applied Optics*, Vol. 58, No. 25, pp. 6755-6761(2019).

P-16

Heat-generating mechanism of polymer-derived SiC fiber under the

microwave

Young Jun Joo[a], Sang Hyun Joo[a], Kwang Youn Cho[a]*

[a]*Fibrous Ceramics & Aerospace Materials Center, Korea Institute of Ceramic Engineering and Technology, 101, Soho-ro, Jinju-si, Gyeongsangnam-do, 660-031 Korea*

E-mail: kycho@kicet.re.kr

Keywords: *SiC fiber, Microwave, Heat-generating, Conduction loss, excess carbon*

Introduction

In a previous study by Korea Institute of Ceramic Engineering and Technology (KICET), SiC fibers were fabricated in the form of multi-layered mats, which showed heat-generating behavior up to 1500°C in few seconds under microwave. However, the microwave-assisted heating mechanism of polymer-derived SiC fibers is not clearly understood. Therefore, the polymer-derived SiC fiber and blocks having various shapes were prepared depending on the pyrolysis temperature to investigate the heat-generating mechanism.

Experimental procedure

Polycarbosilane (PCS) was melt-spun above melting point and its fibers were continuously received by a circular winder at 160 rpm. Then, PCS green fibers and iodine of 1:1 weight ratio were put into graphite crucible, and then heat-treated at 120–180℃ for 2 h under the low pressure. Also, the cured PCS powder was prepared by the same curing method after the ball-milling for 24 h. The cured PCS fiber and powder were pyrolyzed at 500–1700℃ under an inert atmosphere. The heat-generating behavior of polymer-derived SiC fiber observed by in-situ using the microwave furnace equipped with 2.45 GHz magnetron and IR camera.

Results and discussion

The polymer-derived SiC fibers generated the high-temperature heat of 1500–1600℃ in a few seconds under the microwave. Unlike general ceramic materials, the heat-generating behavior of polymer-derived SiC started at the center of the specimen and increased in proportion to the degree of π-electrons. As a result, the heat-generating mechanism of polymer-derived SiC fiber mats under the microwave showed more dependent on the conduction loss than the dipole loss. Although polymer-derived SiC fiber mats degraded by decomposition in the form of SiO and CO gases above 1500℃, SiC fiber mats fabricated at 1450℃ had the lowest oxygen content and improved life-time.

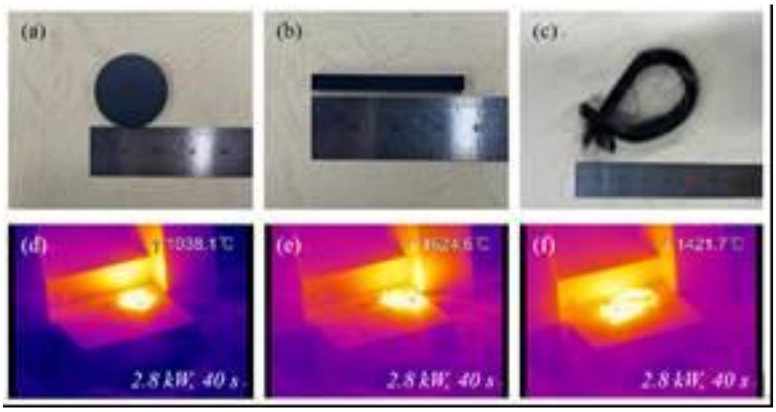

Fig. The (a-c) photographs and (d-f) infrared images of polymer-derived SiC with different shpaes.

References:

1. R.R. Mishra, A.K. Sharma, Compos. Part A. 81 (2016) 78-97.
2. H. Ichikawa, Annu. Rev. Mater. Res. 46 (2016) 335-356

Structural analysis of zirconium-added SiC fibers prepared via blend and electrospinning methods

Young Jun Joo[a], Sang Hyun Joo[a], Kwang Youn Cho[a]*

[a]*Fibrous Ceramics & Aerospace Materials Center, Korea Institute of Ceramic Engineering and Technology, 101, Soho-ro, Jinju-si, Gyeongsangnam-do, 660-031 Korea*

E-mail: kycho@kicet.re.kr

Keywords: *SiC fiber, Zirconium, Heat resistance, SEM, TEM*

Introduction

Silicon carbide (SiC) fibers having a diameter of about 10 ~ 12 μm are fabricated by a precursor route including the sequence of melt-spinning, curing, and pyrolysis, and polycarbosilane (PCS) consisting of silicon and carbon in the backbone is mainly used as a SiC precursor. High-performance SiC fibers with high oxidation resistance and tensile strength at extreme environment have been emerged as a structural material in the field of aerospace and military industries.

Experimental procedure

Polycarbosilane (PCS) was blended with a zirconium acetylacetonate (Zr-acac) at room temperature, and then zirconium-added PCS solution spun into fiber felts by electro-spinning. PCS and zirconium-added PCS fiber felts were heat-treated at 150–200℃ for 10 h in an atmosphere of hot air flowing. Subsequently, the cured PCS fiber felts were converted into SiC fiber felts via pyrolysis process at 1400℃ in an inert atmosphere. The SiC and Si-Zr-C-O fiber felts cut to a size of about 25 x 20 mm were heat-treated at 1500℃ and 1600℃ for 1 h to test heat-resistance.

Results and discussion

SEM and TEM analysis showed that Zr, which has a high oxygen coordination number than Si and undergoes a phase transition at high temperature, remains in the final SiC fibers and has an effect of improving the thermal resistance of about 150℃. Figure shows the TEM images of zirconium-added SiC fiber before and after heat treatment at 1600℃. Before the heat treatment, Si-Zr-C-O fibers had little crystalline phase and showed a ring pattern in selected area diffraction (SAD) pattern. The zirconium-added SiC fibers heat-treated at 1600℃ showed many crystalline phases compared to fibers before heat-treatment but still had a ring pattern because small crystalline phases were piled up.

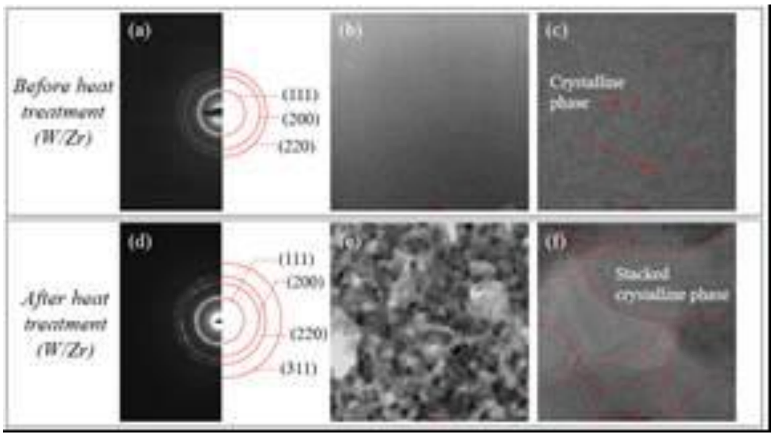

Fig. SAD and TEM images of Si-Zr-C-O fiber felts (a-c) before and (d-f) after heat treatment at 1600℃ for 1h.

References:

3. H. Yamamura, T. Ishikawa, K. Kumagawa, J. Mater. Sci. 34 (1999) 1333-1339.
4. S. Cao, J. Wang, H. Wang, Cryst. Eng. Comm. 18 (2016) 3674-3682.

Densification and Mechanical properties of amorphous Silicon carbide block fabricated from the precursor route

Sang Hyun Joo[a], Young Jun Joo[a], Kwang Youn Cho[a]*

[a]Fibrous Ceramics & Aerospace Materials Center, Korea Institute of Ceramic Engineering and Technology, 101, Soho-ro, Jinju-si, Gyeongsangnam-do, 660-031 Korea

E-mail: kycho@kicet.re.kr

Keywords: SiC block, Densification, Flexural strength, Morphology

Introduction

Silicon carbide (SiC) having the excellent mechanical and thermal properties, is generally synthesized through solid state sintering using α-SiC and β-SiC powder at high temperature (> 2000°C) under the high pressure. In this study, amorphous SiC block was easily fabricated using polycarbosilane (PCS), a ceramic precursor mainly used for SiC fibers or SiC coating. In addition, the synthesis conditions were optimized for densification of amorphous SiC block via the control of pressing load and pyrolysis temperature. Amorphous SiC blocks can be fabricated easily and inexpensively compared to SiC sintered bodies, therefore, it is expected to be applied to industrial fields as a structural material in a vicinity of 1300°C.

Experimental procedure

Polycarbosilane (PCS) as a ceramic precursor was ground into a powder, and then PCS powder and iodine were placed in graphite mold and heat-treated at 180°C for 2 h. The ceramic yield-controlled PCS powder was pressed using a uniaxial press. PCS blocks were pressed in the range of 2 to 8 ton, and then pyrolyzed at temperature ranging from 1000 to 1400°C for 2 h under inert atmosphere.

Results and discussion

Amorphous SiC blocks have been successfully fabricated using the precursor route. The flexural strength of polymer-derived SiC blocks was increased with increasing pressing load and with decreasing pyrolysis temperature. The density of amorphous SiC blocks showed similar tendency of the mechanical strength. All SiC blocks also exhibit only broad β-SiC peak. In SEM images, the microstructure of SiC block became slightly porous as the heat treatment temperature increased.

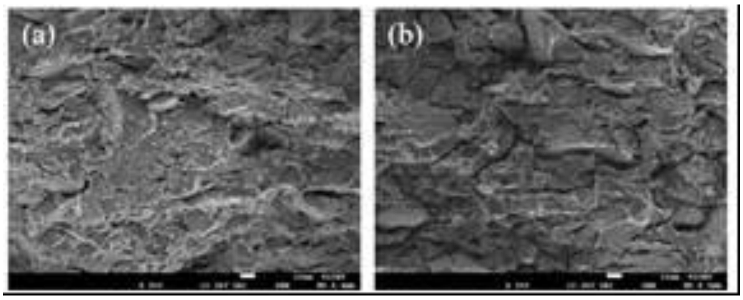

Fig. SEM image of polymer-derived SiC blocks fabricated at (a) 1000℃ and (b) 1400℃

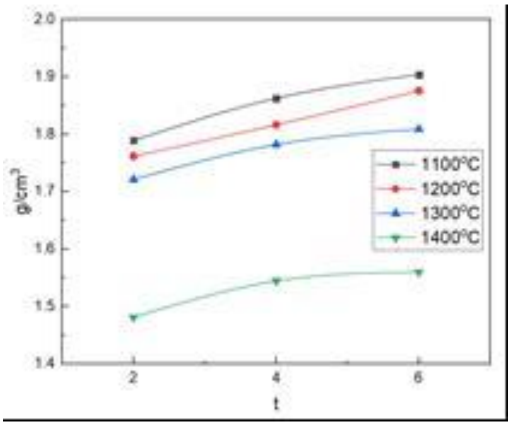

Fig. The density of polymer-derived SiC blocks depending on the pressing load

References:

5. Y. J. Joo, K. Y. Cho, and C. J. Kim, *J. Ceram. Process. Res.* **20** (2019) 1-7

Treatment of the Waste Generated from N_2H_4-Cu^+-H_2SO_4 Decontamination Solution

Huijun Won* and Naon Chang

Decommissioning Technology Research Division, Korea Atomic Energy Research Institute, Daejeon 305-353, Korea

Email: nhjwon@kaeri.re.kr, Fax: +82-42-868-4797

Abstract

The objectives of this study are to predict the decomposition performance of hydrazine using hydrogen peroxide and to evaluate the precipitation characteristics of sulfate ions by Ba^{2+} and Sr^{2+} ion. KAERI developed a decontamination solution that consists of N_2H_4, H_2SO_4 and Cu^+ ions. N_2H_4 and H_2SO_4 can be removed by the decomposition of hydrazine and the precipitation of sulfate ions.

The decomposition characteristics of N_2H_4 in a N_2H_4-H_2SO_4-Cu^+ solution by H_2O_2 were investigated in a temperature range of 50 ℃ to 80 ℃. The decomposed portion of N_2H_4 at a given quantity of H_2O_2 was increased with the temperature and solution pH. The catalytic effect of cuprous ions on the decomposition of N_2H_4 was negligible within the experimental range. N_2H_4 was decomposed perfectly into N_2 and H_2O by the continual addition of H_2O_2. The removal performance of SO_4^{2-} ions in the remaining solution using a precipitation method was also investigated. SO_4^{2-} ions were precipitated into $BaSO_4$ by the same equivalence of Ba^{2+} ions and satisfactorily removed from the solution.

Key words: hydrazine; sulfate; decontamination; waste; treatment

Effect of Silica Nanoparticles on Foaming Stability of Foam Decontaminating Agents

Chong-Hun Jung

Decommissioning Technology Research Division, Korea Atomic Energy Research Institute,

111, Daedeok-daero 989, Yuseong-gu, Daejeon, 34057, Korea

Corresponding author:*E-mail:*[*nchjung@kaeri.re.kr*](mailto:nchjung@kaeri.re.kr)

Key words: Decontamination, Silica Nano particles , Foam, Surfactant, Stability

Abstract

An experiments was conducted to evaluate the stability of nano foaming agents by adding various types of surfactants, silica nanoparticles, and viscosifiers for the purpose of increasing the stability of foaming agents containing nanoparticles. Nonionic surfactants such as EM100 showed higher stability as compared to the Sodium Dodecyl Sulfate (SDS) anionic surfactant, and the foam stability decreased as the surfactant concentration increased. Among some viscosifiers tested, Xantan gum showed the highest foam stability. When silica nanoparticles were added to the surfactant EM100, the foam stability was further improved. In particular, the foam stability of the nano foaming agent was observed to be the maximum when a partially hydrophobic nanoporous silica such as KAERI 1 was added, as compared to the addition of a hydrophilic dry silica such as M5. This is because the partially hydrophobic particles were distributed over the liquid film between the foams, thereby preventing drainage and increasing the stability of the foaming agent fluid. The manufactured nano foaming agent can be used not only for the effective decontamination of large-sized equipment or large facilities but also for overcoming the problem of production of a large amount of radioactive waste during chemical decontamination.

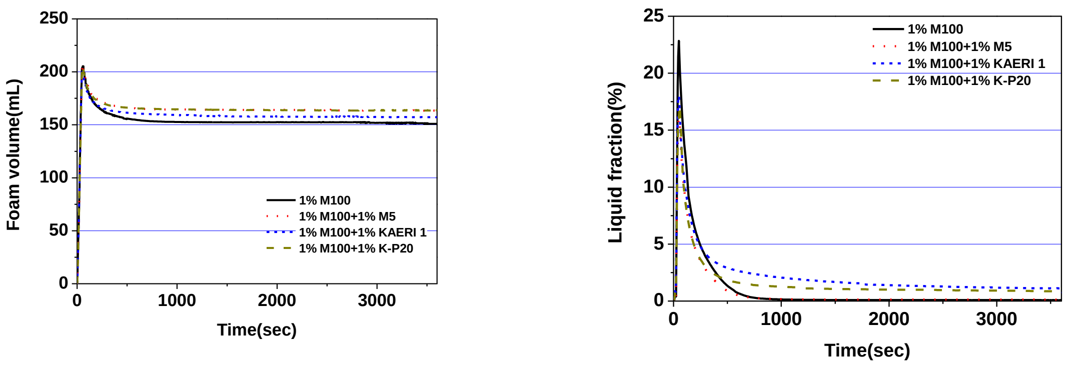

Variation of (a) foam volume and (b) liquid fraction in foam of 1% EM100 with M5, KAERI 1, and K-P20.

Study on the Removal Method of Radioactive Oxide Layer from the Metal in the Nuclear Facility using Perfluorocarbon Emulsion

Naon Chang[1,2] and Huijun Won[1*]

[1]*Decommissioning Technology Research Division, Korea Atomic Energy Research Institute, Daejeon 34057, Korea*

[2]*Department of Nuclear Engineering, Hanyang University, Seoul 04763, Korea*

[1]*cno0622@kaeri.re.kr*

[*]*Corresponding author. Tel: +82-428682331, Email: nhjwon@kaeri.re.kr*

In a nuclear facility, the radioactive oxide layers can be generated on the base metal by neutron absorption during operation. The oxide layers are necessary to be removed to reduce the radiation exposure to workers before decommissioning. However, it is possible that the large amount of radioactive wastes are generated when the high radioactive nuclear facilities are decontaminated. To solve this problem, the PFC (Perfluorocarbon) emulsion including inorganic acid and anionic surfactant, which can be recovered, was developed. The object of this study are to perform the applicability of the PFC emulsion to the removal of radioactive oxide layers and investigate the stability. Before analysis, the PFC emulsions are prepared by the ultrasonic method.

The applicability of PFC emulsion to the removing the radioactive oxide layer was evaluated by decontamination test of simulated Cr oxide layer on the SUS304. It was observed that the oxide layers were removed by the PFC emulsion by using SEM-EDS. The stability of the PFC emulsion was analyzed by measuring interfacial tension, droplet size, and zeta potential. From the results, it was confirmed that the anionic surfactant concentration in the PFC emulsion affected the stability of the emulsion. Furthermore, all the PFC emulsions are stabilized over 24 h regardless of the composition of emulsions in the experimental conditions.

Keywords: Nuclear facility, Oxide layer, Decontamination, PFC, Emulsion

Preparation and photocatalytic properties of MoS_2/Ag_3PO_4 composites

Wu Fuli[1], **Li Bin**[2], **Huang Youpeng**[1], **Yang Benhong**[2]*

1.School of Biology Food and Environmental Engineering, Hefei University, Hefei 230601, China;2. School of Energy Materials and Chemical Engineering, Hefei University Hefei 230601, China

Introduction

In order to solve the problem of organic pollutants in water, semiconductor photocatalysis technology as a new green energy saving technology has attracted the attention of many researchers. Ag_3PO_4 has the characteristics of suitable band gap, strong visible light absorption and high photocatalytic efficiency, so it has certain research value. However, photocorrosion is easy to occur under a long period of light irradiation, which affects its photocatalytic activity and stability, and is bound to limit its application. Therefore, it is worthwhile to study how to overcome the photocorrosion of Ag_3PO_4 and improve its photocatalytic activity and stability.

In recent years, researchers mainly modify Ag_3PO_4 from two directions in order to improve its photocatalytic activity. On the one hand, from the perspective of Ag_3PO_4 itself, the photocatalytic activity of Ag_3PO_4 was improved by changing its morphology and structure. On the other hand, Ag_3PO_4 is compounded with other semiconductors, such as $Ag_3PO_4/BiVO_4$[1], g-$C_3N_4/AgBr/Ag_3PO_4$[2], and Ag_3PO_4/CNTs@$MoSe_2$[3],etc. In this way, the photocatalytic activity of Ag_3PO_4 was much improved. MoS_2 is a transition metal sulfide with narrow band gap, large specific surface area, strong edge reactivity and easy to form complex structure with other substances. MoS_2/Ag_3PO_4 photocatalyst was prepared by chemical precipitation method. The samples were characterized by XRD, SEM, PL, UV-VIS DRS,etc.

Experimental procedure

MoS_2 was prepared by hydrothermal method. An appropriate amount of MoS_2 was taken in distilled water for 3 h ultrasonic, and 3mmol $AgNO_3$ was added into MoS_2 solution under agitation. After stirring for 30 minutes, 1mmol Na_2HPO_4 dissolved in 20mL distilled water was slowly added to the dispersion. After stirring for 3h, MoS_2/Ag_3PO_4 was prepared by centrifugation, washing and drying.

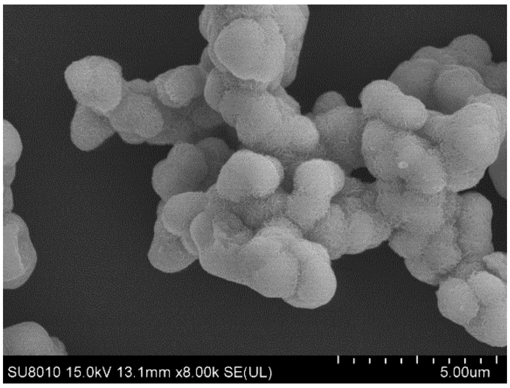

Figure 1 SEM photo of MoS_2

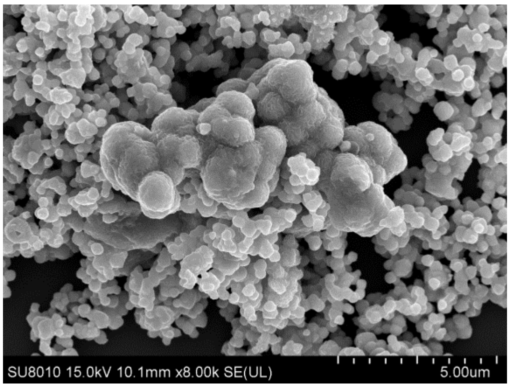

Figure 2 SEM Photo of MoS_2/Ag_3PO_4

Results and discussion

Figure 1 is a SEM Photo of MoS_2, as shown in the figure, MoS_2 presents a layered flower-like structure, clustered together to form a flower cluster. Figure 2 is a SEM Photo of MoS_2/Ag_3PO_4, as shown in the figure, globular Ag_3PO_4 particles are distributed on the flower-like surface of MoS_2. The results showed that photocatalytic degradation of RhB by MoS_2/Ag_3PO_4 with mass percentage of 1% was significantly higher than that of pure Ag_3PO_4, and the degradation rate could reach 97.95%. After repeated use of the same photocatalyst for 4 times, the RhB degradation rate still remained 81.03%. Photogenerated hole (h^+) and superoxide radical ($\bullet O_2^-$) are the main active species in catalytic degradation of RhB. HPLC and UV-VIS analysis showed that RhB may be photodegraded to H_2O and CO_2.

References

[1]Xiaoming Gao, Chunhua Liang, Kailong Gao, et al. Z-scheme heterojunction $Ag_3PO_4/BiVO_4$ with exposing high-active facets and stretching spatial charge separation ability for photocatalytic organic pollutants degradation[J]. Applied Surface Science, 2020, 524.1-11.

[2]Pengfei Zhu, Jing Xu, Ming Duan, et al. Fabrication of a double Z-type g-C_3N_4 /AgBr/Ag_3PO_4 composite with enhanced visible-light photocatalytic activity for organic dye elimination[J]. Optical Materials,2020, 107.1-33.

[3]Li Dongsheng, Wang Wei, Shang Xianyao, et al. Solar-driven photocatalytic water oxidation of Ag_3PO_4/CNTs@$MoSe_2$ ternary composite photocatalyst[J]. Applied Surface Science ,2020, 505(C).1-33.

Preparation and photocatalytic application of Ti_3C_2/Bi_2WO_6 composites

Li Bing[1]， Hu Youpeng[2],Wu Fuli[2],Yang Ben-hong[1*]

（1.School of Energy Materials and Chemical Engineering, Hefei University Hefei
230601 ;2.Department of Biological and Environmental Engineering，Hefei
University，Hefei，230601,China）

1.Introduction

Photocatalytic degradation technology uses sunlight as energy to degrade organic pollutants into CO_2 and H_2O, and it is considered to be one of the most environmentally friendly and effective methods to degrade organic pollutants[1]. Since TiO_2 photocatalysts were first reported in 1972, more and more semiconductor photocatalysts have been reported. Among them, bismuth tungstate (Bi_2WO_6) with its narrow energy gap, excellent stability and unique energy band structure has been used as a common photocatalyst. However, pure Bi_2WO_6 has relatively low photodegradation efficiency[2] due to the high recombination rate of light-excited electrons and holes. This is also a problem with most photocatalytic materials. In order to improve the photocatalytic activity, researchers tend to combine two semiconductors to overcome this shortcomings.

Ti_3C_2 as the earliest and most widely studied two-dimensional material in the MXene family [3], it not only has a two-dimensional layered structure similar to graphene, but also inherits the dual characteristics of ceramic and metallic MAX phase. It has lower carrier density, higher electrical conductivity, good mechanical properties, optical properties and hydrophilicity. However, pure Ti_3C_2 materials also have defects such as poor chemical stability and low photoelectric conversion rate. The combination of Ti_3C_2 and Bi_2WO_6 is likely to improve some of the deficiencies.

In this paper, Ti_3C_2/Bi_2WO_6 composite material was prepared by hydrothermal method, and its photocatalytic performance was studied.

2. Experiment

2.1 Preparation of Ti_3C_2 and Bi_2WO_6

Ti_3C_2 material was prepared via HF etching Ti_3AlC_2 ; Bi_2WO_6 material was prepared by hydrothermal method.

2.2 Preparation of Ti_3C_2/Bi_2WO_6

Disperse 50 mg of Ti_3C_2 in 40 mL of deionized water with ultrasound for 30 min, add 2 mmol $Bi(NO_3)_3\cdot 5H_2O$ and stir for 1 h, and record it as solution (A); take 1 mmol $Na_2WO_4\cdot 2H_2O$ and 0.05 g CTAB to dissolve in Record as solution (B) in 40 mL of deionized water. Then the solution (B) was slowly added to the solution (A), and after stirring for 30 min, the solution was transferred to a 100 mL polytetrafluoroethylene lined stainless steel autoclave, and hydrothermally treated at 180 ℃ for 24 h. After being naturally cooled to room temperature, the white precipitate was collected by centrifugation, washed repeatedly with ethanol and deionized water, and then dried at 60 ℃ for 12 h. The prepared sample is Ti_3C_2/Bi_2WO_6.

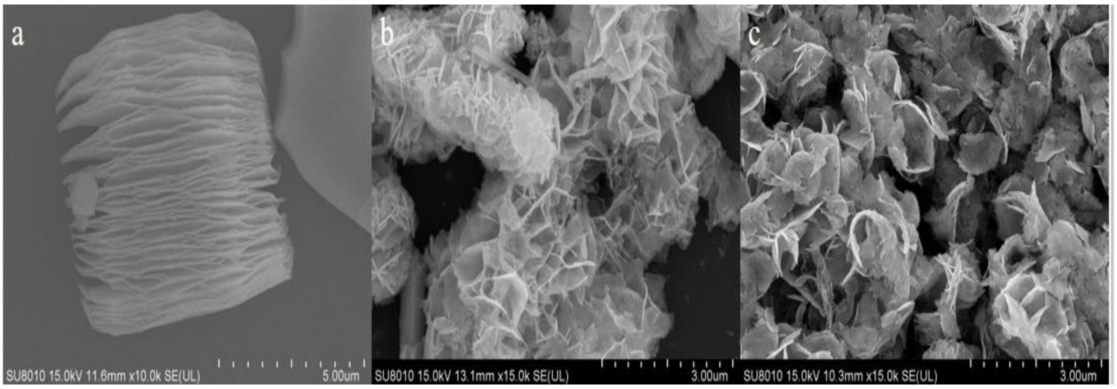

Fig 1. SEM pictures of Ti_3C_2, Bi_2WO_6 and Ti_3C_2/Bi_2WO_6

3.Results and discussion

Ti_3C_2/Bi_2WO_6 composite material was prepared by hydrothermal method and characterized by SEM, XRD, UV-Vis and PL methods. The results show that Ti_3C_2 presents an accordion layered structure, Bi_2WO_6 has a network porous structure, and Ti_3C_2/Bi_2WO_6 has a coiled sheet structure. When the content of Ti_3C_2 in the composite material was 7%, the photocatalytic activity was the best. After 60 min of visible light irradiation, the degradation rate of AF reached 92.17%. After repeated use of the same photocatalyst for 4 times, the degradation rate remained 80.02%. Studies on degradation mechanism show that h^+ and $\cdot O^{2-}$ are the main active substances that degrade AF.

References

[1] Xiao Yi,Wang Ting,Qiu Ganhua,Zhang Kun,Xue Changguo,Li Benxia. Synthesis of EDTA-bridged CdS/g-C_3N_4 heterostructure photocatalyst with enhanced performance for photoredox reactions.[J]. Journal of colloid and interface science,2020,577:459-470.

[2] Shelja Sharma,Alex O. Ibhadon,M. Grazia Francesconi,Surinder Kumar Mehta,Sasikumar Elumalai,Sushil Kumar Kansal,Ahmad Umar,Sotirios Baskoutas. Bi_2WO_6/C-Dots/TiO_2: A

Novel Z-Scheme Photocatalyst for the Degradation of Fluoroquinolone Levofloxacin from Aqueous Medium[J]. Nanomaterials,2020,10(5):1-19

[3] Yiying Zhang,Xilin Zhang,Cheng Cheng,Zongxian Yang.Recent progress of MXenes as the support of catalysts for the CO oxidation and oxygen reduction reaction[J].Chinese Chemical Letters,2020,31(04):931-936.

Research on microwave activated persulfate technology to remove organic matter in landfill leachate

Yongyao Xu[a], Yin Liu[a, b,*]

[a]*School of Materials Science and Engineering, Anhui University of Science and Technology, Huainan 232001, Anhui, China*
[b]*State Key Laboratory of Mining Response and Disaster Prevention and Control in Deep Coal Mines, Anhui University of Science and Technology, Huainan 232001, Anhui, China*

Abstract

In order to treat the organic matter contained in the waste leachate, microwave radiation is used to activate persulfate (MW/PS) and hydrogen peroxide (MW/H_2O_2) to remove the organic matter in the membrane bioreactor (MBR) treatment. Reactive oxygen species (ROS) and the degradation and transformation mechanism of organic matter. Study the influence of microwave power, oxidant dosage and pH on these two processes, and get the best process conditions. Increasing the amount of oxidant can increase the removal rate and kobs (initial reaction rate) of the two processes. Increasing the microwave output power can improve the removal rate of organic matter by the two processes, but too high microwave output power can only increase the removal rate of the two processes, and the removal effect of organic matter is not significant. The microwave/ H_2O_2 process only quickly removes organics under acidic conditions, while the microwave/PS process causes strong degradation of organics in a wide range of pH. The quenching experiment using alcohol shows that both SO_4^- and OH exist in the microwave/polystyrene process, SO_4^- plays a leading role in the degradation of organics, and OH plays a leading role in the microwave/ H_2O_2 process.

Keywords: Microwave, Oxidant dosage, Microwave power,pH

First principles study on photocatalytic hydrogen production of V-doped $SrTiO_3$ improved by P

Jingyu Wang[a], Yin Liu[a, b,*]

[a]*School of Materials Science and Engineering, Anhui University of Science and Technology, Huainan 232001, Anhui, China*

[b]*State Key Laboratory of Mining Response and Disaster Prevention and Control in Deep Coal Mines, Anhui University of Science and Technology, Huainan 232001, Anhui, China*

Abstract

In this study, we used first-principles calculations to study the effects of P and V single doping and (P+V) co-doping on the electronic structure and photocatalytic activity of SrTiO3. We found that although V doping can well improve the visible light absorption performance of $SrTiO_3$, the oxidation potential of VBM at this time is more negative than that of water, which will cause the photocatalyst to fail to split water to produce hydrogen. Moreover, the unoccupied intermediate states above the valence band formed by V single doping are likely to enhance the recombination of photogenerated electron-hole pairs and reduce the photocatalytic efficiency. We have constructed three models of (P+V) co-doped at different positions, which are respectively denoted as: P+V@STO-n (near), P+V@STO-m (middle) and P+V@STO-f (far), the free energy of the system in the near case is the lowest, and will be synthesized first in actual experiments, but the middle and far cases are also formed with a certain probability. So we did research on all these three situations. The co-doped $SrTiO_3$ at these three positions has formed a new state below the valence band, which provides a cleaner energy band structure for the photocatalyst. Not only that, but their band gap values are also all reduced to about 2 eV, moreover, the CBM is more negative than reduction potential of water reduction level (H^+/H_2) and the locates of VBM below the water oxidation (O_2/H_2O). This shows that (P+V) co-doping not only reduces the recombination of photogenerated electron-hole pairs, but also makes the light absorption spectrum of $SrTiO_3$ produce a red shift, and at the same time meets the basic conditions for photocatalytic water splitting. Therefore, the introduction of P improves the photocatalytic performance of V-doped $SrTiO_3$ and becomes a theoretically feasible photocatalytic hydrogen production material.

Key words: Photocatalysis; Hydrogen production; First-principle calculation.

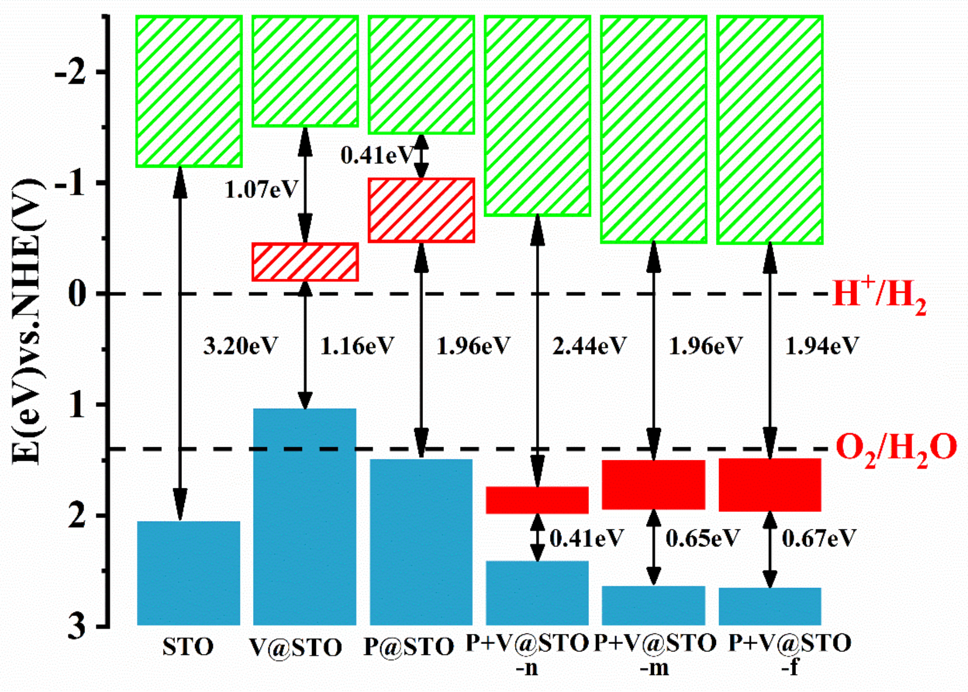
E(eV)vs.NHE(V)
-2
-1
0
1
2
3
1.07eV
0.41eV
H+/H2
3.20eV
1.16eV
1.96eV
2.44eV
1.96eV
1.94eV
O2/H2O
0.41eV
0.65eV
0.67eV
STO
V@STO
P@STO
P+V@STO -n
P+V@STO -m
P+V@STO -f

Purification and dissociation of raw palygorskite through wet ball milling as a carrier to enhance the microwave absorption performance of Fe_3O_4

Sheng Wang[a], Yin Liu[a, b,*]

[a]School of Materials Science and Engineering, Anhui University of Science and Technology, Huainan 232001, Anhui, China
[b]State Key Laboratory of Mining Response and Disaster Prevention and Control in Deep Coal Mines, Anhui University of Science and Technology, Huainan 232001, Anhui, China
*Corresponding authors: yinliu@aust.edu.cn

Abstract:

The effect of ball-to-powder weight ratio on the crystal composition, microscopic morphology and pore structure of palygorskite was systematically studied by using the conventional wet ball milling process. The quartz can be effectively separated from palygorskite through low-speed centrifugal treatment in aqueous solutions, while the strength of ball milling has a significant influence on disaggregation degree of the crystal bundles. When the ratio is 1:2, the rod crystal bundles are well dissociated, while preserving the inherent aspect ratio of the nanofibers. After the treatment, the specific surface area, micropore volume and micropore area are increased from 206.87 m^2/g, 0.0347 cm^3/g and 76.07 m^2/g to 255.03 m^2/g, 0.0502 cm^3/g and 109.42 m^2/g, respectively. For the first time, the purified palygorskite was used as a template to prepare palygorskite/Fe_3O_4 nanocomposite using by hydrothermal method, for microwave absorbing applications. As expected, the introduction of palygorskite can effectively prevent the aggregation of the Fe_3O_4 magnetic particles. Meanwhile, the specific surface area of the composite is enlarged from 10.29 m^2/g to 40.73 m^2/g, as the weight ratio of Fe_3O_4 and palygorskite is 2:1, thus leading to enriched interface polarizations and hence resulting in a maximum reflection loss (RL) of -40.41 dB at 4.80 GHz, with effective absorption frequency that can be adjusted over 2-18 GHz by controlling thickness of the composite.

Keywords: Palygorskite, Dissociation, Palygorskite/Fe_3O_4, Nanoparticle dispersion, Microwave absorption

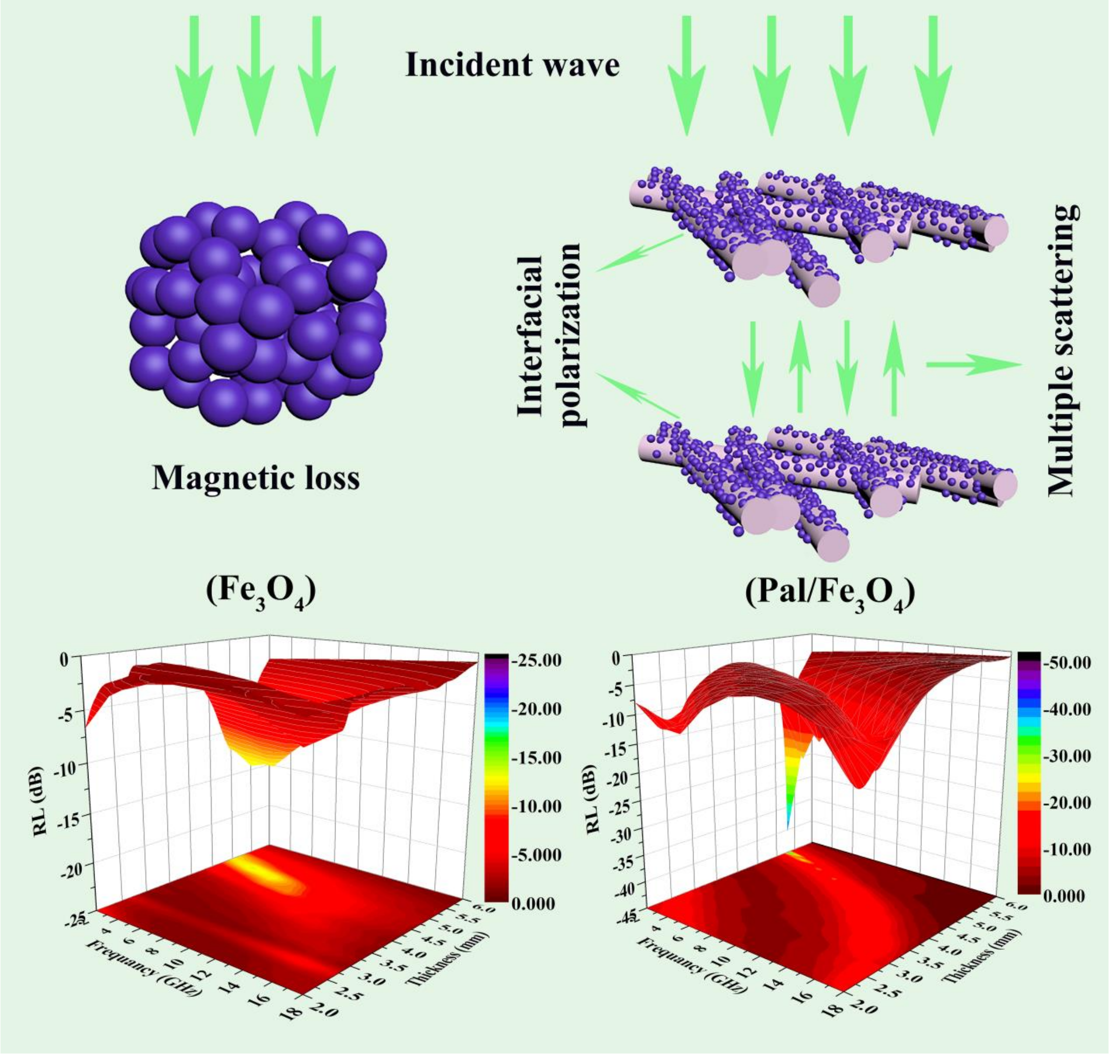

Scheme 1. Schematic illustration of possible microwave loss mechanisms and three-dimensional (3D) RL profiles of the pure Fe_3O_4 and Pal/Fe_3O_4 (S2) composites.

In-situ synthesis of coal-based carbon/Ni magnetic composite with potential microwave absorption performance

Hengdong Ren,Yin Liu*

School of Materials Sciernce and Engineering,Anhui University of Science and Technology,Huainan 232001,China

***Corresponding authors: yinliu@aust.edu.cn (Yin Liu)

Abstract

Due to the rapid development of electronic communication equipment, the resulting microwave pollution can damage human health and cause electronic equipment to fail to operate normally. In order to solve this problem, coal-based carbon/Ni magnetic composite was prepared by using Ningxia anthracite as carbon source. In this work, the prepared pure carbon shows an optimum reflection loss of -31.84 dB at 9.52 GHz with a coating thickness is 2.29 mm. At the same temperature, coal-based carbon/Ni magnetic composite synthesized by coal in a ratio of 1:1 than nickel chloride hexahydrate achieved a reflection loss of -56.64 dB and a thickness of 2.31 mm at 10.40 GHz. It is proved that the coal-based carbon has excellent microwave absorption properties. Besides, we explored the effect of temperature and nickel doping ratio on microwave absorption performance. By adding magnetic metal, the magnetic loss of the carbon material can be improved, and a better impedance matching is obtained, so that the microwaves pass through the material with less reflection and more absorption. In addition, carbon is an ideal microwave absorbing material because of its light weight, high stability and low cost.

Key words: Microwave absorption; Coal-based carbon; Magnetic metal; Electrical conductivity

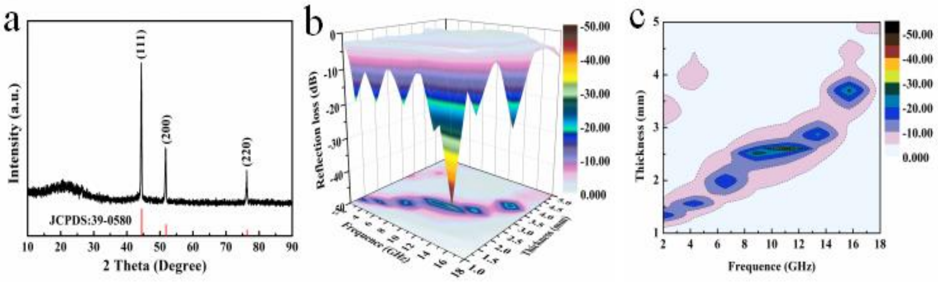

Fig.1. (a) XRD patterns, (b) 3D reflection loss and (c) contour maps of the carbon/Ni.

ZIF-Derived Porous Co/Zn/C Nanocomposites with Excellent Microwave Absorption Properties

Ximing Zhang[a], **Yin Liu**[a, b,*]

[a]*School of Materials Science and Engineering, Anhui University of Science and Technology, Huainan 232001, Anhui, China*

[b]*State Key Laboratory of Mining Response and Disaster Prevention and Control in Deep Coal Mines, Anhui University of Science and Technology, Huainan 232001, Anhui, China*

Abstract

Zeolitic-Imidazolate-Frameworks (ZIFs)-derived carbon materials have been considered as promising candidates in microwave absorption materials. In this study, using Zn-based MOFs (ZIF-8) and Co-based MOFs(ZIF-67) as an example, the feasibility of this synthetic strategy was demonstrated by the successful fabrication of porous Co/Zn/C composite nanomaterials. ZIF-8 is used as the core and ZIF-67 is used as the shell to prepare a double-layer molecular cage structure. Finally, the Co/Zn/C absorbing material is obtained by high temperature pyrolysis. The micro-meso-macropores, enhanced conductive loss, strong dipolar/interfacial polarizations and core-shell carbon layer favor the absorbers with high porosity, improved dielectric loss and promoted impedance matching. The shell thicknesses of ZIF-67 can be adjusted simply by varying the feeding molar ratios of Co2+/Zn2+. The composites exhibited excellent impedance matching and strong absorption. With a filler loading of 50%, the maximum reflection loss reaches -80.19dB at 11.28GHz, and the effective absorption bandwidth exceeding −10 dB is 4.88 GHz (from 8.88 GHz to 13.76 GHz) with a thickness of only 2.50 mm. Furthermore, this work offers a simple and effective strategy in the fabrication of MOF-derived microwave absorption material and improved impedance matching for lightweight and high-efficiency electromagnetic wave absorption materials.

Keywords: Zeolitic-Imidazolate-Frameworks, Hollow structure, Carbon nanocages, Microwave absorption

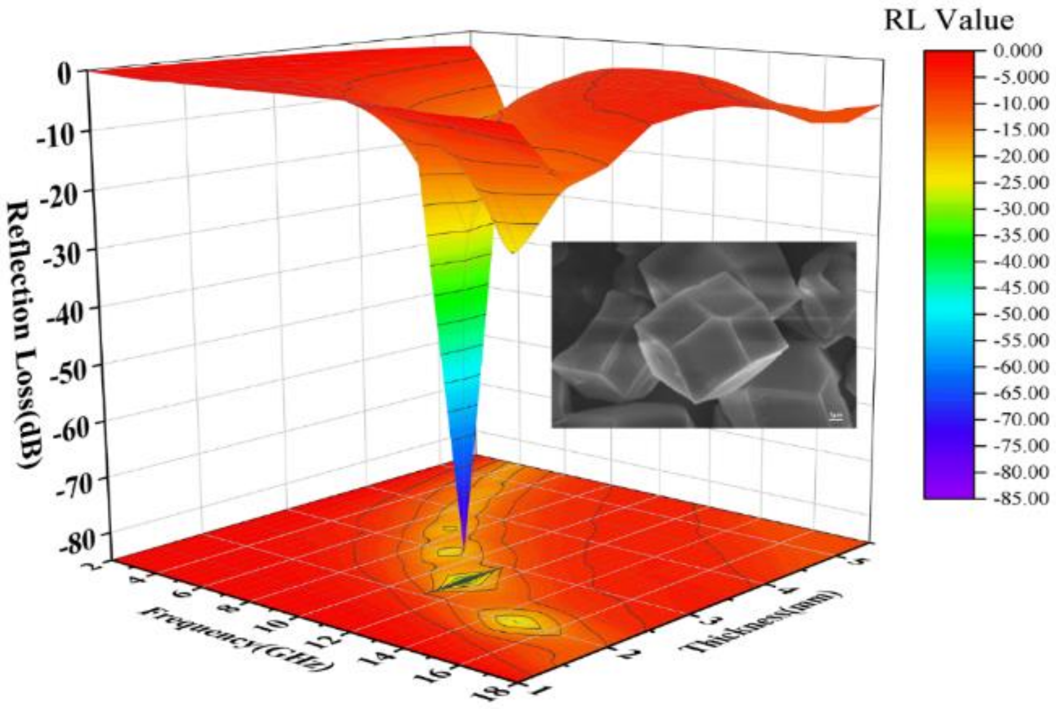
RL Value
0.000
-5.000
-10.00
-15.00
-20.00
-25.00
-30.00
-35.00
-40.00
-45.00
-50.00
-55.00
-60.00
-65.00
-70.00
-75.00
-80.00
-85.00
Reflection Loss(dB)
0
-10
-20
-30
-40
-50
-60
-70
-80
Frequency(GHz)
2
4
6
8
10
12
14
16
18
Thickness(mm)
1
2
3
4
5

Theoretical Study on Asymmetric [2+2] Cycloaddition of Disubstituted Ketenes with *N*-benzylisatins Catalyzed by Chiral *N,N*'-Dioxide-Sc(III) Complex

Xiangxiang Meng[1], Min Wang[1], Changwei Hu[1], Zhishan Su*[1], Chan Kyung Kim*[2]

[1] Key Laboratory of Green Chemistry and Technology, Ministry of Education, College of Chemistry, Sichuan University, Chengdu, Sichuan 610064, P. R. China.

[2] Department of Chemistry, Inha University, 100 Inha-ro, Michuhol-gu, Incheon 22212, Korea.

Abstract.

The mechanism and stereoselectivity of the disubstituted ketenes (R1) and *N*-benzyl isatins (R2) catalyzed by a chiral *N*, *N′*-dioxide-Sc(III) complex were studied by DFT method at the B3LYP-D3(BJ)/6-311G**(SMD,CH_2Cl_2)//B3LYP-D3(BJ)/def2-SVP(SMD,CH_2Cl_2) level. The calculations indicated the reaction occurred in a concerted but asynchronous manner. The four-membered was constructed by nucleophilic attack of the O(2) atom in the *N*-benzyl isatin toward the C(β) atom in the disubstituted ketene in the initial stage of reaction, which was responsible to the high regioselectivity of the cycloadditions. The π-π stacking interaction between two deformed reactants stabilized the corresponding transition state in 2-rs pathway. As a result, the reaction barrier affording enantiomer P-*SR* was lower than that of the diastereoisomer P-*SS*. In catalytic reaction, N-benzyl isatin coordinated to the Sc^{3+} in bidentate manner to form a hexacoordinate Sc(III)-complex. Similar to the background reactions, cycloadditions mediated by chiral *N,N′*-dioxide-Sc(III) complex occurred in a concerted but nonsynchronous manner. However, the C(α)-C(1) bond was formed by interaction between the most nucleophilic Cα atom in the disubstituted ketenes and the most electrophilic terminal C(1) atom in the *N*-benzyl isatins, followed by C(β)-C(2) bonding. The *o*-*i*Pr in aniline of the ligand shielded the *si*-face of the isatin and induced the ketenes to approach the isatin from less hindered *re*-face, leading to high enantioselectivity of reaction. Suffering from the steric repulsion from benzyl group in isatins, the ketene substrate preferred to approach the *re*-face of *N*-benzyl isatins with its *si* face, affording predominant product P-*SS* with *S,S′*-configuration. When the bulky benzyl group in the isatin was replaced by methyl group, the steric repulsion between the two reactants significantly weakened. Accordingly, the difference of distortion energy (ΔE_{starin}) of the reacting species along the competing reaction paths for the diastereoisomers reduced, leading to inferior stereochemical outcomes. These results were in good agreement with the experimental observations.

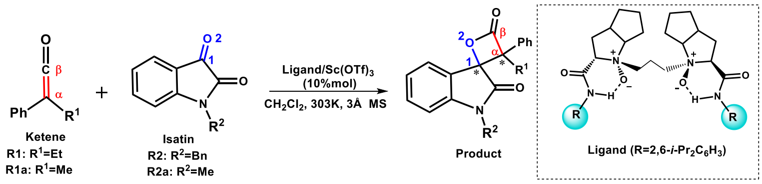

Scheme 1 Asymmetric cycloaddition of disubstituted ketene (R1) with isatin (R2) catalyzed by Sc(III)-complex.

References.

1. Liu X, Lin L, Feng X (2014), Chiral *N*, *N'*-dioxide ligands: synthesis, coordination chemistry and asymmetric catalysis. Org. Chem. Front. 1: 298-302.
2. Wang J, Zuo Y, Hu C, Su Z (2017), Theoretical and experimental studies on the structure–property relationship of chiral *N*,*N*'-dioxide–metal catalysts probed by the carbonyl–ene reaction of isatin. Catal. Sci. &Techol. 7: 2183-2193.
3. Hao X, Liu X, Li W, Tan F, Chu Y, Zhao X, Lin L, Feng X. (2014), Chiral Lewis acid catalyzed asymmetric cycloadditions of disubstituted ketenes for the synthesis of β- Lactones and δ- lactones. Org. Lett. 16: 134.

Acknowledgement

This research was funded by International Cooperation Program managed by the National Research Foundation of Korea (2019K2A9A2A06023069, FY2019) and National Natural Science Foundation of China (21911540465).

Asymmetric Cyanation of Activated Olefins with Ethyl Cyanoformate Catalyzed by Ti(IV)-Catalyst: A Theoretical Study

Zhishan Su[1], Changwei Hu[1], Nasir Shahzad[2], Chan Kyung Kim*[2]

[1] Key Laboratory of Green Chemistry and Technology, Ministry of Education, College of Chemistry, Sichuan University, Chengdu, Sichuan 610064, P. R. China.

[2] Department of Chemistry, Inha University, 100 Inha-ro, Michuhol-gu, Incheon 22212, Korea.

Abstract.

The reaction mechanism and origin of asymmetric induction for conjugate addition of cyanide to the C=C bond of olefin were investigated at the B3LYP-D3(BJ)/6-31+G**//B3LYPD3(BJ)/6-31G**(SMD,toluene) theoretical level. The release of HCN from the reaction of ethyl cyanoformate (CNCOOEt) and isopropanol (HOiPr) was catalyzed by cinchona alkaloid catalyst. The cyanation reaction of olefin proceeded through a two-step mechanism, in which the C-C bond construction was followed by H-transfer to generate a cyanide adduct. For non-catalytic reaction, the activation barrier for the rate-determining C-H bond construction step was 34.2 kcal mol^{-1}, via a four-membered transition state. The self-assembly Ti(IV)-catalyst from tetraisopropyl titanate, (R)-3,3'-disubstituted biphenol, and cinchonidine accelerated the addition of cyanide to the C=C double bond by a dual activation process, in which titanium cation acted as a Lewis acid to activate the olefin and HNC was orientated by hydrogen bonding. The steric repulsion between the 9-phenanthryl at the 3,3'-position in the biphenol ligand and the Ph group in olefin raised the Pauli energy ($\Delta E^{\neq}_{Pauli}$) of reacting fragments at the re-face attack transition state, leading to the predominant R-product.

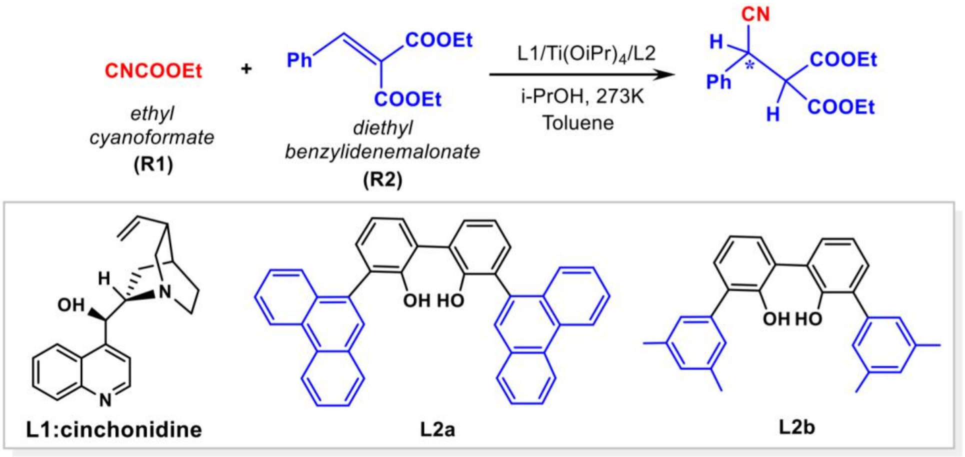

Scheme 1 Asymmetric cyanation of activated olefin catalyzed by Ti(IV)-complex.

References.

1. Wang, J.; Hu, X.L.; Jiang, J.; Gou, S.H.; Huang, X.; Liu, X.H.; Feng, X.M. Asymmetric Activation of Tropos 2,2’-Biphenol with Cinchonine Generates an Effective Catalyst for the Asymmetric Strecker Reaction of N-Tosyl-Protected Aldimines and Ketoimines. *Angew. Chem. Int. Ed.* **2007**, *46*, 8468.

2. Su, Z.S.; Li, W.Y.; Wang, J.; Hu, C.W.; Feng, X.M. A theoretical investigation on the Strecker reaction catalyzed by a Ti(IV)-complex catalyst generated from a cinchona alkaloid, achiral substituted 2,2’-biphenol, and tetraisopropyl titanate. *Chem. Eur. J.* **2013**, *19*, 1637.

3. Su, Z.S.; Hu, C.W.; Shahzad, N.; Kim, C.K. Asymmetric Cyanation of Activated Olefins with Ethyl Cyanoformate Catalyzed by Ti(IV)-Catalyst: A Theoretical Study, *Catalysts*, **2020**, *10*, 1079.

Acknowledgement

This research was funded by International Cooperation Program managed by the National Research Foundation of Korea (2019K2A9A2A06023069, FY2019) and National Natural Science Foundation of China (21911540465).

COMPARATIVE STUDY OF FACTORS CAUSING FALSE POSITIVE IN METHAMPHETAMINE SCREENING TESTS BY IMMUNOCHROMATOGRAPHY

Wimol Palarach[1] Maitree Pakarasang[2] and Rachadaporn Benchawattananon[3]

[1]Forensic Science Faculty of Science, Khon Kaen University, Khon Kaen 40002, Thailand;
[2] Clinical Microbiology Faculty of Associated Medical Sciences, Khon Kaen University, Khon Kaen 40002, Thailand.
[3]*Integrated Science, Forensic Science, Faculty of Science, Khon Kaen University, Khon Kaen 40002, Thailand.
Corresponding Author: Benchawattananon, R.; Email: rachadaporn@kku.ac.th

Abstract

This research focusing on comparative study of factors causing false positive in methamphetamine screening tests by immunochromatography. Several medications for mental disorders can lead to false positive tests. Screening drug tests are often required for pre-employment in the private and government sector, for athletes, students, healthcare workers, for probation or criminal activity, to avoid test in the clinic, or after vehicle or workplace accidents. Drug screening results can be influenced by many circumstances; therefore, accuracy is significant. The results can cause loss of employment ,jail time, exclusion from competitive sports, loss of privileges in a probation setting and inappropriate medical care. Objective of this study is to find factors causing false positive in methamphetamine screening tests by i- lab Methamphetamine Test Device immunochromatography)at lest 1,000 ng/ml(then run the test again using High Performance Liquid Chromatography (HPLC). The samples of this study are focusing on 4 groups of drugs include Pseudoephedrine, Chloroquine , Antibiotic and Procaine. Found Procaine, Pseudoephedrine and Chloroquine show positive, but Antibiotic (Rifampicin) show unclear light stripes.The test results with a different screening test or additional analytical tests are essential to avoid adverse consequences for the suspects.

Keywords: false positive, immunochromatography, methamphetamine, Pseudoephedrine, Chloroquine, Procaine

Phosphoric acid micro-corrosion coral aggregates and its effect on the performance of concrete

Aiguo Wang[1*], Xingyao Wang[1], Kaiwei Liu [1], Yan Li[1], Rui Ma[1],Daosheng Sun [1]

（1 Anhui key laboratory of advanced building materials, Anhui Jianzhu University, Hefei 230022, China）

Abstract

This article proposes the use of phosphoric acid micro-corrosion coral aggregate to enhance the interface bonding ability. In order to make up for the performance defects of traditional cement-based coral aggregate concrete, geopolymer-based coral concrete (CAGC) is prepared by combining geopolymer as a cementing material with modified coral aggregate. The results shows that with the increase of phosphoric acid concentration and soaking time, the quality loss rate of coral aggregate gradually showed a downward trend; the CAGC strength first increased and then decreased and reached the peak under the P_4 treatment condition, and its 7d flexural and compressive strength can reach 3.5MPa and 34.2MPa. During the acid treatment process, phosphoric acid reacts violently with coral aggregate to release CO_2 gas. The release of CO_2 helps to remove impurities such as sand on the surface and pores of the three geometric forms of aggregates. At the same time, Phosphate crystals can be attached to the aggregates. The main components of the waste liquid after pickling are $CaHPO_4$, $Ca(H_2PO_4)_2$ and SiO_2. Aggregate residual PO_4^{3-} can effectively delay the setting and hardening of geopolymer concrete. Compared with W_1, the initial and final setting time of W_5 is increased by 48min and 84min, and the interval between initial and final setting time is extended by 36min, which can be conducive to engineering construction operation. However, excessive contents of phosphoric acid and times of immersion also produce over corrosion effect with the damage of the coral skeletons and enlargement of the connected pore size, which finally resulted in mechanical properties' deterioration of CAGC.

Key words: coral aggregates; phosphoric acid micro-corrosion; geopolymer; interface bonding; pore characteristics

Acknowledgments: The research was the financially supported by the National Natural Science Foundation of China project (51778003).

Preparation of $BaFe_{12}O_{19}$ magnetic nanoparticles using CMC as chelating agent for photocatalytic degradation of methylene blue

Parintip Rattanaburi[1], Prawit Nuengmatcha[1,2*]

[1]Creative Innovation in Science and Technology, [2]Nanomaterials Chemistry Research Unit,
Department of Chemistry, Faculty of Science and Technology, Nakhon Si Thammarat Rajabhat
University, 80280, Thailand.

[*]Corresponding author : pnuengmatcha@gmail.com, Tel. +66-7537-7443, Fax +66-7537-7443

Abstract

Methylene blue is an organic dye that mostly used in the textile industries. These chemicals are responsible for generating significant amounts of toxic. Recently, magnetic nanoparticles have been considered as the new alternative material for wastewater treatment. In this study, $BaFe_{12}O_{19}$ has been successfully employed in the green synthesis of sol-gel auto combustion method using carboxymethyl cellulose (CMC) as chelating agent. The obtained catalyst is efficient, cost effective, easy magnetic separation, high surface and environmentally friendly. The morphology and elemental composition of the synthesized composites were characterized by Scanning electron microscope (SEM), Fourier transform infrared spectroscopy (FT-IR) and X-ray diffraction (XRD). The x-ray spectrum revealed that affected $BaFe_{12}O_{19}$ phase formation. Vibrating sample magnetometer (VSM) technique was used to identify the magnetization of particles. The $BaFe_{12}O_{19}$ was use as catalyst for photocatalytic degradation of methylene blue in aqueous solution. The magnetic $BaFe_{12}O_{19}$ nanoparticles was found active under visible light irradiation.

Keywords: CMC, sol-gel auto combustion, magnetic materials, methylene blue

Study on antibacterial activity of Vinegar-graphene Quantum Dots against *Escherichia coli*, *Pseudomonas aeruginosa*, *Staphylococcus aureus*, and *Bacillus cereus*

Amnuay Noypha[1], Prawit Nuengmatcha[2]

[1]Creative Innovation in Science and Technology, [2]Nanomaterials Chemistry Research Unit,

Department of Chemistry, Faculty of Science and Technology, Nakhon Si Thammarat Rajabhat

University, 80280, Thailand.

Corresponding author: amnuay.noypha@gmail.com, Tel. +66-7537-7443, Fax +66-7537-7443

Abstract

Vinegar–graphene quantum dots (Vg-GQDs) were successfully synthesized hydrothermal and co-pyrolysis method using acetic acid as the precursor. All samples were characterized using ultraviolet-visible spectrophotometry (UV-vis), scanning electron microscopy (SEM), and energy-dispersive X-ray spectroscopy (EDX). The antibacterial activity of Vg-GQDs against strains of *Escherichia coli*, *Pseudomonas aeruginosa*, *Staphylococcus aureus*, *and Bacillus cereus* was determined by using the disc diffusion method for preliminary screening. Their minimum inhibitory concentration (MIC) and minimum bactericidal concentration (MBC) were determined by the broth macro dilution method. Their inhibition zones were compared with those of acetic acid. It was found that the synthesized Vg-GQDs demonstrated excellent antibacterial activity against *Escherichia coli* 97.3 %, Pseudomonas aeruginosa 97.4 %. *Staphylococcus aureus* 95.6 %*, and Bacillus cereus* 99.2 %. Whereas, the MIC of Vg-GQDs against *Escherichia coli 3.125 mg/ml Pseudomonas aeruginosa* 1.56 mg/ml, *Staphylococcus aureus* 1.56 *mg/ml, Bacillus cereus* was 1.56 mg/ml, and the MBC values of Vg-GQDs against *Escherichia coli, Pseudomonas aeruginosa, Staphylococcus aureus* was 6.25 mg/ml, 6.25 mg/ml, and 12.5 mg/ml, respectively, while *Bacillus cereus* was not exhibited at 50 mg/ml.

Keywords: Antibacterial activity, Vinegar-graphene Quantum Dots

Electrical properties of $BiFeO_3$ Perovskite according to magnetization direction

H. S. Kang[1], W. S. Kim[1], S. J. On[1], H. M. Jung[1], J. H. Lee[1], H. S. Choi[1], T. H. Kim[2], H. S. Kim[1*], H. H. Kim[1*]

[1]*Department of Environmental and Bio-chemical Engineering, Sun Moon University, Asan, Republic of Korea*
[2]*Research Center for Eco-Multi-Functional Nano Materials, Sun Moon University, Asan, Republic of Korea*

* Corresponding authors

E-mail address: hskim@sunmoon.ac.kr, hhkim@sunmoon.ac.kr

Abstract

Enhancement in the efficiency of TiO_2 dye sensitized solar cell (DSSC) has been demonstrated by introducing ferromagnetic perovskite $BiFeO_3$ and controlling the magnetic field, which induces two-dimensional material-like properties in the bulk of TiO_2 DSSC (a 3-dimensional material). The effect of the concentration $BiFeO_3$ as well as the magnetization direction on performance of the TiO_2 DSSC have been investigated. After magnetization, it was confirmed that current density, efficiency, and open circuit voltage of $BiFeO_3$-doped DSSC were increased. The observed phenomena have been explained in terms of Hall effect which is responsible for the reduction of the degree of freedom of the electron movement resulting in the two-dimensional material-like properties in the bulk of $BiFeO_3$-doped TiO_2 DSSC. Ferromagnetic perovskite $BiFeO_3$ incorporated TiO_2 DSSC has been proved the effect of the concentration of $BiFeO_3$ as well as the magnetization direction on performance of the TiO_2 DSSC have been investigated.

Real Time Pen Position Estimation Algorithm for Electromagnetic Input Device

Hyun Woo Yu*, Dong Jin Kim
**Department of Electrical Engineering, The Pennsylvania State University, University Park, Pennsylvania 16802,*
Email; hyunwooyu7525@gmail.com
Department of Mechanical Engineering, Korea Advanced Institute of Science and Technology, Daejeon, Korea, 34141,
Email: *dj.kim@kaist.ac.kr*

Abstract:

An electromagnetic induction input device measures an electromagnetic induction signal emitted from an electronic pen and provides information on a user's pen position in real time. Such an electromagnetic induction input device provides a high resolution, hovering function indicating a position even when the electronic pen does not touch the screen, and excellent durability at the rear of the display. In order to measure the position of the electronic pen, an algorithm that calculates the position of the maximum value after curve fitting a number of AD-converted sensor values is used. Such a conventional method requires a large amount of computation and has a limitation in speeding up. In this study, we proposed an algorithm that measures pen coordinates in real time with only three sensor signals that detect pen signals. In order to show the performance of the proposed algorithm, a simple sensor was realized, and a control board was designed. From results of measuring the pen position along the diagonal line of the center of the sensor, it was found that it showed good performance.

Optimization of Ultrasound-assisted Extraction of Bioactive Compounds and Identification of vanillin from Dried Garlic Stem with Skin-whitening and Regeneration Effects

Ji Woo Hong[1], Suh Hee Yeom[1], Hye Lin Kim[1], Da Hye Gam[1], Ha Young Park[1] and Jin Woo Kim[1,2,3]*

[1]*Department of Food Science, Sunmoon University, Natural Science Building, 70 Sunmoon-ro 221, Tangjeong-myeon, Asan-si, Chungnam 336-708, Korea*

[2]*FlexPro Biotechnology, Sunmoon University, Start-up incubation center #306, 70 Sunmoon-ro 221, Tangjeong-myeon, Asan-si, Chungnam 336-708, Korea*

[3]*Center for Next-Generation Semiconductor Technology, Sun Moon University*

Correspondence: kimjw1028@sunmoon.ac.kr; Tel.: +82-41-530-2226

Abstract

This study was performed to establish optimization of ultrasound-assisted extraction (UAE) conditions, including extraction time (X_1), extraction temperature (X_2), and ethanol concentration (X_3) for the production of bioactive ingredients with antioxidant, skin whitening, and skin regeneration activities from dried garlic stems (DGS). By applying multiple regression analysis, the actual data and response variable was correlated by the quadratic equation. Coefficients of determination (R^2) of independent variables existed in the range of 0.90~0.95 to indicate that the regression model sufficiently reflected the actual data and proving their suitability for prediction of optimum condition. Ethanol concentration showed the most significant effect on tyrosinase activity inhibition (TAI, $p < 0.0001$) and collagenase activity inhibition (CAI, $p < 0.0001$). The antioxidant effect (radical scavenging activity, RSA) was significantly affected by the extraction temperature than other variables. The optimum UAE condition for simultaneously satisfying the maximum of the three responses, including RSA, TAI, and CAI, were 73.9℃, 24.2 min, and 88.5% ethanol concentrations. Under the optimum conditions, maximum RSA of 44.8%, TIA of 68.8%, and CIA of 92.5% were predicted. Polyphenolic compounds in DGS extract were then characterized by HPLC-DAD and vanillin was identified as a major component with antioxidant, skin whitening, and skin regeneration properties. Therefore, the excellent bioactive properties of DFS extracts is believed to be available as naturally derived functional ingredients in the cosmetics, food, and pharmaceutical industries.

Keywords: Dried garlic stem, Optimization, Ultrasound-assisted extraction, Antioxidant, Skin whitening, Skin regeneration

Optimization of Ultrasound-assisted Extraction Conditions for Production of Bioactive Compounds with Skin-whitening and Anti-wrinkle Effects from Peanut Shell

Da Hye Gam, Ji Woo Hong and Jin Woo Kim*

Department of Food Science, Sunmoon University, Natural Science 118, 70 Sunmoon-ro 221,
Tangjeong-myeon, Asan-si, Chungnam 336-708, Korea

[*] Correspondence: kimjw1028@sunmoon.ac.kr; Tel.: +82-41-530-2226

Abstract

Response surface methodology (RSM) was applied to optimize the ultrasound-assisted extraction (UAE) conditions for maximization of radical scavenging activity (RSA), tyrosinase activity inhibition (TAI), and collagenase activity inhibition (CAI) of peanut shell extracts. The effects of extraction time (5.0 ~ 55.0 min, X_1), extraction temperature (26.0 ~ 94.0℃, X_2), and ethanol concentration (0.0 ~ 99.5%, X_3) on RSA (Y_1), TAI (Y_2), and CAI (Y_3) were evaluated. Based on data from each experimental condition, quadratic regression models were derived for prediction of optimum condition, and the coefficient of determination (R^2) of the independent variable was in the range of 0.89 to 0.96, demonstrating that the regression model is suitable for prediction purposes. In predicting optimal UAE conditions based on the superimposing method, 20.9 min of extraction time, 34.5°C of extraction temperature, and 50.1% of ethanol concentration were identified, and 83.9%, TAI 41.0%, and CAI 91.0% were predicted under this condition, showing good agreement with experimental values. The prediction of UAE conditions using statistically-based optimization in extracting bioactive compounds from peanut shell has been proven effective, and it is expected that peanut shell extracts, an agricultural by-product using UAE, have a great potential as bioactive compounds and could be used as ingredients of food, cosmetics, and medicine materials.

Keywords: Peanut shell; Optimization; Whitening; Anti-wrinkle; Antioxidant; Tyrosinase; Collagenase

Effect of viscosity to formation of porous PDMS for applying the wearable devices

Dong-Hyun Baek[1,2], Hachul Jung[3], Jeong Hun Kim[3], Dae Wook Kim[1], Ho Seob Kim[1,2], Seungjoon Ahn[1], and Young-Jin Kim[3]

[1]Department of Display/Semiconductor Engineering, College of Engineering, Sun Moon University, Asan-si Chungnam Korea, 31460
[2]Center for Next-Generation Semiconductor Technology, Sun Moon University, Asan-si Chungnam Korea, 31460
[3]Integrated Medical Technology Team, Department of Research & Development, Medical Device Development Center, Osong medical innovation Foundation, Osong-si Chungbuk Korea, 28160

E-mail: dhbaek@sunmoon.ac.kr

Abstract:

The demand for medical devices has increased with development of awareness to maintain better life. The various skin-like soft materials have been developed to be applied to wearable devices. We have developed porous substrate by using polydimethylsiloxane (PDMS) elastomer for stretchable electronics. To achieve optimized porous structure, we have proposed fabrication process by using high pressure and steam with 4 different viscosities of uncured PDMS solutions. The proposed method could make porous structures simpler and more cost-effective than other technologies. The mechanical and electrical properties of the porous PDMS are compared with different porous structures. The results that porous PDMS fabricated with 2999 cP has a 3-dimensional porous structure like a sponge compared to other conditions, and it can be increased up to 25% elongation and relative resistance is changed 1,000 times. Repeated tensile strain test during 1,500-cycles with 20 % strain shows that the relative resistance increased about 10 times the initial resistance (R_0). The patch-type wearable devices based on skin-like soft materials can be provided a new platform to connect with human skin for robotics, continuous health monitoring.

P-40

X-Ray Diffraction Analysis of Various Calcium Silicate-based Materials

Youn-Soo Shim[a], Myung-Jin Lee[b], Min-Kyung Kang[c], So-Youn An [d*]
[a] Department of Dental Hygiene, Sunmoon University, Asan, Chungcheongnam-do, 31460, Republic of Korea
[b] Department of Dental Hygiene, Division of Health Science, Baekseok University, Cheonan, Chungcheongnam-do, 31065, Republic of Korea
[c] Department of Dental Hygiene, Hanseo University, Seosan, Chungcheongnam-do, 31963, Republic of Korea
[*d] Department of, Pediatric Dentistry & Wonkwang bone regeneration research Institute, College of Dentistry, Wonkwang University, Iksan-si, Jeollabuk-do, 5453, Republic of Korea
Corresponding to So-Youn An (9543sue@hanmail.net)

ABSTRACT

The purpose of this study was to evaluate the composition of the crystal phases of various calcium silicate-based materials (CSMs): ProRoot white MTA® (WMTA), Ortho MTA® (OM), Endocem MTA® (EM), Retro MTA® (RM), Endocem Zr® (EN-Z), Biodentine™ (BD), EZ-seal™ (EZ) and OrthoMTA III (OM3). In a sample holder, 5 g of the powder sample was placed, and the top surface of the material was packed flat using a sterilized glass slide. The prepared slides were mounted on an XRD instrument (D8 Advance; Bruker AXS GmbH, Germany). The X-ray beam 2θ angle range was set at 10 - 90° and scanned at 1.2° per minute. The Cu X-ray source set to operate at 40 kV and 40 mA in the continuous mode. The peaks in the diffraction pattern of each sample were analyzed using the software Diffrac (version 2.1). Then, the peaks were compared and matched with those of standard materials in the corresponding Powder Diffraction File (PDF-2, JCPDS International Center for Diffraction Data). Powder samples of the materials were analyzed using X-ray diffraction and the peaks in diffraction patterns were compared against the Powder Diffraction File data provided by the International Diffraction Data Center. Eight CSMs showed a similar diffraction pattern because their main component was calcium silicate. Eight CSMs showed similar diffraction peaks because calcium silicate was their main component. This was caused by the presence of Brushite, which is believed to have resulted in crystal growth in a particular direction for a specific purpose.

Keywords: *Biocompatibility, Calcium silicate, Mineral trioxide aggregate (MTA), R canal filling materials, X-ray diffraction analysis (XRD)*

P-41

Role of zinc-doped bioactive glass encapsulated with microspherical

gelatin in localized immune supplementation: A review article

Dokyeong Kim[a], Youn-Soo Shim[b], So-Youn An[c], Myung-Jin Lee[d]*

[a] *Department of Dental hygiene, Jeonju Kijeon College, Jeonju, Jeollabuk-do, 54989, Republic of Korea*

[b] *Department of Dental Hygiene, Sunmoon University, Asan, Chungcheongnam-do, 31460, Republic of Korea*

[c] *Department of, Pediatric Dentistry & Wonkwang bone regeneration research Institute, College of Dentistry, Wonkwang University, Iksan-si, Jeollabuk-do, 5453, Republic of Korea*

[*d] *Department of Dental Hygiene, Division of Health Science, Baekseok University, Cheonan, Cheonan, Chungcheongnam-do, 31065, Republic of Korea*

Corresponding to Myung-Jin Lee (dh.mjlee@bu.ac.kr)

ABSTRACT

The aim of this study was to synthesize and characterize the gelatinous microsphere of bioactive glass and investigate the role of zinc-doped bioactive glass with microspherical gelatin in localized immune supplementation. Gelatin microspheres containing zinc-doped bioactive glass were prepared by phase separation method and evaluated gelatin microsphere size. Mechanism and functional activities of zinc-doped bioactive glass were investigated. The microspheres were ranged in size from 1 µm to 4.5 µm. Gelatin particle was dispersed on the surface of microsphere. ZBGs have shown application with positive effects towards wound healing by contributing to the acceleration of the hemostasis, reduction in localized inflammation, and stimulating anabolic activities for epithelial and osteoblast lineage cells. Therefore, these findings can be expressed with controlled delivery and thus pushing the boundaries of biomedical research to develop a functional and accessible modality for application of ZBG.

Keywords: Zn-doped bioactive glass, ZBG, local immunomodulation, controlled release, gelatin microspheres

P-42

Surface characterization, biocompatibility, and antifungal efficacy of

a denture-lining material containing *Cnidium officinale* extracts

Myung-Jin Lee[a], Youn-Soo Shim[b], So-Youn An[c], Min-Kyung Kang[d*]

[a] *Department of Dental Hygiene, Division of Health Science, Baekseok University, Cheonan, Chungcheongnam-do, 31065, Republic of Korea*

[b] *Department of Dental Hygiene, Sunmoon University, Asan, Chungcheongnam-do, 31460, Republic of Korea*

[c] *Department of, Pediatric Dentistry & Wonkwang bone regeneration research Institute, College of Dentistry, Wonkwang University, Iksan-si, Jeollabuk-do, 5453, Republic of Korea*

[*d] *Department of Dental Hygiene, Hanseo University, Seosan, Chungcheongnam-do, 31963, Republic of Korea*

Corresponding to Min-Kyung Kang (kmk0709@hanseo.ac.kr)

ABSTRACT

Herein, we investigated the surface characterization and biocompatibility of a denture-lining material containing *Cnidium officinale* extracts and its antifungal efficacy against *Candida albicans*. To achieve this, a denture-lining material containing various concentrations of *C. officinale* extract and a control group without *C. officinale* extract were prepared. The surface characterization and biocompatibility of the samples were investigated. In addition, the antifungal efficacy of the samples on, *C. albicans* was investigated using spectrophotometric growth and LIVE/DEAD assay. The results revealed that there was no significant difference between the biocompatibility of the experimental and control groups ($p > 0.05$). However, there was a significant difference between the antifungal efficiency of the denture material on *C. albicans* and that of the control group ($p < 0.05$), which was confirmed by the LIVE/DEAD assay. These results indicate the promising potential of the *C. officinale* extract-containing denture-lining material as an antifungal dental material.

Keywords: Antifungal efficacy, Biocompatibility, Candida albicans, Cnidium Officinale, Denture-relining material, Surface characterization

P-44

Study on Improvement of throughput and the Design of Waferscale

Structure of Multi Electron-Beam System Based on Microcolumn

Youngbok Lee[1, 3], Dae Wook Kim[1, 2, 3], Seung Joon Ahn[1, 2, 3], Tae Sik Oh[1, 2, 3], and Ho Seob Kim[1, 2, 3*]

[1] *Department of Physics and Nanoscience, Sun Moon University, 70, Sunmoon-ro 221, Tangjeong-myeon, Asan-si, Chungcheongnam-do 31460, South Korea*

[2] *Department of Display and Semiconductor Engineering, Sun Moon University, 70, Sunmoon-ro 221, Tangjeong-myeon, Asan-si, Chungcheongnam-do 31460, South Korea*

[3] *Center for Next-Generation Semiconductor Technology, Sun Moon University, Asan-si Chungnam Korea, 31460*

[*] *Corresponding author : hskim3@sunmoon.ac.kr*

Abstract:

Multi electron-beam system is one of the ways to solve the low throughput problem of electron-beam device. Multi electron-beam system use multiple electron columns simultaneously to increase throughput. microcolumn has features that are easy to miniaturize and easy to control, making it suitable for multi electron-beam systems. Multi electron-beam system based on microcolumn consists mainly of three types: arrayed microcolumn, monolithic array and waferscale microcolumn. Among these, the waferscale microcolumn is complex in structure and design but can simultaneously produce and control large numbers of electron columns with uniformed specifications and characteristics. In a multi electron-beam system, the throughput that varies with the quantity of the electron column can be determined by calculation. As the number of columns increases by N, processing time per wafer is reduced by approximately 1/N rate. When using microcolumns of initial structure, it can be seen that about 240 electron columns are required for processing 25 wafer per hour, and about 480 electron columns are required for 50 wafer per hour. In order to reduce the quantity of electron columns needed to increase throughput, the study of microcolumns applied with improved structure electron optics was conducted. Efficient design is needed to place hundreds of electron columns in a wafer. The quantity of the deployable electron column is determined by the size of the column and distance of column to column, thereby determining the size of the required electrodes and wiring. Electrodes in microcolumns are easy to miniaturize, but wiring connecting each electrode is difficult to miniaturize below a certain size. In this paper, we check the difference between structure and characteristics of existing microcolumn and improved microcolumn and discuss column layout and wiring design optimized and change in efficiency for waferscale structure.

This study was supported by National Research Foundation of Korea (NRF) grant funded by the Korean government (MEST) (NRF-2018R1D1A1B07046695).

P-45

Study on Silicon Lens Surface by Raman Spectroscopy

Geon Woo Lee[1,3], Hyun Se Choi[1,3], Young Bok Lee[1,3] and Ho Seob Kim[1,2,3*]

[1] Department of Physics and Nanoscience, Sun Moon University, 70, Sunmoon-ro 221, Tangjeong-myeon, Asan-si, Chungcheongnam-do 31460, South Korea

[2] Department of Display and Semiconductor Engineering, Sun Moon University, 70, Sunmoon-ro 221, Tangjeong-myeon, Asan-si, Chungcheongnam-do 31460, South Korea

[3]Center for Next-Generation Semiconductor Technology, Sun Moon University, Asan-si Chungnam Korea, 31460

** Corresponding author : hskim3@sunmoon.ac.kr*

Abstract:

The microcolumn consists of electron emitter, source lenses, deflectors, and an einzel lens which are fabricated by using micro electromechanical system (MEMS) process. The electron lenses used in microcolumns are made of silicon highly-doped with boron. Most of the electrons emitted from CNT (Carbon nanotube) emitter pass through the aperture hole of the silicon electron lens, but a large amount of electrons that do not pass the hole collide around the aperture hole. After using the microcolumn for a long time, the area around the aperture hole of the electron lens turns into a contaminated form by the emitted electron bombardment. In this study, a Raman spectroscopy was used to investigate the surface propertied of the electron lenses after 6 months of operating the microcolumn. In order to compare the used lens surface properties with regular lenses, we acquired the Raman signal of the fresh lens surface as well as the CNT tip, carbon contaminated silicon, etc. and we will present a comparison of Raman spectra.

Acknowledgment:

This study was supported by the National Research Foundation of Korea (NRF) grant funded by the Korea government (MSIT) (No. 2020R1A2C1008944)

P-46

Protocol for MTA Biomineralization & Regeneration Retrograde filling and Replantation of Avulsed Primary Incisors ; a SEM Study

Youn-Soo Shim^{a}, Myung-Jin Lee^{b}, Min-Kyung Kang^{c}, So-Youn An ^{d*}

[a] Department of Dental Hygiene, Sunmoon University, Asan, Chungcheongnam-do, 31460, Republic of Korea

[b] Department of Dental Hygiene, Division of Health Science, Baekseok University, Cheonan, Chungcheongnam-do, 31065, Republic of Korea

[c] Department of Dental Hygiene, Hanseo University, Seosan, Chungcheongnam-do, 31963, Republic of Korea

[*d] Department of, Pediatric Dentistry & Wonkwang bone regeneration research Institute, College of Dentistry, Wonkwang University, Iksan-si, Jeollabuk-do, 5453, Republic of Korea

Corresponding to So-Youn An (9543sue@hanmail.net)

ABSTRACT

According to the recent guidelines for dental trauma (IADT2012), the replantation of a avulsed primary incisor is not recommended. However, in some cases, under the age of three, if there is no fracture and there is relatively no contamination, the guardian may want a replantation even if it fails. In the case of our pediatric dental hospital, if the guardian's sufficient understanding and consent form is prepared, primary tooth is preserved in PBS, and a disk is used to cut one-third of the root under saline solution, and the tooth is performed retrograde filling using MTA. The tooth replant into the tooth alveolar socket and perform RESIN-WIRE fixation. Periodically observe whether the peri-alveolar bone regenerates around the replanted MTA through dental radiography and clinical evaluation. MTA (Mineral Trioxide Aggregate) has the ability of periodontium regeneration, but this material has drawbacks such as difficult handling properties, causes discoloration of the tooth, contains heavy metals and problems with retrievement. The main focus of this protocol is to introduce the Biomineralization and Regeneration research result and the easy grafting technique of a new Biomaterial which is capable of periodontium regeneration. The purpose of this study is to evaluate by SEM on avulsed primary incisor exposed outside of 45 minutes or more that were replanted more than six months after the application of retrograde MTA filling in 27-month old child.

Keywords: *Avulsion, Mineral trioxide aggregate (MTA), Primary tooth, Retrograde fil materials, Replantation, scanning electron microscopy (SEM)*

P-47

Application of Silver Diamond Fluoride (SDF) in Primary Molar dental caries surfaces

Youn-Soo Shim[a], **So-Youn An**[b*]
[a] Department of Dental Hygiene, Sunmoon University, Asan, Chungcheongnam-do, 31460, Republic of Korea
[*b] Department of, Pediatric Dentistry & Wonkwang bone regeneration research Institute, College of Dentistry, Wonkwang University, Iksan-si, Jeollabuk-do, 5453, Republic of Korea
Corresponding to So-Youn An (9543sue@hanmail.net)

ABSTRACT

As a way to stop the progress of dental caries and prevent the occurrence of new dental caries, fluoride varnishes are mainly applied to experts. Silver Diamond Fluoride (SDF), another sanction for the prevention of dental caries, is a colorless base liquid made up of a combination of silver nitrate and fluoride, consisting of about 24 to 28% (weight/volume) silver, 5 to 6% (weight/volume) fluoride, and about 8% ammonia. SDF is a cost-effective, non-invasive, and safe prevention of dental caries, and can effectively prevent dental caries through antibacterial action, suppression of decomposition of dentin, suppression of aberration of enamel and dentin, and promotion of re-lightening. According to the Systematic Review published in 2016, the rate of suspension of dentin caries in vitro by treatment of 38% SDF was 81% (95% Confidence interval, 68 to 89% and p0.0.001). In addition to the prevention of eating well, SDF has the effect of reducing perceptual hypertrophy by forming silver ion salts in the hypersensitive dentin and blocking the dentinal tubes. In the United States, SDF has been approved as a perceptual hypersensitive treatment. The purpose of this study is to evaluate by MicroCT on primary molar exposed SDF application.

Keywords: *Dental caries, MicroCT, Primary tooth, Replantation, Silver Diamond Fluoride (SDF)*

P-48

Study on feasibility of large area image acquisition using stage transfer synchronization methods

Youngbok Lee[1, 3], Dae Wook Kim[1, 2, 3], Seung Joon Ahn[1, 2, 3], Ho Seob Kim[1, 2, 3], and Tae Sik Oh[1, 2, 3*]

[1]*Department of Physics and Nanoscience, Sun Moon University, 70, Sunmoon-ro 221, Tangjeong-myeon, Asan-si, Chungcheongnam-do 31460, South Korea*

[2]*Department of Display and Semiconductor Engineering, Sun Moon University, 70, Sunmoon-ro 221, Tangjeong-myeon, Asan-si, Chungcheongnam-do 31460, South Korea*

[3]*Center for Next-Generation Semiconductor Technology, Sun Moon University, Asan-si Chungnam Korea, 31460*

[*]*Corresponding author : ots99@sunmoon.ac.kr*

Abstract:

We have studied stage transfer synchronization method (STSM) to improve the low throughput which is the biggest drawback of the raster scan method being applied for image acquisition in a low energy microcolumn system. STSM means acquiring image of the sample by repeating sequential processes with single microcolumn, the line-scan is performed once by electron beam in specific direction followed by the stage mounted sample is transferred once in the direction perpendicular to the line scan, for a certain period of time. Through preliminary experiments, we were able to acquire some sample images by applying STSM to a conventional single microcolumn system. Through preliminary experiments, we were able to acquire some images of measured sample by applying STSM to a conventional single microcolumn system. The image of this preliminary experiment was 3 times larger than raster scan method in the vertical direction. In this study, we have tried two types of STSM's; the first method is acquiring image by horizontal electron beam scanning followed by vertical stage transfer (V-STSM), and the second method is acquiring image by vertical electron beam scanning followed by horizontal stage transfer (H-STSM). By applying V-STSM, we could acquire larger image than the conventional raster scan method, the V-STSM image was1.8 times larger in the horizontal direction and 6 times larger in the vertical direction. In addition, a larger image of about 9 times in the horizontal direction and 5 times in the vertical direction was acquired by applying H-STSM.

This study was supported by the National Research Foundation of Korea (NRF) grant fu
by the Korea government (MSIT) (No. 2020R1A2C1008944)

P-49

Synthesis of molecularly polymer nanoparticles using surface iniferter

miniemulsion polymerization in presence of amphiphilic ionic liquid as surfactant

Renyuan Song[1*], **Yanfang Tai**[1], **Xiaofeng Yu**[1]

[1] *Anhui Provincial Engineering Laboratory of Silicon-based Materials, School of Material and Chemical Engineering, Bengbu University, Bengbu, 233030, PR China*

Corresponding author: E-mail: songrenyuan0726@163.com, Tel: +86-552-317-9368

Abstract

By adopting the long-chain alkyl ionic liquids (1-dodecyl-3-methyl imidazolebromide) as solubilizer of template and co-stabilizer of continuous phase, the glutathione (GSH) imprinted polymers (ILs-MIPs) microspheres with large specific surface area and high selectivity were synthesized by surface iniferter miniemulsion polymerization. The effects of the ionic liquids on the stability of complex of the template and functional monomer were investigated by UV-vis spectroscopy, 1H-NMR spectroscopy and fluorescence spectroscopy respectively, which suggested that the complex of the template and functional monomer has a good stability in the mini-emulsion polymerization systems. In addition, the effects of the ionic liquids on the apparent morphology and recognition property of ILs-MIPs were investigated in detail. The N2 adsorption tests manifested that the ILs-MIPs have larger specific surface area (34.58 m2·g-1), well-distributed pore size and good hydrophilicity to improve the biocompatibility of materials surface. The results of batch adsorption tests indicated that the saturated adsorption capacity of ILs-MIPs was 68.24 mg·g-1 and the imprinting factor reach was up to 3.77. Moreover, the recognition performance of ILs-MIPs was superior to that of MIPs (2.02) without ionic liquids as addition. The experimental data of ILs-MIPs was fitted to Langmuir isotherm model and the adsorption of ILs-MIPs towards GSH follows the pseudo-second-order kinetic model, indicating that the adsorption process is chemical in nature. The dynamic adsorption tests demonstrated that the ILs-MIPs have outstanding selectivity towards the template.

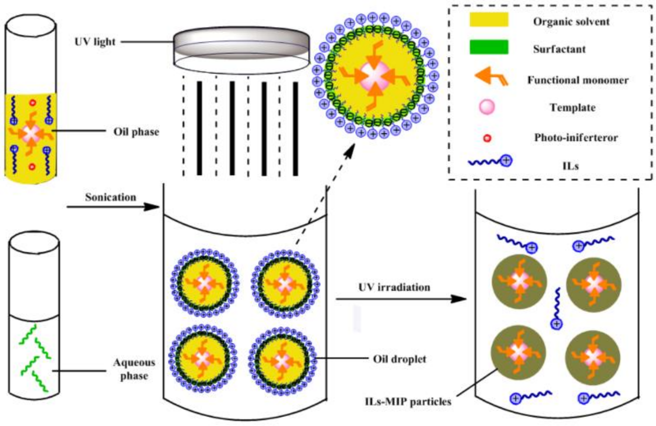

Fig.1 Schematic illustration for the preparation of GSH imprinted polymer microspheres in the presence of ILs via iniferter miniemulsion polymerization.

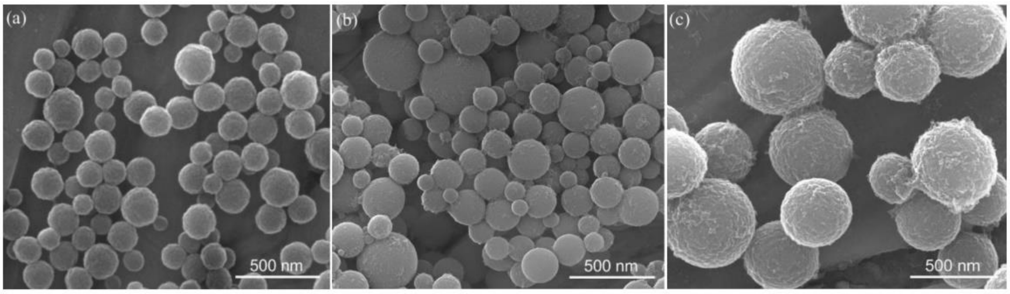

Fig. 2 The effects of the amount of ILs on the morphologies of ILs-MIPs particles.

References

1 Wang Z, Qiu T, Guo L, et al. *Reactive and Functional Polymers*, 2018, 126(1):1-8.

Acknowledgments

The work was supported by the Provincial Natural Science Foundation of Anhui (No. 2008085ME174)

Carbon quantum dots sensitized hollow TiO_2 spheres for visible light photocatalytic degradation of organics

Xianfeng Zhang*, Zongqun Li, Shaowen Xu, Yaowen Ruan

Anhui Provincial Engineering Laboratory of Silicon-based Materials, School of Material and Chemical Engineering, Bengbu University, Bengbu, 233030, PR China

[*] Corresponding author: E-mail: zxf@bbc.edu.cn, Tel: +86-552-317-9368

Abstract

The carbon nanospheres prepared by the hydrothermal method using glucose as carbon source were used as the template, the coated composite was formed by wrapping with n-butyl titanate, and after temperature-programming calcination to remove the carbon nanosphere templates, the hollow-structured TiO_2 nanospheres were formed. Then with carbon quantum dots (CQDs) prepared with citric acid as a carbon source, a nano-CQDs/TiO_2 composite was prepared by covalent connection. Using X-ray diffractometer (XRD), specific surface area method (BET), transmission electron microscope (TEM) and other means to characterize carbon sphere templates, carbon quantum dots, TiO_2 nanospheres and their composites. The photocatalytic degradation of methyl orange solution by composite nanomaterials CQDs/TiO_2 was studied. The results show that the obtained nanocomposite has a hollow structure, the diameter of the TiO_2 shell is about 1.1 μm, the thickness of the shell wall is about 50 nm, and the specific surface area is about 27.9 m^2/g. When the composite dosage is 50 mg, the degradation rate of 100 mL methyl orange solution (10 mg/L) can reach 39.1% after 2 hours of light irradiation.

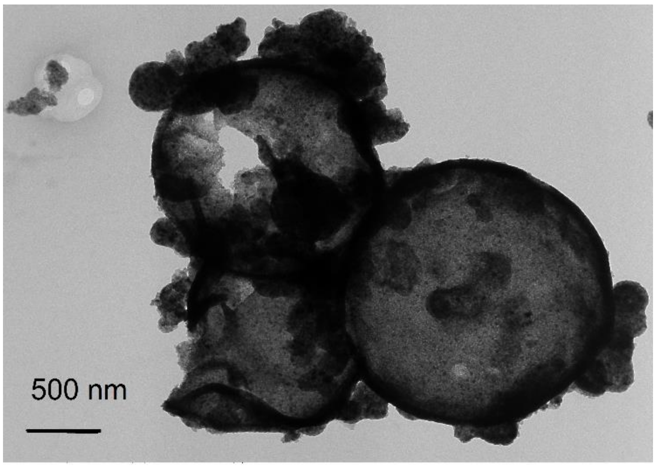

Fig.1 Transmission electron microscopy of CQDs/TiO_2 nanocomposites.

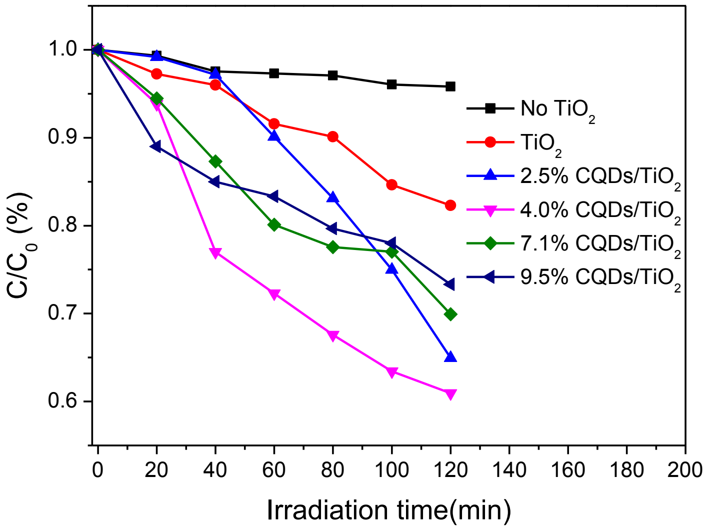

Fig.2 Photocatalytic degradation of methyl orange by TiO_2 and CQDs/TiO_2 nanocomposite.

References

[1] Li H., He X., Kang Z., et al, Angew. Chem., Int. Ed., 2010, 49, (26), 4430-4434.

[2] Wu L., Fu C., Huang W. Phys. Chem. Chem. Phys., 2020, 22, 9875-9909.

Acknowledgments

The work was supported by the National Natural Science Foundation of China (No. 21503004) and Key Natural Science Research Projects in Universities of Anhui Province (No. KJ2019A0851).

Preparation of the mesoporous silica composite nanoparticles coated with biodegradable temperature/pH sensitive copolymer and their application in drug release

Xiaoqi Jin, Jinlong Ge, Qiuqin Wang, Yan Gao

Department of Materials Science and Chemical Engineering, Anhui province Engineering Laboratory of Silicon-based Materials Bengbu University, Bengbu 233000, P.R. China

Abstract

In this work, we have synthesized the biodegradable and temperature/pH- sensitive copolymer PEG-PLA-P(NIPAM-co-AA) by emulsion copolymerization method with the modified of Poly(ethylene glycol)-co-(L-lactic acid) as crosslinker[1]. Then the structural composition and temperature/pH-sensitive properties were characterized by using ^{1}HNMR, FT-IR and Dynamic light scattering (DLS) techniques. Furthermore, the Ibuprofen as the model drug , the copolymer was encapsulated on the surface of modified mesoporous silica nanoparticles MSNs-NH_2 using “grafted to” method. We preliminary investigated the performance of drug release in the difference release conditions. The results showed that the copolymer had rapidly temperature/pH dual stimuli responsive. Moreover, the resultant composite nanoparticles PEG-PLA-P(NIPAM-co-AA)@ MSNs exhibited excellent property of drug-controlled release, as shown in Fig.1. Therefore, the copolymer is expected to apply in the field of controlled drug release as intelligent drug carried.

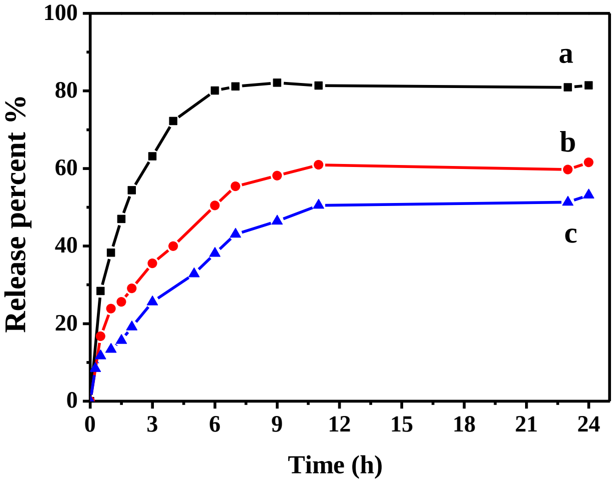

Fig.1 Release profiles of ibuprofen from composite nanoparticles (a) pH=7.4 PBS 40℃(b) pH=2.0 PBS 40℃ (c) pH=7.4 PBS 25℃

Keywords: mesoporous silica nanoparticles, biodegradable; pH/temperature sensitivity; controlled drug release

Acknowledgments: This project was supported by the Key Research Project of Natural Science

from Provincial Bureau of Education, Anhui, China (KJ2018A0567)

References:

[1] Dong W. L., Tae G. P. Stereocomplex formation between enantionmeric PLA-PEG-PLA triblock copolymers; Characterization and use as protein-delivery microparticulate carriers [J]. J Appl Polym Sci, 2000, 75(13):1615-1623.

Ultrasonic-microwave synergistic synthesis of Co-MCM-41: effect of Co molar ratio on its microstructural property and catalytic activity

Ying-Yue Qin*, Liang Li[1], Mu-Xin Liu[1]

[1] *Anhui Provincial Engineering Laboratory of Silicon-based Materials, School of Material and Chemical Engineering, Bengbu University, Bengbu, 233030, PR China*

*Corresponding author. Tel: +863865527939 E- mail: qinyingyue@126.com

Abstract:

Under the ultrasonic-microwave synergistic irradiation, Co-MCM-41 mesoporous materials with different Co Molar Ratios were synthesized in the alkaline system using cobalt chloride ($CoCl_2$) as cobalt source. The as-prepared samples were characterized by Powder X-ray diffraction (XRD), infrared (IR), Energy dispersive X-ray detector (EDX) and Transmission electron microscopy (TEM). All the samples exhibited typical hexagonal mesoporous structure and the cobalt was incorporated into the framework of MCM-41, with a regular straight pore size around 0.5nm. The catalytic activities of the obtained Co-MCM-41 composites were evaluated by the oxidation of benzene. The optimized dosage of Co-MCM-41(10) is 2.5g/L when the yield of Phenol is highest as 26.18%.

Keywords: mesoporous; Co-MCM-41; synergistic irradiation; Catalytic activity

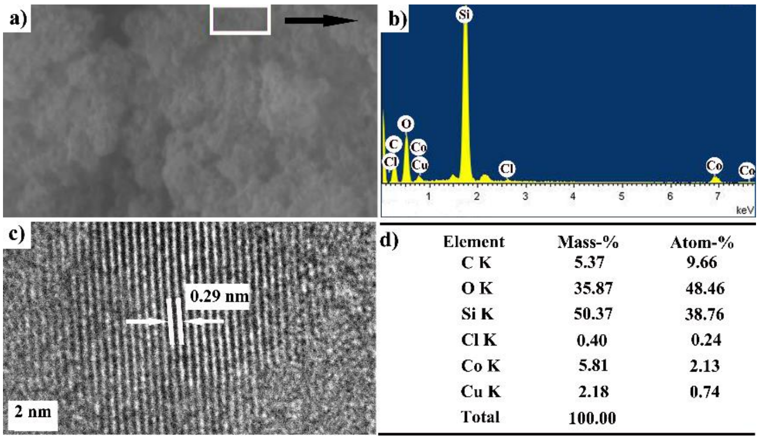

Element	Mass-%	Atom-%
C K	5.37	9.66
O K	35.87	48.46
Si K	50.37	38.76
Cl K	0.40	0.24
Co K	5.81	2.13
Cu K	2.18	0.74
Total	100.00	

Fig. 1 TEM-EDS spectrum of Co-MCM-41(10)

Acknowledgments

Thanks to the financial support of the National Natural Science Foundations of China (21978003), and Major Projects of the Natural Science Fund for High Education of Anhui Province(KJ2019A0850; KJ2019ZD62).

References

[1] B. Han, H. Wang, Y. Kong, J. Wang. Mater. Lett. , **100**,159(2013)

[2]P. A. Robles-Dutenhefner, K.A.D.S. Rocha, E.M.B. Sousa, E.V. Gusevskaya. J. Catal. , **265**,72(2009)

Fabrication of NH_2-Al-53 for Adsorptive Desulfurization

Zongqun Li,* Chao Feng, Wen Han

Anhui Provincial Engineering Laboratory of Silicon-based Materials, School of Material and Chemical Engineering, Bengbu University, Bengbu, 233030, PR China

* Corresponding author: E-mail: bbxylzq@163.com, Tel: +86-552-317-9368

Abstract

Due to the air pollution caused by SO_x produced from combustion of sulfur-containing fuel, new challenges have been posed to the desulfurization technology. Adsorption desulfurization is a promising technology for clean production of zero sulfur fuel. Metal-organic framework NH_2-Al-53 was synthesized by hydrothermal method with Al^{3+} as the central ion and aminotropephthalic acid. The material was modified by benzoic acid to adjust the pore size and characterized by XRD, BET and FT-IR. The results showed that the mesoporous NH_2-Al-53 was synthesized by changing the ratio of ligands to control the pore size and has good adsorption capacity for benzothiophene in gasoline. The maximum adsorption capacity is 15 mg/g. The fluorescence properties of the materials show that the materials have good fluorescence properties. The fluorescence sensing properties of thiophene and benzothiophene with 2.5 ppm to 75 ppm are tested. The fluorescence sensing properties are obvious in the range of 2.5 ppm to 25 ppm. The online detection of low concentration organic sulfides can be achieved. The material is expected to have a certain application prospect in industrial desulfurization and fluorescence detection.

.

References

[1] Zong-Qun Li,Ling-Guang Qiu,Tao Xu,Yun Wu,Wei Wang,Zhen-Yu Wu,Xia Jiang. Ultrasonic synthesis of the microporous metal–organic framework Cu 3 (BTC) 2 at ambient temperature and pressure: An efficient and environmentally friendly method[J]. Materials Letters, 2008, 63(1).

[2] Khan N A, Jhung S H. Effect of central metal ions of analogous metal-organic frameworks on the adsorptive removal of benzothiophene from a model fuel [J]. Journal of Hazardous Materials, 2013: 1050-1056.

Acknowledgments

The work was supported by the the Program of College Students Innovation of Laboratory Construction (2016ckjh116).

Title: Stereo-Defined co-doping of sp-N and O atoms in porous carbon nanosheets for Oxygen Reduction Reaction

Zhong Wu*[a,b,c]

[a]*Materials and Chemical Engineering Department, Bengbu College, Anhui, 233030, China*

[b]*Anhui Provincial Engineering Laboratory of Silicon-based Materials, Anhui, 233030, China*

[c]*Engineering Technology Research Center of Silicon-based Materials, Anhui, 233030, China*

Abstract

Nitrogen-doped carbon (NC) materials have been proposed as next-generation oxygen reduction reaction (ORR) catalysts to significantly improve scalability and reduce costs, but these alternatives usually exhibit low activity and/or gradual deactivation during use. Here, as a proof-of-concept experiment, N,O-codoped porous carbon nanosheets (GCNs) have been fabricated. Compared to commercial Pt/C catalyst, the GCNS show comparable onset potential, higher current density, and superior durability in the ORR. Those properties might be attributed to a synergistic effect between NC and graphene with regard to structure and composition. The resultant uniform porous carbon nanospheres show the ultralarge pore size, high surface area and abundant N content, which deliver high current density and excellent durability toward oxygen reduction reaction in alkaline solution.

Keywords: heteroatom-doping; carbon nanosheets; oxygen reduction reaction

References:

1. Z. Wu, and X. Zhang, Acta Phys. -Chim. Sin. 33, 305 (2017).
2. Z. Wu, and X. Zhang, Sci. China Mater. 59, 547 (2016).
3. H. B. Tao, J. Zhang, J. Chen, L. Zhang, Y. Xu, J. G. Chen, and B. Liu, J. Am. Chem. Soc. 141, 13803 (2019).
4. J. Gao, Y. Wang, H. Wu, X. Liu, L. Wang, Q. Yu, A. Li, H. Wang, C. Song, Z. Gao, M. Peng, M. Zhang, N. Ma, J. Wang, W. Zhou, G. Wang, Z. Yin, and D. Ma. Angew. Chem. 58, 15089 (2019).
5. X. Han, X. Ling, D. Yu, D. Xie, L. Li, S. Peng, C. Zhong, N. Zhao, Y. Deng, and W. Hu, Adv. Mater. 31, 1905622 (2019).

Acknowledgments: This study was funded by Doctoral Scientific Research Start-up Foundation of Bengbu University (Grant No. BBXY2018KYQD16), Anhui Department of Education University Natural Science Research Project (Grant No. KJ2019A0848).

High hydrophobic graphene/functionalized SiO_2 composites as efficient absorbent in oil-water separation

Liyuan Zhang *, Linlin Zhu, Xiaoqi Jin, Zhenwei Li

School of Material and Chemical Engineering, Bengbu University, Bengbu, Anhui 233000, People's Republic of China

Abstract

The high hydrophobic graphene/functionalized SiO_2 composites were prepared via self-assembly of graphene sheets on the surface of vinyl-functionalized silica nanoparticles. The resulting graphene/functionalized SiO_2 composites exhibited rapid absorption rate, high absorption capacity and convenient separation in oil-water separation. Furthermore, the composites could be easily recovered and reused at least 12 times without any loss of its activity and showed great potential for large-scale application in water treatment.

Keywords: Graphene; Silica; Nanocomposites; Water treatment.

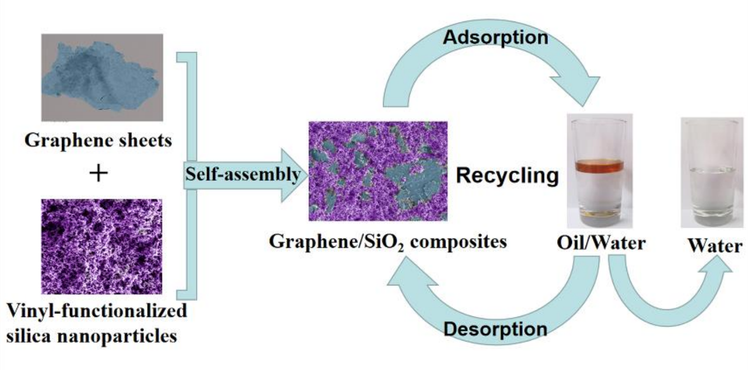

Scheme 1. The preparation of high hydrophobic graphene/functionalized SiO_2 composites via self-assembly and their application in oil-water separation.

Research Support Fund: The Natural Science Foundation of Anhui Province's Higher Education of China (KJ2019A0847, KJ2018A0567), the Natural Science Foundation of Bengbu University (2019ZR05zd).

FROM: Zhang LY, Zhu LL, Jin XQ, Li ZW. High hydrophobic graphene/functionalized SiO_2 composites as efficient absorbent in oil-water separation. Fullerenes, Nanotubes, and Carbon Nanostructures, 2020, Article ID FNCN2070.

Process development for detoxification of fermentation inhibitors from acid-hydrolysate of microalgae

Song Yi Kim[1], Seong Jin Jeon[1], Dong Ho Baek[1], Ho Seob Kim[2,3,4], and Jin Woo Kim[1,3]*

[1]*Department of Food Science, Sunmoon University, Natural Science Building, 70 Sunmoon-ro 221, Tangjeong-myeon, Asan-si, Chungnam 336-708, Korea*

[2]*Department of Physics and Nano-science, Sun Moon University, Natural Science Building, 70 Sunmoon-ro 221, Tangjeong-myeon, Asan-si, Chungnam 336-708, Korea*

[3]*Center for Next-Generation Semiconductor Technology, Sun Moon University*

[4]*CEBT Co. Ltd.*

[*]*Correspondence: kimjw1028@sunmoon.ac.kr; Tel.: +82-41-530-2226*

Abstract:

The aim of this study was to remove toxic compounds including 5-hydroxymethyl (5-HMF) and furfural known as fermentation inhibitors in acid-hydrolysates obtained from the acid-pretreatment of microalgae (*Scenedesmus obliquus*) using activated carbon. For this purpose, synthetic hydrolysate containing glucose, xylose, 5-HMF, and furfural was prepared, and response surface methodology (RSM) was applied to optimize the detoxification condition. Detoxification temperature (16.5~58.5℃), time (0.5~5.5 hr), and solid-liquid ratio of activated carbon (0.6~7.4 w/v %) were used as independent variables. Statistical analyses showed that three variables had significant effects on the removal of toxic compounds. The optimum detoxification conditions with the maximum removal of 5-HMF and furfural were as following: temperature of 76.1℃, extraction time of 7.7 hr, and solid ratio of 3.3 w/v %. Under these conditions, the removal of 5-HMF was 86.2%, furfural was 84.3%, and sugars (glucose and xylose) were 1.41% from acid-hydrolysate of *S. obliquus* which agreed with the predicted values of 89.9%, 87.9%, and 1.28%, respectively. When the acid-hydrolysate and detoxified acid-hydrolysate were used for ethanol fermentation by *S. cerevisiae*, the ethanol products were obtained 2.7 and 20.8 g/L respectively, which confirmed that the detoxification using activated carbon was effective in removing toxic compounds from acid-hydrolysate of *S. obliquus*.

Keywords*:* Microalgae, fermentation, detoxification, HMF, furfural, sugars, pretreatment

Microwave employed sol-gel synthesis of $Ho^{3+}/Yb^{3+}/Tm^{3+}$ tri-doped $NaGd(WO_4)_2$ phosphors and their spectroscopic properties for biomedical applications

Chang Sung Lim[1*], **Won-Chun Oh**[1], **Aleksandr S. Aleksandrovsky**[2,3], **Victor V. Atuchin**[4,5,6,††], **Maxim S. Molokeev**[7,8,9], **Aleksandr S. Oreshonkov**[8,10]

[1]*Department of Aerospace Advanced Materials Engineering, Hanseo University, Seosan 31962, Korea*
[2]*Laboratory of Coherent Optics, Kirensky Institute of Physics Federal Research Center KSC SB RAS, Krasnoyarsk 660036, Russia*
[3]*Institute of Nanotechnology, Spectroscopy and Quantum Chemistry, Siberian Federal University, Krasnoyarsk 660041, Russia*
[4]*Laboratory of Optical Materials and Structures, Institute of Semiconductor Physics, SB RAS, Novosibirsk, 630090, Russia*
[5]*Laboratory of Semiconductor and Dielectric Materials, Novosibirsk State University, Novosibirsk 630090, Russia*
[6]*Research and Development Department, Kemerovo State University, Kemerovo 650000, Russia*
[7]*Laboratory of Crystal Physics, Kirensky Institute of Physics, Federal Research Center KSC SB RAS, Krasnoyarsk 660036, Russia*
[8]*Siberian Federal University, Krasnoyarsk 660041, Russia*
[9]*Department of Physics, Far Eastern State Transport University, Khabarovsk 680021, Russia*
[10]*Laboratory of Molecular Spectroscopy, Kirensky Institute of Physics Federal Research Center KSC SB RAS, Krasnoyarsk 660036, Russia*
*E-mail: cslim@hanseo.ac.kr

Abstract

In recent years, rare earth-doped upconversion (UC) nanoparticles have attracted great interest due to the luminescent properties and potential applications in products such as lasers, three-dimensional displays, light-emitting devices, and biological detectors[1]. The binary tungstate compounds with general composition of $NaR(WO_4)_2$ (R: trivalent rare earth ion) belong to a group of double alkaline earth lanthanide tunghstates. It is possible that the trivalent rare earth ions in the disordered tetragonal phase could be partially substituted by Er^{3+}/Yb^{3+}, Ho^{3+}/Yb^{3+} and $Ho^{3+}/Yb^{3+}/Tm^{3+}$ ions, and the ions are effectively doped into the crystal lattice of the tetragonal phase due to the similar radii of trivalent rare earth ions of R^{3+}, resulted in the excellent UC photoluminescence properties[2-4]. In this study, double tungstate

NGW:Ho^{3+}/Yb^{3+}/Tm^{3+} white phosphors were successfully synthesized by microwave employed sol-gel method. The synthesized particles brought superior microcrystalline morphology with particle size of 1-2 μm. Under excitation at 980 nm, the UC doped particles revealed white emissions based on blue, green and red emission bands, which correspond to the $^1G_4 \rightarrow {}^3H_6$ transitions of Tm^{3+} in the blue region, the $^5S_2/{}^5F_4 \rightarrow {}^5I_8$ transitions of Ho^{3+} in the green region, the $^5F_5 \rightarrow {}^5I_8$ transitions of Ho^{3+} as well as the $^1G_4 \rightarrow {}^3F_4$ and $^3H_4 \rightarrow {}^3H_6$ transitions of Tm^{3+} in the red region. The calculated slope value $n = 2.23$ for blue emission at 475 nm, $n = 1.69$ for green emission at 545 nm, and $n = 1.95$ and 1.73 for red emissions at 655 and 695 nm, respectively. The calculated chromaticity coordinates were corresponding to the standard equal energy point in CIE diagram. The strong disordered peaks at higher and lower frequencies in Raman spectroscopy were attributed the strong mixing between the W-O bonds and the WO_4 stretching in framework of local distortions of WO_4 tetrahedra. The results led to superior emitting efficiency and NGW:Ho^{3+}/Yb^{3+}/Tm^{3+} white phosphors can be considered as potentially active PL materials in new optoelectronic devices and in the field of biomedical applications.

References

1. M.V. DaCosta, S. Doughan, U.J. Krull, Analyca Chimica Acta, **832**, 1-33 (2014).

2. Chang Sung Lim, Aleksandr Aleksandrovsky, Maxim Molokeev, Aleksandr Oreshonkov, Victor Atuchin,, Physical Chemistry Chemical Physics, **17**, 19278-19287 (2015).

3. Chang Sung Lim, Aleksandr Aleksandrovsky, Maxim Molokeev, Aleksandr Oreshonkov, Victor Atuchin, J. Solid State Chemistry, **228**, 160-166 (2015).

4. Chang Sung Lim, Materials Research Bulletin, **75**, 211-216 (2016).

Development of natural luminescent powder for the detection of latent fingerprint

Choosak Poonsawat ,Supatcharee Siriwong and Rachadaporn Benchawattananon*

Chemistry , Faculty of Science, Khon Kaen University, Khon Kaen, Thailand 40002

Integrated Science ,Faculty of Science, Khon Kaen University, Khon Kaen, Thailand 40002

Synchrotron Light Research Institute (Public Organization) Nakhon Ratchasima, Thailand

* Corresponding Author: Benchawattananon, R.; Email: rachadaporn@kku.ac.th

Abstract

Nowadays, Dyes is widely used to improve fingerprints identification test. Natural Dyes is another interesting way that be used instead of chemical dyes because natural dyes is less toxic and lower cost than chemical dyes. In this research, the development of rush powder for fingerprints identification due to ability of fluorescence under UV was applied to fingerprints identification technique include dust technique which was for detecting hidden fingerprints on non-porous objects and small particle reagent (SPR) that contain suspension of zinc carbonate used for detecting hidden fingerprints for drowning objects. This research studied physical properties, adhesion characteristics between zinc carbonate particles and rust powder by scanning microscope (SEM). Analysis functional group and elements in compound of rush powder by using UV-visible spectroscopy (UV-VIS), Fourier-transform infrared spectroscopy (FTIR) and Energy-Dispersive X-ray (EDX). Fingerprints identification by dust technique by using rush powder, provide fingerprints can fluorescent under UV light and have a good efficiency but small particle reagent technique (SPR) doesn't appear under UV light. Adhesion characteristics between zinc carbonate particles and rust powder by scanning microscope (SEM) is found that both particles don't adhere well to each other. However, fluorescence properties of rush powder is still interesting to improve rush powder to be a good natural dyes that can interact with zinc carbonate to help increasing more efficiency of fingerprints identification test.

Keywords : rush powder, FTIR, EDX, SEM, non-porous objects, SPR

Variable Focusing Liquid Crystal Lens with Polarization Free

Seok Je Lee[1], Chul Gyu Jhun[1]†

[1]*Division of Electronics and Display Engineering, Hoseo University, Asan 31499, Korea*

Tel : +82 41 540 5899, Fax : + 82 41 540 5618, email : cgjhun@hoseo.edu

Abstract:

We predicted and demonstrated changing diopter values by designing a variable focus lens through simulation and fabricating a device based on the results. The variable focus lens is a technology that can change the focus according to the input signal, and can be used as a lens that improves the problem of complex eyes. It is mainly controlled by an electric signal using liquid crystal, and was first proposed in 1979 [1]. So far, many researchers have studied focal lenses [1-4]. We have studied a variable focusing lens with liquid crystals to apply for the VR/AR device. In this paper, we demonstrates the facrication process of variable focusing lens with liquid crystal materials. Simulation results of variable focusing liquid crystal lenses were compared with the measured results of that.

Key words: variable focusing lens, liquid crystal, polarization free

[1] S. Sato, Liquid-crystal lens-cells with variable focal length, Jpn, J. Appl. Phys. 18, (1979) 1679

[2] G. Williams, N. J. Powell, A. Purvis, and M. G. Clark, Electrically controllable liquid crystal Fresnel lens, Proc. SPIE, 1168, (1989) 352-357

[3] J. S. Patel and K. Rastani, Electrically controlled polarization-independent liquid-crystal Fresnel lens arrays, Opt. Lett. 16, (1991), 532-534

[4] K. Hamanaka, H. Nemoto, M. Oikawa, E. Okuda, and T. Kishimoto, Multiple imaging and multiple Fourier transformation using planar microlens arrays, Appl. Opt. 29, (1990) 4064

Enhanced Electrical Properties of Organic-Light Emitting Diode by Controlling Molecular Ordering

Seok Je Lee[1], Chul Gyu Jhun[1]†

[1]*Division of Electronics and Display Engineering, Hoseo University, Asan 31499, Korea*

Tel : +82 41 540 5899, Fax : + 82 41 540 5618, email : cgjhun@hoseo.edu

Abstract:

We demonstrate enhanced electrical properties of organic light-emitting diode (OLED) by controlling the molecular ordering. We fabricated the OLED device with poly[2-methoxy-5-(2-ethylhexyloxy)-1,4-phenylenevinylene] (MEH-PPV) by the solution process [1]. When the emssion layer (EML) was coated by a directional coating method, EML has molecular crystal phase [2-3]. In this paper, we compared the electrical properties of OLED fabricated by the directical coating method and the conventional spin coating method. To figure out the underlying mechanism, we analysis the device properties by various method such as atomic force microscopy (AFM), spectroscopic ellipsometry (SE), X-ray diffraction (XRD), LCR meter, I-V-L system.

Key words: OLED, MEH-PPV, molecular ordering, enhanced conductivity

[1] J. H. Burroughes, D. D. C. Bradley, A. R. Brown, R. N. Marks, K. Mackay, R.H. Friend, P. L. Burns & A. B. Holmes, Light-emitting diodes based on conjugated polymers, Nature, 347, (1990) 539-541

[2] D. Yokoyama, Molecular orientation in small-molecule organic light-emitting diodes, Journal of Materials Chemistry, 21 (2011) 19187-19202

[3] A. R. Inigo, Y. F. Huang, J. D. White, Y. S. Huang, W. S. Fann, K. Y. Peng and S. A. Chen, Review of Morphology Dependent Charge Carrier Mobility in MEH- PPV, Journal of the Chinese Chemical Society, 57 (2010) 459-468

Effects of calcination temperature on the preparation of ZnO nanoparticles by mechanochemical method

Zhou Zhou[1], Wang Jing[2], Chul Gyu Jhun[1†]

[1]*Division of Electronics and Display Engineering, Hoseo University, Asan 31499, Korea*

[2]*School of Materials Science and Engineering, Anhui University of Science and Technology, Huainan 232001, China*

Tel : +82 41 540 5899, Fax : + 82 41 540 5618, email : cgjhun@hoseo.edu

Abstract:

ZnO is a direct bandgap n-type semiconductor with a large forbidden band width (3.37 eV) and high exciton binding energy (60 meV). High-energy ($\lambda < 400$ nm) UV light, however, this part of light accounts for less than 5% of the energy of sunlight, and the application of solid-pure ZnO is greatly limited. Therefore, numerous studies on the modification of ZnO photocatalytic activity have been reported in recent years. Microscopic properties such as the morphology, particle size, and specific surface area of the photocatalyst have been consistently shown to influence its photocatalytic activity. Herein, we have prepared ZnO nanopowders with excellent photocatalytic properties using alkaline zinc carbonate as a precursor by first activating them with high-energy ball milling and then calcining them. The effect of high-energy ball milling time on the alkaline zinc carbonate and the effect of two different calcination temperatures on the size and microscopic morphology of the final calcined product ZnO were studied in detail.

Key words: ZnO, Nanoparticles, Mechanochemistry, Photocatalytic， RhB

[1] C.C. Lin, Y.J. Chiang, Feasibility of using a rotating packed bed in preparing coupled ZnO/SnO_2 photocatalysts, J. Ind. Eng. Chem., 18 (2012) 1233–1236.

[2] C.L. Yu, K. Yang, Y. Xie, Q.Z. Fan, J.C. Yu, Q. Shu, C.Y. Wang, Novel hollow Pt-ZnO nanocomposite microspheres with hierarchical structure and enhanced photocatalytic activity and stability, Nanoscale, 5 (2013) 2142–2151.

[3] D.M. Kong, J. Wang, L.N. Zhu, Y.W. Jin, X.Z. Li, H.X. Shen, H.F. Mi, Oxidative DNA cleavage by Schiff base tetraazamacrocyclic oxamido nickel(II) complexes, Chinese J. Catal., 102 (2008) 824-832.